

**ANALYTICAL STUDIES OF THE VETERINARY  
TRYPANOCIDE ISOMETAMIDIUM  
AND RELATED SUBSTANCES**

A thesis submitted in accordance with the regulations governing the award  
of the Degree of Doctor of Philosophy in Pharmaceutical Sciences.

by

Gesa Johanna Schad Dipl. Ing. (FH), MSc.

Strathclyde Institute of Pharmacy and Biomedical Sciences,  
University of Strathclyde,  
The John Arbuthnott Building,  
27 Taylor Street,  
Glasgow G4 0NR

MAY, 2010

This thesis is the result of the author's original research. It has been composed by the author and has not been previously submitted for examination which has lead to the award of a degree.

The copyright of this thesis belongs to the author under the terms of the United Kingdom Copyright Acts as qualified by University of Strathclyde Regulation 3.50. Due acknowledgement must always be made of the use of any material contained in, or derived from, this thesis.

Signed:

Date:

## Acknowledgements

I wish to thank Dr. J.N. Tetley, Dr G.G. Skellern and Prof. M.H. Grant for their invaluable support, advice and supervision of this work.

Special thanks go to Prof. M.R. Euerby from Hichrom Ltd., for his continuous interest and enthusiasm in supporting me through my work as well as the advice while writing up the thesis.

I would also like to thank the following collaborators who provided materials, advice and support without which the work in this thesis would have been impossible: Merial (Lyon, France) for samples and standards used in this study. Hichrom Ltd. (Reading, UK) for several HPLC columns.

Dr. R. Edrada-Ebel, Dr. T. Zhang and Prof. A.I. Gray (Strathclyde Institute for Pharmacy and Biomedical Sciences (SIPBS), University of Strathclyde) for their assistance with NMR spectroscopy of the phenanthridines and their willingness to share their expertise on the subject.

Furthermore I wish to thank the technical staff in SIPBS, University of Strathclyde, for their friendly advice and assistance throughout the course of this work.

The studentship provided by Merial SAS and the University of Strathclyde, which made the project and this further education possible for me is gratefully acknowledged.

Finally, I wish to thank my family and friends, for their constant love and support.

## CONTENTS

Acknowledgements	iii
Abstract	viii
Glossary	x
List of Figures	xiii
List of Tables	xviii
List of Equations	xix
1. Introduction	
1.1. African Trypanosomiasis	1
1.1.1. The Parasite	4
1.1.2. Control Strategies	8
1.1.3. The Problem of Drug Resistance	11
1.1.4. Counterfeiting	12
1.2. Analysis of Isometamidium	14
1.2.1. Chromatographic Methods (HPLC)	16
1.3. Aims and Objectives	18
2. An Analytical Method for the Quality Control of ISM Formulations	
2.1. Introduction	19
2.1.1. Isometamidium	20
2.1.2. Aims and Objectives	23
2.2. Experimental	24
2.2.1. Materials	24
2.2.2. Preparation of Standard and Sample Solutions	25
2.2.3. HPLC and HPLC-MS analysis	26
2.2.4. Validation Studies	26

2.3.	Results and Discussion	28
2.3.1.	Method Development	28
2.3.2.	Validation	31
2.3.3.	Analysis of Commercial ISM Preparations	35
2.4.	Conclusions	40
3.	Bioanalytical Assay for the Determination of Residual Isometamidium and Related Substances in Plasma	
3.1.	Introduction	43
3.1.1.	Pharmacokinetics of Isometamidium	43
3.1.2.	Metabolism of Isometamidium	46
3.1.3.	Aims and Objectives	48
3.2.	Experimental	49
3.2.1.	Materials	49
3.2.2.	Lowry Assay	52
3.2.3.	Metabolism Studies	52
3.2.4.	Preparation of Standard and Sample Solutions	54
3.2.5.	Solid Phase Extraction	55
3.2.6.	HPLC-MS Analysis	55
3.2.7.	Validation Studies	56
3.3.	Results and Discussion	58
3.3.1.	Method Development	58
3.3.1.1.	HPLC-MS Analysis	58
3.3.1.2.	Internal Standard	60
3.3.1.3.	Solid Phase Extraction	62
3.3.2.	Metabolism Studies	67
3.3.3.	Validation of the Bioanalytical Assay	70
3.4.	Conclusions	75

4.	Comparative Study of the Effect of Stationary Phase Chemistry and Mobile Phase Selectivity on the HPLC Separation of Isometamidium and Related Substances	
4.1.	Introduction	77
4.1.1.	The Resolution Equation	77
4.1.2.	Selectivity	79
4.1.3.	Efficiency	85
4.1.4.	Gradient Analysis	87
4.1.5.	Computer Simulation	89
4.1.5.1.	Theoretical Background	89
4.1.5.2.	Potential Sources of Error in Computer Simulation	91
4.1.5.3.	Practical Application of DryLab®	91
4.1.6.	Aims and Objectives	93
4.2.	Experimental	94
4.2.1.	Materials	94
4.2.2.	Preparation of a Mixed Standard Solution	96
4.2.3.	HPLC Columns	96
4.2.4.	HPLC Analysis	97
4.2.5.	DryLab® Input Data	98
4.3.	Results and Discussion	100
4.3.1.	Effect of Changes on Mobile Phase Composition	100
4.3.2.	Effect of Changes in Stationary Phase Chemistry	103
4.3.3.	Effect of Organic Solvent Content	110
4.3.4.	DryLab® Modelling and Identification of Optimum Separation Conditions	113
4.4.	Conclusions	121

5. Isolation and Characterisation of Isometamidium and Structurally Related Compounds	
5.1. Introduction	124
5.1.1. Establishment of Quality Standards	125
5.1.2. Preparative HPLC	126
5.1.3. Synthesis of Isometamidium: Influence of Reaction Conditions on the Presence of Related Substances	128
5.1.4. Structure Elucidation of ISM and Related Compounds	131
5.1.5. Aims and Objectives	133
5.2. Experimental	134
5.2.1. Materials	134
5.2.2. HPLC-UV analysis	135
5.2.3. HPLC-MS analysis	135
5.2.4. NMR Spectroscopy	136
5.2.5. DryLab® Input Data	137
5.3. Results and Discussion	138
5.3.1. Preparative HPLC	138
5.3.2. UV-Spectroscopy	144
5.3.3. NMR Spectroscopy	146
5.3.4. High Resolution Mass Spectrometry	162
5.4. Conclusions	166
6. Conclusions and Future Work Suggestions	
6.1. Conclusions	168
6.2. Suggestions for Future Work	176
7. References	178
Appendix	192

## **Abstract**

Isometamidium (ISM) is a veterinary trypanocide, extensively used for chemotherapy and chemoprophylaxis against African animal trypanosomiasis in many prime areas of sub-Saharan Africa. Synthesis of ISM results in production of varying amounts of process-related impurities, with pharmacological activity primarily attributed to the principal component (ISM; M&B4180A).

This thesis reports the development and validation of a selective, reproducible and precise assay for the separation and quantification of ISM and process-related by-products present in ISM formulations.

A simple isocratic HPLC-UV assay has been developed and validated, which enables fast HPLC profiling of commercially available ISM products. The method has been successfully applied to a range of samples obtained from the open market in Africa, amongst which several counterfeit products were identified.

Aiming at the determination of residual trypanocide in biological material of treated animals, the method was coupled with MS detection for increased sensitivity. A solid phase extraction (SPE) sample preparation procedure was developed and successfully optimised for the extraction of ISM and related substances from spiked plasma samples. The HPLC-MS assay however failed to provide good precision of the quantification at the very low concentrations of the analytes as present in biological samples from treated animals.

Optimisation of the HPLC assay with respect to selectivity and efficiency in order to improve sensitivity was achieved in a comparative study of the effect of stationary phase chemistry and mobile phase selectivity on the HPLC separation. Computer-assisted method development resulted



in an improved gradient method for highly sensitive determination of ISM and related substances.

A semi-preparative HPLC method was developed for the specific isolation of ISM and related substances. Once isolated, the single compounds were characterised using MS, UV- and NMR-spectroscopy for the first time since their introduction on the market in 1958.

This work will facilitate quality control of ISM products, and permit greater understanding of the pharmacokinetics of the drug in treated animals. It may ultimately lead to definition of further active compounds of the ISM formulation, and also perhaps new, therapeutically useful compounds with trypanocidal activity.

## Glossary

$\alpha$	Selectivity factor alpha
$\alpha_{B/P}$	Ion exchange capacity
$\alpha_{CH_2}$	Hydrophobic Selectivity
$\alpha_{C/P}$	Hydrogen bonding capacity
$\alpha_{T/O}$	Shape selectivity
AB	Amylbenzene
As	Asymmetry factor
$\Delta\%B$	Gradient range
BB	Butylbenzene
$^{\circ}C$	Degrees Celsius
CEIA	Competitive enzyme immunoassay
CW	Weak Cation Exchanger
$d_c$	inner column diameter
DMCS	Dimethylchlorosilane
DMSO	Dimethyl sulfoxide
DNA	Deoxyribonucleic acid
e. g.	for example
ELISA	Enzyme-linked immunosorbent assay
ESI	Electrospray ionisation
F	Flow rate
FAO	Food and Agriculture Organization
G	Units of Gravitational Force
h	Hour(s)
H	Theoretical plate height
HMBC	Heteronuclear multiple bond correlation (NMR)
HMQC	Heteronuclear multiple quantum coherence (NMR)
HPLC	High performance liquid chromatography
IAEA	International Atomic Energy Agency
IFAH	International Federation of Animal Health

ISM	Isometamidium
<i>k</i>	Solute retention factor
<i>k</i> *	Relative retention factor in gradient analysis
L	Column length
l	Litre(s)
LOD	Limit of detection
LOQ	Limit of quantification
<i>m/z</i>	Mass-to-charge ratio
mAU	Milli absorbance units
Max	Maximum
MeCN	Acetonitrile
MeOH	Methanol
mg	Milligram(s)
min	Minute(s)
Min	Minimum
ml	Millilitres(s)
mM	Millimolar
mm	Millimetre(s)
MS	Mass spectrometry
MSD	Mass spectrometric detector
µg	Microgram(s)
µm	Micrometre(s)
N	Number of theoretical plates (Efficiency)
n	Number of experiments carried out
NADP	Nicotinamide Adenine Dinucleotide Phosphate
ng	Nanogram(s)
NMR	Nuclear magnetic resonance spectroscopy
PAAT	Program against African Trypanosomiasis
PCA	Principal component analysis
pKa	Logarithmic measure of the acid dissociation constant

psi	pound-force per square inch, unit of pressure
PW	Peak width
QA	Quality assurance
QC	Quality control
R <sup>2</sup>	Regression coefficient
RIA	Radioimmunoassay
RNA	Ribonucleic acid
ROESY	Rotating frame Overhauser effect (ROE) spectroscopy
RP-HPLC	Reversed phase high performance liquid chromatography
rpm	Revolutions per minute
Rs	Resolution
RSD	Relative standard deviation
RSM	Reference standard mixture
S/N	Signal-to-noise ratio
sec	Second(s)
SPC	Spectra
T	Temperature
TOCSY	Total correlation spectroscopy
t <sub>0</sub>	Dead time
t <sub>G</sub>	Gradient time
t <sub>R</sub>	Retention time
UV	Ultraviolet light
V	Volt
v/v	Volume per volume
V <sub>m</sub>	Dead volume
vs.	Versus
VSG	Variable surface glycoprotein
W <sub>1/2</sub>	Width at half peak height
W <sub>B</sub>	Width at peak base
WHO	World Health Organization

<b>List of Figures</b>	<b>Page No.</b>
Figure 1.1: Reported cases of sleeping sickness and between 1939–2004	2
Figure 1.2: Distribution of tsetse infestation and cattle breeding areas on the African continent	3
Figure 1.3: Abbreviated classification of the family trypanosomatidae	5
Figure 1.4: Generalized life cycle of a fly-transmitted trypanosome	6
Figure 1.5: Chemical structures of trypanocides for chemotherapy of human trypanosomiasis	9
Figure 1.6: Chemical structures of the most commonly used trypanocides for chemotherapy and chemoprophylaxis of African trypanosomiasis in cattle	10
Figure 1.7: Chemical structures of the red and purple isomers present in metamidium	14
Figure 2.1: Chemical structures of phenanthridine compounds with trypanocidal activity	19
Figure 2.2: Reaction scheme of the synthesis of ISM from homidium by electrophilic substitution	21
Figure 2.3: Proposed chemical structures of ISM and related substances	22
Figure 2.4: Representative HPLC-UV chromatograms of the separation of the major components of ISM formulations	30
Figure 2.5: Plots of peak area vs. concentration of for ISM and related substances	31
Figure 2.6: Representative HPLC-MS total ion count chromatogram of the separation of the major components of ISM formulations	34
Figure 2.7: (a) Mass spectrum of M&B4596 and (b) Mass spectrum of homidium	34
Figure 2.8: Front and rear images of sachets of a genuine and counterfeit version of Samorin® product and chromatograms of HPLC analysis of the contents	38
Figure 3.1: Proposed pathways for the metabolism of ISM	47
Figure 3.2: Representative total ion count chromatogram obtained from HPLC-MS analysis of M&B4180A and related substances	59
Figure 3.3: Mass spectra obtained from HPLC MS analysis of M&B4180A and related substances	60
Figure 3.4: Chemical structure of a possible internal standard, dimidium	61

Figure 3.5:	a) Total ion chromatogram obtained from HPLC-MS analysis of M&B4180A and related substances with added dimidium bromide as internal standard and mass spectrum of dimidium bromide	61
Figure 3.6:	Total ion chromatogram obtained from HPLC-MS analysis of M&B4180A and related substances and selected ion chromatograms obtained for the ions with $m/z = 230$ and $m/z = 300$	62
Figure 3.7:	Selected ion chromatograms from ISM sample after SPE extraction from bovine plasma	64
Figure 3.8:	Effect of the blockage of adsorptive sites on the adsorption of ISM on glassware	66
Figure 3.9:	Metabolic scheme of flurazepam in rat liver microsomes	67
Figure 3.10:	HPLC-MS selected ion mass chromatograms obtained from analysis of incubation of flurazepam with rat liver microsomes	68
Figure 3.11:	Representative HPLC-MS selected ion mass chromatograms obtained from analysis of incubation of ISM	69
Figure 3.12:	Plots of peak area vs. concentration for ISM and related substances	70
Figure 3.13:	HPLC-MS selected ion mass chromatograms of ISM and homidium at a concentration of 5 ng/ml	71
Figure 3.14:	HPLC-MS selected ion mass chromatograms of ISM and homidium at a concentration of 20 ng/ml and M&B4250 and M&B38897 at a concentration of 5 ng/ml	72
Figure 4.1:	Relative impact of retention, selectivity and efficiency on resolution	78
Figure 4.2:	Graphical demonstration of selectivity	80
Figure 4.3:	Chromatograms of 15 min and 45 min gradients on ACE 5 C8 HPLC column, with mobile phase consisting of 15 mM ammonium formate and acetonitrile	100
Figure 4.4:	Chromatograms of 15 min and 45 min gradients on ACE 5 C8 HPLC column, with mobile phase consisting of 15 mM ammonium formate and methanol	101
Figure 4.5:	Chromatograms of 15 min and 45 min gradients on ACE 5 C8 HPLC column with mobile phase consisting of 0.1 %v/v formic acid and acetonitrile	103
Figure 4.6:	Chromatograms of 20 min gradient on Phenomenex, Gemini 5u C18, ACE 5 C18 and ACE 5 C18-HL, with mobile phase consisting of 0.1 %v/v formic acid and acetonitrile	105

Figure 4.7:	Chromatograms of 20 min gradient on ACE 5 C8 and ACE 5 C4, with mobile phase consisting of 0.1 %v/v formic acid and acetonitrile	106
Figure 4.8:	Chromatograms of 20 min gradient on ACE 5 Phenyl and ACE 5 CN, with mobile phase consisting of 0.1 %v/v formic acid and acetonitrile	107
Figure 4.9:	Chromatograms of 20 min gradient on ACE 5 AQ and ACE 5 C18-AR with mobile phase consisting of 0.1 %v/v formic acid and acetonitrile	108
Figure 4.10:	Plot of log k versus % organic solvent	111
Figure 4.11:	Chromatograms of 15 min and 45 min gradients on ACE 5 SIL, with mobile phase consisting of 15 mM ammonium formate buffer and acetonitrile	112
Figure 4.12:	Chromatograms of 20 min gradient as predicted by DryLab <sup>®</sup> and obtained from an experiment run on ACE 5 C8, with mobile phase consisting of 15 mM ammonium formate buffer and acetonitrile	114
Figure 4.13:	DryLab <sup>®</sup> generated two dimensional resolution map	115
Figure 4.14:	Chromatograms of 21 min gradient as predicted by DryLab <sup>®</sup> and obtained from experiment run on ACE 5 C8, with mobile phase consisting of 15 mM ammonium formate buffer and acetonitrile	116
Figure 4.15:	DryLab <sup>®</sup> generated one dimensional resolution map	118
Figure 4.16:	Chromatograms of isocratic separation of ISM and related substances as predicted by DryLab <sup>®</sup> and obtained from an experiment run on ACE 5 C8	118
Figure 4.17:	Chromatograms obtained with isocratic conditions on Gemini 5u C18 and 4 min gradient on ACE 5 C8, with mobile phase consisting of 15 mM ammonium formate and acetonitrile	119
Figure 5.1:	Theoretical separation as a function of sample weight	128
Figure 5.2:	Proposed chemical structures of ISM and related substances	129
Figure 5.3:	Participation of the 3-amino group in a resonance configuration with the quaternary nitrogen	130
Figure 5.4:	Provisionally assigned chemical structures for isomers contained in metamidium	131
Figure 5.5:	Proposed chemical structure of the purple isomer present in metamidium	132

Figure 5.6:	DryLab® generated resolution map, predicting isocratic conditions for optimum resolution of the compounds of interest	138
Figure 5.7:	DryLab® prediction and experimental data of an isocratic separation of ISM and related compounds	139
Figure 5.8:	Representative chromatogram of the isocratic, semi-preparative separation of ISM and related compounds and picture of Fractions I – V obtained from a 1 %w/v solution of a mixed reference standard of ISM and related compounds	140
Figure 5.9:	Representative HPLC-MS selected ion mass chromatograms of ions m/z 230.5 and m/z 314 obtained for fractions III, IV and V	142
Figure 5.10:	Mass spectra of fractions I and II	143
Figure 5.11:	UV absorption spectrum of homidium	144
Figure 5.12:	UV absorption spectra of M&B4250, M&B38897 and M&B4180A	145
Figure 5.13:	UV absorption spectra of pure samples of the isolated unknown ISM process related compound and M&B4596	146
Figure 5.14:	400 MHz <sup>1</sup> H-NMR spectrum of homidium in DMSO-d <sub>6</sub>	147
Figure 5.15:	Chemical structure of homidium with coloured bonds correlating to <sup>1</sup> H- <sup>1</sup> H TOCSY NMR correlations	147
Figure 5.16:	400 MHz <sup>1</sup> H- <sup>1</sup> H TOCSY spectrum of homidium in DMSO-d <sub>6</sub>	148
Figure 5.17:	400 MHz <sup>1</sup> H- <sup>13</sup> C HMBC spectrum of homidium in DMSO-d <sub>6</sub> with chemical structure of homidium	148
Figure 5.18:	400 MHz <sup>1</sup> H-NMR spectrum of ISM in DMSO-d <sub>6</sub>	150
Figure 5.19:	New proposed structure of ISM based on NMR data with coloured bonds corresponding to TOCSY correlations	151
Figure 5.20:	400 MHz <sup>1</sup> H- <sup>1</sup> H TOCSY spectrum of ISM in DMSO-d <sub>6</sub>	151
Figure 5.21:	New proposed chemical structure of ISM with coloured arrows corresponding to <sup>1</sup> H- <sup>13</sup> C correlations	152
Figure 5.22:	400 MHz <sup>1</sup> H- <sup>13</sup> C HMBC spectrum of ISM in DMSO-d <sub>6</sub>	152
Figure 5.23:	400 MHz <sup>1</sup> H- <sup>1</sup> H ROESY spectra of ISM in DMSO-d <sub>6</sub> and new proposed chemical structure of ISM with coloured arrows corresponding to <sup>1</sup> H- <sup>1</sup> H correlations	154
Figure 5.24:	400 MHz <sup>1</sup> H-NMR spectrum of M&B4250 in DMSO-d <sub>6</sub>	156
Figure 5.25:	New proposed structure of M&B4250 based on obtained NMR data with coloured bonds corresponding to TOCSY correlations	157
Figure 5.26:	400 MHz <sup>1</sup> H- <sup>1</sup> H TOCSY spectrum of M&B4250 in DMSO-d <sub>6</sub>	157



Figure 5.27:	New proposed chemical structure of ISM with coloured arrows corresponding to $^1\text{H}$ - $^{13}\text{C}$ correlations	158
Figure 5.28:	400 MHz $^1\text{H}$ - $^{13}\text{C}$ HMBC spectrum of M&B4250 in DMSO- $d_6$	158
Figure 5.29:	400 MHz $^1\text{H}$ - $^1\text{H}$ ROESY spectra of M&B4250 in DMSO- $d_6$ and new proposed chemical structure of M&B4250	160
Figure 5.30:	High resolution mass spectra of pure samples of ISM and M&B4596	162
Figure 5.31:	New proposed structure of ISM with an exact mass of 461.2328 g/mol and a protonated mass ion at $m/z = 460.2244$	164
Figure 5.32:	New proposed structure of M&B4250 as supported by NMR and high resolution MS data	164
Figure 5.33:	New proposed structure of M&B38897 and M&B4596 as supported by NMR and high resolution MS data	165
Figure 6.1:	Chromatograms obtained with isocratic conditions on Gemini 5u C18 and optimised 4 min gradient on ACE 5 C8	173
Figure 6.2:	Previously reported and new proposed structures of M&B4180A (ISM) and M&B4250	175
Figure A1:	400 MHz $^1\text{H}$ - $^{13}\text{C}$ HMQC spectrum of homidium in DMSO- $d_6$	191
Figure A2:	400 MHz $^1\text{H}$ - $^{13}\text{C}$ HMQC spectrum of ISM in DMSO- $d_6$	192
Figure A3:	400 MHz $^1\text{H}$ - $^{13}\text{C}$ HMQC spectrum of M&B4250 in DMSO- $d_6$	193

<b>List of Tables</b>	<b>Page No.</b>
Table 1.1: Trypanocides used in animal African trypanosomiasis	10
Table 2.1: Regression analysis of calibration curves obtained from the analysis of M&B4180A (ISM) and related substances	31
Table 2.2: Sensitivity of HPLC assay	32
Table 2.3: Repeatability of HPLC method	32
Table 2.4: MS data from analysis of ISM and related substances	33
Table 2.5: Precision of HPLC analysis of ISM and related substances in a commercial sample	35
Table 2.6: Results of HPLC analyses of various commercial ISM products	37
Table 3.1: Volumes used for the microsomal incubation of ISM and flurazepam with rat liver microsomes	53
Table 3.2: Comparison of recovery of ISM and related substances from plasma using four different SPE cartridges	65
Table 3.3: Regression analysis of calibration curves generated from the analysis of M&B4180A (ISM) and related substances in spiked plasma	70
Table 3.4: Sensitivity of HPLC-MS assay	72
Table 3.5: Precision of the bioanalytical method for the determination of ISM and related substances in spiked plasma samples	73
Table 4.1: Potential sources of error in computer simulation	91
Table 4.2: Gradients used for initial DryLab <sup>®</sup> input	98
Table 4.3: Optimised gradients for separation on ACE 5 C8	98
Table 4.4: Column characterisation parameters	104
Table 4.5: Comparison of column performance	109
Table 4.6: Comparison of actual and DryLab <sup>®</sup> predicted chromatographic data	114
Table 4.7: Retention times of ISM and related substances over one week	117
Table 5.1: HPLC-MS data of stability testing of the fractions collected from semi-preparative separation of ISM and related compounds	141
Table 5.2: <sup>1</sup> H-NMR and <sup>13</sup> C-NMR data of homidium in DMSO-d <sub>6</sub> at 400 MHz	149
Table 5.3: <sup>1</sup> H-NMR and <sup>13</sup> C-NMR data of ISM in DMSO-d <sub>6</sub> at 400 MHz	155
Table 5.4: <sup>1</sup> H-NMR and <sup>13</sup> C-NMR data of M&B4250 in DMSO-d <sub>6</sub> at 400 MHz	161

<b>List of Equations</b>	<b>Page No.</b>
Equation 1: Resolution Equation	78
Equation 2: Calculation of Selectivity	79
Equation 3: Calculation of Retention Factor	80
Equation 4: Calculation of Column Dead-Volume Time	80
Equation 5: Calculation of Column Dead-Volume	80
Equation 6: Van't Hoff Equation	81
Equation 7: Calculation of Plate Number	85
Equation 8: Van Deemter Equation	86
Equation 9: Calculation of Average Retention Factor	88
Equation 10: Relationship between retention and % organic solvent	89
Equation 11: Prediction of retention time in DryLab®	90
Equation 12: Prediction of band width in DryLab®	90
Equation 13: Equilibration of a column between gradient runs	120
Equation 14: Adjusting flow rate to changes in column dimensions	139

# 1. Introduction

## 1.1. African Trypanosomiasis

African trypanosomiasis is a vector transmitted parasitic disease that, if left untreated, is fatal to humans and animals. Infection is caused by protozoan blood parasites of the genus *Trypanosoma*, transmitted to mammalian hosts by a bite of the tsetse fly.

First written records on trypanosomiasis from Africa date back as far as the 12<sup>th</sup> century, when the Arabian geographer Abu Abdallah Yaqut (1179 – 1229) referred to “an underground village whose inhabitants and even their dogs were just skin and bones and asleep” (Steverding, 2008; Winkle, 2005). Throughout the 19<sup>th</sup> century detailed medical reports, describing swollen lymph glands as an early sign of infection (early stage disease), and also neurological symptoms, lethargy and coma of the late stage disease were published and “sleeping sickness” became a well-recognised illness (Cox, 2004). In 1852, the Scottish missionary and explorer David Livingston (1813 – 1875) was the first to identify the tsetse fly as the carrier of the disease called Nagana (from Zulu: N’gana = “useless / powerless”) in cattle. Subsequently in 1895, the Scottish pathologist and microbiologist David Bruce (1855 – 1931) identified trypanosomes as the causative agent. In following years he also provided coherent evidence on the transmission of the disease by the tsetse fly and described the life cycle of the parasites (Cox, 2004; Steverding, 2008).

During the 20<sup>th</sup> century, and up to the present day there were three incidences of severe sleeping sickness epidemics in Africa (WHO, 2006). From 1896 to 1906 an estimated number of 800,000 people died from the infection in the Congo, Uganda and Kenya alone (de Raadt, 2005; Hide, 1999). This disastrous epidemic gave rise to development of the first chemotherapeutic agents for the treatment of early- and late-stage disease,

which also helped to combat the second major trypanosomiasis epidemic in the 1920s to 1940s. Mobile teams were introduced, systematically monitoring and treating the population in threatened areas. In combination with vector and host reservoir control, these measures led to a substantial decline in the incidence of the disease (de Raadt, 2005; Vickerman, 1997). Continued research and the introduction of further medication not only for human but also for African animal trypanosomiasis, as well as use of insecticides for vector control and systematic case detection led to further reduction of the prevalence of sleeping sickness by the early 1960s (Figure 1.1) (Steverding, 2008).

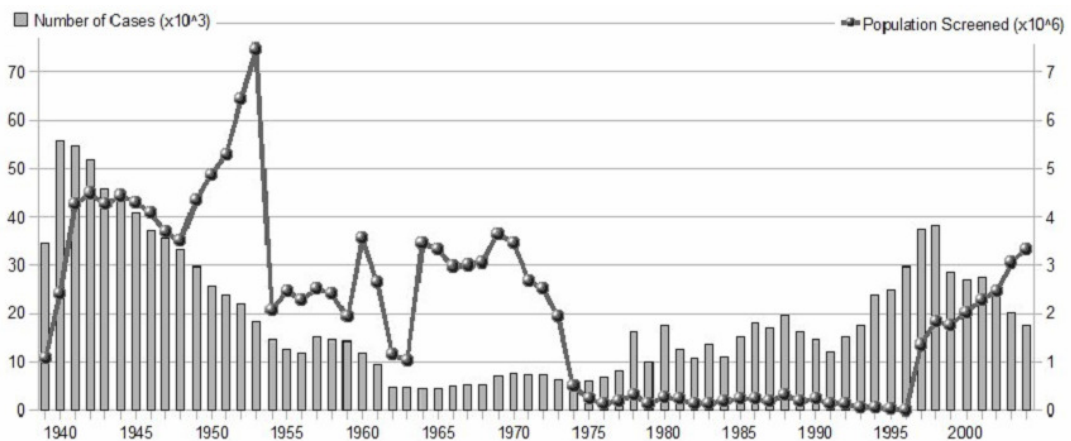


Figure 1.1: Reported cases of sleeping sickness between 1939 and 2004.

Grey columns, number of reported cases; black circles, population screened as adapted from Steverding, 2008

As the histogram (figure 1.1) shows, the third and latest sleeping sickness epidemic is currently in decline. With decolonialisation, political instability and the economic ruin of many African countries in the mid 1960s, health care and trypanosomiasis control were neglected with the result of a steady re-emergence of the disease in the 1970s. When prevalence levels had reached dramatically high levels yet again in 1999, the World Health Organization (WHO) negotiated with some leading pharmaceutical

companies and arranged for the supply of trypanocides for endemic countries free of cost. From 1997 monitoring and control of the disease were reinstated with major initiatives for vector eradication and surveillance of the population at risk, which resulted in a constant decrease in the risk of infection (Steverding, 2008). However, even careful control in all areas will only help to significantly reduce the occurrence of the hazardous illness. Complete eradication of sleeping sickness in tsetse infested areas is very unlikely. As recent developments show, disregard of the control regime inevitably leads to re-emergence of the disease with alarming proportions.

The habitats of the tsetse fly are spread over 36 countries of sub-Saharan Africa, infesting about 10 million km<sup>2</sup> of land in the area extending 10 degrees above and below the equator. Over 60 million people who live in this so called tsetse fly “belt” are at risk of being infected (WHO, 2006), and the threat of infection with animal African trypanosomiasis severely restricts stock farming in the most endemic areas (figure 1.2).

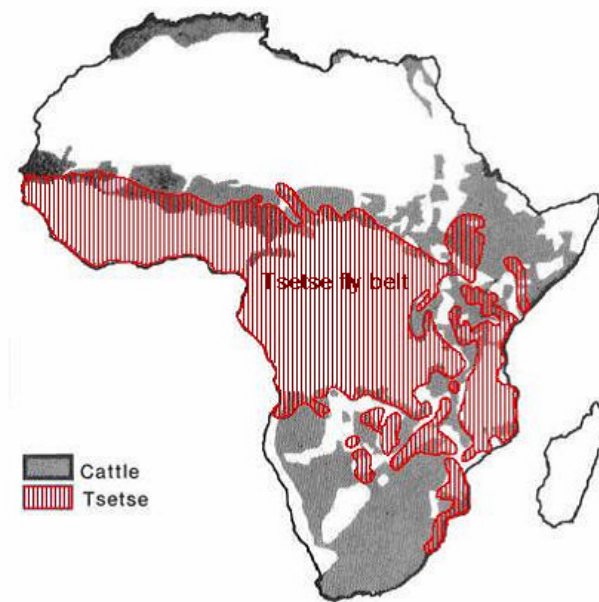


Figure 1.2: Distribution of tsetse infestation and cattle breeding areas on the African continent as adapted from Dalan *et al.*, 1989

This potentially fatal disease not only has an impact on the health care system in many prime areas of Africa, but also on agricultural economies and the nutrition of millions of people living there. As animal husbandry is the source of dairy and meat products and Africa's economic growth largely depends on its agriculture, the widespread infection of cattle, sheep, goats, pigs, horses and other species of domestic and wild animals is a major issue in the African food supply problem (Swallow, 1999). Animal trypanosomiasis, also called Nagana in cattle puts an estimated 50 million head of cattle at risk of infection (Steverding, 2008). The disease causes a loss in live animal gains, lower milk yield and reduced work efficiency of oxen used for cultivation of the land. Also there is requirement for frequent treatment with trypanocidal drugs of animals kept in areas of moderate risk. As a result the disease causes economic losses as great as US\$ 4.5 billion per annum (Budd, 1999; Gilbert *et al.*, 2001; Swallow, 1999).

### **1.1.1. The Parasite**

The organism causing African trypanosomiasis is a single-celled, eukaryotic protozoan parasite, belonging to the order of the *Kinetoplastida*, suborder *Trypanosomatina*, family *Trypanosomatidae* from the phylum *Sarcomastigophora* (Bush *et al.*, 2001). The genus *Trypanosoma* is divided into two sections, *Stercoraria* and *Salivaria* (figure 1.3) depending on the way of transmission. *Trypanosoma cruzi*, causative agent of American trypanosomiasis, or Chagas disease, widespread in Central- and South America, is an important representative of the *Stercoraria* group. It is also transmitted by an insect vector, the blood-sucking assassin bug, however not through bite, but via contamination with parasite infected feces. All trypanosomes widespread in

the African continent are *salivarian* trypanosomes with infection of the mammalian host as the result of an insect bite.

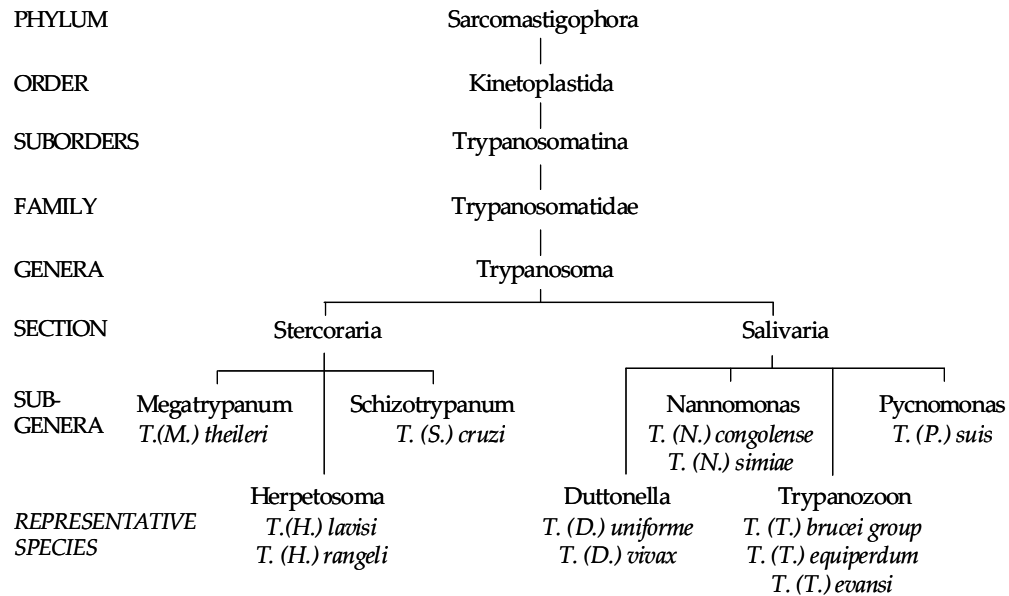


Figure 1.3: Abbreviated classification of the family trypanosomatidae (Bush *et al.*, 2001)

*Trypanosoma brucei* is further differentiated into three morphologically identical subspecies: *T. b. brucei*, *T. b. rhodesiense* and *T. b. gambiense* (El-Sayed *et al.*, 2000). Only *T. b. rhodesiense* and *gambiense* infect humans, causing acute infection in Eastern Africa and a chronic disease in the West African countries, respectively. *T. brucei brucei*, as well as *T. vivax* and *T. congolense* affect cattle, sheep, goats and pigs; *T. simiae* affects pigs while *T. evansi* is hazardous only in camels. Trypanosomes present in the blood of the mammalian host induce anemia, tissue lesions and immunosuppression. The host reacts with fever, weakness, lethargy, weight loss and ultimately death (Maré, 1998). Wild hosts, mainly game animals are immune to the parasite and act as reservoirs of trypanosomes, rendering their eradication by treating domestic hosts and people impossible (Williams *et al.*, 1993).



Trypanosomiasis is spread via the bite of infected bloodfeeding tsetse flies (Genus: *Glossina*, Family: *Glossinidae*). While taking a bloodmeal on an infected host, the insect picks up the bloodstream trypomastigotes, which transform into procyclic trypomastigotes in the fly's midgut (Figure 1.4).

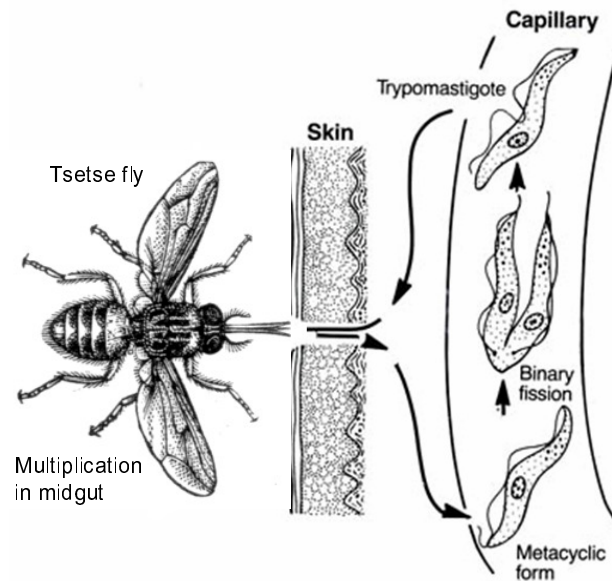


Figure 1.4: Generalized life cycle of a fly-transmitted trypanosome that reproduces by binary fission in the host as adapted from Gardiner *et al.*, 1988

After proliferation, the parasites leave the midgut and transform into epimastigotes, migrate in the intestinal mucosa to the fly's salivary glands and continue multiplication. With the next blood meal the resulting non-dividing metacyclic organisms in the fly's saliva are injected into the mammalian host's skin tissue. The metacyclic trypomastigotes enter a macrophage, transform into amastigotes and proliferate by binary fission. When the host cell bursts eventually the parasite is freed into the bloodstream where it can enter another macrophage and is carried to other sites throughout the body, reaching other blood fluids (e.g. lymph, spinal fluid) and continuing proliferation. At the injection site initial replication of trypanosomes proceeds, causing a sore swelling. Subsequently the parasites

continuously replicate while spreading to blood and lymph nodes. After initially residing in the bloodstream, lymphatic system and interstitial spaces, trypanosomes eventually enter the central nervous system inducing the latter stages of the infection (Bush *et al.*, 2001; El-Sayed *et al.*, 2000).

Once infected, the host immune system develops antibodies to the glycoprotein coat on the trypanosome surface which enables elimination of some of the parasites from the system. However, this so called Variable Surface Glycoprotein (VSG) enables a number of trypanosomes to evade the immune defences by switching to another variant of the surface protein, which is not recognised by the antibodies which were specifically developed for one VSG coat. The residual pathogens proliferate, causing a next wave of infection (Barrett *et al.*, 2003). The persistent infection results in an ongoing cycle of parasite replication, antibody production, development of immune complexes and a changing of the VSG coat. This antigenic variation explains the disease pattern of an intermittent parasitaemia with a long, partially asymptomatic incubation period, with fluctuant fever, disease chronicity, and failure to develop an effective immune defence. It also renders development of an efficient vaccine impossible (Barrett *et al.*, 2003).

Treatment for the early stage disease is usually highly effective. In this haemolymphatic phase, when parasites are still restricted to the blood and lymph system, drug administration is easier and the medicaments in use are less toxic to the host than those used for the late stage disease. Once the pathogen reaches the cerebrospinal fluid in the second or late stage of the disease, known as the neurological phase, therapy depends on compounds that can cross the blood-brain barrier. Those substances are more difficult to introduce and are highly toxic to the mammalian host, causing serious adverse effects, sometimes death. Hence, an important tool for treatment

with good prospect of cure is an early diagnosis of the infection (Steverding, 2008; WHO, 2006).

African trypanosomiasis is diagnosed by microscopic examination of stained lymph node or blood smears, or a more sensitive antigen-detecting enzyme linked immunosorbent assay (ELISA). Species-specific DNA probe technology even allows the identification of coexistent infections with several pathogenic species, which can not be distinguished by the conventional techniques. However, the high costs of this approach limits its utilisation in the endemic countries (Clair, 1988).

### **1.1.2. Control Strategies**

There are three basic strategies to manage the spread of African trypanosomiasis in areas of risk: vector control, chemotherapy and in case of African animal trypanosomiasis the breeding of trypanotolerant species. Vector control involves reducing the fly density by means of bush clearing, ground and aerial spraying with insecticides and use of flytraps. This has been useful in areas where the procedures were applied consistently by the communities. However, it is a rather expensive approach considering its limited success (Bhalla, 2002; Budd, 1999).

Another means of combating the spreading of African animal trypanosomiasis is the breeding of certain autochthonal animal species that tolerate infection with trypanosomes while maintaining productivity. These trypanotolerant African cattle have coexisted with the tsetse fly in the area for over 5,000 years and during this time have developed the tolerance trait (Maré, 1998). With increasing risk of Nagana, however, trypanotolerant animals will also be affected (Trail *et al.*, 1994). By far the most important strategy for trypanosomiasis control is the use of chemotherapeutic drugs.

Treatment of human trypanosomiasis relies entirely on the use of only four approved drug substances, as shown in figure 1.5.

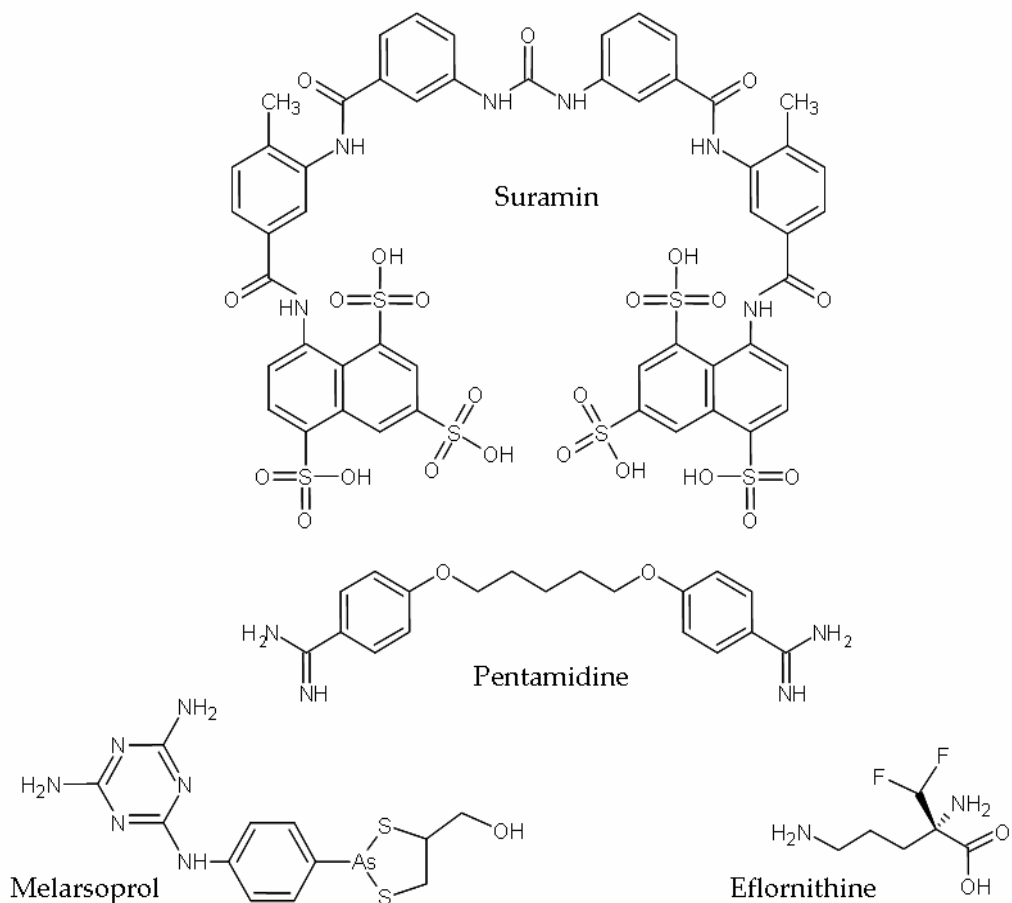


Figure 1.5: Chemical structures of trypanocides for chemotherapy of human trypanosomiasis

Suramin (1922) and pentamidine (1940) were introduced over 60 years ago and still are the medication of choice to cure early stage sleeping sickness. The second stage of the disease is commonly treated with the highly toxic arsenical drug melarsoprol (1950) and the more tolerable, but highly expensive drug eflornithine (1990). Both drugs can enter the central nervous system, a premise for curing the late stage disease (Croft *et al.*, 2005; WHO, 2006).

Chemotherapy of African trypanosomiasis in cattle essentially relies on the salts of only three compounds: diminazene, an aromatic diamidine, homidium, a phenanthridine and isometamidium (ISM), a phenanthridine-aromatic amidine (table 1.1, figure 1.6) (Anene *et al.*, 2001).

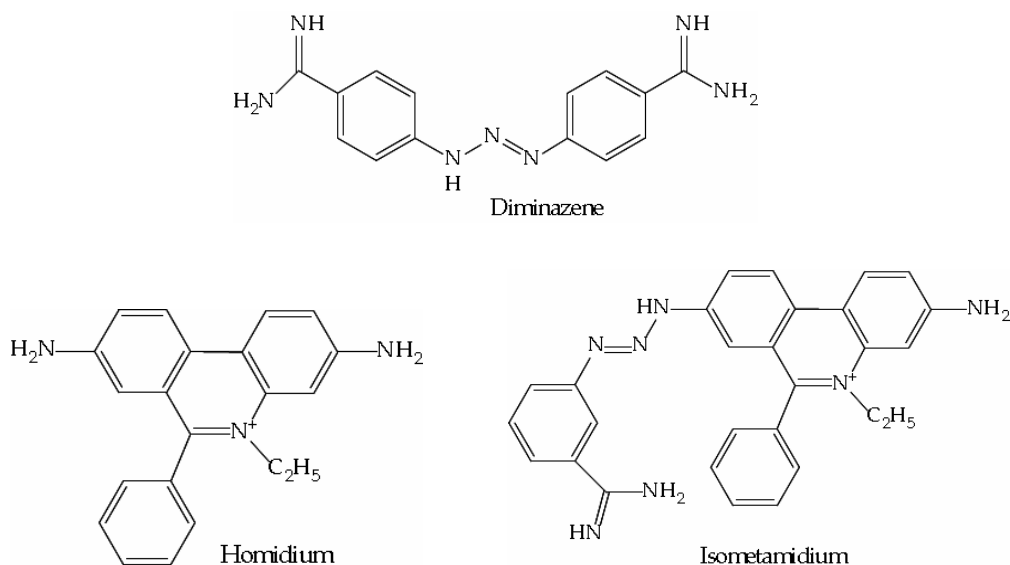


Figure 1.6: Chemical structures of the most commonly used trypanocides for chemotherapy and chemoprophylaxis of African trypanosomiasis in cattle

Table 1.1: Trypanocides used in animal African trypanosomiasis

Active ingredient	Salt	Trade Name	Dosage (mg/kg i.m.)	Effective against
Isometamidium	- chloride	Samorin®	0.25-1.0	T. congolense
		Trypamidium®	(Therapy) 0.25-1.0 (Prophylaxis)	T.b. brucei T. vivax
Homidium	- chloride	Novidium®	1.0 (Therapy)	T. congolense
	- bromide	Ethidium®		T. vivax
Diminazene	- aceturate	Berenil®	3.5 (Therapy)	T. congolense
		Veriben®		T. vivax
		Ganaseg®	7.0 (T. b. brucei)	T. b. brucei

While the salts of diminazene and homidium are used as chemotherapeutic agents only, ISM is marketed as both, a prophylactic and a therapeutic agent (table 1.1). It has been in use for almost 50 years and is still effective for prophylaxis against all three African animal trypanosomes providing protection for 3 - 6 months (Eisler *et al.*, 1996b; Olila *et al.*, 2002; Sinyangwe *et al.*, 2004).

### **1.1.3. The Problem of Drug Resistance**

Drug resistance is generally defined as the heritable ability of a pathogen to withstand a therapeutic drug to which it has previously been sensitive. The use of veterinary trypanocides for the management of African animal trypanosomiasis in sub-Saharan Africa has been effective and generally affordable for a long period of time (Anene *et al.*, 2001). However, the number of reported cases of chemoresistance to each of the commonly used trypanocides is increasing (Matovu *et al.*, 2001). Diminazene and isometamidium have been regarded as the best therapeutic and prophylactic trypanocides respectively in veterinary use for over half a century. The former was considered the only drug to which trypanosomes do not readily develop resistance, due to its rapid elimination from the body (Anene *et al.*, 2001; Matovu *et al.*, 2001). Unfortunately, diminazene resistant trypanosomes, isometamidium treatment failures and shortened prophylactic intervals as a result of infections with drug resistant trypanosome species have been reported from over 13 African countries (Geerts & Holmes, 1998; Geerts *et al.*, 2001). The biochemical basis of trypanosome resistance to these trypanocides has not been fully characterised. However, because anti-microbial agents interact with a drug target, it would follow that drug resistance can arise either as a consequence

of changes in drug concentration at the target site or alteration in the target, or both (Delespaux & de Koning, 2007). It has been demonstrated that sensitive trypanosome populations show a faster drug uptake into the cells than resistant trypanosome species, which also exhibit a rapid backflow of compound from the cell (Mäser *et al.*, 2003). On a genetic level three different routes leading to drug resistance are described, gene mutations, gene amplifications and gene transfer mechanisms. Whilst trypanosomes exhibit the ability of gene transfer when exposed to killing agents, it could not be determined whether this mechanism was responsible for the formation of drug resistance in trypanosomes (Sutherland & Holmes, 1993).

Despite these genetic aspects, which can not be directly influenced by consumers or manufacturers, there are also assessable factors which can cause the evolution of drug resistance. Inappropriate storage, incorrect application or defective preparations can lead to the loss of therapeutic effect of the active ingredient (Matovu *et al.*, 2001). Several reports also indicate the widespread phenomenon of counterfeit and poor quality trypanocides in sub-Saharan Africa (Eisler *et al.*, 1996b; Newton *et al.*, 2006).

#### **1.1.4. Counterfeiting**

A counterfeit medicine is one which is produced and sold with the intent to deceptively represent its origin, authenticity or effectiveness. It can contain the correct amount of active ingredient as stated, contain an insufficient quantity or not contain any active compound at all. It can also consist of entirely incorrect active or inactive ingredients which might also be harmful (Newton *et al.*, 2006). Counterfeits are typically sold with inaccurate, fake packaging. The production of counterfeit or substandard anti-infective drugs is a widespread and under-recognised problem that contributes to morbidity,

mortality and drug resistance and leads to spurious reporting of resistance and toxicity (Kapp, 2002). Additionally the use of poor quality trypanocides has severe implications for animal health and food safety, posing problems with unspecified, unwanted chemicals, their metabolites and residues in the food chain (Seiter *et al.*, 2005) .

Considering the high cost of new drug development and the comparatively small African market, the prospect of an advance in the development of new drugs for the treatment of African animal trypanosomiasis is small (Sones, 2001). Hence, maintenance of the effectiveness of available drug substances is of vital importance. Despite being in use for more than 50 years, up to the present day internationally agreed standards for trypanocides with documented specifications and pharmacopoeial monographs for veterinary trypanocides are either lacking or inaccurate (PAAT/FAO, 2008). Also lacking are references to recommend methods of analysis of drug residues in food. Furthermore, with the absence of elaborate veterinary drug registration procedures and post-marketing pharmacovigilance activities in most African countries the quality of products cannot be guaranteed (PAAT/FAO, 2008).

With the problem of counterfeiting and drug resistances on the rise a well defined quality control of those formulations in all stages of the production and treatment process is an immediate need. In 2003, the Animal Health Service of the Food and Agriculture Organization of the United Nations (FAO) and the International Federation for Animal Health (IFAH) developed a joint concept note on quality assurance and quality control (QA/QC) of trypanocides, with the main objective to pursue internationally and scientifically agreed standards and protocols for QA/QC of trypanocides. Just recently, these organisations have signed a “Memorandum of



Understanding” to address the widespread presence of counterfeit and poor quality ISM and diminazene based trypanocidal drugs on the open market in sub-Saharan Africa (WHO, 2009a). The FAO Animal Health Service, in partnership with the Joint FAO/IAEA (International Atomic Energy Agency) Division and the IFAH, emphasize the importance of the development of reference standards and protocols for quality control and quality assurance of trypanocidal drugs on the African market. Validated protocols for drug quality control should be provided to the relevant regulatory bodies in countries where these drugs are most used, and the developed technical analytical methods should be transferred to Africa-based laboratories (WHO, 2009a). Marketing of sub-standard or counterfeit drugs will be hindered by these procedures.

## 1.2. Analysis of Isometamidium

When isometamidium was first introduced in the late 1950s a mixture of isomers called metamidium was reported (Wragg *et al.*, 1958). The red (I) and purple (II) compound as shown in figure 1.7 were separated by paper electrophoresis and by fractional crystallizations from water and methanol respectively, due to their different solubilities (Wragg *et al.*, 1958).

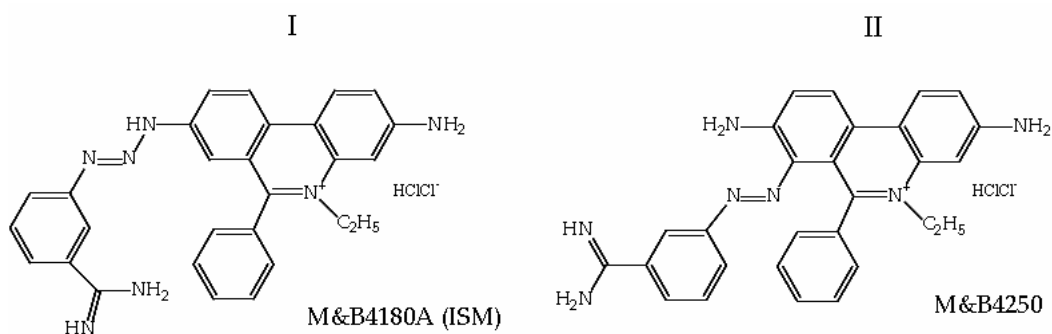


Figure 1.7: Chemical structures of the red (I) and the purple (II) isomer present in metamidium

Early attempts at structure elucidation relied solely on a diagnostic test for the presence of a diazoamino group in the molecule and the interpretation of infrared spectra (Berg *et al.*, 1961; Wragg *et al.*, 1958). When the red isomer (M&B4180A) was identified as a more active curative and prophylactic agent against trypanosome infection, than the purple isomer (M&B4250), it was introduced on the market as isometamidium (ISM). Formulations, such as Samorin<sup>®</sup>, however still contain a mixture of related compounds.

Clarke (1969) describes a system for paper chromatography of an ISM preparation (Samorin<sup>®</sup>) that separates a dark yellow, an orange and a blue compound, indicating that there are even more than these two positional isomers present. Also the ultraviolet absorption spectrum reported for ISM, is one of the mixture, rather than the pure compound (Clarke, 1969). Early pharmacokinetic studies were performed using non-specific spectrophotometric methods (Ali & Hassan, 1984; Braide & Eghianruwa, 1980; Philips *et al.*, 1967). Since the advance of high performance liquid chromatography (HPLC) in pharmaceutical analysis HPLC methods for the determination of ISM have been published (Kinabo & Bogan, 1988c; Perschke & Vollner, 1985; Tettey *et al.*, 1998). However, analysis of ISM containing products remains difficult due to the presence of its isomers, degradation products and other process related compounds, all of which are positively charged and bear at least one strongly basic amidino moiety, which makes separation by HPLC challenging. The choice of method also depends on the intended use of the acquired data. If the purpose is the quality control of commercially available products a HPLC-UV assay is appropriate, as it enables separation and selective quantification of all compounds of interest (Tettey *et al.*, 1998). For metabolic and bioavailability studies enzyme-linked immuno sorbent assay (ELISA) has so far been the method of choice (Eisler *et al.*, 1996a; Whitelaw

*et al.*, 1991), as this is capable of detecting sub-nanogram quantities of the drug in sera of treated cattle for several weeks after treatment (Eisler, 1996). However, an ELISA is not a selective detection method, as it is not able to distinguish between structurally related compounds like ISM and related substances. Alternatively a HPLC-MS assay could allow quantification as sensitive as the immuno assay, while offering the advantage of selectivity for ISM in the presence of all its isomers and related compounds.

### **1.2.1. Chromatographic Methods (HPLC)**

The presence of the quaternary nitrogen atom and strongly basic amidino moieties in ISM and related substances results in pronounced tailing of chromatographic peaks due to interaction with residual silanol groups in silica based chromatographic columns (Tettey *et al.*, 1998). The incorporation of mobile phase additives to improve peak shape results in reduction of column efficiency (Kinabo & Bogan, 1988c). Attempts at the indirect determination of ISM by converting it to homidium prior to analysis (Perschke & Vollner, 1985) did not allow the specific quantification of the drug of interest. Not only is homidium the main degradation product of ISM, it is also extensively used as a veterinary trypanocide and needs to be separated and quantified separately. In general previously reported methods are not specific with respect to ISM and its related substances. Quantification is achieved by detecting one peak which represents ISM and its isomers, which do not exhibit the intended pharmacological activity (Brown *et al.*, 1961). Therefore the obtained concentrations are falsely high with regard to active drug, and reported limits of detection and quantification are incorrect. The intrinsic fluorescence of ISM was successfully used for quantitative analysis (Perschke & Vollner, 1985; Zilberstein *et al.*, 1993). UV detection

however has been demonstrated to exhibit better sensitivity (Tetty *et al.*, 1998).

A simple, fast and inexpensive HPLC method for the separation and quantification of ISM in the presence of manufacturing and degradation impurities by RP-HPLC was reported by Tetty *et al.* in 1998. With a base-deactivated silica-based stationary phase and an acidic pH to suppress interactions with residual silanol groups acceptable peak shape for the compounds of interest was achieved. If this method was further improved in terms of selectivity and efficiency it could enable the absolute quantification of the four major components of ISM formulations and provide a powerful tool for the control of sub-standard and counterfeit products in international commerce. Furthermore with the elimination of mobile phase additives and use of volatile buffers it could be readily adapted for use with mass spectrometry for enhanced selectivity and sensitivity. Such a well defined, highly sensitive, quantitative assay for ISM could be used to determine concentrations of residual trypanocide in biological material from treated animals. Not only would that enable the quality control of meat products for human use, but also highly selective metabolic and bioavailability studies could be carried out to improve the understanding of the mechanisms of action of the drug. Since chemoresistance is prevalent and new trypanocides are lacking, these studies could limit the development of chemoresistance to existing trypanocides. Furthermore, this knowledge could optimise the use of existing drugs in the field, and the design of new trypanocides.

An existing HPLC method could also be developed into a preparative HPLC separation, with the goal of the isolation of pure standards of all analytes present in a common ISM formulation.

### 1.3. Aims and Objectives

The objectives of this study were:

1. The development and validation of an improved HPLC method for specific separation and quantitation of ISM and its related substances. The method should enable fast, reproducible assays for quality control of the manufacturing process and authenticity testing of commercial products.
2. The development and validation of an HPLC method with mass spectrometry detection for enhanced sensitivity which could be used to determine residual ISM and related substances in animal body fluids and tissues. This would also involve designing an appropriate extraction method for the selective and quantitative extraction of the compounds of interest from biological material.
3. The development of a selective bioanalytical method for both, the parent compound and its putative metabolites. Therefore the metabolic pathways of ISM and related substances are to be investigated.
4. The development and validation of a semi-preparative HPLC method for the isolation of pure ISM (M&B4180A) and related substances, namely M&B4596, M&B4250 and M&B38897. For the demonstration of selectivity and specificity of any analytical method pure reference standards of the compounds of interest are needed. Once isolated the single compounds were to be characterised using MS, UV- and NMR-spectroscopy and used for development of an analytical method based on a single isomer only.

## 2. Analytical Method for the Quality Control of ISM

### Formulations

#### 2.1. Introduction

The trypanocidal action of phenanthridine compounds was recognised in the late thirties when phenidium chloride (figure 2.1) was found to be active against trypanosomes (Browning *et al.*, 1938). As a result of the chemotherapeutic action of several phenanthridines these compounds were extensively investigated and in 1958 isometamidium (figure 2.1) was introduced on the market (Wragg *et al.*, 1958). It proved to be more active and less toxic than the precursor phenanthridines, dimidium and homidium (figure 2.1). It additionally possesses chemoprophylactic effects, unlike any of the other trypanocides in use (Brown *et al.*, 1961).

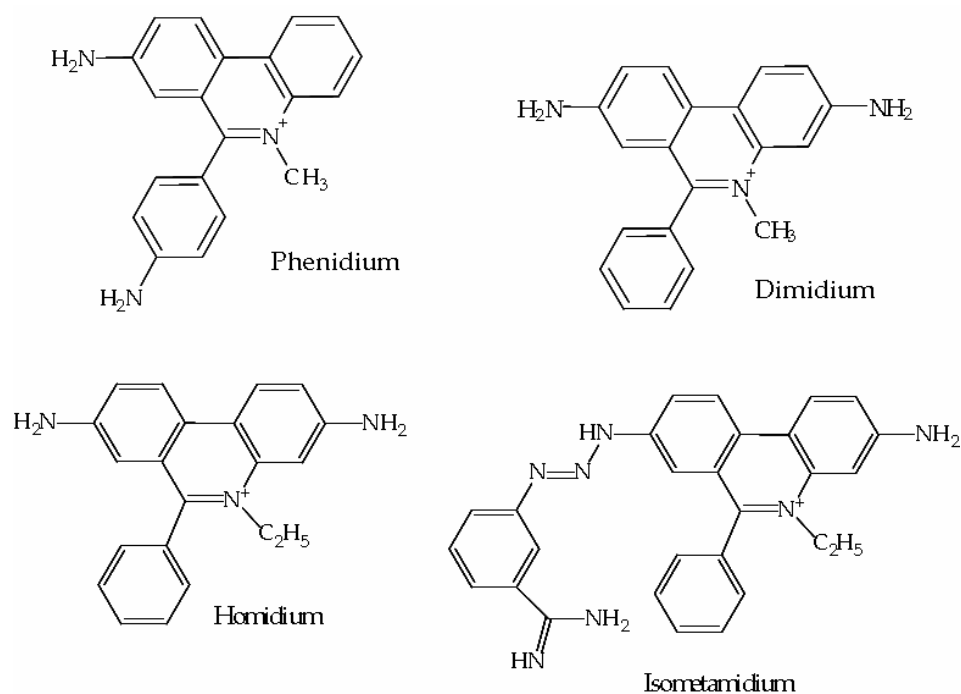


Figure 2.1: Chemical structures of phenanthridine compounds with trypanocidal activity

Until today the design of effective vaccines against trypanosomes is difficult due to their ability to vary their cell surface antigens (Barry, 1997), and with the high costs involved in any vector control technique the control of African animal trypanosomiasis still relies principally on chemotherapy and chemoprophylaxis (Anene *et al.*, 2001).

Considering the high cost involved in research and development of new trypanocides and the relatively small total African market (\$20 million per annum) (Sones, 2001), the likelihood that pharmaceutical companies will start investing more money into the development of new trypanocidal drugs is small. A fact, that renders maintenance of the effectiveness of available drug substances even more essential. With the current drug regime on the market for almost 50 years the problem of drug resistance is evolving. ISM treatment failures and shortened prophylactic intervals as a result of infections with drug resistant trypanosome species have been reported (Geerts *et al.*, 2001). Also incidences of counterfeit and poor quality drugs of isometamidium based trypanocides in sub-Saharan Africa have been described (Eisler *et al.*, 1996b) (see also sections 1.1.3 & 1.1.4).

### **2.1.1. Isometamidium**

The synthesis of isometamidium, [8-(3-*m*-amidinophenyl-2-triazeno)-3-amino-5-ethyl-6-phenylphenanthridiniumchloride hydrochloride (ISM; M&B4180)] as illustrated in figure 2.2, comprises the reaction of diazotised *m*-aminobenzamide monohydrochloride with 3, 8-diamino-5-ethyl-6-phenyl phenanthridinium chloride (homidium chloride). The diazoamino compound is formed by coupling of a diazonium salt with an aromatic primary amine. This electrophilic substitution reaction involves the diazonium ion and the non-ionised amine (Wragg *et al.*, 1958).

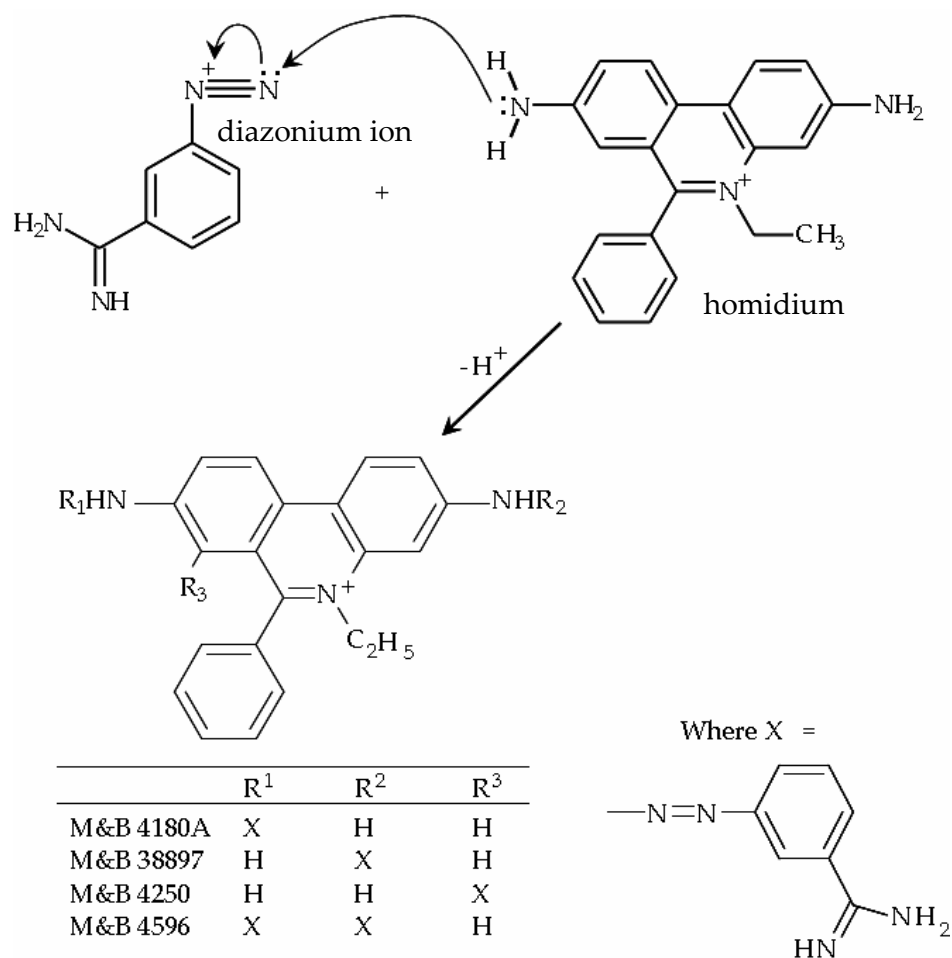


Figure 2.2: Reaction scheme of the synthesis of ISM from homidium by electrophilic substitution

The reactivity of the parent benzenediazonium ion is enhanced by the presence of the amidino substituent, which leads to an increase in the range of coupling reactions, resulting in the production of several by products, namely M&B38897, M&B4250 and M&B4596. The proposed full structures of M&B4180A and its related substances are shown in figure 2.3 (Tetty *et al.*, 1999).

The reaction conditions influence the nature and extent of the coupling and thus the relative ratios of the isomers. Commercial products, such as Samorin<sup>®</sup> or Trypamidium<sup>®</sup> contain a mixture of these five



compounds (Tettey *et al.*, 1998) but the pharmacological action has been ascribed principally to M&B4180A (Berg, 1960). Therefore therapeutic equivalence from batch to batch is dependent on the optimisation, robustness and reproducibility of the manufacturing process which is susceptible to significant variability (Berg *et al.*, 1961; Tettey *et al.*, 1999).

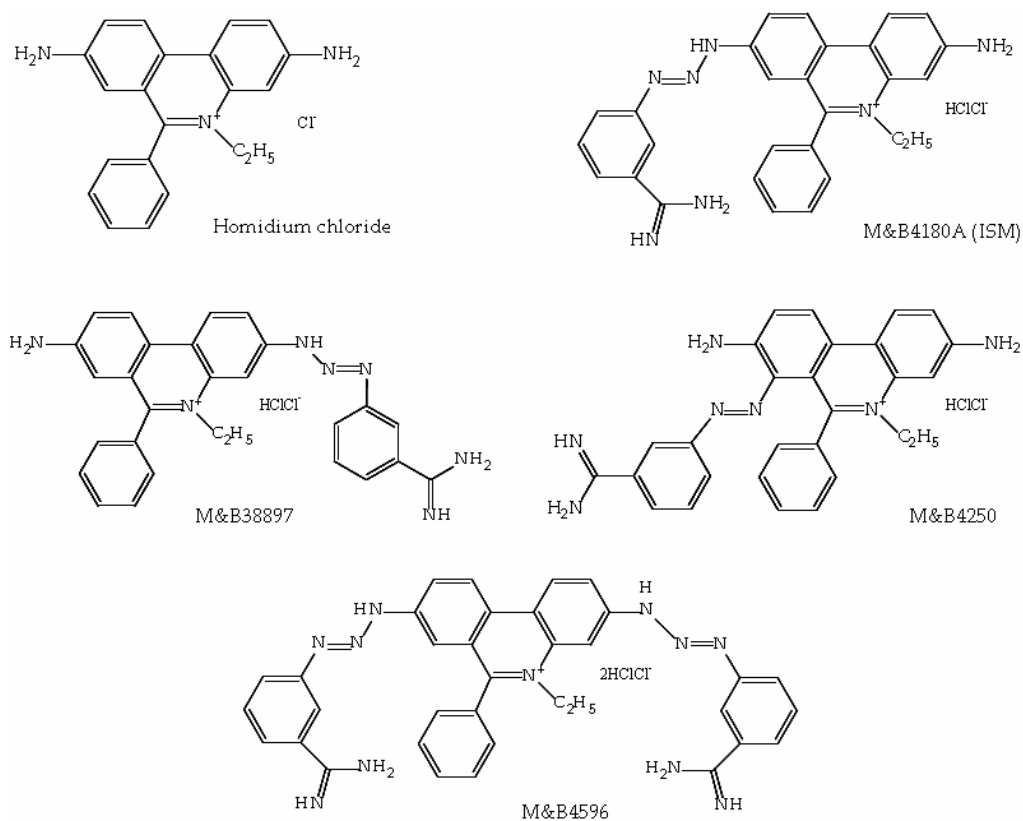


Figure 2.3: Proposed chemical structures of ISM and related substances (Tettey *et al.*, 1999)

A suitable method for the quality control of isometamidium formulations has to allow the baseline separation of M&B4180A and all the process related by-products in question. Due to their structural and physicochemical similarities the separation of these compounds by HPLC is challenging. Moreover the presence of quaternary nitrogen atoms and strongly basic amidino moieties in all components can result in poor peak shape due to interactions with residual silanols in the silica-based stationary phases (Tettey *et al.*, 1998).

### **2.1.2. Aims and Objectives**

Manufacture of commercial ISM formulations always results in production of a mixture of related substances. There are no monographs or internationally agreed standards for the quality control of these formulations, and with problems like counterfeiting and drug resistance on the rise, accurate, specific and well characterised methods for assurance of suitable quality control of these products are an immediate need. The aim of this part of the study is the development and validation of an improved HPLC method for specific separation and quantitation of ISM in the presence of its process related by-products. The method should enable fast, reproducible assays for quality control of the manufacturing process and authenticity testing of commercial products on the market.

## 2.2. Experimental

### 2.2.1. Materials

HPLC-grade acetonitrile, methanol and isopropyl alcohol were obtained from VWR International Ltd. (Poole, UK). Analytical reagent grade glacial acetic acid and formic acid were obtained from Sigma-Aldrich (Dorset, UK) and ammonium acetate, formate and chloride were obtained from BDH Laboratory Supplies (Poole, UK). A secondary reference standard mixture (RSM) of isometamidium and related substances containing 8-(*m*-amidinophenyldiazoamino)-3-amino-5-ethyl-6-phenylphenanthridinium chloride [(58.6 %w/w), isometamidium, ISM, M&B4180A], 3-(*m*-amidinophenyldiazoamino)-8-amino-5-ethyl-6-phenylphenanthridinium chloride [(13.3 %w/w), M&B38897], 7-(*m*-amidinophenyldiazo)-3,8-diamino-5-ethyl-6-phenylphenanthridinium chloride [(13.7 %w/w), M&B4250] and 3,8-di-(3-*m*-amidinophenyltriazeno)-5-ethyl-6-phenylphenanthridinium chloride [(8.1 %w/w), M&B4596] and an authentic standard of homidium (3,8-diamino-5-ethyl-6-phenylphenanthridinium chloride) were a kind gift from Merial Limited (Toulouse, France). Commercial preparations of isometamidium were obtained from the open market in West Africa.

*Ammonium acetate buffer (10 mM, pH 4.0)*

Ammonium acetate (7.71 g) was accurately weighed, dissolved in approximately 800 ml of water and the pH adjusted to a value of 4.0 with acetic acid. The resulting solution was made up to 1 l with distilled water.

*Ammonium formate buffers (50 mM and 15 mM, pH 2.8)*

Ammonium formate (3.15 g or 0.95 g) was accurately weighed, dissolved in approximately 800 ml of water and the pH adjusted to a value of 2.8 with formic acid. The resulting solution was made up to 1 l with distilled water.

## **2.2.2. Preparation of Standard and Sample Solutions**

*ISM standard solutions*

For HPLC analysis, 21.4 mg of the reference standard mixture (RSM) was accurately weighed using a Mettler AT20 analytical balance (readability 0.01 mg). The weighed sample was dissolved in, and made up to 25 ml with water to produce a stock solution containing 0.05 %w/v M&B4180A, 0.007 %w/v M&B4596, 0.01 %w/v M&B38897 and 0.01 %w/v M&B4250. Aliquots of the stock solution were suitably diluted with 25 %v/v acetonitrile in water to produce calibration solutions containing 0.002, 0.004, 0.006, 0.008 and 0.01 %w/v M&B4180A; 0.0003, 0.0006, 0.0008, 0.0011 and 0.0014 %w/v M&B4596; 0.0005, 0.0009, 0.0014, 0.0018, 0.0023 %w/v M&B38897 and 0.0005, 0.0010, 0.0014, 0.0019, 0.0024 %w/v M&B4250 (based on the %w/w values provided by Merial [section 2.2.1]).

*Sample preparation*

Samples (85 mg) of different commercial preparations of isometamidium chloride hydrochloride were weighed accurately, dissolved in and made up to 100 ml with water. The resultant solution was diluted ten-fold with 25 %v/v acetonitrile in water prior to analysis.

### 2.2.3. HPLC and HPLC-MS Analysis

An Agilent HP1100 series quaternary pump with ChemStation® software version 10.02 for data acquisition equipped with a HP1100 series UV-Vis detector was used. The HPLC was also coupled to an Agilent MSD SL single-quadrupole mass spectrometer via an electrospray ionisation source. M&B4180A and the related substances were separated at ambient temperature on a Gemini C18 column (150 x 4.6 mm, 5 µm particle size, 110Å, Phenomenex, Cheshire, UK) coupled with a Phenomenex C18 Securigard® column. The mobile phase, composed of a mixture of acetonitrile and 50 mM ammonium formate buffer, pH 2.8 (25 : 75 v/v) was delivered at a flow rate of 1 ml/min with a split ratio of 1 in 50 for MS detection. With the UV-Vis detector compounds were detected at a wavelength of 320 nm. For mass spectrometric analysis the following conditions were used: nebulising gas pressure: 10 psi; drying gas flow rate: 7 l/min; drying gas temperature: 300 °C; capillary voltage: 4000 V; positive ion mode; gain: 1; threshold: 150; step size: 0.10; peak width: 0.10 min; cycle time: 1.02 sec/cycle. Data were acquired in full scan mode ( $m/z = 100 - 650$ ) at a fragmentor voltage of 70 V.

### 2.2.4. Validation Studies

The rectilinear relationship between concentrations of the analytes and the UV detector response was evaluated. The concentrations of the calibration series of the analytes examined were 20, 40, 60, 80 and 100 µg/ml M&B4180A; 5, 10, 14, 19 and 24 µg/ml M&B4250; 5, 9, 14, 18 and 23 µg/ml M&B38897 and 3, 6, 8, 11 and 14 µg/ml M&B4596 (based on the %w/w values provided by Merial [section 2.2.1]).

The repeatability of the method was assessed at three different concentrations within the aforementioned ranges. M&B4180A: 20, 50 and

100 µg/ml; M&B4250: 5, 12 and 25 µg/ml; M&B38897: 5, 12 and 25 µg/ml; M&B4596: 3, 7 and 14 µg/ml. Three different preparations of the analytical standard were analysed in triplicate on the same day for the determination of intra-day assay precision. These determinations were repeated using freshly prepared standard solutions on three separate days to determine inter-day precision of analysis. The analysis, in triplicate, of a commercial sample using freshly prepared solutions (as described in section 2.2.2) on three separate days was used to compute the inter-day ( $n = 3$  separate determinations) and intra-day precision of the method.

The stability of the analytical solutions while stored in the autosampler was determined for M&B4180A, M&B4250, M&B38897 and M&B4596 at the concentrations described above for the assessment of repeatability. Analytical solutions were injected repeatedly ( $n = 30$ ) over a 60 h period and %RSD computed for the peak areas due to the respective analytes.

The performance characteristics of the method were based on the resolution between the critical pair (M&B4180A and M&B38897) and the robustness of the method as a function of small changes in pH (between 2.8 and 3.5), buffer strength (25 and 50 mM ammonium formate) of the mobile phase, stability of analytical solutions and the effect of temperature (20 - 40 °C) on resolution. The limits of detection and quantitation for each analyte were determined as signal-to-noise ratio (S/N) of three and %RSD  $\leq 5$ , respectively (Kromidas, 1999).

## 2.3. Results and Discussion

### 2.3.1. Method Development

ISM and its major related substances (figure 2.3) contain highly basic amidino and quaternary nitrogen moieties which interact avidly with residual silanols on silica-based columns. Although Kinabo and Bogan proposed the use of ion pairing reagents to overcome these interactions (Kinabo & Bogan, 1988c), the method failed to achieve separation between the related substances, especially the two positional isomers M&B4180A and M&B38897 (figure 2.3). Subsequently a RP-HPLC method based on the use of phosphate buffer (20 mM, pH 3) as the aqueous component of the mobile phase was reported (Tetty *et al.*, 1998). The method that was fully validated with respect to the principal component (M&B4180A) was successful in giving baseline separation of all the known constituents in commercial ISM preparations. However, the method did not facilitate absolute quantification of the major manufacturing impurities M&B38897 and M&B4250 which can vary significantly in the manufacturing process (Berg, 1963). This was due to the unavailability of authentic reference standards at the time. Boibessot *et al.* (2006) reported an MS compatible method involving the use of formic acid in the mobile phase for the analysis of the putative metabolites of the single component M&B4180A (Boibessot *et al.*, 2006). However, the method was neither designed nor validated for the known manufacturing impurities. In the present study, using a well-characterised analytical standard of M&B4180A and the known impurities, the suitability of  $\text{NH}_4^+$ -containing mobile phases, providing a competing ion to reduce analyte-silanol interactions, was investigated. Generally, the increase in the ionic strength of either the ammonium formate or ammonium acetate buffers up to concentrations of 50 and 100 mM respectively resulted in an improvement in

the chromatographic peak shapes. This observation is consistent with competition between the highly basic moieties in the phenanthridinium salts and the ammonium ions for electrostatic interactions with residual silanols. Optimal separation of the analytes (figure 2.4), as judged by the resolution between the critical pair M&B4180A and M&B38897, was achieved with mobile phases containing either ammonium acetate (100 mM, pH 4.0, figure 2.4 a) or ammonium formate (50 mM, pH 2.8, figure 2.4 b). Although the ammonium acetate buffer produced an  $R_s$  value of 2.5 for the critical pair, the asymmetric nature of the peak due to M&B4596 ( $A_s = 4.1$ ) precluded the use of this buffer salt (figure 2.4 a). The presence of two highly basic amidino moieties in addition to the quaternary nitrogen in M&B4596 makes it particularly susceptible to peak tailing due to interactions with residual silanols. Ammonium formate, in contrast to ammonium acetate, produced a better peak shape for M&B4596 with a peak symmetry factor of approximately 2.3 and an improved  $R_s$  value of 3.0 for the critical pair at a pH of 2.8 (figure 2.4 b). This was achieved at a reduced buffer concentration of 50 mM compared with 100 mM for ammonium acetate. Due to the instability of some silica-based columns at pH values of below 2.8, the method was further evaluated using ammonium formate buffer at a pH of 3.5 (figure 2.4 c). Although this change in mobile phase produced an increase in the retention times of the analytes, the  $R_s$  value for the critical pair was  $\geq 2.5$  and illustrated a flexibility of the proposed conditions in terms of choice of pH within the effective buffering range (pH 2.8 - 4.8) of ammonium formate. An assessment of the effect of temperature over a range of 20 - 40 °C on the separation showed a gradual, albeit insignificant, decrease in retention times with increase in temperature which did not compromise resolution of the critical pair. Further analyses were carried out at ambient temperature.



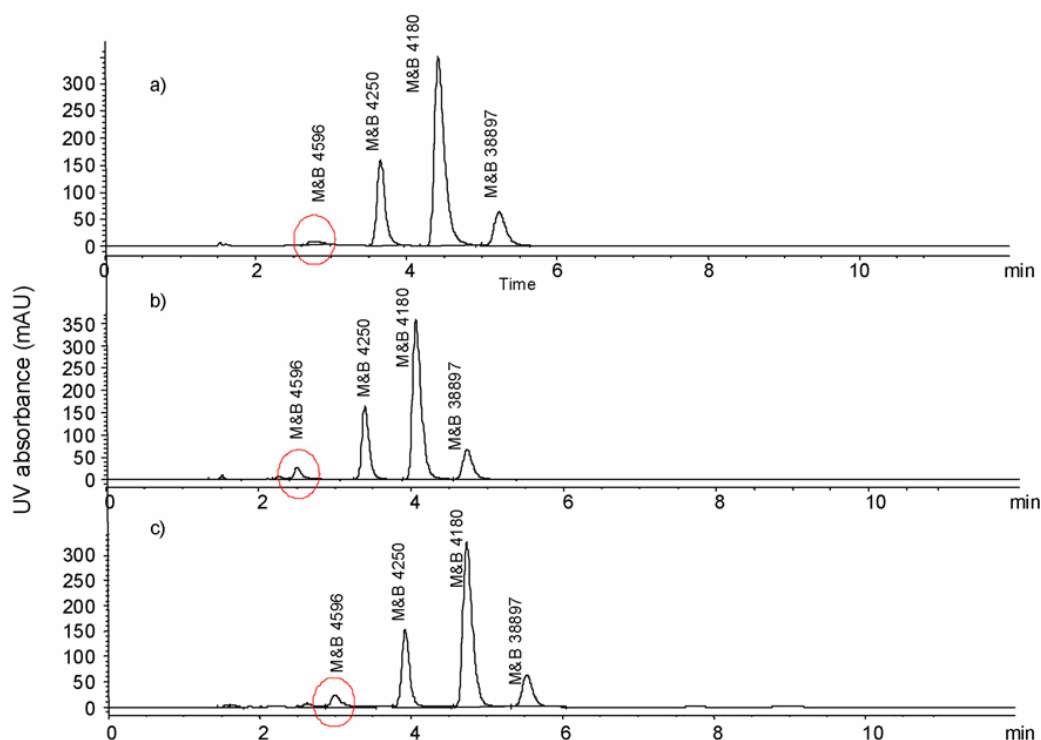


Figure 2.4 Representative chromatograms of the separation of the major components of ISM formulations using the conditions described in section 2.2.3 with mobile phase composition: a) mixture of acetonitrile and ammonium acetate buffer (100 mM, pH 3.8) (25 : 75 v/v), b) mixture of acetonitrile and ammonium formate buffer (50 mM, pH 2.8) (25 : 75 v/v) and c) mixture of acetonitrile and ammonium formate buffer (50 mM, pH 3.5) (25 : 75 v/v). The peak due to the highly basic bis-amidino compound M&B4596 is highlighted to illustrate the effect of the analytical conditions on peak shape.

The stability of analytical solutions assessed at three different concentrations for each component of ISM as described in section 2.2.4 gave %RSD values ( $n = 36$  injections over 60 h) for peak areas which were typically less than 3.0, 1.7 and 0.7 % for the low, intermediate and high concentrations respectively. Thus solutions are sufficiently stable to justify the analysis of freshly prepared samples over a 24 h period.

### 2.3.2. Validation

The chromatographic peak areas showed rectilinear relationships with respect to analyte concentration within the specified ranges (figure 2.5; table 2.1), which are consistent with the expected concentrations in diluted samples of commercial isometamidium formulations.

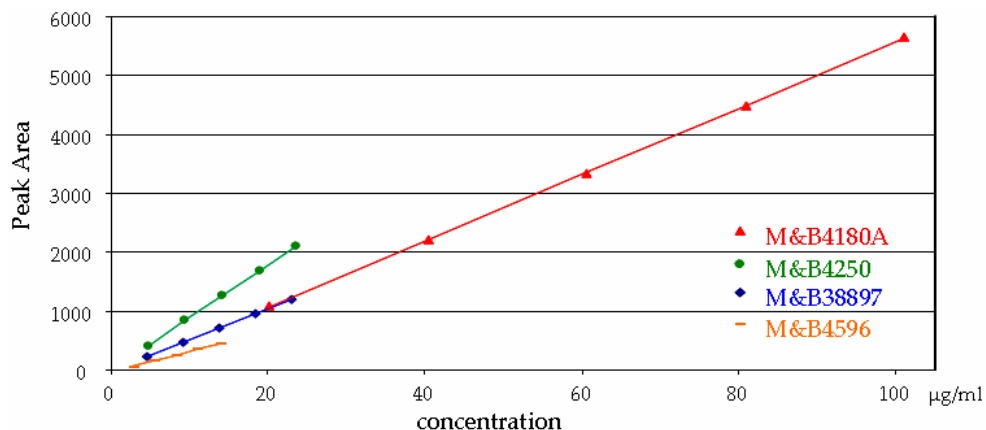


Figure 2.5: Plots of peak area vs. concentration for ISM and related substances

Linear regression analysis showed that the correlation coefficients ( $R^2$ ) of all calibration curves were  $\geq 0.995$  with minimal variations in the slopes and intercepts (table 2.1).

Table 2.1: Regression analysis of calibration curves obtained from the analysis of M&B4180A (ISM) and related substances

Analyte	Range (µg/ml)	<i>n</i>	Slope	Intercept	Correlation coefficient ( $R^2$ )
M&B 4596	3 – 15	4	$34.7 \pm 0.3$	$41.1 \pm 4.6$	$0.9998 \pm 0.0001$
M&B 4250	5 – 25	4	$89.6 \pm 0.1$	$18.4 \pm 1.6$	$1.0000 \pm 0.0000$
M&B 4180	20 – 100	4	$56.3 \pm 0.1$	$74.7 \pm 4.2$	$1.0000 \pm 0.0001$
M&B 38897	5 – 25	4	$52.2 \pm 0.1$	$14.3 \pm 2.1$	$1.0000 \pm 0.0001$

Limits of detection and quantitation of the method as shown in table 2.2 confirm that the assay is sufficiently sensitive for the quality control of commercial products. The LOD and LOQ values for M&B4596 are considerably higher than for the positional isomers.

Table 2.2: Sensitivity of HPLC assay

		M&B4180A	M&B38897	M&B4250	M&B4596
LOD	S/N = 3	0.04 µg/ml	0.05 µg/ml	0.02 µg/ml	1.40 µg/ml
LOQ	%RSD ≤ 5	0.20 µg/ml	0.10 µg/ml	0.05 µg/ml	2.80 µg/ml

The broad, small peaks are not as well integrated and show higher variability in peak area at low concentrations. M&B4596 contains two highly basic amidino moieties in addition to the quaternary nitrogen and is more prone to peak tailing ( $A_s = 2.3$ ) than M&B4180A and its isomers. That can also be observed in the inter- and intra-day assay precision (%RSD) for the determination of M&B4596 (table 2.3).

Table 2.3: Repeatability of HPLC method

	M&B4180A			M&B4250		
	µg/ml	Peak Area	%RSD	µg/ml	Peak Area	%RSD
<b>Inter-day precision</b>						
Day 1 ( $n=3$ )	20	1306 ± 14.8	1.13	5	542 ± 2.9	0.54
Day 2 ( $n=3$ )	50	3283 ± 22.7	0.69	12	1303 ± 25.0	1.92
Day 3 ( $n=3$ )	100	6586 ± 79.7	1.21	25	2693 ± 15.1	0.56
<b>Intra-day precision</b>						
Solution 1	20	1304 ± 9.8	0.75	5	545 ± 6.65	1.22
Solution 2	50	3277 ± 17.4	0.53	12	1297 ± 6.1	0.47
Solution 3	100	6546 ± 30.1	0.46	25	2685 ± 12.9	0.48
	M&B38897			M&B4596		
	µg/ml	Peak Area	%RSD	µg/ml	Peak Area	%RSD
<b>Inter-day precision</b>						
Day 1 ( $n=3$ )	5	317 ± 18.0	5.69	3	138 ± 8.9	6.30
Day 2 ( $n=3$ )	12	767 ± 6.7	0.87	7	346 ± 3.9	1.13
Day 3 ( $n=3$ )	25	1567 ± 9.7	0.62	14	679 ± 6.4	0.95
<b>Intra-day precision</b>						
Solution 1	5	325 ± 20.4	6.27	3	126 ± 16.6	13.16
Solution 2	12	748 ± 19.7	2.64	7	318 ± 29.0	1.15
Solution 3	25	1547 ± 25.7	1.66	14	678 ± 23.5	3.47

The intra-day assay precision (%RSD) of peak areas for M&B 4180A at the working concentration range of 50 - 100 µg/ml (0.53 % ; 0.46 %) is comparable to the value of 0.51 % previously reported (Tetty *et al.* 1998). With the exception of M&B4596, which produced a high %RSD for intra-day precision (3.47 %) at the proposed working concentrations, the other compounds of interest gave a repeatability value of  $\leq 2.7$  % (table 2.3).

Specificity of the method was confirmed by comparing the peak retention values of chromatographic peaks of M&B4596, M&B4250, M&B4180A and M&B38897 acquired from injections of single standard solutions with those obtained from injections of a standard solution of a compound mixture and injections of commercial samples (Tetty, 2006). The chromatographic peaks of the four compounds were clearly resolved with M&B4180A and M&B38897 as the critical peak pair ( $R_s > 3.0$ ).

Robustness was assessed by determining the resolution between the critical peak pair M&B4180A and M&B38897 when different system parameters were slightly modified as described in section 2.3.1. A shift in retention times could be observed (figure 2.4) but resolution obtained remained  $> 2.5$ . Baseline separation was achieved for all compounds of interest even with the modified conditions.

The method was compatible with mass spectrometric detection (figure 2.6), the obtained data is summarised in table 2.4.

Table 2.4: MS data from analysis of ISM and related substances using the conditions described in section 2.2.3

Compound	$t_R$ (min)	Molecular Ion ( $m/z$ )	Major Ion ( $m/z$ )
M&B4180A	5.01	460 [M] <sup>+</sup>	230.5 [M+H] <sup>2+</sup>
M&B4250	4.21	460 [M] <sup>+</sup>	230.5 [M+H] <sup>2+</sup>
M&B38897	6.02	460 [M] <sup>+</sup>	230.5 [M+H] <sup>2+</sup>
M&B4596	3.19	606 [M] <sup>+</sup>	303.5 [M+H] <sup>2+</sup>
Homidium	12.07	314 [M] <sup>+</sup>	314 [M] <sup>+</sup>

The structural similarity of the related substances (figure 2.3) makes it difficult to distinguish between M&B4180A, M&B4250 and M&B38897 based on MS data alone. The refinement of the MS data with chromatographic retention times enables unambiguous identification of these compounds.

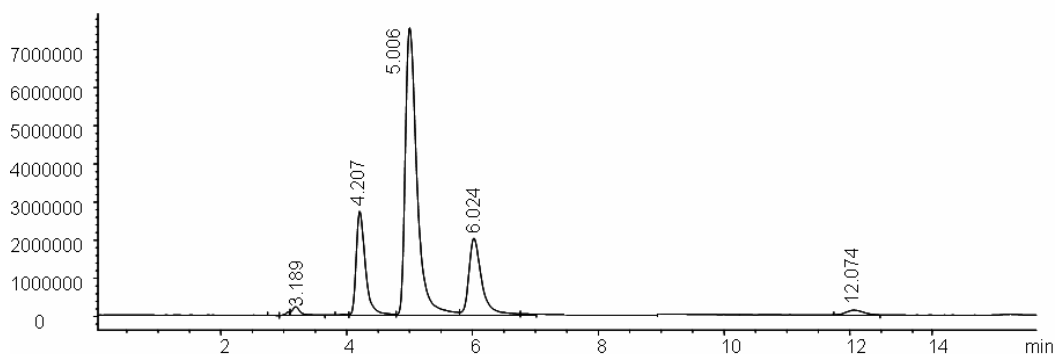


Figure 2.6 Representative total ion count chromatogram of the separation of the major components of ISM formulations using the conditions described in section 2.2.3 with MS detection.

However, distinct MS data were obtained for the bis-amidino substituted analogue, M&B4596 (figure 2.7 a) and the precursor and degradation product homidium (figure 2.7 b). The LC-MS method subsequently provides selectivity in analysis with respect to the degradation product homidium, which is also well resolved from the other analytes (figure 2.6).

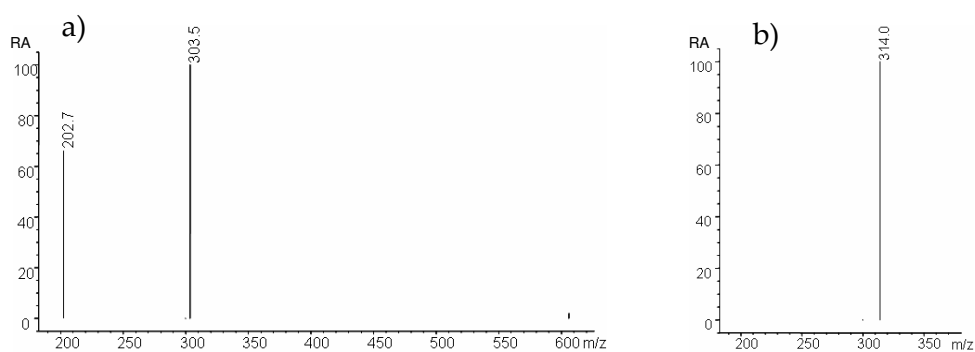


Figure 2.7: a) Mass spectrum of M&B4596 ( $t_R = 3.2$ ,  $m/z = 606$ ,  $303.5$  and  $202.7$  for  $[M]^+$ ,  $[M+H]^{2+}$  and  $[M+H]^{3+}$ ) b) Mass spectrum of homidium ( $t_R = 12.1$ ,  $m/z = 314$  for  $[M]^+$ )

### 2.3.3. Analysis of Commercial Preparations

The challenges involved in the commercial production of a consistent mixture of components in ISM led to the incidence of non-chemically equivalent products in the past (Tettey *et al.*, 1999). Samorin®/Trypamidium®, currently the only World Health Organization (WHO)-FAO Joint Expert Committee on Food Additives (JECFA) approved product, recognizes these challenges and provides a workable range for the contents (%w/w) of M&B4180A (55 – 65 %), M&B4596 (5 – 10 %), M&B38897 and M&B4250 (10 - 20 %) in commercial samples (*source*: Merial SAS, Lyon, France). The validation of the repeatability (inter- and intra-day precision) of the proposed HPLC method using the JECFA approved product (table 2.5) yielded %RSD values typically less than 2 % with exception of the highly basic M&B4596 which contains two amidino moieties in addition to a quaternary nitrogen.

Table 2.5: Precision of HPLC analysis of ISM and related substances in a commercial sample

	M&B4180A	M&B38897	M&B4250	M&B4596
<b>Inter-day precision</b>				
Mean (%w/w) ± SD ( <i>n</i> = 3)	62.9 ± 0.54	8.0 ± 0.02	7.6 ± 0.09	5.8 ± 0.15
%RSD	0.87	0.25	1.17	2.67
<b>Intra-day precision</b>				
Mean (%w/w) ± SD ( <i>n</i> = 3)	62.3 ± 1.13	8.0 ± 0.12	7.5 ± 0.11	5.5 ± 0.06
%RSD	1.82	1.49	1.53	1.15

The reproducibility of the method, as assessed by comparative analysis of the same five commercial products in two different laboratories (University of Strathclyde and International Atomic Energy Agency Laboratory, Seibersdorf, Austria) showed no significant difference ( $p < 0.05$ ) using a two-sample paired comparison test. The lack of consistency in the amounts of additives and excipients added to commercial products, which is reflected in

the actual weight of contents (table 2.6), makes it difficult to assess equivalence in terms of %w/w. Rather a useful comparison is obtained based on the amounts of the analytes per 125 mg or 1 g sachet of product. The data (table 2.6) show a significant variation in profiles of these products with respect to the content of the known chemical entities and excipients or additives. The WHO recognizes counterfeit medicines as part of a broader phenomenon of sub-standard pharmaceuticals (WHO Fact sheet 275). The WHO definition of sub-standard medicines as ones “which are manufactured below established standards of quality and therefore dangerous to patient’s health and ineffective for the treatment of diseases” is difficult to apply to ISM in the absence of an internationally established specification or standard of quality for the product. Therefore, it is not immediately apparent if the lack of chemical and pharmaceutical similarity between the innovator and some commercially available product results from the manufacture of sub-standard products. Counterfeit ISM products, which are deliberately and fraudulently mislabelled with respect to source or identity, may however be assigned as sub-standard without ambiguity. For example, the analysis of a counterfeit version of Samorin<sup>®</sup> (figure 2.8) found on the West-African market by the HPLC and HPLC-MS methods previously described showed the complete absence of M&B4180A, M&B4596, M&B38897 and M&B4250. Moreover, the labelling and dosage instruction on the counterfeit version, compared to authentic Samorin<sup>®</sup>, was incomplete. Eisler *et al.* (1996) speculated that the absence of protective concentration of ISM in cattle following treatment under field conditions was probably attributable to the use of adulterated or counterfeit drugs. This study confirmed that assertion and also demonstrated marked differences in chemical composition and formulation of current commercially available ISM products.

Table 2.6: Results of HPLC analyses of various commercial ISM products

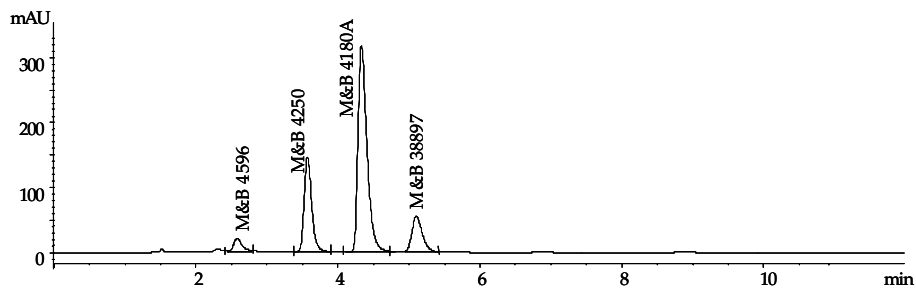
	Manufacturer	Wt. of contents of sachet	M&B4596	M&B38897	M&B4250	M&B4180A
<b>Innovator specifications (mg) for 125 mg sachet<sup>(a)</sup></b>			6.25 - 12.5	12.5 - 25.0	12.5 - 25.0	68.75 - 81.3
Trypamidium®-Samorin®	Merial, France	125 mg	11.3 mg	16.4 mg	17.6 mg	74.0 mg
Kelamidium (lot n°8898)	Kela, Belgium	3000 mg	5.6 mg	9.1 mg	15.8 mg	64.4 mg
<b>Innovator specifications (mg) for 1 g sachet<sup>(a)</sup></b>			50 - 100	100 - 200	100 - 200	550 - 650
Inomidium	Inouko Generics, France	1.04 g	60.3	65.5	99.0	653.5
Lobidium	LOBS, France	1.04 g	55.7	79.3	125.4	602.6
Isometamidium	PKM International	1.30 g	92.4	145.6	143.6	773.8
Veridium™ (lot 93A1)	Ceva, France	1.08 g	50.8	99.5	103.1	640.2
Veridium™ (lot 101A1)	Ceva, France	1.08 g	62.6	86.4	82.1	679.3
Kelamidium (lot 7937)	Kela, Belgium	2.15 g	79.2	37.4	15.3	419.0
Kelamidium (lot 9536)	Kela, Belgium	1.86 g	72.8	114.3	127.3	608.7

<sup>a</sup>Based on the innovator specification of M&B4180A (55 - 65 %), M&B4596 (5 - 10 %), M&B38897 (10 - 20 %) and M&B4250 (10 - 20 %)





a)



b)

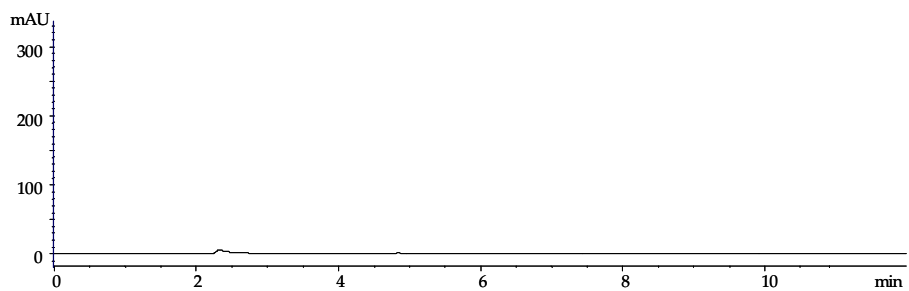


Figure 2.8 Front and rear images of sachets of a genuine (a, top) and counterfeit (b, bottom) Samorin® product and chromatograms of HPLC analysis of the contents.

These observations have significant implications with respect to treatment failures and toxicity of unknown additives/ adulterants. Isometamidium remains the only chemical agent for the prophylaxis and treatment of veterinary trypanosomiasis. It is obvious that the difficulties in its synthesis, the absence of regulatory standards and drug counterfeiting have resulted in the marketing of products, which bear no chemical or pharmaceutical similarity to each other, or the innovator product.

The application of this proposed validated method which allows for absolute quantitation of the four major components and LC-MS screening of the authenticity of products should facilitate the control of the quality of these products in international commerce.

## 2.4. Conclusions

With the method described successful resolution of ISM and related compounds, namely M&B4596, M&B4180A, M&B4250 and M&B38897 was achieved and the advantage of using  $\text{NH}_4^+$ -containing mobile phases could be demonstrated. The ammonium ion acts as a competing ion to the basic centre in the compounds of interest and the low, acidic pH suppresses silanol ionization. This leads to reduced analyte-silanol interactions, giving rise to better chromatography. Strong peak tailing could be overcome and the improved peak shape offered better resolution and efficiency.

Experiments showed that the use of formate buffer was superior to using acetate buffer in the mobile phase. Also with the ammonium acetate buffer baseline separation of the critical peak pair was achieved ( $R_s = 2.5$ ), but the asymmetric nature of the peak due to M&B4596 ( $A_s = 4.1$ ) was considerably improved by the use of ammonium formate. Compared to chromatograms obtained with 100 mM acetate buffer (pH 4.0) a better peak shape for this bis-amidino substituted analogue was obtained using 50 mM formate buffer (pH 2.8) ( $A_s = 2.3$ ) as well as an improved  $R_s$  value of 3.0 for the critical pair (figure 2.4). As M&B4596 bears two highly basic amidino moieties in addition to the quaternary nitrogen it is specifically susceptible to peak tailing due to interactions with residual silanols.

The results for the robustness study also showed, that a pH of the mobile phase of 3.5 produced good separations of all compounds of interest, with only slightly increased analysis time (figure 2.4). These mobile phase conditions could thus be used with silica based columns which are unstable at pH values below 3. Changes in temperature within the range of 20 - 40 °C did not significantly affect separation.

The linear relationship between detector response and concentration was shown by linear regression analysis, which gave a correlation coefficient ( $R^2$ ) for calibration curves of all analytes of  $\geq 0.995$  and also precision was indicated by very little variation in the slopes and intercepts of all calibration curves obtained (table 2.1). Repeatability and reproducibility of the method was further demonstrated by an intra-day and inter-day assay precision of usually  $< 2\%$  (%RSD) for replicate ( $n = 3$ ) injections of separately prepared standard solutions of different concentration (table 2.3). With a %RSD value of 3.95 in the repeatability studies the related substance M&B4596 is an exception. This high value can be explained by the low concentrations of M&B4596 in the analytical reference standard as well as in the sample substances, which are close to the limit of quantification. The %RSD values are  $< 10\%$  and the quantification shows a good precision for this compound, thus the method is still applicable.

With limits of quantification of  $0.2\ \mu\text{g/ml}$  for M&B4180A and  $\leq 0.1\ \mu\text{g/ml}$  for its isomers (table 2.2) the method is sufficiently sensitive for the quality control of commercial products.

The developed method is specific, precise and robust and a linear relationship between concentration and the detector signal for the compounds of interest has been demonstrated within the specified range. The method was successfully employed for the quality evaluation of several generic formulations of ISM (table 2.6).

The method employs standard isocratic HPLC instrumentation with UV detection and widely available reagents and chemicals. The relatively low cost and simple procedure of the approach renders it suitable for transfer to laboratories in developing countries where the improved quality control of veterinary trypanocides is an immediate need.

The method was also compatible with mass spectrometric detection. The determination of homidium ( $m/z = 314$ ), well separated from ISM ( $m/z = 460$ ; 230.5) and other related substances (figure 2.6), shows selectivity of the method with respect to the main degradation product and the method's capability of indicating the stability of ISM.

The highly selective and sensitive LC-MS method offers the possibility to decrease the limit of detection and quantification to a considerable degree. It consequently enables the determination of very low concentrations of analytes present in plasma and tissues from animals treated with ISM. This approach would be developed into a bioanalytical method for the determination of residual ISM in biological material (chapter 3).

### **3. Bioanalytical Assay for the Determination of Residual Isometamidium and Related Substances in Plasma**

#### **3.1. Introduction**

If it was possible to markedly decrease the limits of detection and quantification of the reported ISM assay (chapter 2) and find a suitable extraction procedure for the analytes of interest from biological material, that would enable the selective determination of nanogram amounts of the drug, as present in plasma and tissue of treated animals (Eisler *et al.*, 1996b). This assay could be used not only for the quality control of meat products from treated cattle but also to carry out pharmacokinetic and bioavailability studies to enable a better understanding of the mechanisms of action and the production of chemoresistance. These insights might help to optimise the use of drugs in the field, as well as the design of new trypanocides. There have been previous studies on pharmacokinetics, drug metabolism and mode of action of ISM, but the assays were neither selective nor sensitive for all the isomers and related substances present in commercially available formulations of the trypanocide.

##### **3.1.1. Pharmacokinetics of Isometamidium**

Previous studies investigating the absorption, distribution and elimination of ISM in mice (Hill & McFadzean, 1963), rats (Hill & McFadzean, 1963; Philips *et al.*, 1967), dogs, monkeys (Philips *et al.*, 1967), goats (Braide & Eghianruwa, 1980; Kinabo & McKellar, 1990; Wesongah *et al.*, 2004), sheep (Wesongah *et al.*, 2004), pigs (Kinabo *et al.*, 1991), camels (Ali & Hassan, 1984) and cattle (Eisler, 1996; Kinabo & Bogan, 1988b; Kratzer *et al.*, 1989; Murilla *et al.*, 1996) relied on the determination of ISM concentrations by non-specific analytical

methods which were not sufficiently sensitive. Spectrophotometry as used by Philips *et al.* in 1967 or Braide and Eghianruwa in 1980 enabled the detection of 1 µg/ml ISM in serum and 2.3 µg/ml in tissue, measuring not only the most active isomer M&B4180A, but all related substances present in the formulation as one. Kinabo and Bogan (1988c) reported a limit of detection of 10 ng/ml in serum and about 500 ng/g of tissue using an HPLC method which included a solid phase extraction sample preparation step. Again the analysis was not specific for M&B4180A only, but produced an unresolved peak for all the known related substances. With a radioimmunoassay (RIA) using [<sup>14</sup>C]ISM as a radioligand, amounts as low as 5.8 pmol (2.7 ng) per assay could be determined, but the assay also showed considerable cross-reactivity of the antibodies with other trypanocidal agents (Kinabo & Bogan, 1988a). Furthermore, none of these methods were able to detect ISM in biological materials beyond 24 h following drug treatment. Development of more sensitive detection methods such as a radiometric technique using [<sup>14</sup>C]ISM as a radioactive marker that could be monitored for up to 120 days after administration (Murilla *et al.*, 1996), allowed pharmacodynamic studies of the drug over an extended time period. An enzyme-linked immunosorbent assay (ELISA) (Eisler *et al.*, 1993; Whitelaw *et al.*, 1991) and a later reported competitive enzyme immunoassay (CEIA) (Eisler *et al.*, 1996a) made the determination of ISM at concentration levels as low as 0.5 ng/ml possible. Those methods were successfully employed to determine plasma concentrations of ISM in cattle up to four months following treatment (Eisler *et al.*, 1996b).

ELISA is able to detect subnanogram quantities of drug in the sera of treated animals and has been the assay of choice for the investigation of the pharmacokinetics of ISM in treated animals. However, it is known to exhibit

significant cross-reactivity with homidium and is not specific for M&B4180A in the presence of its isomers and related substances (Eisler *et al.*, 1993; Eisler *et al.*, 1996b; Wesongah *et al.*, 2004).

All biological studies however have shown a similar outcome, in that ISM is detectable in plasma shortly after intra-muscular injection and achieves its maximum concentration after about an hour, followed by a rapid decrease to very low levels within 24 h. Kinabo suggested that this accelerated decrease in plasma concentrations was due to the fast distribution of the drug into various tissues, where ISM is accumulated. This explains the higher concentrations of ISM in tissue than in plasma (Kinabo, 1993). The distribution and elimination of ISM is biphasic. Peak plasma levels of about 160 ng/ml were reached 15 to 30 min after administration (1 mg/kg) followed by a rapid decline with half lives of approximately 1.5 h to levels of 14 ng/ml (Kratzer *et al.*, 1989). Despite this rapid distribution phase, the drug exhibits a bioavailability of as low as 27 % in goat (Kinabo & McKellar, 1990) and up to 66 % in cattle (Eisler, 1996). In the second phase the decline in plasma with an apparent half life of 23 days reaches concentrations of about 0.5 ng/ml after three months (Eisler *et al.*, 1996b). Extensive tissue binding of ISM at the intramuscular injection site, from where it gets slowly released into the plasma has also been shown. It has been suggested that this primary depot is responsible for most of the prolonged chemoprophylactic effect of ISM. Additionally, secondary drug depots are formed by tissue binding in liver and kidney, the primary organs of excretion, particularly after intravenous administration (Eisler, 1996; Hill & McFadzean, 1963).

The apparent half-life of ISM in sera from intramuscularly treated cattle was 23 days with these cattle protected against trypanosome infections for at least 18 weeks following treatment (Eisler *et al.*, 1996b).



Although the precise mechanism of the selective toxicity of phenanthridines toward certain organisms remains unknown, one accepted therapeutic mechanism is based on the selective inhibition of nucleic acid synthesis by intercalation between adjacent base pairs of the DNA-double helix (Denise & Barrett, 2001; Gambari & Nastruzzi, 1994). Furthermore inhibition of DNA- and RNA-polymerase, and spurious integration of precursor nucleic acids in DNA- and RNA-molecules are assumed (Kinabo, 1993). Another reported mechanism is the selective cleavage of kinetoplast DNA minicircles (Shapiro & Englund, 1990).

It has been shown, that the drug uptake of ISM by trypanosomes is severely reduced by its binding to serum albumin and that this is significantly related to cellular damage (Girgis-Takla & James, 1974).

### **3.1.2. Metabolism of Isometamidium**

Despite extensive biological investigations relatively little is known about the metabolism of ISM. Studies of the metabolism and distribution of phenanthridine trypanocides in trypanosomes showed that ISM is accumulated in the kinetoplast and that no metabolite formation could be detected. However, in isolated rat hepatocytes ISM was only shown to be metabolised to a small extent (approx. 1 %) (Boibessot *et al.*, 2002). In 2006 possible metabolic pathways of ISM were proposed indicating the formation of two metabolites (figure 3.1) (Boibessot *et al.*, 2006). Putative metabolites represented only 1 % of the parent. Low recoveries of the parent compound and putative metabolites from cell macromolecules might be due to the strong binding of ISM to DNA and other macromolecules. Recovery of total ISM was only one third of that reported for homidium. Unmetabolised drug

and possible metabolites are mainly excreted in bile (Boibessot *et al.*, 2006; Coolbear & Midgley, 1986).

It has been suggested that the use of persistent organochlorine compounds and other agents used for aerial and ground spraying of the tsetse habitats, as a means of vector control, may have contributed to the generation of trypanocide resistance (Boibessot *et al.*, 2006). Organochlorines possess cytochrome P450 inducing properties (Walker *et al.*, 2006) and thus could accelerate the metabolism pathways of the trypanocides, which are catalysed by the P450 system (Boibessot *et al.*, 2006). It is not known whether the metabolism of the trypanocide by the parasite contributes to their activity, selective toxicity for these parasites or to the development of chemoresistance (Boibessot *et al.*, 2002). Furthermore the proposed pathway of metabolism of ISM in rat hepatocytes as shown in figure 3.1 is not unambiguous and needs further confirmation (Boibessot *et al.*, 2006).

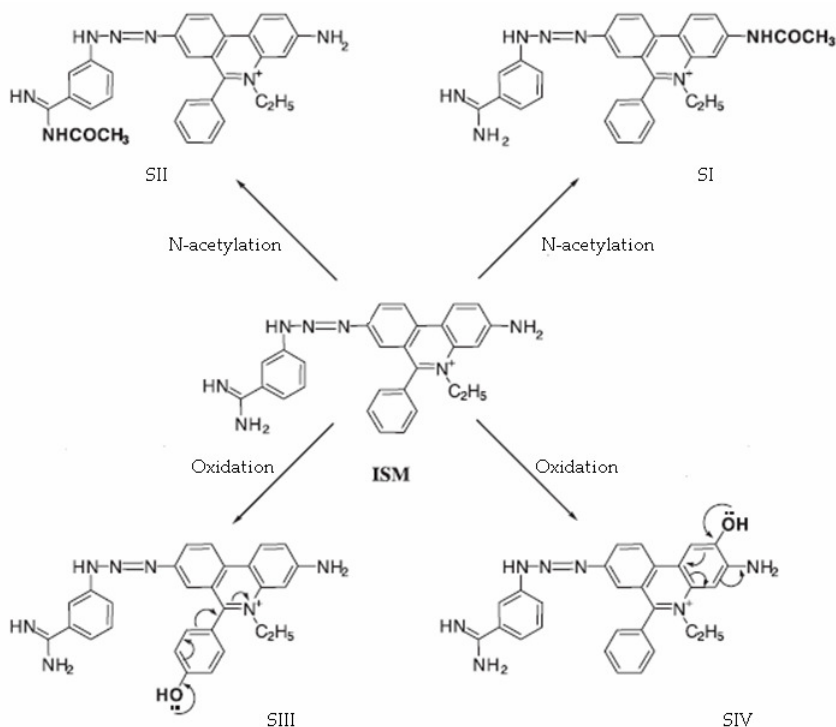


Figure 3.1: Proposed pathways for the metabolism of isometamidium (adapted from Boibessot *et al.*, 2006)

These studies of the metabolism of ISM carried out by Boibessot *et al.* (2006) used a generic HPLC-MS assay that was not specific for only ISM (M&B4180A), but resulted in one peak for all three isomers and related substances. It is thus not possible to establish which of the three isomers present is metabolised or whether different metabolites from the various isomers and related substances are being formed. Data were collected in full scanning mode, rather than in selected ion mode for better selectivity and sensitivity of the ions in question.

### **3.1.3. Aims and Objectives**

The aim of this part of the study was the development and validation of an HPLC method with mass spectrometry detection for enhanced sensitivity, which could be used to determine residual ISM and related substances in animal body fluid and tissue. This also involved designing an appropriate extraction method for the selective and quantitative extraction of the compounds of interest from biological material.

Development of a selective bioanalytical method requires knowledge of putative metabolites of the compound of interest. Therefore studies of the metabolic pathways of ISM and related substances were also carried out, using rat liver microsomes.

## 3.2. Experimental

### 3.2.1. Materials

HPLC-grade acetonitrile, 2-propanol and methanol were obtained from VWR International Ltd. (Poole, UK). Dibasic potassium phosphate (98 % purity), potassium chloride (approx. 99 % pure), sodium tartrate, sodium hydroxide (> 98 % purity), flurazepam dihydrochloride, Folin-Ciocalteu's phenol reagent (2 N),  $\beta$ -nicotinamide adenine dinucleotide phosphate (NADPH; reduced tetrasodium salt; 96 % purity), dimethylsulfoxide ( $\geq$  99.5 % pure), analytical reagent grade formic acid, orthophosphoric acid ( $\geq$  85 % wt. in H<sub>2</sub>O), 5 % dimethylchlorosilane (DMCS) in toluene, magnesium chloride, anhydrous glycerol (> 99.5 % pure), dimidium bromide (95 % purity) and bovine serum albumin were obtained from Sigma-Aldrich (Dorset, UK). Ammonium formate, ammonium chloride, sucrose (AnalaR<sup>®</sup>) and toluene (AnalaR<sup>®</sup>) were obtained from BDH Laboratory Supplies (Poole, UK). Cupric sulphate (98.5 %) was purchased from Fisons Scientific Apparatus (Loughborough, Leicestershire, UK). A pure standard of 3,8-diamino-5-ethyl-6-phenylphenanthridinium chloride (homidium) was supplied by Laprovet (France). A secondary reference mixture of isometamidium and related substances containing 8-(3-*m*-amidinophenyl-2-triazeno)-3-amino-5-ethyl-6-phenylphenanthridinium chloride (ISM, M&B4180A, 58.6 %w/w), 7-(*m*-amidinophenyldiazo)-3,8-diamino-5-ethyl-6-phenylphenanthridinium chloride (M&B4250, 13.7 %w/w), 3-(3-*m*-amidinophenyl-2-triazeno)-8-amino-5-ethyl-6-phenylphenanthridinium chloride, (M&B38897, 13.3 %w/w), and 3,8-di-(3-*m*-amidinophenyltriazeno)-5-ethyl-6-phenylphenanthridinium chloride (M&B4596, 8.1 %w/w) was a kind gift from Merial Limited (Toulouse, France). Strata-X, C<sub>18</sub> and C<sub>8</sub> SPE cartridges (30 mg; 1 ml) were obtained from Phenomenex (Macclesfield, UK).

*Ammonium formate buffer (15 mM, pH 2.8)*

Ammonium formate (0.95 g) was accurately weighed, dissolved in approximately 800 ml of water and the pH adjusted to a value of 2.8 with formic acid. The resulting solution was made up to 1 l with water.

*Methanol saturated with ammonium chloride*

Ammonium chloride (2.0 g) was weighed into a 50 ml volumetric flask and made up to mark with methanol. To achieve a supersaturated solution, the salt was dissolved at 50 °C with the aid of an ultrasonic waterbath.

*Washing buffer for preparation of rat liver microsomes (0.01 M K<sub>2</sub>HPO<sub>4</sub>, 1.15 %w/v KCl, pH 7.6)*

K<sub>2</sub>HPO<sub>4</sub> (1.74 g) and KCl (11.5 g) were accurately weighed and dissolved in approximately 800 ml of distilled water. The pH was adjusted to 7.6 using phosphoric acid. The solution was transferred into a 1 l volumetric flask and made up to mark with distilled water. The buffer solution was stored in a cold room at 4 °C.

*Homogenising buffer for preparation of rat liver microsomes (0.01 M K<sub>2</sub>HPO<sub>4</sub>, 0.25 M sucrose, 15 %v/v glycerol, pH 7.6)*

K<sub>2</sub>HPO<sub>4</sub> (1.74 g) and sucrose (85.58 g) were accurately weighed and dissolved in approximately 600 ml of distilled water. Glycerol (150 ml) was added and the pH was adjusted to 7.6 using phosphoric acid. The solution was transferred into a 1 l volumetric flask and made up to mark with distilled water. The buffer solution was stored in a cold room at 4 °C.

*Preparation of rat liver microsomes*

The liver from a male Sprague-Dawley rat (215 g) was chopped up and placed in about 150 ml of cold washing buffer, and kept on ice. Liver pieces were washed to remove blood using ice cold washing buffer and transferred into 50 ml of ice-cold homogenising buffer. The beaker was kept on ice while

blending the liver using a BRAUN hand blender. The resulting blend was homogenised using two strokes of a motor driven homogeniser. All beakers, vessels and instrument parts were kept on ice to maintain the homogenate temperature below 4 °C to avoid denaturation of the enzymes.

The homogenate was transferred into 5 ml centrifugation tubes, accurately weighed to obviate unbalance of the ultracentrifuge, and centrifuged on a Beckman preparative ultracentrifuge (model L8-80M; Beckman Instruments, California) at 15,000 G (10,500 rpm) for 20 minutes. The centrifuge temperature was set to 4 °C.

The resultant supernatant was decanted into fresh centrifugation tubes and topped up with ice cold homogenising buffer, to avoid collapse of the tube during centrifugation. Again the tubes had to be accurately weighed and contents adjusted if necessary. The supernatant was then centrifuged at 180,000 G (33,000 rpm) for 65 minutes at 4 °C.

The resulting pellet was washed in homogenising buffer and centrifuged for another 65 min at 180,000 G.

The clean pellets were suspended in a small amount of homogenising buffer, the suspensions combined and re-homogenised by stirring with a glass pestle. Aliquots (0.5 ml) of the microsome-containing suspension were stored at - 80 °C.

#### *Deactivation of glassware*

HPLC and sample preparation vials used in the bioanalytical investigation of ISM and related substance were silanized by treatment with a solution of 5 %w/v of dimethylchlorsilane (DMCS) in toluene for 30 minutes. The deactivated glassware was then immediately rinsed with toluene and methanol (Supelco, 1997).

### 3.2.2. Lowry Assay

The protein concentration of the microsomal suspension was determined by the Lowry method (Lowry *et al.*, 1951).

Reagent A: 1 ml of a 1 %w/v CuSO<sub>4</sub> solution and 1 ml of a 2 %w/v sodium tartrate solution in 98 ml of a 2 %w/v NaCO<sub>3</sub> solution.

Reagent B: Four-fold dilution of Folin and Ciocalteu's phenol reagent [a mixture of phosphotungstic- and phosphomolybdic acid (Folin & Ciocalteu, 1927)] in distilled water

Both reagents were freshly prepared on the day of use.

A calibration standard curve was prepared with solutions of bovine serum albumin in 0.5 M NaOH with concentrations of 0, 25, 50, 100, 150 and 200 µg/ml of protein. The sample solution was prepared by pipetting 250 µl of the microsome preparation into a 100 ml volumetric flask and making up to mark with 0.5 M NaOH.

Volumes of reagent A (5 ml) were pipetted into six sample tubes containing 1 ml of a protein standard solution and into a tube containing 1 ml of sample dilution. After 10 minutes a volume of solution B (0.5 ml) was added to each tube and the mixtures left standing for further 30 - 90 minutes. The absorption of each solution was measured on a Shimadzu UV-2401PC UV-Vis recording Spectrophotometer at a wavelength of 750 nm.

### 3.2.3. Metabolism Studies

Rat liver microsomes were incubated with the reference standard mixture (RSM) containing ISM, its isomers and related substances in order to determine whether metabolites were formed. The microsomal preparations were also incubated with flurazepam to confirm that they were metabolically active.

NADPH-solution: NADPH (8.33 mg) was accurately weighed into a 1 ml Eppendorf tube and dissolved in 1 ml of ice-cold homogenising buffer.

MgCl<sub>2</sub>-solution: MgCl<sub>2</sub> (20.33 mg) was accurately weighed into a 1 ml Eppendorf tube and dissolved in 1 ml of ice-cold homogenising buffer.

A 50 mM solution of ISM in water, was prepared by accurately weighing the reference standard mixture (23 mg) into a 1 ml Eppendorf tube followed by the addition of 1 ml of distilled water.

A 50 mM solution of flurazepam in DMSO was prepared by accurately weighing flurazepam (19.4 mg) into a 1 ml Eppendorf tube followed by the addition of 1 ml of DMSO.

Aliquots (30 µl) of the microsomal suspension, containing approximately 1 mg of protein, was pipetted into five glass test vials containing 100 µl MgCl<sub>2</sub> solution and an appropriate amount of ice-cold homogenising buffer to make a final volume of 1 ml after addition of substrate and / or NADPH (table 3.1).

Table 3.1: Volumes used for the microsomal incubation of ISM and flurazepam with rat liver microsomes

Vial	microsomes	substrate	NADPH	MgCl <sub>2</sub>	buffer
1 (Blank)	30 µl	-	100 µl	100 µl	770 µl
2 (Ctrl. ISM)	30 µl	2 µl	-	100 µl	868 µl
3 (Ctrl. flurazepam)	30 µl	2 µl	-	100 µl	868 µl
4 (ISM)	30 µl	2 µl	100	100 µl	768 µl
5 (flurazepam)	30 µl	2 µl	100	100 µl	768 µl

A blank was also prepared only containing microsomes, MgCl<sub>2</sub>, buffer and the NADPH solution. Incubation samples of each analyte were prepared in duplicate. They were made up with all the above and 2 µl of substrate solution. Another control solution was prepared containing only substrate without the addition of NADPH. Test tubes were kept on ice during



the entire preparation procedure and placed in a water bath of 37 °C immediately after addition of the substrate solution. After one minute of pre-incubation time NADPH solution was added into the appropriate vials (table 3.1). After 30 minutes incubation the samples were taken from the water bath and 2 ml of ice-cold acetonitrile was added to stop the reaction and initiate protein precipitation. The samples were centrifuged for five minutes at 3000 rpm. The supernatants were then analysed by HPLC-MS to screen for potential metabolites.

### 3.2.4. Preparation of Standard and Sample Solutions

#### *Reference standard solutions*

To prepare a standard stock solution containing 100 µg/ml M&B4180A, 20 µg/ml M&B4250, 20 µg/ml M&B38897 and 100 µg/ml homidium, 17.1 mg of the mixture of standards (RSM) and 10 mg of the homidium standard were accurately weighed using a Mettler AT20 analytical balance (readability 0.01 mg). The weighed RSM was dissolved in and made up to 100 ml with HPLC water containing 1 %v/v of isopropyl alcohol to prevent adsorption of the isomers to silica in glassware. Aliquots of the stock solution were diluted 2, 4, 10, 20, 50 and 250 - fold with HPLC grade water containing 1 %v/v of isopropyl alcohol to produce calibration solutions ranging in concentrations of M&B4180A from 0.4 - 50 µg/ml.

An internal standard stock solution of dimidium bromide (0.01 %w/v) in HPLC grade water containing 1 %v/v of isopropyl alcohol was also prepared, and diluted with the same solvent to contain 5 µg/ml of internal standard.

#### *ISM spiked plasma*

Plasma samples spiked with M&B4180A, M&B4250, M&B38897, homidium and dimidium as internal standard were prepared by mixing blank bovine

plasma (3.92 ml) with 40  $\mu$ l of the internal standard solution (5  $\mu$ g/ml) and 40  $\mu$ l of the mixed standard solution (ranging in concentrations of M&B4180A from 0.4 - 50  $\mu$ g/ml) to produce final concentrations of 4, 20, 50, 100, 250 and 500 ng/ml M&B 4180A and homidium; 1, 5, 12, 23, 59, 117 ng/ml M&B4250 and M&B38897 and 50 ng/ml dimidium in plasma.

### **3.2.5. Solid Phase Extraction**

The spiked plasma samples (section 3.2.4) were diluted 1 : 1 with distilled water. Solid phase extraction cartridges were activated by eluting them with 1 ml of methanol followed by 1 ml of distilled water. An aliquot (2 ml) of the spiked and diluted plasma samples were loaded onto each cartridge. After sample extraction the cartridges were washed with a volume (1 ml) of methanol followed by distilled water (1 ml) and run dry under vacuum. The retained compounds were then eluted with two volumes (0.5 ml) of methanol saturated with ammonium chloride. The extracts were dried under a stream of nitrogen and reconstituted in 200  $\mu$ l of a mixture of acetonitrile and water (30 : 70 v/v), containing 1 %v/v of isopropyl alcohol. Prior to analysis by HPLC samples were stored at room temperature.

### **3.2.6. HPLC-MS Analysis**

An Agilent HP1100 series quaternary pump with ChemStation® software version 10.02 for data acquisition was coupled to an Agilent MSD SL single-quadrupole mass spectrometer. M&B4180A and the related substances were separated at ambient temperature on a HyperClone BDS C18 column (150 x 3.2 mm, 3  $\mu$ m particle size, 130Å, Phenomenex, Cheshire, UK) coupled with a Phenomenex C18 Securigard® column. The mobile phase was a mixture of acetonitrile and 15 mM ammonium formate buffer, pH 2.8 (25 : 75 v/v) which

was delivered at a flow rate of 0.4 ml/min. The HPLC was connected to the mass spectrometer via an electrospray ionisation (ESI) interface. The MS was calibrated using the automated MS system tuning and mass calibration function of the Agilent system. For mass spectrometric analysis, compounds were detected using the following conditions: nebulising gas pressure: 20 psi; drying gas flow rate: 7 l/min; drying gas temperature: 350 °C; capillary voltage: 4000 V; positive ion mode; gain: 5; threshold: 150; step size: 0.10; peak width: 0.10 min; cycle time: 0.60 sec/cycle. Data were acquired in full scan mode ( $m/z = 100- 650$ ) at a fragmentor voltage of 70 V and in selected ion mode ( $m/z = 606, 303.5$  and  $202.7$  for single, double and triple charged M&B4596 respectively,  $m/z = 460$  and  $230$  for the single and double charged ions respectively of M&B4180A and its isomers M&B4250 and M&B38897,  $m/z = 314$  for homidium). The internal standard dimidium generates an ion of  $m/z = 300$ .

### 3.2.7. Validation Studies

The rectilinear relationship between concentrations of the analytes and detector response was evaluated. The internal standard stock solution (section 3.2.4) was diluted by a factor of 50, giving a concentration of dimidium bromide of 2 µg/ml. The standard stock solution containing ISM and related substances (section 3.2.4) was diluted by a factor of 20, 40, 80, 200 or 500 giving dilutions with concentrations of 5, 2.5, 1.25, 0.5 and 0.1 µg/ml for M&B4180A and homidium; 1.1, 0.6, 0.3, 0.1, and 0.05 µg/ml for M&B38897 and 1.2, 0.6, 0.3, 0.1 and 0.05 µg/ml for M&B4250.

Aliquots (1 ml) of pure bovine plasma were spiked with 10 µl of internal standard solution and 10 µl of one of the dilutions containing ISM and related substances, resulting in plasma concentrations of 20 ng/ml for

internal standard and 50, 25, 12.5, 5 or 1 ng/ml for M&B4180A and homidium; 11, 6, 3, 1 or 0.5 ng/ml for M&B38897 and 12, 6, 3, 1, or 0.5 ng/ml for M&B4250 respectively. Sample preparation included a concentration step, so that analysed samples were five times more concentrated than the concentration in spiked plasma.

The recovery efficiency for the compounds of interest was determined by comparing the area ratios of compound to internal standard obtained after extraction from spiked plasma to the area ratios obtained with the control standards. For preparation of control standards unspiked bovine plasma was passed through SPE cartridges. The same concentration of internal and reference standard stock solutions as present in spiked plasma samples was added to those pure extracts after the extraction step.

Precision of the method was assessed by analysis of nine separately prepared sample solutions with plasma concentrations of 250, 50 and 4 ng/ml M&B4180A and homidium and 60, 12 and 1 ng/ml M&B38897 and M&B4250 to cover the whole validation range. Three samples of each concentration were prepared (n = 9; 3 samples of each concentration). Intra-day assay precision was based on the %RSD of recovery obtained from replicate analyses on one day, whilst the inter-day assay precision was based on %RSD of replicate determinations of freshly prepared sample solutions analysed on three separate days (n = 27; 9 samples of each concentration).

The limits of detection and quantitation for each analyte were determined as S/N of 3 and %RSD  $\leq$  10 % respectively.

### 3.3. Results and Discussion

#### 3.3.1. Method Development

##### 3.3.1.1. HPLC-MS Analysis

The determination of residual drug and identification of possible metabolites in the plasma and tissue of treated animals is an important tool for the investigation of the pharmacological and toxicological characteristics of any drug substance. Currently there is no record of a sufficiently sensitive, as well as selective assay for the quantification and qualification of the veterinary trypanocide isometamidium, in the presence of its major related substances. Spectrophotometric assays using ultraviolet fluorescence microscopy enabled the detection of a concentration of 1 µg/ml in serum, measuring all isomers and related substances present in the formulation as one compound (Ali & Hassan, 1984; Braide & Eghianruwa, 1980; Philips *et al.*, 1967). An indirect HPLC method developed by Perschke and Vollner (1985) used the transformation of ISM to its degradation product homidium prior to quantification and thus is not specific in its presence. Furthermore the limit of quantification of all these approaches only allowed detection of the total drug up to 24 h after administration. Consequently, pharmacokinetic studies over an extended period of time were not possible. The advent of immunoassays with detection limits down to 0.5 ng/ml in serum, overcame that problem (Eisler *et al.*, 1993; Eisler *et al.*, 1996a). However, still no separation and selective quantification of the related substances was possible. Furthermore, immunoassays exhibit cross-reactivity with structurally related compounds, such as homidium, which is also used as a trypanocidal drug and can thus lead to falsely high results. A reversed phase HPLC-UV assay for the selective qualification and quantification of ISM in the presence of its isomers and other process related substances has been

described (chapter 2). The assay was shown to be compatible with mass spectrometric detection using the conditions described in section 3.2.6. Baseline separation of M&B4180A, its isomers M&B4250 and M&B38897, the related substance M&B4596 and the main degradation product homidium was achieved (figure 3.2). Mass spectra of the compounds are shown in figure 3.3.

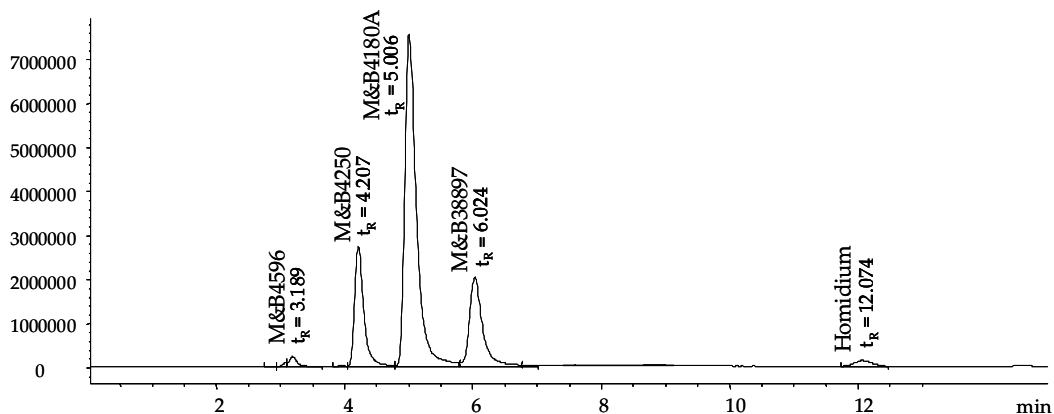


Figure 3.2: Representative total ion chromatogram obtained from HPLC-MS analysis of M&B4180A and related substances. Experimental conditions as described in section 3.2.6.

The mass spectra show the most abundant ion generated in the source for each analyte. For the isomers M&B4250, M&B4180A and M&B38897 these are double charged ions at  $m/z = 230.5$ , for the bis-amidino substituted analogue M&B4596 it is a double charged ion at  $m/z = 303.5$  and the single charged ion at  $m/z = 314$  for homidium (see also table 2.4). These highly abundant ions were chosen for most sensitive detection of the analytes in selected ion mode. Use of selected ion mode not only decreases the limits of detection and quantification compared to a UV detector or MS detection in full scan mode, but also results in better selectivity for compounds with different mass to charge ratios.

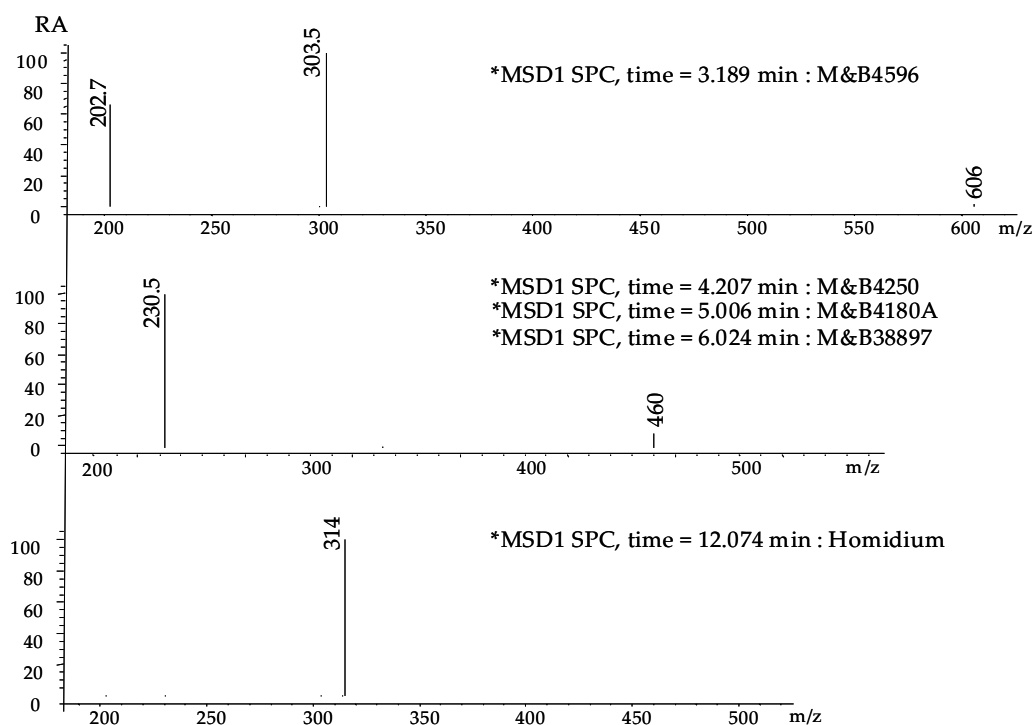


Figure 3.3: Mass spectra obtained from HPLC-MS analysis of M&B4180A and related substances. Retention times relate to peaks as seen in figure 3.2.

### 3.3.1.2. Internal standard

To compensate for variations during sample preparation, a known concentration of internal standard needs to be added to every sample. This internal standard experiences the same preparation procedure, including the same possible losses as the compounds of interest. The ratio between peak areas of analyte and internal standard is used for quantitation, rather than peak areas only. Ideally the internal standard should possess physicochemical properties similar to those of the compounds of interest, without affecting the separation. Dimidium bromide (figure 3.4), a structurally related compound, which itself is not used as a trypanocide anymore, was examined for that purpose.

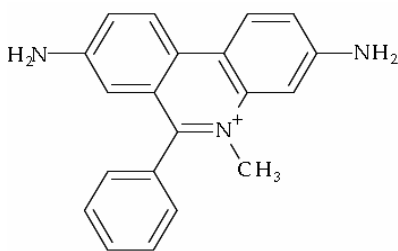


Figure 3.4: Chemical structure of the possible internal standard dimidium

It elutes from the column just after M&B38897 and before homidium and is completely resolved from all the components of the mixture (figure 3.5 a).

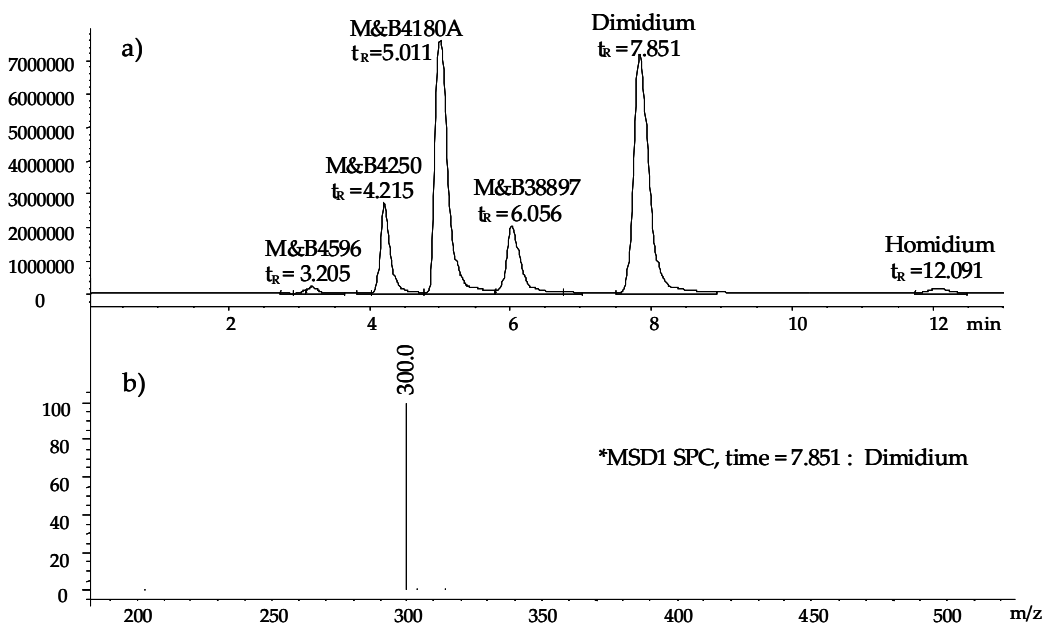


Figure 3.5: a) Total ion chromatogram obtained from HPLC-MS analysis of M&B4180A and related substances with added dimidium bromide as an internal standard b) Mass spectrum of dimidium bromide; retention time relates to peak as seen in figure 3.4 a).

Figure 3.5 b) shows the mass spectrum of dimidium and the molecular ion  $[M^+]$  with a  $m/z$  value of 300, which enables selective MS detection in the presence of the other compounds of interest as can be seen in figure 3.6. Therefore dimidium bromide was considered suitable as an internal standard for the bioanalytical investigation of ISM and related substances and it was used in subsequent experiments.



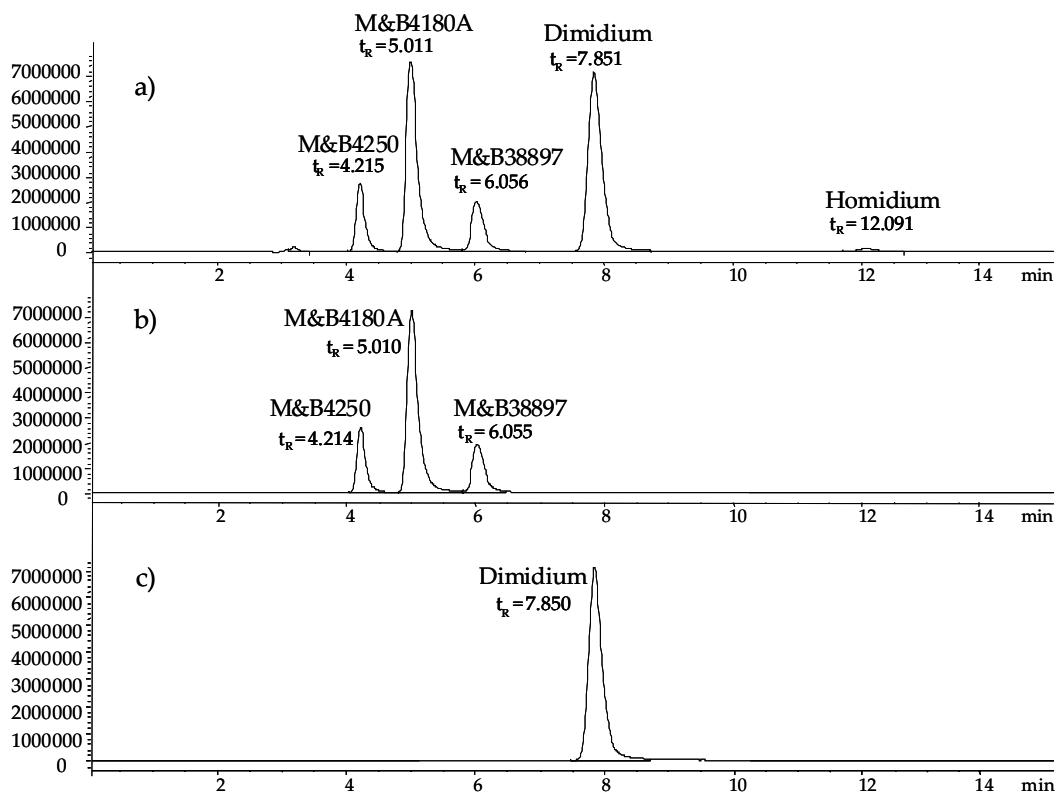


Figure 3.6: a) Total ion chromatogram obtained from HPLC-MS analysis of M&B4180A and related substances with added dimidium bromide as internal standard b) Selected ion chromatogram obtained for the isomer ions with  $m/z = 230.5$  c) Selected ion chromatogram obtained for the internal standard ion with  $m/z = 300$

### 3.3.1.3. Solid Phase Extraction

As by their nature quaternary ammonium compounds are ionized at all pH values and are not readily extracted into organic solvents, the extraction of ISM from biological matrices is problematic (Russ-Kirschenbaum *et al.*, 1989). Although solvent extraction using an ion-pairing reagent has been reported, this procedure is rather time consuming and involves high organic solvent consumption. Alternatively protein precipitation is possible but could cause the loss of a considerable amount of analyte, as ISM is known to strongly and irreversibly bind to plasma and tissue macromolecules (Philips *et al.*, 1967).

A solid phase extraction (SPE) sample preparation procedure using C8 Bond Elut cartridges has been successfully employed for the extraction of ISM from plasma (Kinabo & Bogan, 1988c). Moreover this approach could be developed into an on-line SPE-LC approach for direct analysis of the drug in small-volume plasma samples (Steiner *et al.*, 2007). The application would benefit from the reduction in sample load, optimized enrichment factors and huge savings in time and solvent consumption.

The choice of a suitable elution solvent is challenging as ISM is unstable in strongly acidic and basic conditions and at high temperatures (Kinabo & Bogan, 1988c). Therefore an appropriate eluent with an intermediate pH that can be readily evaporated to allow sample reconstitution is required. Sample extraction was previously described using a mixture of methanol, heptane sulphonic acid and triethylamine (92 : 8 : 0.1 v/v/v) (Kinabo & Bogan, 1988c) with reported recoveries over 80 %. However, this assay did not consider that ISM formulations contain a mixture of compounds with at least three isomers in considerable concentrations. Furthermore, the presence of the strong ion pair reagent, heptane sulfonic acid, in the reconstituted samples can cause significant suppression of MS signals of the compounds under investigation. The non-volatile ion-pair hinders the analytes from escaping the droplets during electrospray ionisation (Miller & Fischer, 2000), rendering this approach unsuitable for analysis with MS detection. In 1989 Russ-Kirschenbaum *et al.* reported the use of a solution of a halide salt, dissolved in methanol as an SPE eluent for quaternary ammonium compounds. Thus, methanol saturated with ammonium chloride was examined as elution solvent for the extraction of ISM from plasma on various SPE cartridges (section 3.2.5). This procedure gave markedly higher recovery values than the previously reported approach (Kinabo & Bogan, 1988c), with

up to 100 % recovery for all the analytes investigated (table 3.2). Also the stability of ISM after extraction with the slightly acidic eluent (pH = 4.51) was examined and no degradation to homidium during the procedure could be detected when analysing six separately prepared samples (figure 3.7).

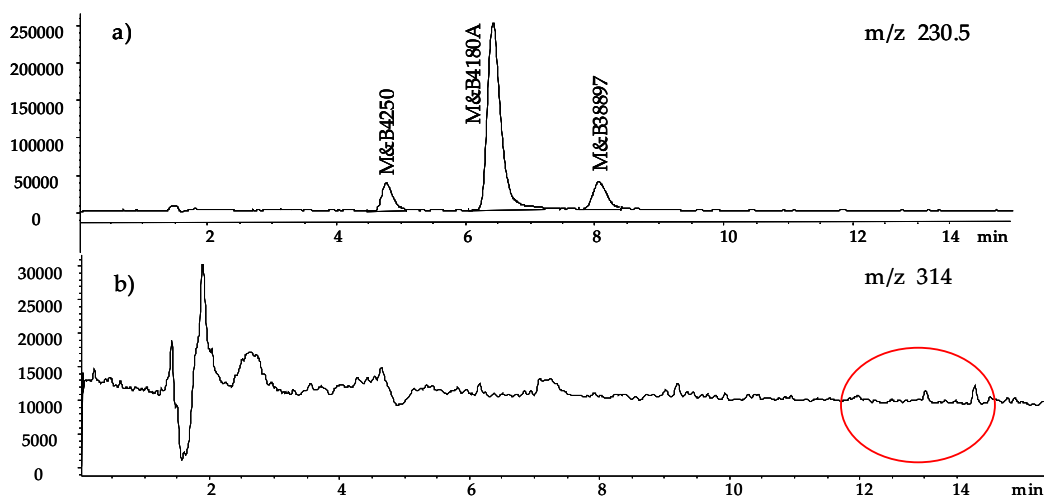


Figure 3.7: a) Selected ion chromatogram obtained for the isomer ions ( $m/z = 230.5$ ) b) Selected ion chromatogram obtained for the degradation product ion (homidium) with  $m/z = 314$  in ISM sample after SPE extraction from bovine plasma using methanol saturated with ammonium chloride as extraction solvent. HPLC-MS conditions as described in section 3.2.6.

Four different kinds of solid phase extraction cartridges were examined (table 3.2). Phenomenex, Strata C8 and C18-E reversed phase cartridges exhibit different selectivities due to differences in their lipophilicities. They differ in retention behaviour of the analytes under investigation due to hydrophobic interaction. Use of a Strata-X-CW column exploits ionic interaction of the permanently charged quaternary ammonium compounds with a weak cation exchanger. With a Strata-X polymeric cartridge retention is due to lipophilic interactions without the additional effect of residual silanol groups as present with the silica based C8 and C18-E reversed phase stationary phases. All four cartridges with different retention mechanisms for the permanently charged organic compounds of interest were examined for

the clean up procedure and recovery of ISM and related substances. The recovery data (table 3.2) showed that best and most reproducible results were obtained using C8 cartridges. Recovery found for all compounds was > 80 % with %RSD of < 15 %.

Table 3.2: Comparison of recovery of isometamidium and related substances from plasma using four different SPE cartridges

SPE cartridge	Concentration of analyte ( $\mu\text{g/ml}$ )	Average recovery (%) ( $\bar{x} \pm \text{R.S.D.}, n = 5$ )
Strata -X	M&B4180A: 0.25	73.3 $\pm$ 17.7
	M&B4250: 0.05	141.6 $\pm$ 40.8
	M&B38897: 0.05	94.6 $\pm$ 14.9
	Homidium: 0.25	113.4 $\pm$ 8.3
Strata-X-CW	M&B4180A: 0.25	51.9 $\pm$ 5.4
	M&B4250: 0.05	108.4 $\pm$ 14.5
	M&B38897: 0.05	50.2 $\pm$ 4.1
	Homidium: 0.25	95.2 $\pm$ 4.5
Strata C18-E	M&B4180A: 0.25	50.0 $\pm$ 2.0
	M&B4250: 0.05	80.4 $\pm$ 11.1
	M&B38897: 0.05	89.2 $\pm$ 3.7
	Homidium: 0.25	83.9 $\pm$ 4.9
Strata C8	M&B4180A: 0.25	82.1 $\pm$ 10.3
	M&B4250: 0.05	112.4 $\pm$ 7.3
	M&B38897: 0.05	90.1 $\pm$ 6.3
	Homidium: 0.25	86.9 $\pm$ 1.8

During method development unexpectedly high values for recovery of over 120 % occurred. This problem was thought to be due to the adsorption of ISM and its isomers that contain a highly basic amidino moiety, to residual silanol groups in silica-based glassware. At low analyte concentrations this effect can seriously affect the accuracy of the assay. The loss due to this problem seemed to be greater in control standards than in spiked plasma samples. It is probable that ammonium chloride, present in samples after extraction, prevents the analytes from adsorbing to the injection vial glass. Another possible reason is the plasma binding capacity of ISM, reducing the

amount of drug that is adsorbed to glassware. To overcome this problem, control standards were then prepared by spiking amounts of internal and reference standards, equal to those in spiked plasma samples into plasma extracts from solid phase extraction of unspiked plasma, rather than just by diluting in mobile phase. Furthermore, this approach does account for any probable matrix effects. Ion suppression or enhancement caused by the sample matrix could otherwise affect accuracy and reproducibility of the assay (Matuszewski *et al.*, 2003). To avoid further loss of a compound due to glassware, the flasks and vials used were deactivated as described (section 3.2.1) and 1 %v/v of isopropyl alcohol was added to any solvent used to dissolve and reconstitute the analytes, as it is thought to compete for the adsorptive sites on the glass surface (Supelco, 1997).

The effect of masking the adsorptive sites and addition of the alcohol to the solvent is graphically demonstrated in figure 3.7.

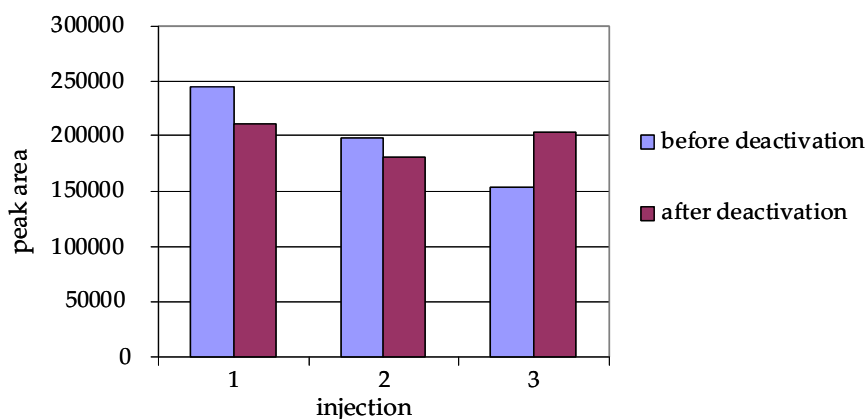


Figure 3.7: Effect of the masking of adsorptive sites on the adsorption of ISM on glassware

Before glassware-deactivation, there is a decrease in peak area (blue columns) for M&B4180A on three successive injections of one sample (concentration of 20 ng/ml). These data result in a %RSD of 22.7 %. After deactivation of glassware and addition of 1 %v/v isopropyl alcohol, the peak

area varied to a lesser extent (purple columns) with the %RSD reduced to 7.6 %. These findings prove the usefulness of this approach to avoid the loss of ISM due to its adsorption to glassware.

### 3.3.2. Metabolism Studies

In order to demonstrate the selectivity of the assay in the presence of possible metabolites, the formation of phase I metabolites using a rat liver microsomal preparation was investigated. Incubation of flurazepam with the microsomal preparation (section 3.2.3) showed the system to be metabolically active, as all the known metabolites (Lau *et al.*, 1987; Schwartz & Postma E., 1970; Song *et al.*, 1994) could be detected by LC-MS. A scheme of the metabolic pathways of flurazepam is shown in figure 3.8.

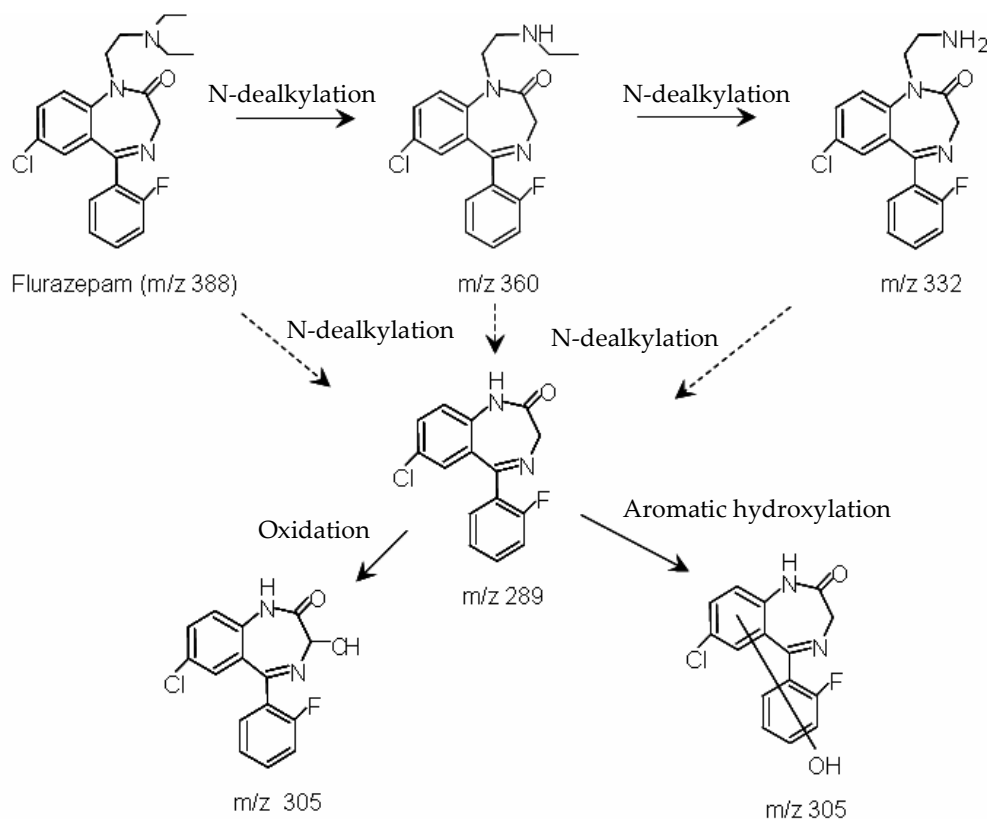


Figure 3.8: Metabolic scheme of flurazepam in rat liver microsomes with *m/z* values for ions produced (Duong Thi *et al.*, 2009)

The selected ion mass chromatograms of the flurazepam samples incubated with rat liver microsomes are shown in figure 3.9.

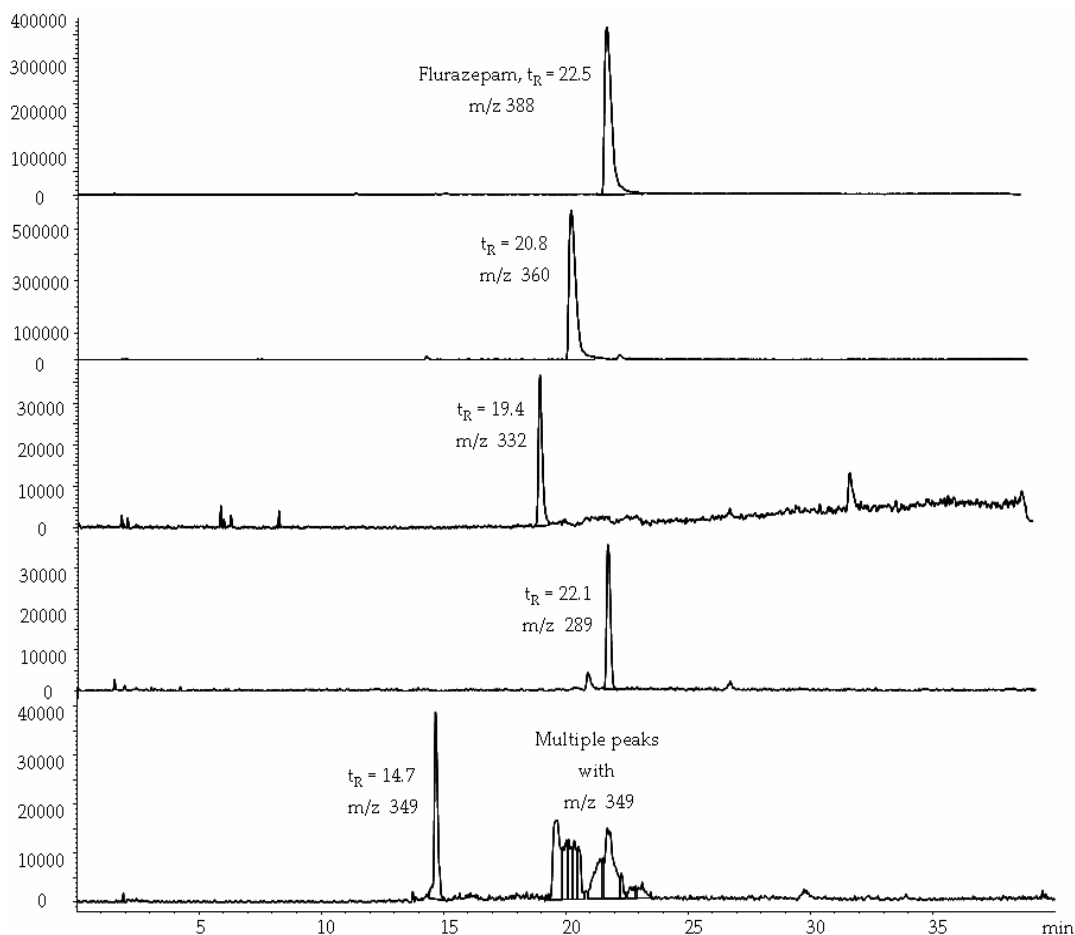


Figure 3.9: HPLC-MS selected ion mass chromatograms obtained from analysis of incubation of flurazepam with rat liver microsomes

The chromatograms show an 80 % decrease in peak area from 42,607,500 AU to 7,720,570 AU in the flurazepam sample incubated with rat liver microsomes as compared to flurazepam in buffer only, indicating extensive metabolism of the drug. Metabolite ions with  $m/z$  values of 360, 332 and 289 are known metabolites (figure 3.8). An expected ion (Duong Thi *et al.*, 2009) at  $m/z = 305$  due to the hydroxylated N-dealkylated metabolite was not detected. Instead multiple ions with  $m/z$  values of 349 were observed. As none of these ions were detected in an incubated sample of flurazepam

containing no microsomes, it was concluded that they were metabolites of flurazepam and the system is shown to be metabolically active. HPLC-MS analysis of the sample from microsomal incubation with ISM does not provide any evidence of phase I metabolite formation. The HPLC-MS chromatograms (figure 3.10) show no apparent difference in the peak areas of ISM samples incubated with rat liver microsomes and samples incubated with buffer only. These results indicate that no metabolism took place. Ions of possible metabolites formed by oxidation, as suggested by Boibessot *et al.* (2006) (figure 3.1) at  $m/z = 475$  or  $m/z = 238$  for double charged ions could not be detected.

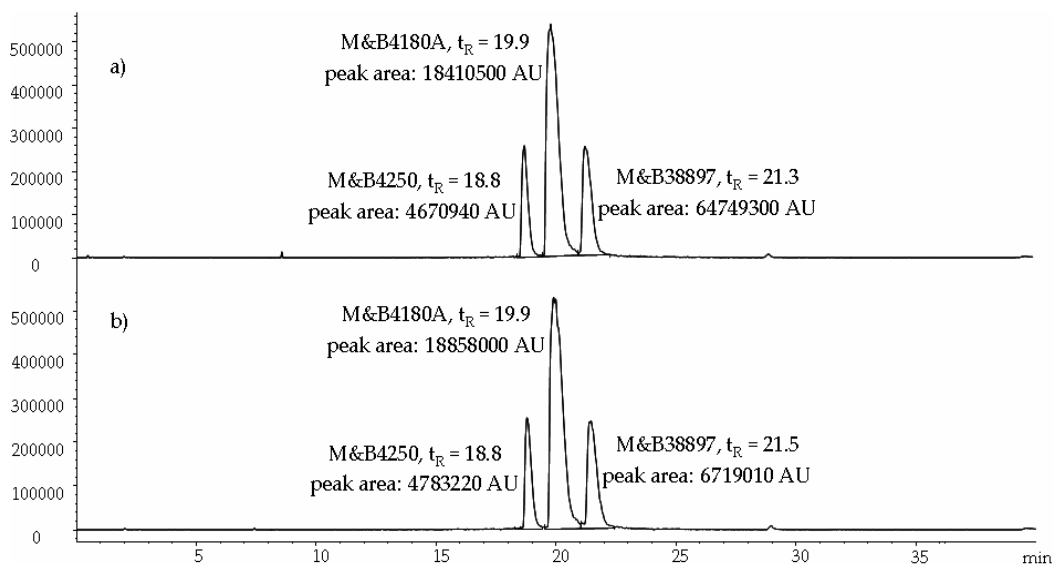


Figure 3.10: Representative HPLC-MS selected ion mass chromatograms obtained from analysis of incubation of ISM and structural isomers with a) homogenising buffer and b) rat liver microsomes

Since drug metabolism is a mechanism to render a lipophilic compound more polar, hence more soluble, to facilitate its excretion through the kidneys, it is plausible that ISM is not extensively metabolised, as it is already sufficiently polar to be excreted. Previous pharmacokinetic studies reported excretion of unaltered drug via faeces, urine and bile (Kinabo & Bogan, 1988d; Murilla *et al.*, 1996). This *in vitro* study showed that no



interference to the HPLC-MS assay from putative metabolites was likely during analysis of ISM plasma samples from treated animals.

### 3.3.3. Validation of the Bioanalytical Assay

The ratios of the peak area of analyte to those of internal standard for M&B4180A and related compounds showed a rectilinear relationship with analyte concentration within the specified ranges (figure 3.11; table 3.3), which are consistent with reported concentrations of residual ISM in serum of treated animals (Eisler *et al.*, 1996b).

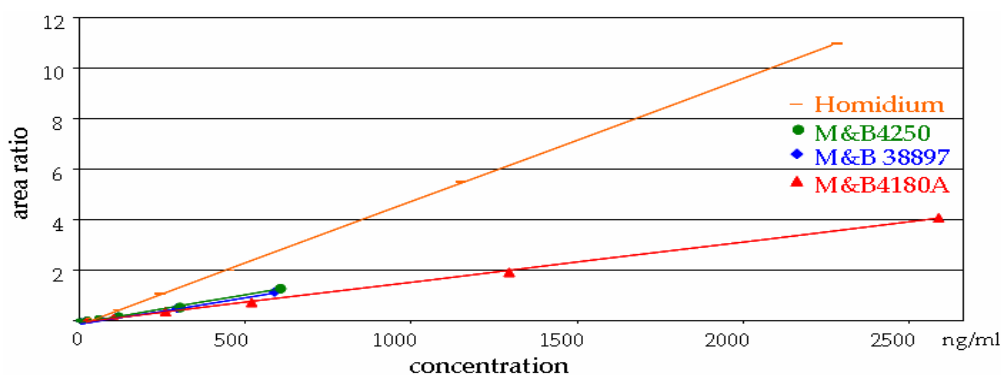


Figure 3.11: Plots of peak area vs. concentration for ISM and related substances

Linear regression analysis showed that the correlation coefficients ( $R^2$ ) for all calibration curves were  $\geq 0.998$  with minimal variation in the slopes and intercepts (table 3.3).

Table 3.3: Regression analysis of calibration curves generated from the analysis of M&B4180A and related substances in spiked plasma

Analyte	Range	<i>n</i>	Slope	Intercept	Correlation coefficient ( $r^2$ )
M&B 4180A	20 – 2500 (ng/ml)	5	$0.002 \pm 0.0001$	$0.007 \pm 0.05$	$0.999 \pm 0.003$
M&B 4250	5 – 600 (ng/ml)	5	$0.002 \pm 0.0002$	$0.026 \pm 0.006$	$0.998 \pm 0.003$
M&B 38897	5 – 600 (ng/ml)	5	$0.002 \pm 0.001$	$0.010 \pm 0.007$	$0.999 \pm 0.0004$
Homidium	20 – 2500 (ng/ml)	5	$0.005 \pm 0.0003$	$0.094 \pm 0.06$	$0.999 \pm 0.0004$

The method was not validated for determination of the bis-amidino substituted analogue M&B4596, as it is unlikely to be present in serum samples of treated animals in detectable concentrations, as it is a minor component in ISM formulations.

The limit of detection for each analyte was determined as the concentration that gave a signal-to-noise ratio  $\geq 3$  (figure 3.12).

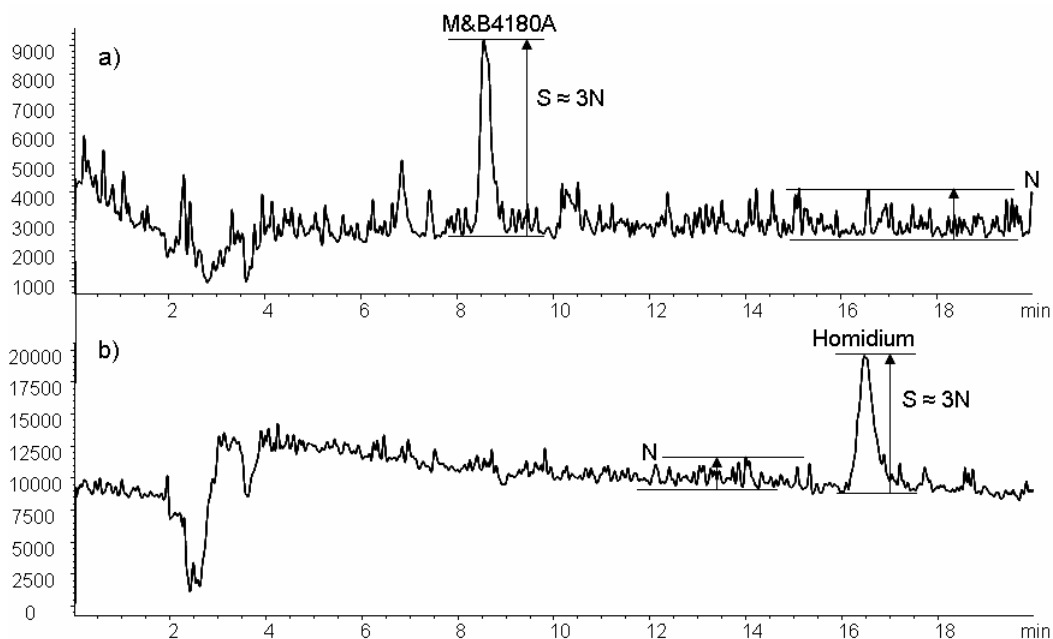


Figure 3.12: HPLC-MS selected ion mass chromatograms of a) ISM and b) homidium at a concentration of 5 ng/ml. Conditions as described in section 3.2.6.

The limit of quantification was established as the concentration that gave a signal-to-noise ratio  $\geq 9$  (figure 3.13) and a %RSD of peak areas  $\leq 10$  %.

Limits of detection and quantification of the method (table 3.4) represent the concentration of analyte present in a reconstituted sample after solid phase extraction. An aliquot (1 ml) of extract is taken to dryness and reconstituted in 200  $\mu$ l of solvent (section 3.2.5). The samples analysed in the HPLC-MS assay are therefore five times more concentrated than the actual amount of compound spiked into the initial volume of plasma.

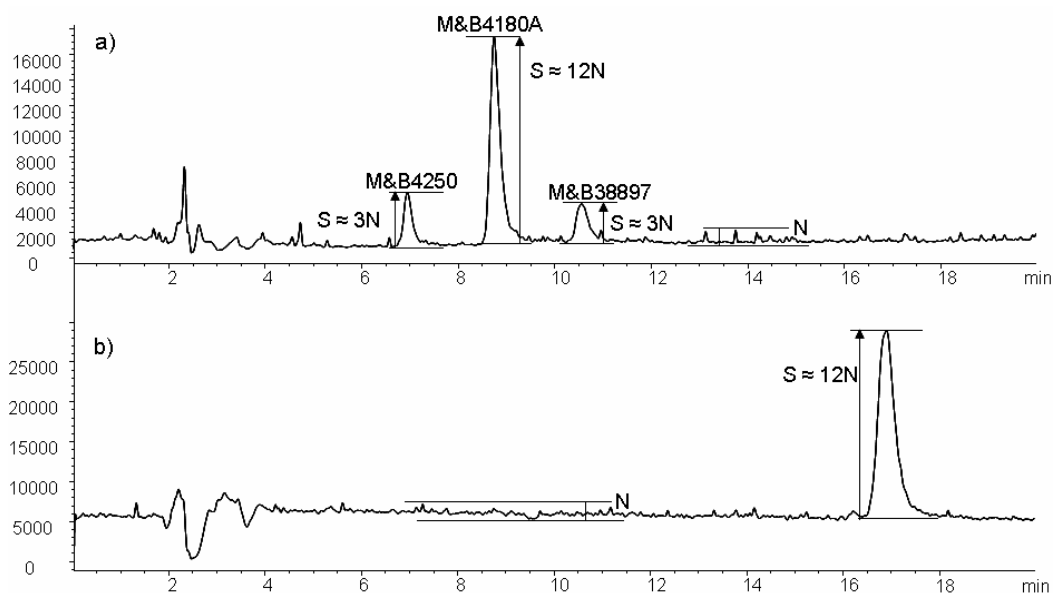


Figure 3.13: HPLC-MS selected ion mass chromatograms of a) ISM at a concentration of 20 ng/ml and M&B4250 and M&B38897 at a concentration of 5 ng/ml and b) homidium at a concentration of 20 ng/ml. Conditions as described in section 3.2.6.

Table 3.4: Summary of the sensitivity of the HPLC-MS assay for ISM, its isomers and the degradation product homidium

		M&B4180A	M&B38897	M&B4250	Homidium
LOD	S/N = 3	5 ng/ml	5 ng/ml	5 ng/ml	5 ng/ml
LOQ	%RSD ≤ 10	20 ng/ml	15 ng/ml	15 ng/ml	20 ng/ml

Because of the final concentration step (5 x), this method potentially has a detection limit of 1 ng/ml in plasma for all the compounds. Therefore the assay is 10 times more sensitive than a previously reported HPLC method (Kinabo & Bogan, 1988c) and almost as sensitive as an immunoassay (0.5 ng/ml) (Eisler *et al.*, 1996a), with the advantage of unambiguous selectivity for all the analytes.

Selectivity of the assay for M&B4180A in the presence of its known isomers, its degradation product homidium and the internal standard dimidium has been demonstrated in section 3.3.1.1 and 3.3.1.2 in figures 3.2 - 3.6.

Despite all precautions to avoid adsorption of the analytes on glassware and use of an internal standard to compensate for any losses during sample preparation, overall the method still failed to prove good precision with respect to recovery. The intra-day assay precision (%RSD) of peak area ratios for M&B4180A at the working concentration of 4 - 250 ng/ml plasma gave values of variation just little higher (10 %) than the results reported by Kinabo and Bogan (6 - 8 %) (Kinabo & Bogan, 1988c). Inter-day precision, however, resulted in variation as high as 30 % (table 3.5).

Moreover, recovery values for the isomers M&B4250 and M&B38897 were also not sufficiently precise (%RSD  $\leq$  15) (Bansal & DeStefano, 2007) to consider the results accurate.

Table 3.5: Precision of the bioanalytical method for the determination of isometamidium and related substances in spiked plasma samples

	<b>M&amp;B4180A</b>			<b>M&amp;B4250</b>		
	ng/ml	% recovery	%RSD	ng/ml	% recovery	%RSD
<b>Inter-day precision</b>						
Day 1 ( $n=3$ )	4	77.7 $\pm$ 5.3	6.9	1	85.1 $\pm$ 12.9	15.1
Day 2 ( $n=3$ )	50	87.5 $\pm$ 13.1	14.9	12	71.6 $\pm$ 8.4	11.7
Day 3 ( $n=3$ )	250	93.0 $\pm$ 28.0	30.1	60	77.2 $\pm$ 7.8	10.1
<b>Intra-day precision</b>						
Solution 1	4	82.1 $\pm$ 2.7	3.3	1	81.3 $\pm$ 7.4	9.1
Solution 2	50	102.4 $\pm$ 10.8	10.5	12	67.1 $\pm$ 2.8	4.2
Solution 3	250	97.5 $\pm$ 4.1	4.2	60	86.0 $\pm$ 8.5	9.9
	<b>M&amp;B38897</b>			<b>Homidium</b>		
	ng/ml	% recovery	%RSD	ng/ml	% recovery	%RSD
<b>Inter-day precision</b>						
Day 1 ( $n=3$ )	1	86.5 $\pm$ 7.0	8.1	4	92.6 $\pm$ 6.3	6.8
Day 2 ( $n=3$ )	12	95.2 $\pm$ 14.9	15.7	50	92.3 $\pm$ 2.3	2.5
Day 3 ( $n=3$ )	60	98.1 $\pm$ 20.9	21.3	250	95.1 $\pm$ 5.2	5.5
<b>Intra-day precision</b>						
Solution 1	1	81.8 $\pm$ 4.0	4.9	4	98.8 $\pm$ 1.8	1.8
Solution 2	12	87.0 $\pm$ 18.8	21.6	50	94.2 $\pm$ 1.8	1.9
Solution 3	60	101.8 $\pm$ 4.2	3.3	250	100.2 $\pm$ 2.3	2.3

Only quantification of homidium gave good values with a relative standard deviation as low as 2.3 % for the intra-day and < 7 % for the inter-day assay precision (table 3.5). These results show that the internal standard dimidium, does compensate for variations during the sample preparation procedure far better for homidium than for ISM and its structural isomers. Dimidium is structurally very similar to homidium but lacks the strongly basic amidino moiety present in ISM (M&B4180A), M&B4250 and M&B38897. The losses due to adsorption to plasma and glassware are not accounted for using this internal standard. Furthermore homidium and dimidium are more stable than ISM and less prone to degradation during sample preparation and analysis time.

These results indicate that further development is required to produce a method suitable for the bioanalytical investigation of ISM and related substances.

### 3.4. Conclusions

With the method described successful extraction of the isomers of isometamidium chloride M&B4180A, M&B4250 and M&B38897 and the main degradation product homidium from spiked plasma samples was achieved and the advantage of using NH<sub>4</sub>Cl saturated methanol as elution solvent could be demonstrated. The problem of adverse matrix effects and analyte absorption to the residual silanol groups in the glassware used could be overcome by preparing reference standards in blank plasma extracts, use of deactivated, silanized glassware and addition of 1 %v/v iso-propanol to the reconstitution solvent to compete for the adsorptive sites on the glass surface.

Dimidium bromide was shown to be a suitable internal standard and was employed to compensate for any variation due to sample preparation. With its structure being very similar to the structure of homidium, only differing in one alkyl group, results for accuracy and precision for the degradation product are far more accurate using this approach than those for ISM and related substances. Lacking the highly basic amidino moiety, higher losses of these compounds, due to adsorption to glassware are not accounted for using dimidium as an internal standard. Use of one of the structural isomers of ISM would be a better choice for this method, however with all of those being present in ISM formulations, this option is not applicable.

The HPLC-MS assay as described in section 2.3.2 was used in selected ion mode for the highly selective and sensitive determination of ISM, its isomers and related substances in question. Interference due to possible phase I metabolites was screened out by an *in vitro* metabolism study.

Limits of detection and quantification were considerably improved compared to previously reported HPLC assays with the further advantage of unambiguous specificity for all compounds present.

The linear relationship between peak area ratios of analyte and internal standard and concentration could be demonstrated by linear regression analysis, which showed a correlation coefficient ( $R^2$ ) for calibration curves of all analytes of  $\geq 0.998$ .

The method however failed to prove good precision for all analytes under investigation. Repeatability and reproducibility of the determination of homidium could be demonstrated by an intra-day and inter-day assay precision of usually  $< 7\%$  (%RSD) for replicate ( $n = 3$ ) injections of separately prepared standard solutions of different concentration (table 3.4). With %RSD of up to 30.1 % in repeatability studies of M&B4180A and its structural isomers M&B4250 and M&B38897 quantification gave poor precision for these compounds and therefore the method does need further examination.

After concentrating on the development and optimisation of a suitable sample preparation procedure during this study the next chapter will focus on optimisation of the HPLC-MS analysis of the prepared samples. If it is possible to further enhance selectivity and sensitivity of the assay, it is likely to achieve more precise data even in very low analyte concentration levels. As interactions of the highly basic compounds of interest with residual silanol groups on the stationary phase still give rise to severe peak tailing, the possibility of using a different, high purity silica phase will be investigated. Also the use of other stationary phase chemistry with altered selectivity for the analytes is an option for additional improvement.

## **4. Comparative Study of the Effect of Stationary Phase Chemistry and Mobile Phase Selectivity on the HPLC Separation of Isometamidium and Related Substances**

### **4.1. Introduction**

The method developed for the bioanalytical investigation of ISM and related substances (chapter 3) failed to provide good precision for the determination of small amounts of residual trypanocide in biological matrices from treated livestock. The HPLC-MS assay required an increase in sensitivity and column performance. As interactions of the highly basic compounds of interest with residual silanols in the silica-based stationary phase still give rise to severe peak tailing resulting in a loss of sensitivity, this chapter will focus on the possibility of using different, high purity silica HPLC phases. Also the use of other stationary phase chemistry with altered selectivity for the analytes will be investigated. If it was feasible to further enhance selectivity and sensitivity of the assay, it might be possible to achieve more precise data even at very low analyte concentrations.

#### **4.1.1. The Resolution Equation**

The goal of any chromatographic separation is the adequate resolution of the components of interest in reasonable time, resolution being defined as the differences in retention time and peak width of two adjacent peaks. Resolution can be improved by either increasing the separation of two analytes or by decreasing the band widths. It is a function of the retention factor ( $k$ ), a measure of how well an analyte is retained, selectivity ( $\alpha$ ), which is a measure of the relative retention of two components in a mixture and the efficiency ( $N$ ), expressed in theoretical plates (Snyder *et al.*, 1997a).



The resolution equation (equation 1) shows the dependency of resolution on the parameters  $\alpha$ ,  $k$  and  $N$ .

Equation 1: Resolution Equation

$$R_s = \left( \frac{1}{4} \right) N^{0.5} \left( \frac{\alpha - 1}{\alpha} \right) \left( \frac{k}{1 + k} \right)$$

Efficiency
Selectivity
Retention factor

In method development the first stage is to get acceptable sample retention times with a selected column and mobile phase combination, with  $0.5 < k < 20$  for all compounds under investigation. After appropriate retention is obtained, selectivity of a separation can be optimised by changes in mobile phase composition, stationary phase chemistry or temperature (Snyder *et al.*, 1997a).

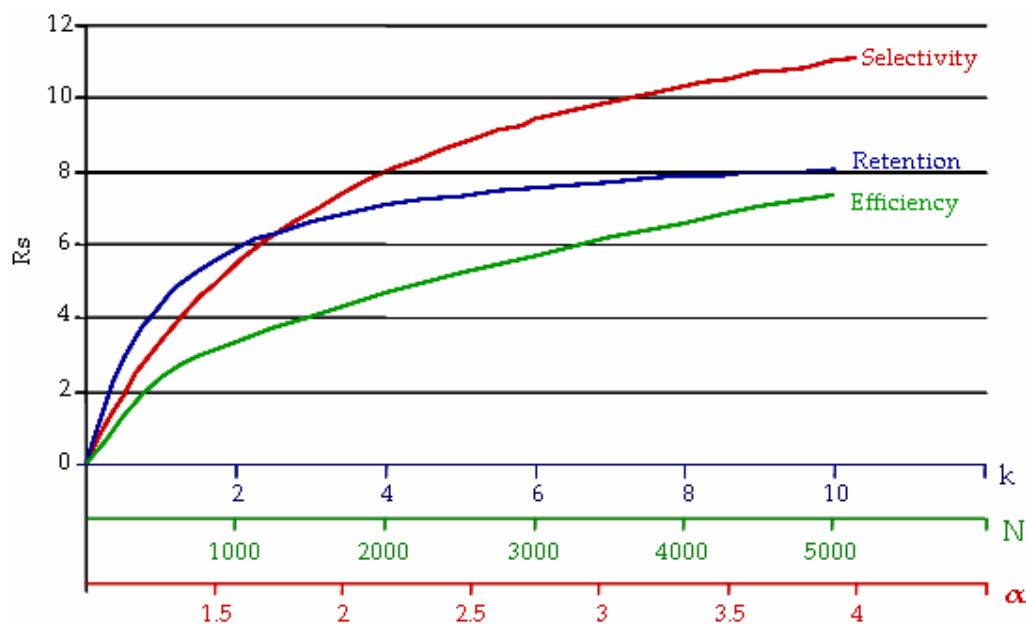


Figure 4.1: Relative impact of retention, selectivity and efficiency on resolution

When satisfactory retention and selectivity are achieved, adjustments in flow rate, particle size and column dimensions can be used to further improve the separation in terms of efficiency. The overall aim is to enable all solutes of one analyte to elute together in a small volume, resulting in small bandwidth and high, well resolved peaks.

Figure 4.1 shows the impact of each of the three factors ( $k$ ,  $\alpha$ ,  $N$ ) on resolution. Once retention reaches a  $k$  value  $> 2$  the curve flattens out and increasing retention does not strongly affect resolution anymore and then changing selectivity has the greatest effect on resolution. Hence, the major focus in method development centres on changing selectivity. The effect of increasing column efficiency is less marked, as doubling the plate count ( $N$ ) increases resolution only by a factor of  $\sqrt{2}$ .

Whilst the developed method for ISM and related substances does provide good retention of the analytes under investigation (chapter 2; figure 2.4) further optimisation will focus on improvements in selectivity and efficiency.

#### 4.1.2. Selectivity

Selectivity ( $\alpha$ ) is defined as the difference in the relative retention of two analytes for given stationary phase and mobile phase conditions (equation 2; figure 4.2).

Equation 2:                      Selectivity                      
$$\alpha = \frac{t'_{R2}}{t'_{R1}} = \frac{k_2}{k_1}$$

The selectivity factor depends on the ratio between the retention factors  $k_2$  and  $k_1$  of late- and early-eluting peaks (figure 4.2).

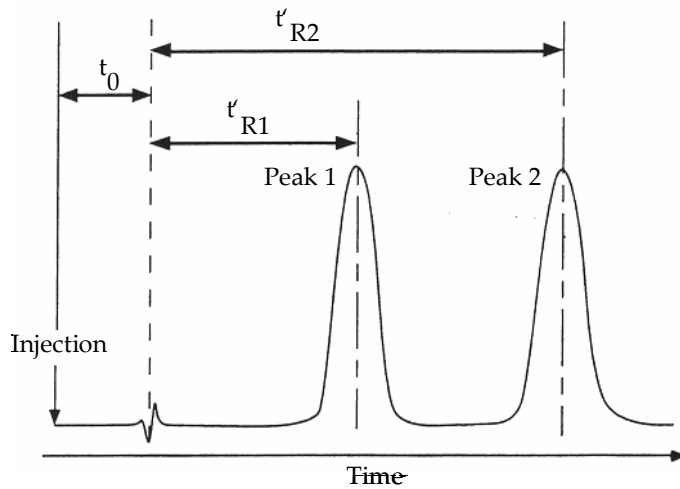


Figure 4.2: Graphical demonstration of selectivity

The retention factor  $k$  can be expressed as stated in equation 3, where  $t_R$  is the retention time of the peak of interest and  $t_0$  is the time an unretained solute takes to travel through the column (“column dead-volume time”) (Haky, 2005).

Equation 3: Retention Factor 
$$k = \frac{(t_R - t_0)}{t_0}$$

Column dead time depends on column dead volume as follows:

Equation 4: Column dead-volume time 
$$t_0 = \frac{V_m}{F}$$

With  $F$  being the flow rate and  $V_m$  being the column dead volume of the column, calculated as:

Equation 5: Column dead-volume 
$$V_m = 0.5 L d_c^2$$

where  $V_m$  is the column dead-volume in ml,  $L$  is the column length in cm and  $d_c$  is the internal diameter of the column in cm.

Retention factor ( $k$ ) and selectivity ( $\alpha$ ) are affected by parameters that determine retention, as defined by the equilibrium distribution of solutes between the stationary and mobile phases. Accordingly selectivity can be altered by changes in stationary phase chemistry, mobile phase composition and also by varying temperature (Snyder *et al.*, 1997a).

Mobile phase solvents should be chosen taking practical properties into account, such as toxicity, commercial availability and compatibility with mass spectrometry if required. Solute molecules are attracted to mobile phase molecules based on a combination of hydrogen bonding and dipole interactions, hence dipole moment, acidity and basicity of a solvent will affect mobile phase selectivity (Snyder *et al.*, 1997a). Once a suitable solvent has been identified, changes in the % organic solvent in the mobile phase have a great impact on solute band spacing in HPLC and should be one of the first parameters to be investigated when optimising selectivity of a given method. Plotting  $\log k$  vs. % organic generally gives a straight line, indicating a linear relationship between these two parameters. This correlation is used to predict HPLC separations using computer simulation software such as DryLab<sup>®</sup>, which will be further described in section 4.1.3.

Temperature also affects selectivity. The van't Hoff equation (equation 6) describes the inverse relationship between the retention factor ( $k$ ) and temperature ( $T$ ) (Wilson *et al.*, 2002a).

Equation 6:            van't Hoff equation             $\log k \propto \frac{1}{T}$

Plotting  $\log k$  vs.  $1/T$  (in Kelvin) gives a straight line, illustrating that higher temperature reduces retention and results in sharper analyte peaks (Marin *et al.*, 2004). Due to this effect on selectivity temperature can also be

used as a computer simulation input parameter in programs such as DryLab®, to optimise a separation (see also section 4.1.3).

When using high temperature for HPLC analysis pre-heating is essential, as axial and radial temperature gradients cause band broadening and retention time shifts (Wolcott *et al.*, 2000). Different analyte distribution between stationary and mobile phase in different parts of the stationary phase bed caused by temperature gradients needs to be avoided as well as differences in mobile phase viscosity and thereby differences in diffusion rates (Greibrokk & Andersen, 2003).

Use of high temperature however can be restricted by the specifications of the equipment. Maximum oven temperature and column stability are limitations, as well as the stability of the compounds under investigation (Greibrokk & Andersen, 2003). Use of higher temperatures has the potential to rapidly degrade not only the stationary phase, due to the higher rate of dissolution of the silica support or cleavage of the bonded ligands, but also analytes with thermolabile functional groups (He & Yang, 2003).

Elevated temperatures also improve sample solubility and can affect selectivity by altering the pKa or the extent of ionisation of an analyte. With state of the art instrumentation including column oven and thermostat, changes in temperature are feasible and a convenient parameter to slightly alter retention of the analytes and possibly improve resolution (Snyder *et al.*, 1997a).

Changing the stationary phase chemistry usually causes a more abrupt change in the selectivity of a separation. Most commercially available HPLC columns consist of a porous silica support with a bonded organic layer. Due to differences of the bonded phase, column packings vary in selectivity. The retention behaviour of a stationary phase depends on its

chemical nature or functionality, surface coverage of the bonded phase, nature of the chemical bonding between organic layer and silica particles and the quality of the silica surface (Snyder *et al.*, 1997a). To successfully exploit these different characteristics in method development it is important to understand which columns show large differences in selectivity and which provide similar retention behaviour (Neue *et al.*, 2006). Over the years various protocols for the chromatographic characterisation of reversed phase columns have been published (Cruz *et al.*, 1997; Engelhardt *et al.*, 1991; Euerby & Petersson, 2003; Kimata *et al.*, 1989; Neue *et al.*, 1999; Snyder *et al.*, 2004). One of the most popular approaches is the hydrophobic-subtraction model proposed by Snyder's group in 2004 (Neue, 2007). It characterises the stationary phases by five different selectivity parameters (Snyder *et al.*, 2004):

- Hydrophobic interactions (H) of analyte and stationary phase, which basically depend on surface area and coverage of organic ligands on the silica support
- Steric selectivity (S), influenced by spacing of the ligands and probably also the shape/functionality of the silylating reagent
- Hydrogen bonding (A) between acceptor solutes and non-ionized silanols, which is based on the number of available silanol groups in the stationary phase and the degree of endcapping
- Hydrogen bonding (B) between donor solutes and an unidentified acceptor group in the stationary phase, which is less significant
- Attraction of positively charged molecules to ionized silanols (C), which depends on the acidic activity of residual silanols in a stationary phase support.

Phases with marked differences in these five parameters should greatly vary in their selectivity (Wilson *et al.*, 2002b).

Another popular approach for the classification of a wide range of stationary phases is the Tanaka protocol (Kimata *et al.*, 1989), which has been modified and used by Euerby *et al.* since 1997 to characterise over 266 different HPLC columns until the present day (Neue, 2007). It provides reliable evaluation of several chromatographic parameters that impact on selectivity (Pettersson & Euerby, 2005) and uses statistical tools, such as Principal Component Analysis (PCA) as a rational way to compare and group different stationary phases (Euerby & Pettersson, 2003). Essentially the protocol comprises six parameters for the characterization of selectivity differences (Cruz *et al.*, 1997):

- the *Retention factor* for amylobenzene, ( $k_{AB}$ ), which reflects the surface area and surface coverage (ligand density).
- *Hydrophobic Selectivity*, ( $\alpha_{CH_2}$ ), which is the retention factor ratio between amylobenzene (AB) and butylbenzene (BB),  $\alpha_{CH_2} = k_{AB} / k_{BB}$ . This is a measure of the surface coverage of the phase as the selectivity between alkylbenzenes differentiated by one methylene group is dependent on the ligand density.
- *Shape selectivity*, ( $\alpha_{T/O}$ ) is the retention factor ratio between triphenylene (T) and o-terphenyl (O),  $\alpha_{T/O} = k_T / k_O$ . This descriptor is influenced by the spacing of the ligands on the phase and probably also the shape/functionality of the silylating reagent.
- *Hydrogen bonding capacity*, ( $\alpha_{C/P}$ ) is the retention factor ratio between caffeine (C) and phenol (P),  $\alpha_{C/P} = k_C / k_P$ . This descriptor is a measure of the number of available silanol groups and the degree of endcapping. However, this value may be falsely high in phenyl phases as caffeine, may be retained by both aromatic and hydrogen bonding mechanisms (Euerby *et al.*, 2007).

- *Total cation exchange capacity*, ( $\alpha_{B/P}$  pH 7.6) is the retention factor ratio between benzylamine (B) and phenol (P),  $\alpha_{B/P}$  pH 7.6 =  $k_B/k_P$ . This is an estimate of the total silanol activity.
- *Acidic cation exchange capacity*, ( $\alpha_{B/P}$  pH 2.7) is the retention factor ratio between benzylamine (B) and phenol (P),  $\alpha_{B/P}$  pH 2.7 =  $k_B/k_P$ . This is a measure of the acidic activity of the silanol groups.

PCA is used to manage the vast amount of data and provides a simple graphical comparison of the datasets. Phases can be classified into groups and similarities and differences are readily identified (Euerby & Petersson, 2003).

In online databases available to the public such as the “Column Selector” ([www.acdlabs.com/download/column\\_selector.html](http://www.acdlabs.com/download/column_selector.html)) these data can be consulted to find equivalent columns when a back up column is needed for a certain separation, as well as stationary phases with very different chromatographic characteristics for method development.

#### 4.1.3. Efficiency

As resolution is a function of square root of the efficiency term  $N$ , relatively large increases in  $N$  are required to make small improvements in resolution ( $R_s$ ) (see equation 1).

The number of theoretical plates ( $N$ ) can be calculated using the peak width either at half height or at base, as stated in equation 7.

Equation 7: Calculation of plate number

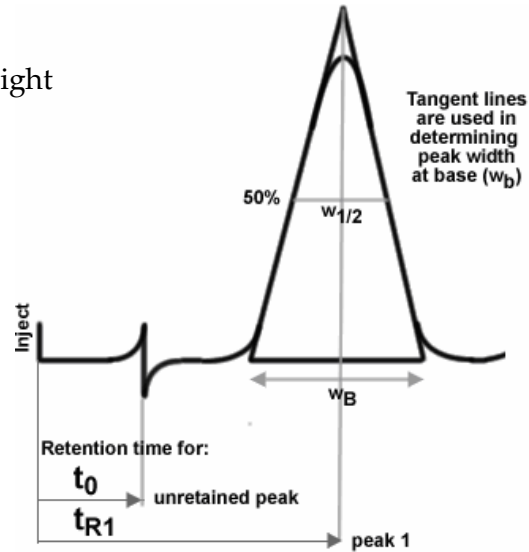
a) using peak width at base

$$N = 16 \left( \frac{t_R}{W} \right)^2$$



b) using peak width at half height

$$N = 5.54 \left( \frac{t_R}{W_{1/2}} \right)^2$$



Efficiency is also described by the Van Deemter Equation (equation 8) which relates efficiency (H) to mobile phase velocity.

Equation 8: Van Deemter Equation

$$a) \quad H = A + \frac{B}{\mu} + C \mu$$

$$b) \quad H = \lambda dp + 2\gamma \frac{D_m}{\mu} + c \frac{dp^2}{D_m} \mu$$

where H represents the plate height and is expressed by column length divided by the plate number ( $H = L / N$ ). Small values of H indicate good column performance. A, B and C are constants influenced by size, distribution and uniformity of the packing material and  $\mu$  describes the linear velocity of the mobile phase, controlled by the flow rate (Watson, 1999). Increased values of diffusion and resistance to mass transfer, due to

packing non-uniformity lead to band broadening and affect resolution. Consequently, the quality of the packed stationary phase largely influences the efficiency of a separation.

#### 4.1.4. Gradient Analysis

In gradient analysis the mobile phase solvent strength is changed as a function of time. Usually as solvent strength increases, the more highly retained analytes are eluted earlier. Typically gradients can be binary, ternary or quaternary solvent mixtures in which solvents are blended to achieve the appropriate strength (Neugebauer, 2001).

The main purpose of gradient elution is to speed up the elution of more strongly retained components of an analyte mixture and having the least retained component still well resolved. Thus all analyte bands are eluted within a reasonable retention factor ( $k$ ) range.

Having initially a low content of the organic component in the eluent allows the least retained components to be separated. Strongly retained components will sit on the adsorbent surface on the top of the column, or will only move slowly. By increasing the amount of organic component in the eluent, the strongly retained components will move faster due the steady increase of competition for the adsorption sites (Jandera & Kucеров, 1997; Neugebauer, 2001).

Furthermore gradient elution increases the quasi-efficiency of a column. Whilst with isocratic elution, the longer a component is retained, the wider its peak, with gradient elution, especially with a smooth gradient shape without flat regions, the tail of the peak is always under the influence of the stronger mobile phase compared to the peak front. Hence, molecules

on the tail of the chromatographic zone (peak) will move faster, compressing the zone and narrowing the resultant peak (Jandera, 1998).

Re-equilibration of the stationary phase is a necessary part of gradient chromatography. HPLC systems and columns must be at initial conditions at the beginning of each run to ensure reproducible chromatographic separations. To equilibrate a column between gradient runs typically 5 - 10 column volumes of mobile phase are required. The column dead-volume ( $V_m$ ) is calculated as described by equation 5.

When changing column dimensions and hence  $V_m$ , the flow rate of a gradient method or the gradient time, care must be taken not to change the average retention factor ( $k^*$ ), and consequently selectivity, by changing the overall gradient profile. The average retention factor ( $k^*$ ) is an analogous term to  $k$  (isocratic). Since with gradient analysis the solvent strength changes on a continuous basis,  $k$  changes during the separation. When changing one or more of the mentioned parameters  $k^*$  must be kept constant to obtain equivalent gradient separation (Romanyshyn & Tiller, 2001).

The average retention factor is calculated using equation 9.

Equation 9: Calculation of average retention factor

$$k^* = \frac{t_g F}{\Delta\%B V_m S}$$

where  $t_g$  is gradient time (min),  $\Delta\%B$  is gradient range,  $F$  is flow rate (ml/min),  $V_m$  is column dead volume and  $S$  is a constant characteristic of the analyte with  $S \approx 4$  for molecules with molecular weights of 100 - 500 (Snyder & Dolan, 1996).

#### 4.1.5. Computer Simulation

DryLab® is software for computer-assisted HPLC method development. It provides “computer simulation” of a separation, which attempts to mimic the strategy followed by chromatographers, while using the computer to reduce the required time and effort. Whilst any number and combination of separation variables can be explored, only a small number of experimental chromatograms are required (Krisko *et al.*, 2006). Despite emphasizing those experimental variables that have a primary effect on sample retention and band spacing as mobile phase conditions and column type, the software also permits computer simulation of changes in column dimensions, particle size and flow rate. Efficiency can be optimized for a given application, with a good compromise among different separation goals such as resolution, run time, pressure and peak volume (Snyder *et al.*, 1989).

##### 4.1.5.1. Theoretical Background

DryLab® computer-simulated predictions are based on the assumption that  $\log k$  changes linearly with % organic solvent in the mobile phase. Two experimental gradient runs are required to determine the solute parameters  $k_w$  and  $S$  for each component of a sample (Snyder *et al.*, 1997b).

The theory behind the simulation can be expressed as:

Equation 10: Relationship between retention and % organic solvent

$$\log k = \log k_w - S\Phi$$

where  $k$  is the retention factor in mobile phase composition  $\Phi$  (volume fraction of organic solvent B),  $k_w$  is the value of  $k$  in water and  $S$  is a constant for a given mobile phase and solute.

Once values of  $k_w$  and  $S$  have been determined experimentally this relationship (equation 10) enables the prediction of a gradient separation for any combination of conditions as gradient time or steepness, initial and final values of % organic solvent and/or gradient shape. The derived values for  $k_w$  and  $S$  allow the calculation of  $k_o$  and  $b$  for each solute and hence permit prediction of retention and band width as a function of experimental conditions as described by equations 11 and 12.

Equation 11: Prediction of retention time in DryLab®

$$t_g = \left( \frac{t_o}{b} \right) \log(2.3k_o b + 1) + t_o + t_D$$

where  $t_g$  is the retention time of solute in gradient elution,  $t_o$  is the column dead time,  $b$  is the gradient steepness parameter,  $k_o$  is the value of  $k$  at the beginning of the gradient and  $t_D$  is the dwell time of the gradient.

Equation 12: Prediction of band width in DryLab®

$$\sigma_t = \frac{t_o G \left[ 1 + \left( \frac{1}{2.3b} \right) \right]}{N^{0.5}}$$

where  $\sigma_t$  is the band width in gradient elution ( $4 \sigma =$  band width,  $w$ ),  $G$  is the gradient compression factor and  $N$  is the column plate number.

Using this approach retention times can generally be predicted with an accuracy of about  $\pm 1 - 3 \%$  (Dolan *et al.*, 1989; Dolan *et al.*, 1999; Euerby, 2005; Snyder *et al.*, 1989).

#### 4.1.5.2. Potential Sources of Error in Computer Simulation

Possible reasons for errors associated with DryLab<sup>®</sup> modelling have been reported (Dolan *et al.*, 1999). These are summarised in table 4.1.

Table 4.1: Potential sources of error in computer simulation

<i>Factor</i>	<i>Comment</i>
Equipment	Problems can arise from gradient or pumping errors, inaccurately measured dwell volumes or excessive rounding of the gradient due to dispersion effects
Column processes	Errors can be caused by demixing of the mobile phase within the column
Changes in stationary phase	Loss of bonded phase or column deactivation during use can lead to changes in retention, which produce errors in the computer simulation
Errors in interpretation	Overlapping bands can cause errors in measured retention; overlooked band reversals can lead to error in predicted retention times and separation
Non-linear plots of log k vs. %B	Non-linear retention plots can lead to errors in predicted retention, particularly for extrapolated runs

#### 4.1.5.3. Practical Application of DryLab<sup>®</sup>

To obtain necessary data to use computer simulation for gradient elution two experimental runs with linear, typically 5 - 100 % organic gradients and different gradient times need to be performed. All other conditions remain the same. The second run should be typically three times longer than the first.

The next step is the generation of a relative resolution map, which can be used to determine the feasibility of the separation and to choose optimum gradient time. An ideal gradient range can be established, providing maximum resolution in minimal run time.

Initial % organic and gradient shape will subsequently be varied to fine tune band spacing and maximise resolution. Also column conditions, such as length and particle size and/or flow rate can be varied to change  $N$  while keeping  $k^*$  and  $\alpha$  constant. Using this approach, little effort is needed to achieve optimum gradient conditions for resolution, run time and column back pressure (Euerby, 2005).

#### 4.1.6. Aims and Objectives

The key aim of the work described in this chapter was to optimise the previously described HPLC assay (chapter 2 & 3) for the bioanalytical investigation of ISM and related substances, as previous work showed that the measurement of small amounts of the trypanocide in biological matrices from treated livestock requires an increase in sensitivity and column performance.

Therefore the effect of stationary phase chemistry and mobile phase selectivity on the isocratic separation of ISM was examined, using a range of stationary phases of different chemistries. Also the usefulness of gradient elution in this case has been investigated.

Computer simulation has been used to model retention behaviour of the compounds as a function of mobile phase composition, column type, column dimensions, particle size and mobile phase flow rate in order to establish optimum conditions for the HPLC assay.



## 4.2. Experimental

### 4.2.1. Materials

HPLC-grade acetonitrile and methanol were obtained from VWR International Ltd. (Poole, UK). Analytical reagent formic acid and dimidium bromide (95 % purity) were bought from Sigma-Aldrich (Dorset, UK) and ammonium formate was supplied by BDH Laboratory Supplies (Poole, UK). A secondary reference standard mixture (RSM) of isometamidium and related substances containing 8-(*m*-amidinophenyldiazoamino)-3-amino-5-ethyl-6-phenylphenanthridinium chloride [(58.6 %w/w), isometamidium, ISM, M&B4180A], 3-(*m*-amidinophenyldiazoamino)-8-amino-5-ethyl-6-phenylphenanthridinium chloride [(13.3 %w/w), M&B38897], 7-(*m*-amidinophenyldiazo)-3,8-diamino-5-ethyl-6-phenylphenanthridinium chloride [(13.7 %w/w), M&B4250] and 3,8-di(3-*m*-amidinophenyltriazeno)-5-ethyl-6-phenylphenanthridinium chloride [(8.1 %w/w), M&B4596] and an authentic standard of homidium (3,8-diamino-5-ethyl-6-phenylphenanthridinium chloride) were a kind gift from Merial Limited (Toulouse, France).

#### *Stock 150 mM ammonium formate buffer (pH 2.8)*

Ammonium formate (9.5 g) was accurately weighed, dissolved in approximately 800 mL of water and the pH adjusted to a value of 2.8 with formic acid. The resulting solution was made up to 1 l with water.

#### *Stock 1 %v/v formic acid solution*

Formic acid (10 ml) was accurately pipetted into a 1 l volumetric flask, using a one mark pipette, and made up to mark with distilled water.

*Mobile Phase A1: 15 mM ammonium formate buffer (pH 2.8)*

A volume (100 ml) of the 150 mM HCOONH<sub>4</sub> buffer stock solution was made up to 1000 ml with purified water.

*Mobile Phase A2: 0.1 %v/v formic acid*

A volume (100 ml) of the 1 % formic acid stock solution was made up to 1000 ml with purified water.

*Mobile Phase B1: 15 mM ammonium formate buffer (pH 2.8) in water/acetonitrile (20:80 v/v)*

A volume (100 ml) of the 150 mM HCOONH<sub>4</sub> buffer stock solution was made up to 200 ml with purified water, to which was added 800 ml of acetonitrile.

*Mobile Phase B2: 0.1 %v/v formic acid in water/acetonitrile (20:80 v/v)*

A volume (100 ml) of the 1 %v/v formic acid stock solution was made up to 200 ml with purified water, to which was added 800 ml of acetonitrile.

*Mobile Phase B3: 15 mM ammonium formate buffer (pH 2.8) in water/methanol (20:80 v/v)*

A volume (100 ml) of the 150 mM HCOONH<sub>4</sub> buffer stock solution was made up to 200 ml with purified water, to which was added 800 ml of methanol.

#### 4.2.2. Preparation of a Mixed Standard Solution

For HPLC analysis weights of the reference standard mixture (RSM) of ISM and related compounds (17.1 mg), homidium standard (10.0 mg) and dimidium bromide (10.0 mg) were accurately weighed using a Mettler AT20 analytical balance (readability 0.01 mg) and transferred to a 100 ml volumetric flask. The flask was made up to the mark with water to produce a stock solution containing 0.1 µg/ml M&B4180A, 0.001 µg/ml M&B4596, 0.02 µg/ml M&B38897 and 0.02 µg/ml M&B4250, 0.1 µg/ml homidium and 0.1 µg/ml dimidium bromide. An aliquot (250 µl) of this stock solution was transferred into a sample vial and made up to 1 ml with 25 %v/v acetonitrile in water to produce sample solutions containing 0.025 µg/ml M&B4180A, homidium and dimidium bromide, 0.005 µg/ml M&B4250 and M&B 38897 and 0.25 ng/ml M&B4596.

#### 4.2.3. HPLC Columns

1. Phenomenex, Gemini 5u C18, 150 x 4.6 mm, 5 µm particles  
CN: 00F-4435-E0SN: 356086-12
2. ACT, ACE 5 C18-HL, 150 x 4.6 mm, 5 µm particles  
CN: ACE-321-1546 SN: A58131
3. ACT, ACE 5 C18, 150 x 4.6 mm, 5 µm particles  
CN: ACE-121-1546 SN: A54754
4. ACT, ACE 5 C8, 150 x 4.6 mm, 5 µm particles  
CN: ACE-122-1546 Batch: V08-1674-N SN: A58125  
Batch: V08-1674-N SN: A67277
5. ACT, ACE 5 C4, 150 x 4.6 mm, 5 µm particles  
CN: ACE-123-1546 SN: A58126

6. ACT, ACE 5 CN, 150 x 4.6 mm, 5 µm particles  
CN: ACE-124-1546 SN: A58127
7. ACT, ACE 5 Phenyl, 150 x 4.6 mm, 5 µm particles  
CN: ACE-125-1546 SN: A58128
8. ACT, ACE 5 AQ, 150 x 4.6 mm, 5 µm particles  
CN: ACE-126-1546 SN: A58129
9. ACT, ACE 5 C18AR 150 x 4.6 mm, 5 µm particles  
CN: ACE-129-1546 SN: A58130
10. ACT, ACE 5 SIL, 150 x 4.6 mm, 5 µm particles  
CN: ACE-127-1546 SN: A67065

#### 4.2.4. HPLC Analysis

An Agilent HP1100 series quaternary pump with ChemStation® software version 10.02 for data acquisition equipped with a HP1100 series UV-Vis detector was used. M&B4180A and related substances were separated on various HPLC columns with different stationary phase chemistries (see section 4.2.3). Compounds were detected at a wavelength of 320 nm.

Initial gradients with mobile phases A2/B2 (section 4.2.1) and a flow rate of 1 ml/min were run on each column, at 30 °C and 50 °C to generate DryLab® input data that was used for computer simulated modelling. To determine the effect of a change in mobile phase composition, gradients with mobile phases A1/B1 and A1/B3 were run only on an ACT, ACE 5 C8 column.

Gradient times for initial and later determined optimised gradient runs are shown in tables 4.2 - 4.4.

Table 4.2: Gradients used for initial DryLab® input

	Time (min)	Time (min)	Time (min)	Time (min)	% B
Initial	0	0	0	0	5
Gradient	<b>15</b>	<b>20</b>	<b>30</b>	<b>45</b>	100
Hold	20	25	35	45	100
Drop down %B	21	26	36	46	5
Post time (9 column volumes)	14	14	14	14	5
Total cycle time	35	40	50	60	

Table 4.3: Optimised gradients for separation on ACT, ACE 5 C8

	Time (min)	% B	Time (min)	% B
Initial	0	5	0	30
Gradient	<b>21</b>	100	<b>4</b>	60
Hold	26	100	6	60
Drop down %B	27	5	7	30
Post time (8 column volumes)	13	5	5	30
Total cycle time	40		12	

#### 4.2.5. DryLab® Input Data

Program: DryLab® 2000 Plus version 3.6.1

##### – Instrument Data

- Dwell volume: 1.75 ml
- Extra-column volume: 0.016 ml
- Time constant: 0.100 sec

– **Elution Data**

- Run Type: Gradient
- Temperature: 30 °C and 50 °C
- Gradient: 5.00 to 100.00 % B in 15 and 45 min
- Solvent A: A1: 100.0 % water, 15 mM formate, pH 2.8  
A2: 100.0 % water, 0.1 % formic acid
- Solvent B: B1: 80.0 % acetonitrile, 20 % water, 15 mM formate, pH 2.8  
B2: 80.0 % acetonitrile, 20 % water, 0.1 % formic acid  
B3: 80.0 % methanol, 20 % water, 15 mM formate, pH 2.8

– **Constant Column Data**

- Column length: 150 mm
- Inner Diameter: 4.6 mm
- Pore Diameter: 10.00 nm
- A-value: 0.80
- Plate number: 6500
- Particle Size: 5 µm
- Flow rate: 1 ml/min
- Peak Width at half peak height: taken from ChemStation integration data

### 4.3. Results and Discussion

#### 4.3.1. Effect of Changes in Mobile Phase Composition

Initial gradient experiments with varying mobile phase compositions to determine the most favourable conditions were undertaken with the ACE 5 C8 column. Chromatograms of the separation using ammonium formate and acetonitrile (mobile phase system A1/B1) as described in chapter 2 are shown in figure 4.3.

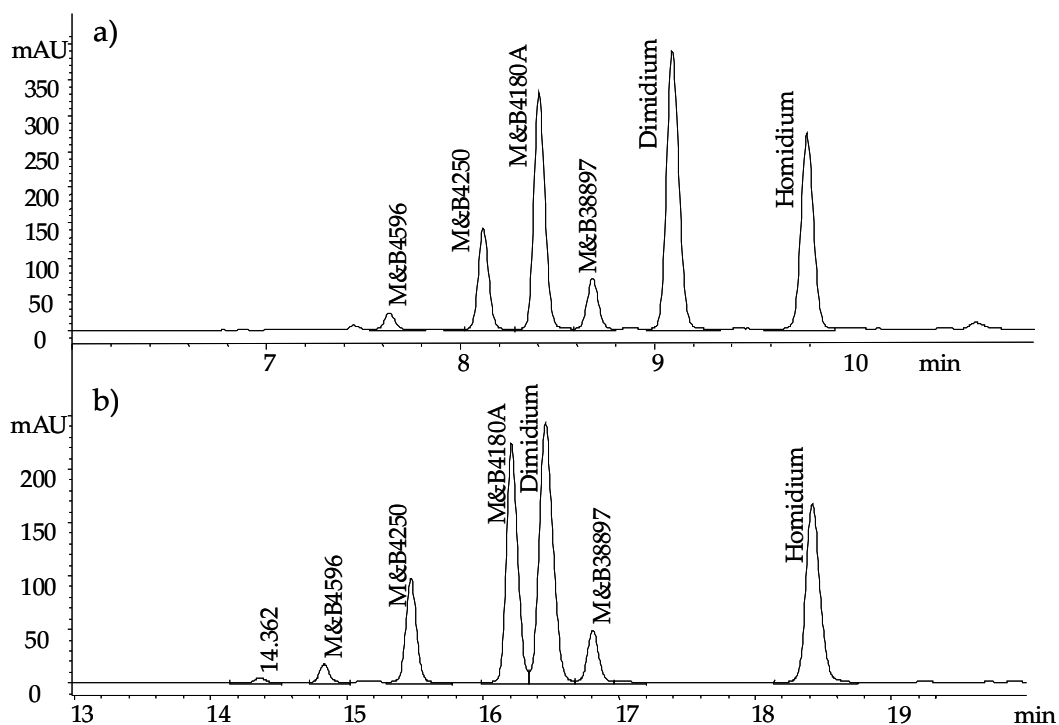


Figure 4.3: Separation of components in the RSM solution by a) 15 min and b) 45 min gradient run on ACE 5 C8, 150 x 4.6 mm, 5  $\mu$ m, HPLC column with mobile phase consisting of 15 mM ammonium formate and acetonitrile at 30 °C

Although the 15 min gradient gave the same order of elution as the original isocratic method (chapter 2), there was a noticeable improvement in peak shape and resolution when compared to previously obtained chromatograms (figures 2.2 and 3.4). The choice and performance of particular columns is discussed in section 4.3.2.

Changes in solvent strength strongly affect retention and thus selectivity (Snyder *et al.*, 1997a). Since the isocratic method (see chapter 2) gave values of  $1.5 < k < 7$  for all the compounds of interest, their retention values lie within a preferable range and should not be markedly altered.

Considering recent developments and the global shortage of acetonitrile (Lowe, 2009; Tullo, 2008), usage of methanol as organic modifier would be favourable. Hence, initially the possibility of replacing acetonitrile in the mobile phase with methanol was explored, running the initial 15 and 45 min gradients using mobile phase A1 and B3 to produce the relevant DryLab® input data. Methanol in a reversed phase separation is a weaker solvent than acetonitrile and an increase in retention would be expected. Figure 4.4 illustrates the results obtained.

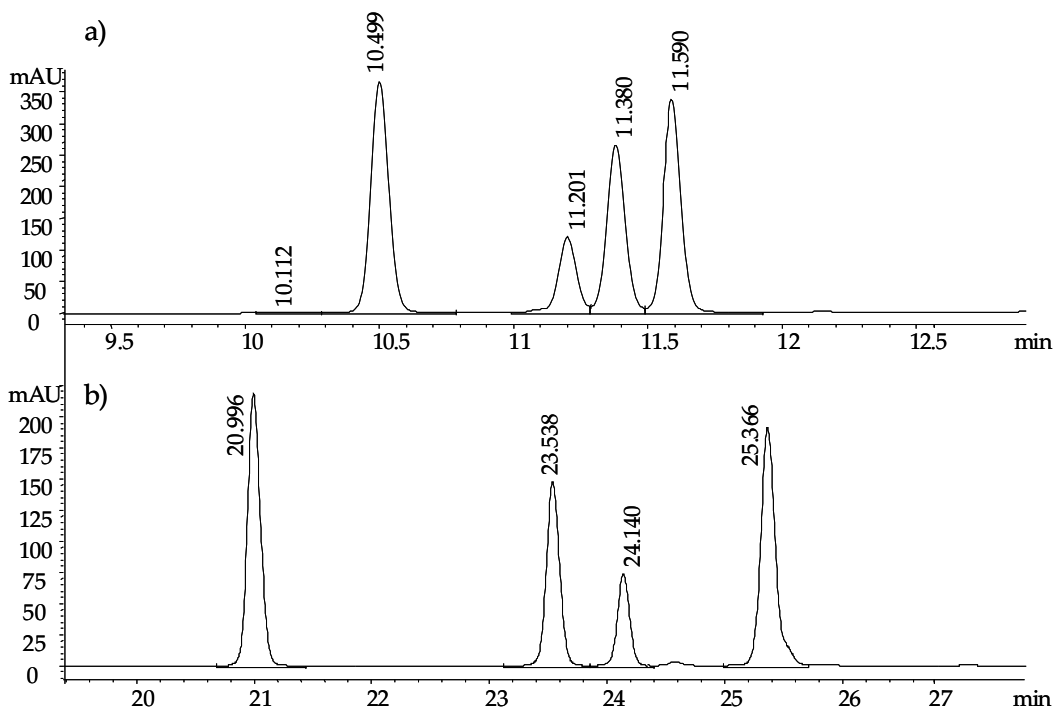


Figure 4.4: Separation of components in the RSM solution by a) 15 min and b) 45 min gradient run on ACE 5 C8, 150 x 4.6 mm, 5  $\mu$ m, HPLC column with mobile phase consisting of 15 mM ammonium formate and methanol at 30 °C



With methanol the chromatograms (figure 4.4) show that not only is there an increase in retention but there are also changes in selectivity of the separation, producing shifts in retention and coelution when compared to chromatograms obtained with the initial conditions (figure 4.3). Consequently, without MS detection, peak assignment was not possible. Furthermore changes in % organic seem largely to affect selectivity, as the two gradients show a completely different elution order, based on peak areas of the four detected peaks. Therefore the separation of the components with a methanol containing mobile phase is strongly affected by small changes in % organic solvent. However, as the experiment resulted in an apparent loss of resolution, rather than any improvement, the possibility of changing the organic solvent was not further investigated.

Another possibility of altering the composition of the mobile phase is to change the aqueous component. In general, use of buffer salt should be avoided when using MS detection, as its presence can lead to contamination of the source or clogging of the vaporizer, leading to a loss in sensitivity and interference with the molecular ion formation within the mass spectrometer (Cech & Enke, 2001). Taking this into account the 15 mM ammonium formate buffer was replaced by 0.1 %v/v formic acid in the mobile phase.

Chromatograms (figure 4.5), obtained with 0.1 %v/v formic acid are comparable to those obtained with ammonium formate buffer, apart from a shorter analysis time. Even though the analytes elute slightly faster (compare figures 4.3 and 4.5), baseline separation of all compounds of interest is achieved with the 15 min gradient, without any further changes in selectivity of the separation. Consequently, subsequent experiments were carried out using 0.1 %v/v formic acid and acetonitrile in the mobile phase (mobile phase system A2/B2).

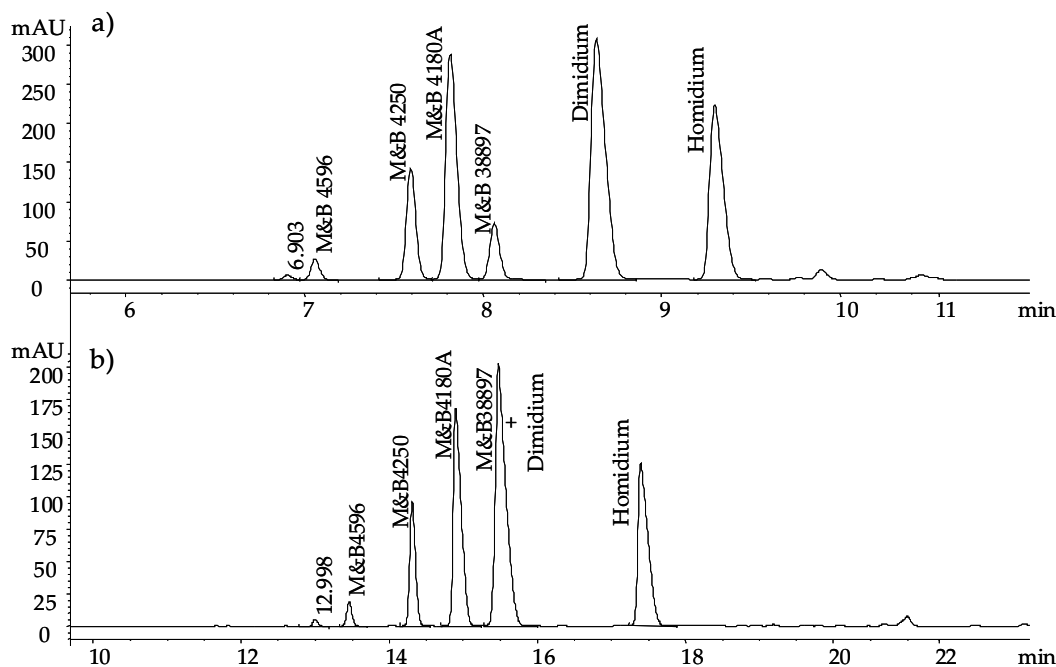


Figure 4.5: Separation of components in the RSM solution by a) 15 min and b) 45 min gradient run on ACE 5 C8, 150 × 4.6 mm, 5 μm, HPLC column with mobile phase consisting of 0.1 %v/v formic acid and acetonitrile at 30 °C

#### 4.3.2. Effect of Changes in Stationary Phase Chemistry

All columns under investigation have been characterised with regards to stationary phase properties that influence retention behaviour as described by Euerby & Petersson (2003).

Those characteristics as stated in table 4.4 are:

- The *Retention factor* for amylbenzene,  $k_{AB}$
- *Hydrophobic Selectivity*,  $\alpha_{CH2}$
- *Shape selectivity*,  $\alpha_{T/O}$
- *Hydrogen bonding capacity*,  $\alpha_{C/P}$
- *Total cation exchange capacity*,  $\alpha_{B/P}$  pH 7.6
- *Acidic cation exchange capacity*,  $\alpha_{B/P}$  pH 2.7

(see also section 4.1.2).

Table 4.4: Column characterisation parameters

Column	Manufacturer	$k_{AB}$	$\alpha_{CH_2}$	$\alpha_{T/O}$	$\alpha_{C/P}$	$\alpha_{B/P}$ pH 7.6	$\alpha_{B/P}$ pH 2.7
Gemini C18	Phenomenex	4.87	1.46	1.21	0.44	0.29	0.08
ACE 5 C18-HL	ACT	7.95	1.50	1.60	0.38	0.32	0.08
ACE 5 C18	ACT	5.19	1.49	1.59	0.38	0.32	0.09
ACE 5 C8	ACT	2.34	1.36	1.00	0.33	0.29	0.10
ACE 5 C4	ACT	1.08	1.29	0.70	0.43	0.35	0.13
ACE 5 CN	ACT	0.26	1.08	1.73	0.51	0.74	0.14
ACE 5 Phenyl	ACT	1.20	1.26	1.00	1.14*	0.46	0.14
ACE 5 AQ	ACT	2.30	1.35	1.22	0.48	0.32	0.11
ACE 5 C18AR	ACT	4.31	1.39	1.77	0.75	0.37	0.12

\*High values are not only due to hydrogen bonding, but aromatic interaction of organic ligand with analyte (caffeine) (Euerby et al., 2007).

Gradients of 15, 20, 30 and 40 min (described in section 4.2.4) were run with each of the columns (table 4.4). The results obtained from the 15 and 45 min gradients were used as DryLab<sup>®</sup> input data, and 20 and 30 min gradients were used to verify computer predictions. Representative chromatograms obtained with the 20 min gradient on each of the ten columns under investigation are shown in figures 4.6 - 4.9.

The Phenomenex Gemini 5u C18 column (figure 4.6 a), that was used in the original method (chapter 2), with 0.1 %v/v formic acid in the mobile phase did not produce a separation of the compounds under investigation, with the principal component M&B4180A and its structural isomer M&B38897 coeluting. Moreover, peak shape was poor compared to those obtained with the ACT, ACE 5 C18 and C18-HL phases (figure 4.6). Worthy of note is the appearance of a second, unidentified, early eluting compound ( $t_{R} = 8.02$  min and  $t_{R} = 7.40$  min on the ACT phases (figures 4.6 b and c) which seems to coelute with the ISM related bis-substituted compound M&B4596 on the Phenomenex column (figure 4.6 a).

Another distinctive feature of the separation is the decreased retention of all the compounds on the high load C18 phase (figure 4.6 c), which bears higher surface coverage of lipophilic ligands than a regular C18 phase. This observation suggests that, for this separation the hydrophobic interaction of organic compounds with the bonded phase is not the major mechanism of retention.

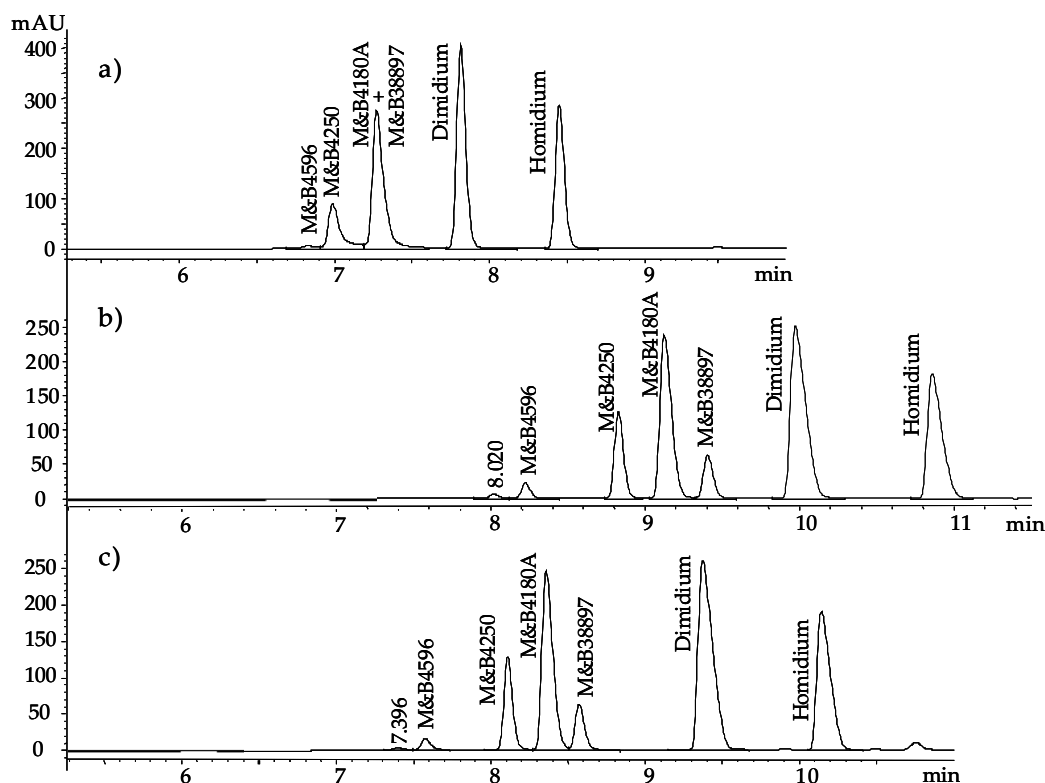


Figure 4.6: Separation of components in the RSM solution by 20 min gradient runs on a) Gemini 5u C18, b) ACE 5 C18 and c) ACE 5 C18-HL, 150 x 4.6 mm, 5  $\mu$ m HPLC columns with a mobile phase consisting of 0.1 %v/v formic acid and acetonitrile at 30  $^{\circ}$ C

The separation of ISM and related compounds on a C8 (figure 4.7 a) and C4 (figure 4.7 b) column gave again the previously observed effect. Compounds are retained for longer on the ACE 5 C4 column, with values for retention factor ( $k_{AB} = 1.08$ ) and hydrophobic selectivity ( $\alpha_{CH_2} = 1.29$ ) lower than those obtained with the ACE 5 C8 phase ( $k_{AB} = 2.34$ ;  $\alpha_{CH_2} = 1.36$ ) (table 4.4).

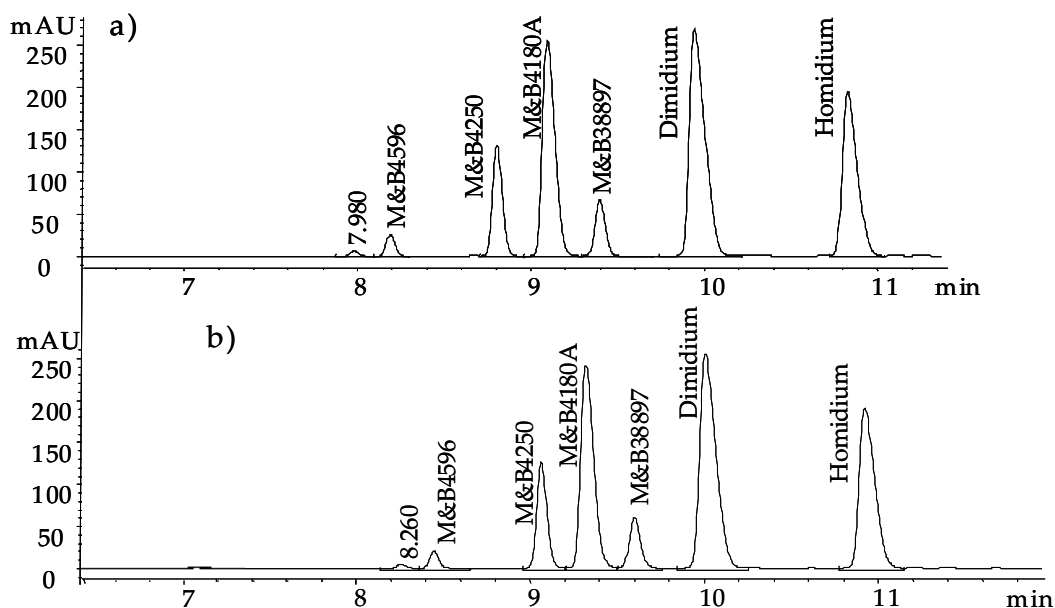


Figure 4.7: Separation of components in the RSM solution by 20 min gradient run on a) ACE 5 C8 and b) ACE 5 C4, 150 x 4.5 mm, 5  $\mu$ m HPLC columns with mobile phase consisting of 0.1 %v/v formic acid and acetonitrile at 30 °C

These findings lead to the hypothesis, that the compounds, which all bear a positively charged quaternary ammonium moiety (figure 2.3), are also retained due to polar interactions with the silica surface rather than just being attracted to the bonded organic layer. This conclusion is supported by the results obtained with a phenyl phase (figure 4.8 a), which has a lower surface coverage ( $k_{AB} = 1.20$ ) and hydrophobic selectivity ( $\alpha_{CH_2} = 1.26$ ) but better accessibility of the silica surface due to lower steric hindrance ( $\alpha_{T/O} = 1.00$ ) (table 4.4). The analytes of interest elute between 9 and 12 minutes on the phenyl phase, compared to between 7 and 11 min on the ACE 5 C18-HL phase (figure 4.6 c) with the same gradient conditions. However, with the phenyl phase aromatic interactions of the phenanthridine compounds with the stationary phase will possibly also contribute to the longer retention times (Euerby *et al.*, 2007).

Moreover, the ACE 5 CN stationary phase provides a complete change in selectivity of the separation (figure 4.8 b). The elution order of the compounds is changed in a way that makes peak assignment difficult. Furthermore only six instead of the seven distinct peaks are observed, suggesting that two of the components of the mixture coelute with these conditions. Use of the CN phase was therefore not further investigated.

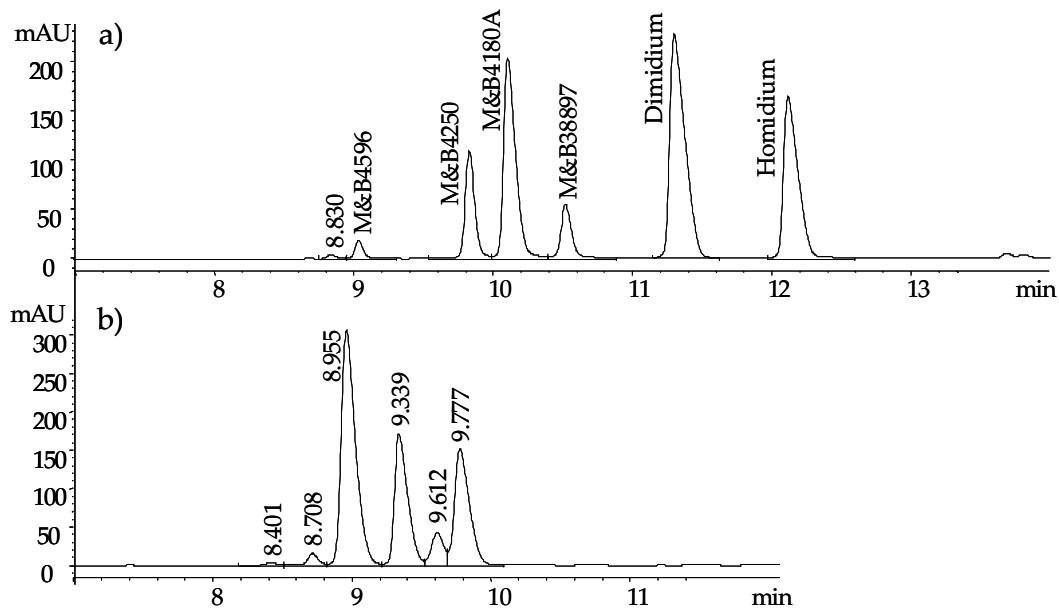


Figure 4.8: Separation of components in the RSM solution by 20 min gradient runs on a) ACE 5 Phenyl and b) ACE 5 CN, 150 x 4.5 mm, 5  $\mu$ m HPLC columns with mobile phase consisting of 0.1 %v/v formic acid and acetonitrile at 30  $^{\circ}$ C

ACE 5 AQ columns are recommended for use with mobile phases of high aqueous content, as the bonded phase provides improved resistance to phase collapse (ACT, 2007), compared to commonly used C18 phases. The stationary phase bears an incorporated polar moiety which could contribute to improved peak shape for the polar analytes and changes in the selectivity of the separation when compared to ordinary C18 phases.

Results obtained with the ACE 5 AQ and an ACE 5 C18-AR column are illustrated in figure 4.9.

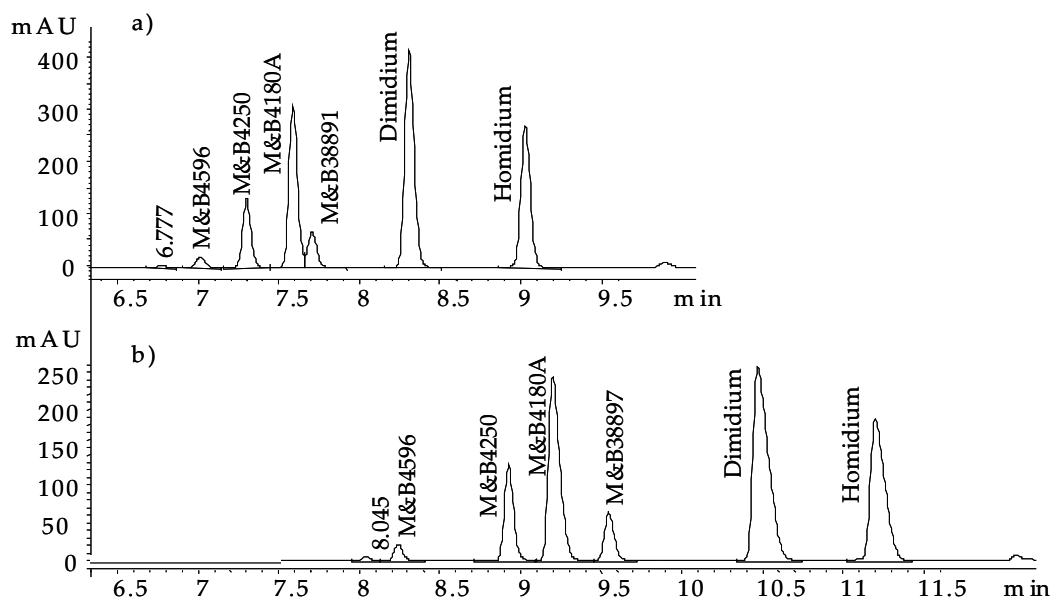


Figure 4.9: Separation of components in the RSM solution by 20 min gradient runs on a) ACE 5 AQ and b) ACE 5 C18-AR, 150 x 4.5 mm, 5  $\mu$ m HPLC columns with mobile phase consisting of 0.1 %v/v formic acid and acetonitrile at 30  $^{\circ}$ C

The chromatogram shown in figure 4.9 a) shows that despite the embedded polar groups within the ACE 5 AQ phase, with retention times between 6 and 9 minutes, ISM and related substances are less retained on this stationary phase than on the regular C18 or the C8 column. The finding is surprising, as values for retention factor, hydrophobic selectivity and acidity of residual silanol (table 4.4) are very similar to those of the C8 phase which exhibits stronger retention for all separated analytes. However, as there is no information of the nature and functionality of the embedded polar group no further conclusions can be drawn from these results. As use of the ACE 5 AQ phase lead to a loss in resolution no further experiments were carried out on this column.

Promising results in terms of peak shape and resolution were achieved with the ACE 5 C18AR phase (figure 4.9 b), which is known to possess an integrated phenyl functionality. This characteristic feature could

add to the retention of the phenanthridine compounds, which were most strongly retained on the previously used phenyl phase (figure 4.8 a).

Results for all the columns that gave good separations of the compounds of interest were examined more closely, with regard to retention times, resolution of the critical peak pair, peak width and peak symmetry, as the sensitivity of an assay is improved when all molecules of one solute elute as one narrow band, producing a sharp peak with increased peak height.

Comparison of chromatographic data obtained from the 20 min gradient experiments on the selected columns, using 0.1 %v/v formic acid and acetonitrile in the mobile phase are summarised in table 4.5.

Table 4.5: Comparison of column performance in 20 min gradients with mobile phase consisting of 0.1 %v/v formic acid and acetonitrile at 30 °C

Column	tr1	tr7	Min Rs	Min PW	Max PW	Symmetry
ACE 5 C18	8.0	10.9	1.82	0.067	0.114	0.5 – 0.8
ACE 5 C18 - HL	7.4	10.1	1.29	0.067	0.111	0.5 – 0.8
ACE 5 C18 - AR	8.1	11.2	1.77	0.066	0.111	0.5 – 0.9
ACE 5 C8	8.0	10.8	2.03	0.061	0.106	0.6 – 0.9
ACE 5 C4	8.3	10.9	1.58	0.066	0.107	0.6 – 0.8
ACE 5 Phenyl	8.8	12.1	1.65	0.071	0.121	0.4 – 0.8

These data show that the C8 stationary phase seems to provide the most favourable separation of the analytes of interest (figure 4.7 a). Resolution of the critical peak pair, which in all cases is the former unknown early eluting peak and the related substance M&B4596, is greater than 2.0 and values for peak width and symmetry are slightly better than those obtained with any other column. For all the columns examined, the symmetry factor values as provided by Agilent ChemStation® suggest marked peak tailing, especially for the late eluting peaks [Peak symmetry = (Area, front) / (Area, tail)].



Further experiments showed improvements in peak shape with 15 mM ammonium formate buffer in the mobile phase instead of 0.1 %v/v formic acid. With the C8 phase, symmetry factors of no less than 0.86 for all compounds of interest were obtained. Also peak widths improve with use of the buffered mobile phase, peaks no wider than 0.083 min were obtained even for the late eluting compounds. A compromise between improvement in peak shape and the loss of sensitivity in a MS detector, due to the ion suppression effect of the buffer salt, would need to be investigated if a MS detector is used.

#### 4.3.3. Effect of Organic Solvent Content

Since in gradient analysis the percentage organic solvent, thus solvent strength, varies with time, gradients of differing times and steepness provide information on the effect of changes in % organic on the separation. Thus plots of  $\log k$  vs. % organic provide information on the similarities and differences in retention mechanisms of the different compounds on a given stationary phase (figure 4.10 a), and the same information for one compound with different stationary phases (figure 4.10 b).

Parallel graphs of  $\log k$  vs. % organic (figure 4.10 a) illustrate that the unknown, early eluting compound exhibits the same retention behaviour as the ISM related bis-substituted compound M&B4596, which suggests that this unidentified analyte also is ISM related. Furthermore, parallel plots for ISM (M&B4180A) and its two structural isomers M&B4250 and M&B38897 (figure 4.10 a) indicated that these three analytes also possess identical chromatographic properties and are well separated on the C8 column at any percentage of organic solvent.

Similarly, the plots of dimidium and homidium are parallel, which suggests similar retention mechanisms on the C8 phase. However, dimidium coelutes with the late eluting isomer M&B38897 with lower organic solvent content.

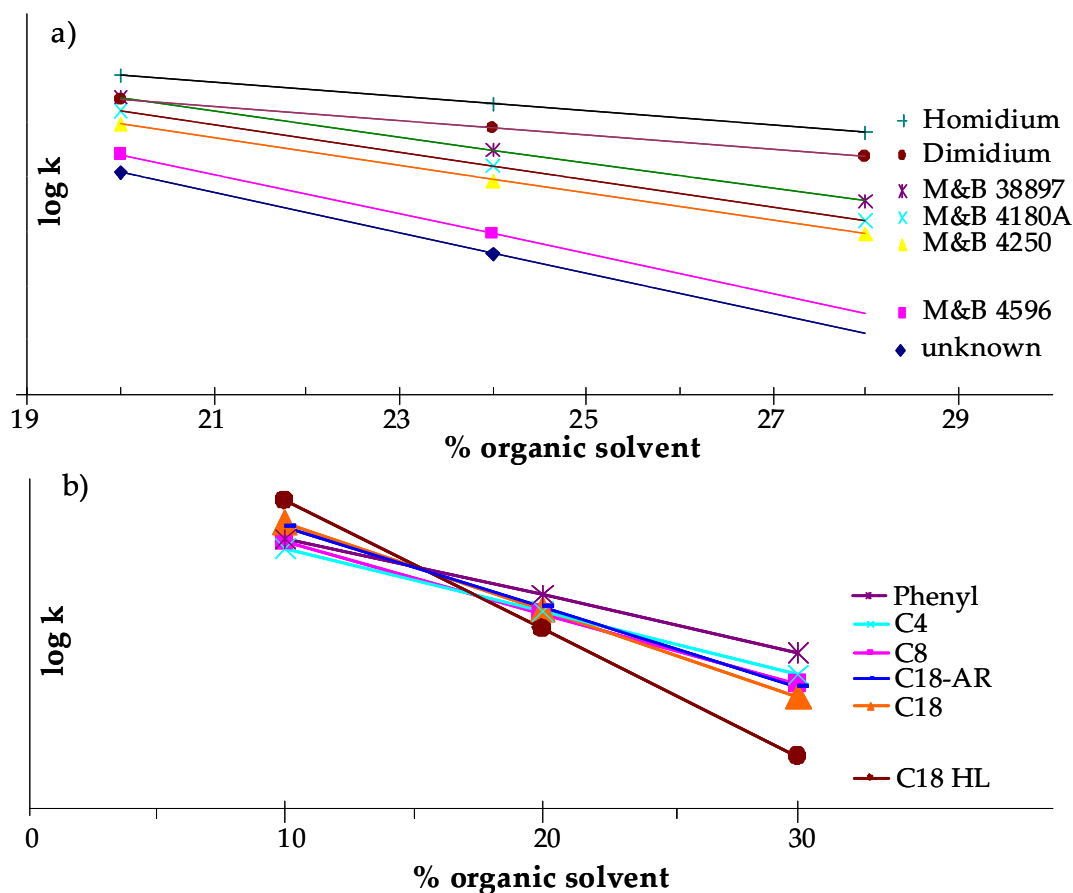


Figure 4.10: Log k versus % organic solvent of a) ISM and related substances on ACE 5 C8, 150 x 4.6 mm, 5  $\mu$ m, stationary phase with mobile phase consisting of 0.1 %v/v formic acid and acetonitrile at 30 °C and b) of M&B4180A on columns of differing stationary phase chemistries

An optimum gradient profile, as well as optimum isocratic conditions for the separation will be described in section 4.3.4 using this data and DryLab<sup>®</sup> computer simulations.

Focusing on the principal isomer M&B4180, differences in retention mechanisms and thus selectivity of the varying stationary phases were observed (figure 4.10 b). Again the apparent reverse order of increasing

retention with decreasing ligand density (see table 4.4) becomes obvious, particularly with increasing % organic content. This observation suggests that with decreasing polarity of the mobile phase, the positively charged analytes are more strongly retained by polar interactions with residual silanols on the silica surface of the stationary phase.

This hypothesis led to an experiment where initial gradient separations were carried out on a bare silica column. The resulting chromatograms are displayed in figure 4.11.

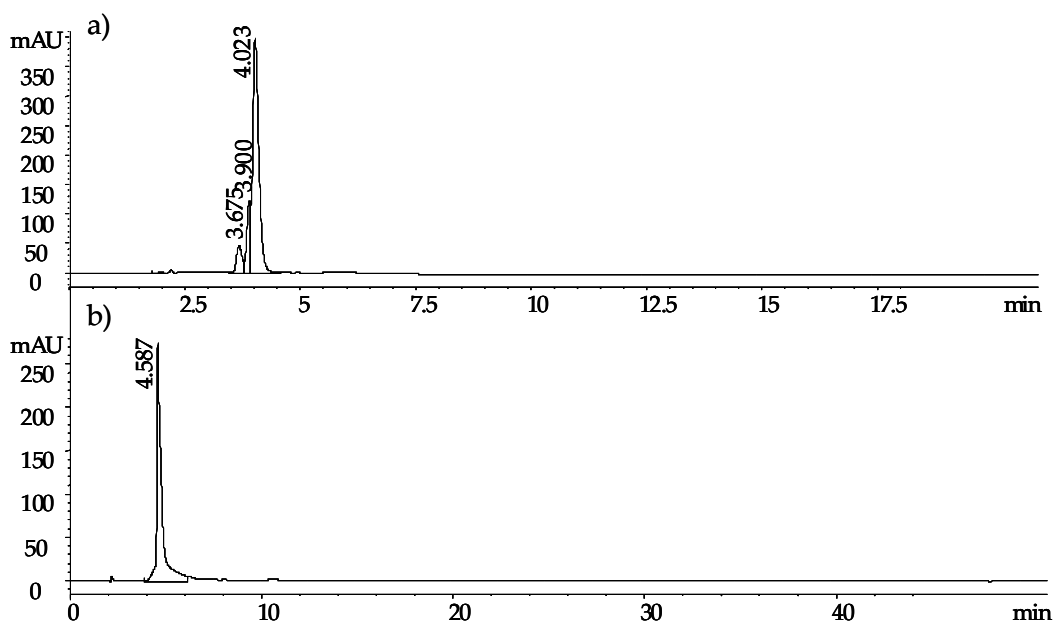


Figure 4.11: Separation of components in the RSM solution by a) 15 min and b) 45 min gradient run on ACE 5 SIL, 150 x 4.6 mm, 5  $\mu$ m, HPLC column with mobile phase consisting of 15 mM ammonium formate buffer and acetonitrile at 30  $^{\circ}$ C

The compounds of interest were not separated under the given conditions, neither with 15 min nor 45 min gradient time. Although, using the shorter, steeper gradient the analytes are partly separated (figure 4.11 b) when compared to complete coelution with the longer gradient (figure 4.11 a). Again, this observation suggests, that with a high percentage organic solvent in the mobile phase, polar interactions of the analytes with the silica support

of the stationary phase increase and add to the separation. The results also show, that without any hydrophobic character to the column, the compounds are not separated by ion exchange interaction alone. The retention mechanism of this separation seems to be a cooperative effect of hydrophobic, aromatic and ionic interactions.

As the ACE 5 C8 column was identified as the most suitable stationary phase to use for the separation of ISM and related substances, gradient data obtained with this column at 30 °C and 50 °C was used as input data for the DryLab® computer simulation software. DryLab® modelling was used to identify the optimum gradient and isocratic separation conditions.

#### **4.3.4. DryLab® Modelling and Identification of Optimum Separation Conditions**

The best column performance in terms of resolution, peak width and peak symmetry was achieved using an ACT, ACE 5 C8, 150 x 4.6 mm, 5 µm stationary phase (figure 4.7 a). Gradients of 15 and 45 min at 30 °C and 50 °C were performed for DryLab® data input, to enable computer simulated prediction of optimum separation conditions for isocratic and gradient analysis. To confirm the accuracy of DryLab® predicted data, 20 and 30 min gradients were also performed and the results obtained from actual experiments of the column under investigation were compared to those from the computer simulation software. The DryLab® version used in this study (version 3.6.1) produced unreliable results when peak width was used as an input data parameter. Consequently, instead of using peak width, a plate number of 6500 was entered as a column parameter, as it provided most accurate results when compared to an actual experiment. Similarly, several estimated values of dwell volume were entered, and predicted results were

compared to actual chromatographic data. The smallest % error was obtained when a dwell volume of 1.75 ml was entered. Results of predicted and actual experimental data are displayed in figure 4.12 and table 4.6.

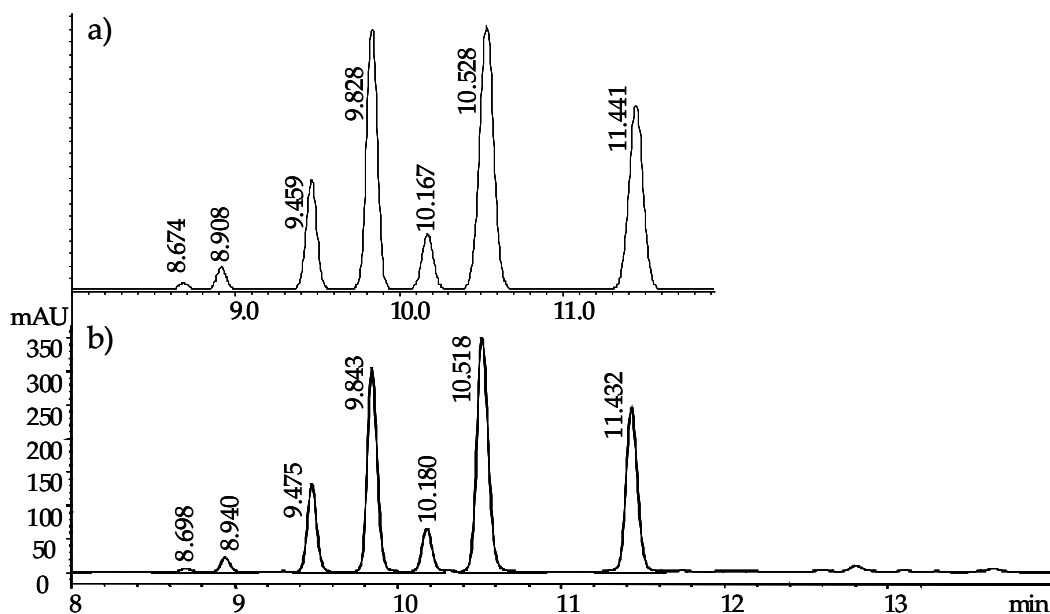


Figure 4.12: Chromatograms of 20 min gradient as a) predicted by DryLab® and b) obtained from an experiment run with an ACE 5 C8, 150 x 4.6 mm, 5  $\mu$ m, HPLC column with mobile phase consisting of 15 mM ammonium formate buffer and acetonitrile at 30 °C

Table 4.6: Comparison of actual and DryLab® predicted chromatographic data for experiment on ACE 5 C8, 150 x 4.6 mm, 5  $\mu$ m, HPLC column with mobile phase consisting of 15 mM ammonium formate buffer and acetonitrile at 30 °C

DryLab prediction			Actual experiment			% error		
$t_r$ (min)	PW (min)	$R_s$	$t_r$ (min)	PW (min)	$R_s$	$t_r$	PW	$R_s$
8.674	0.062	2.22	8.698	0.0830	1.89	0.3	25.3	17.3
8.908	0.062	4.81	8.940	0.0674	4.65	0.4	8.0	3.5
9.459	0.072	2.98	9.475	0.0677	3.12	0.2	6.4	4.5
9.828	0.074	2.66	9.843	0.0714	2.77	0.2	3.6	4.0
10.167	0.076	2.47	10.180	0.0717	2.59	0.1	6.0	4.8
10.528	0.096	5.56	10.518	0.0815	6.55	0.1	17.8	15.2
11.441	0.097	-	11.432	0.0827		0.1	17.3	

As can be seen from these figures (table 4.6), DryLab® predicted values for peak width, and consequently resolution, show some quite high values for the % error, which is partly due to a known software problem. Modelling using a later, updated DryLab® version (version 3.9 OUS Build 7.2411.1) provided % errors of generally < 2 %. Another known source for inaccurate predictions is input data from partly or fully overlapping peaks, where peak width and retention time cannot be entered with 100 % accuracy. These variations also add to errors in simulated results. However, the simulated retention times are very accurate (table 4.6) and the model could be used with confidence for computer assisted method development.

A DryLab® generated two dimensional resolution map (figure 4.13) provides information on optimum separation conditions with regard to gradient time and oven temperature. Maximum resolution for all compounds of interest is achieved with conditions where the map shows a deep red colour, in this case for a 21 min gradient at 30 °C.

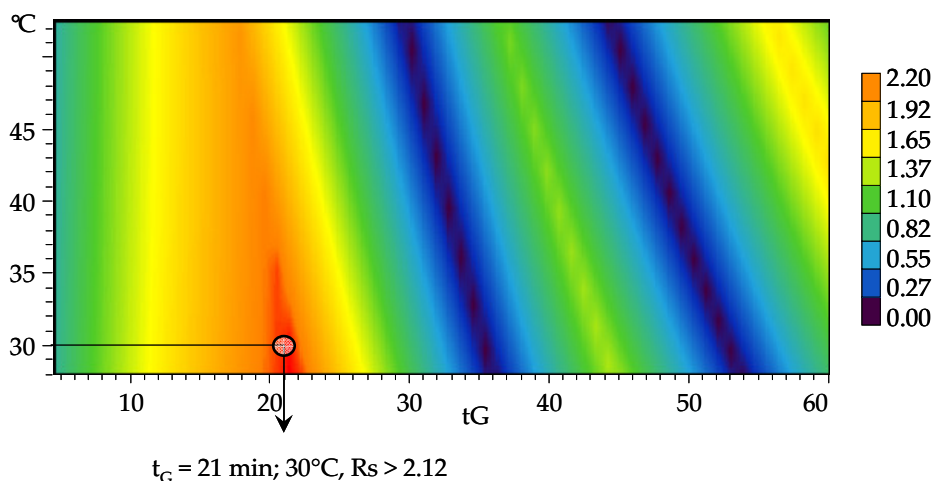


Figure 4.13: DryLab® generated two dimensional resolution map, predicting optimum resolution of all compounds of interest on a ACE 5 C8, 150 × 4.6 mm, 5 µm, HPLC column with mobile phase consisting of 15 mM ammonium formate buffer and acetonitrile

Chromatographic data of the DryLab® prediction and the experimental run with this gradient are illustrated in figure 4.14. Comparison of the actual and predicted data, shows a shift of the retention times in the experimental chromatogram (figure 14 b), as compared to the DryLab® chromatogram (figure 14 a).

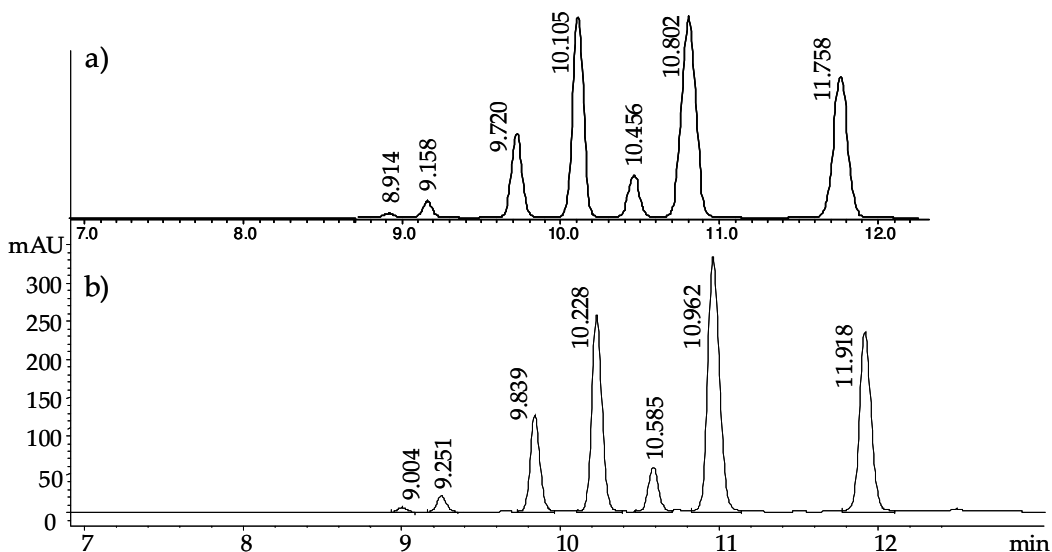


Figure 4.14: Chromatograms of 21 min gradient as a) predicted by DryLab® and b) obtained from experiment run on ACE 5 C8, 150 x 4.6 mm, 5 µm, HPLC column with mobile phase consisting of 15 mM ammonium formate buffer and acetonitrile at 30 °C

The % error in  $t_R$  increased from < 0.5 % to up to 1.5 % due to the longer retention of the analytes with the C8 phase. The fact that initially the predicted and experimental data for the 20 min gradient run on the exact same column were in good agreement (table 4.6) suggests that, with weeks of carrying out experiments on this phase, some changes to the surface chemistry have taken place, changing the retention behaviour of the compounds on this column. This possibility was investigated further by analysing the mixture of ISM and related substances on a new, unused ACE 5 C8 (150 x 4.6 mm, 5 µm) column and injecting one sample every hour for a week.

After 168 injections no obvious shift to longer retention times was observed (table 4.7). If the variations seen on the previously used C8 phase were due to the positively charged phenanthridine compounds being adsorbed on to the column, altering stationary phase chemistry, then a greater exposure to the analyte mixture is required.

Table 4.7: Retention times of ISM and related substances over one week on ACE 5 C8, 150 x 4.6mm, 5 µm, HPLC column with mobile phase consisting of 15 mM ammonium formate buffer and acetonitrile at 30 °C

	Day 1	Day 2	Day 3	Day 4	Day 5	Day 6	Day 7
Compound	t <sub>R</sub> (min)	t <sub>R</sub> (min)	t <sub>R</sub> (min)	t <sub>R</sub> (min)	t <sub>R</sub> (min)	t <sub>R</sub> (min)	t <sub>R</sub> (min)
Unknown	2.79	2.80	2.81	2.79	2.79	2.77	2.75
M&B4596	3.21	3.23	3.24	3.22	3.22	3.20	3.18
M&B4250	4.00	4.01	4.02	4.00	4.01	3.99	3.98
M&B4180A	4.31	4.33	4.33	4.32	4.33	4.31	4.30
M&B38897	4.59	4.61	4.62	4.60	4.61	4.59	4.58
Dimidium	5.10	5.13	5.14	5.12	5.13	5.11	5.11
Homidium	5.71	5.74	5.74	5.73	5.74	5.71	5.71

(run with optimised 4 min gradient, see section 4.2.4; table 4.3)

As the *k* values for all the compounds are within a narrow range, the analysis of ISM and related compounds does not necessarily require gradient analysis. Use of an isocratic method is an advantage, as column re-equilibration between injections is not necessary, saving solvent, and it can be used with more simple equipment. Thus DryLab<sup>®</sup> was used to predict optimum isocratic conditions for the separation, by generating isocratic data sets with the gradient model. These generated data were used as an input data set for an isocratic DryLab<sup>®</sup> model, providing an isocratic resolution map which plots resolution versus % organic solvent in the mobile phase (figure 4.15).



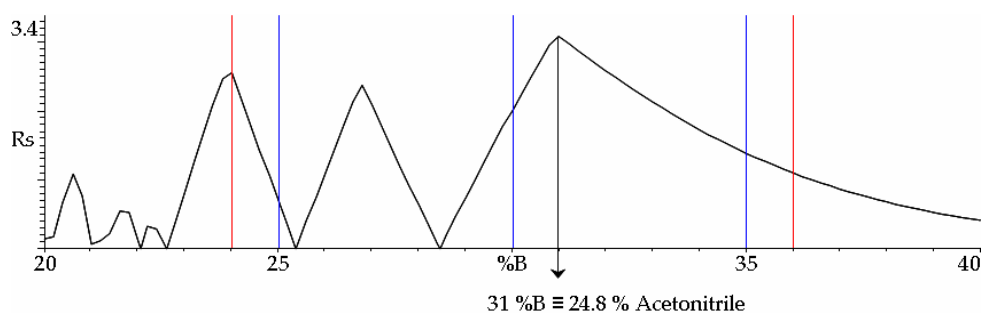


Figure 4.15: DryLab® generated resolution map, predicting isocratic conditions for optimum resolution of all compounds of interest on an ACE 5 C8, 150 x 4.6 mm, 5  $\mu$ m, HPLC column with mobile phase consisting of 15 mM ammonium formate buffer and acetonitrile

Comparison of chromatographic data as predicted by DryLab® (figure 4.16 a) with chromatograms obtained isocratically on the ACE 5 C8 column (figure 4.16 b) shows that isocratic modelling is not as accurate as predictions obtained for a gradient experiment. Moreover, the fact that the early eluting compounds run off very close to the solvent front was not estimated by the simulation software. However, using the conditions determined by DryLab®, baseline separation ( $R_s > 2.2$ ) of all analytes of interest is achieved with an overall analysis time of 10 minutes.

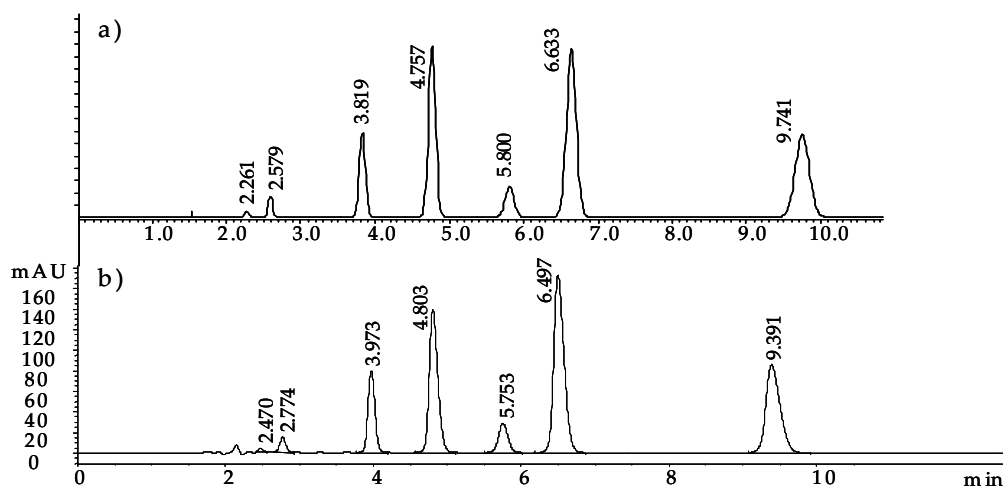


Figure 4.16: Chromatograms of isocratic separation of ISM and related substances as a) predicted by DryLab® and b) obtained from experiment run on an ACE 5 C8, 150 x 4.6 mm, 5  $\mu$ m, HPLC column with mobile phase consisting of 15 mM ammonium formate buffer/acetonitrile; (75 : 25 v/v) at 30 °C

The major advantages of isocratic elution over gradient analysis is the shorter overall analysis time, which means a lower solvent consumption. The 21 min gradient however does provide exceptionally good peak shape even for the late eluting analytes (figure 4.14 b). Peak widths of 0.110 - 0.152 min with the isocratic separation are reduced to peaks with a bandwidth of 0.071 - 0.075 min using the gradient, giving a peak height for ISM of 259 mAU instead of 140 mAU with the same sample concentration. Consequently, as sensitivity is a major goal, a gradient would be the favoured method for the analysis of trace amounts of residual ISM in the plasma of treated cattle.

Examination of the chromatogram obtained with the 21 min gradient on the ACE 5 C8 column (figure 4.14 b) shows that the first analyte elutes at 9 min. Starting the gradient with a higher percentage of organic solvent without changing the overall gradient profile should enable earlier elution of all compounds, while maintaining selectivity.

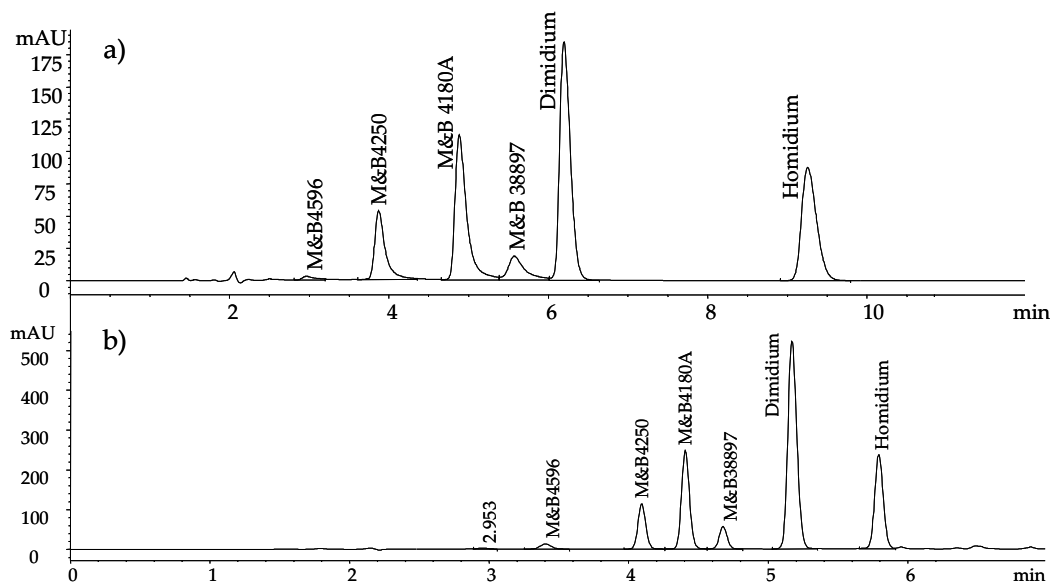


Figure 4.17: Chromatograms obtained with a) isocratic conditions (ammonium formate buffer, pH 2.8 / acetonitrile; 75 : 25 v/v) on Gemini 5u C18 and b) 4 min gradient on ACE 5 C8, 150 x 4.5 mm, 5  $\mu$ m HPLC columns, with mobile phase consisting of 15 mM ammonium formate and acetonitrile at 30  $^{\circ}$ C.

Again DryLab® modelling was used to explore this possibility so that the gradient time could be reduced to only 4 minutes. Furthermore, given the narrower gradient range from 30 - 60 %B instead of 5 - 100 %B, less column re-equilibration is required (Euerby, 2010) (equation 13). Post time can be reduced to 5 min, giving a total cycle time of 12 min, instead of 40 min.

Equation 13: 
$$V_D + (5V_M \Delta\Phi) \leq V_{equilibration} \leq V_D + (10V_M \Delta\Phi)$$

where  $V_D$  is the system dwell volume (1.75 ml),  $V_M$  is the column dead-volume (1.6 ml) and  $\Delta\Phi$  = gradient range (0.3).

A typical chromatogram of the separation and comparison of the improved method to the originally reported assay (chapter 2) is shown in figure 4.17. With the 4 min gradient (figure 4.17 b) the two early eluting analytes elute under isocratic conditions, producing wider, flatter peaks than expected in a gradient, due to the system delay volume. However, for a bioanalytical investigation of ISM and related substances these two minor compounds can possibly be neglected, as no detectable concentrations would be present in the plasma of animals treated with an ISM formulation. Bearing this in mind, this improved, highly sensitive gradient method could well be employed for the intended purpose.

Comparison of figures 4.17 a) and b) does show very well the improvements achieved in peak shape and resolution by using this short gradient on a high purity silica C8 phase. Those chromatograms derive from injection of samples with identical ISM concentrations. The increase in peak height, only due to column performance and gradient conditions becomes very obvious. Use of an equivalent column with a smaller inner diameter, to be used with a lower flow rate compatible with MS detection needs further investigation, as well as the re-validation of the bioanalytical assay using the improved HPLC method.

#### 4.4. Conclusions

As the earlier reported HPLC assay for the bioanalytical investigation of ISM and related substances (chapter 3) failed to prove good precision for the analysis of trace amounts of the trypanocide in spiked plasma samples, the possibility of improving the assay with respect to selectivity and efficiency was investigated. Evaluation of different mobile phase compositions confirmed the previous choice of an ammonium formate buffered mobile phase with an acidic pH of 2.8 to suppress silanol ionisation does provide optimum peak shapes for the charged, basic analytes of interest. Changes in temperature do not seem largely to affect the separation. Gradients run at 30 °C and 50 °C resulted in almost identical chromatograms. Robustness against changes in temperature is an advantage when taking into account that the method might be used for field studies in laboratories situated in Africa.

Furthermore, ten different stationary phases with varying surface chemistries were tested for their effect on the selectivity of the separation. It was found that hydrophobic interactions of the phenanthridine compounds with the bonded organic layer are not the only factor accounting for retention and selectivity of the separation. The retention mechanism of these analytes seems to be multi faceted, with ion exchange and aromatic  $\pi$ - $\pi$  interactions markedly contributing to the retentive potential of a stationary phase. Plotting  $\log k$  versus % organic (see figure 4.10) provided an insight into the retention behaviour of M&B4180A on various columns. The results showed that retention decreases with increasing surface coverage of the organic ligands, and increases with increasing polar character of the stationary phase, indicating that ionic interactions play an important part in the retention mechanism of this compound. Enhanced retention on columns with an

aromatic functionality suggests that also  $\pi$ - $\pi$  interactions of the stationary phase with the aromatic solute add to this effect.

Comparison of the obtained data led to the choice of a C8 HPLC column, rather than the previously reported C18 phase for this separation. This finding correlates well with results obtained during method development of a solid phase extraction method (see section 3.3.1.3) where C8 cartridges proved to be the method of choice.

DryLab<sup>®</sup> computer simulation software was successfully employed to model optimum separation conditions for gradient and isocratic separations of ISM and related substances. The disadvantage of gradient analysis, producing an increased run time due to long column re-equilibration times could be overcome by decreasing the gradient time from 21 min to 4 min and the gradient range from 95 to 30 %. The analysis was started with an increased % organic solvent of 30 % rather than 5 %, causing the compounds to elute after 3 instead of 9 minutes, and with the narrower gradient range column equilibration time was reduced to 5 instead of 13 min. Gradient analysis is favourable to use as a bioanalytical assay of traces of ISM and related substances in plasma samples, as the constant increase of organic solvent produces distinctively narrower peak shapes, compared to an isocratic separation. The result is a marked improvement in the signal-to-noise ratio, peak height is increased and sensitivity of the method improved. Comparison of a chromatogram obtained with the optimised 4 min gradient analysis on an ACE 5 C8 column with one obtained with the original isocratic conditions on the Gemini 5u C18 column (figure 4.17) highlights the dramatic improvements in peak shape and sensitivity due to column performance and improved separation conditions.

This gradient method has not yet been tested with an equivalent column with a narrower inner diameter and packed with smaller particles, to use with a lower flow rate. This measure is required as there is a need for compatibility with MS detection and an ESI interface. Splitting the mobile phase flow prior to detection would cause sample losses, thus an increase in the detection limit, which should rather be avoided. If the method can be proven to be adaptable to MS compatible conditions it should provide a highly sensitive, while selective alternative to ELISA tests for the determination of residual trace amounts of ISM in the plasma of treated animals. Until then, with UV detection, after validation, the assay can be used as an improved quality control method for quality assurance of commercial ISM formulations.

## 5. Isolation and Characterisation of Isometamidium and Structurally Related Compounds

### 5.1. Introduction

Despite recent efforts to advance the development of standards and protocols for the quality control and quality assurance of ISM formulations (FAO, 2006; PAAT/FAO, 2008; WHO, 2009a) at present there is no internationally agreed reference standard or official monograph available for the evaluation of commercially available ISM products. With the same limited number of veterinary trypanocides available on the market over the past fifty years, and the unlikelihood of new products being introduced (Sones, 2001), maintenance of the effectiveness of available drug formulations is essential. Without approved protocols a standardised quality control is lacking, leading to the undetected distribution of sub-standard and counterfeit therapeutic agents (Eisler *et al.*, 1996b) (see also sections 1.1.3 & 1.1.4). Drug resistance to the trypanocides is evolving (Geerts *et al.*, 2001) and the only way to protect the current drug regime and retain efficacy is to apply stringent quality controls and assure good practice in their use.

Monographs, as provided by the official pharmacopoeias for human trypanocides, include a definition of the drug, its physicochemical properties, the identification and dosage of the active principle and identification and content of impurities (Karembé, 2008). In ISM formulations the principal component ISM (M&B4180A) is present to only about 60 % (section 2.2.1). The major by-products which need to be controlled are its structural isomers M&B4250 and M&B38897, a process related bis-amidino compound M&B4596 and the degradation product homidium (figure 2.3). Unfortunately, with the exception of homidium, there are no analytical

reference standards available of the single compounds. The only chemical reference substance supplied by the innovator company is a reference standard mixture (RSM) with known relative amounts for each constituent which does not allow the specific characterisation of a single component. Furthermore, as the sphere of interest in these compounds and their evaluation is small, albeit extremely important in parts of the world, efforts to isolate and characterise pure standards of ISM and related compounds have been limited. There are no published reports of any structure elucidation studies using techniques such as MS and NMR spectroscopy, and the known physicochemical properties mostly refer to the mixture rather than each single component (Clarke, 1969; JECFA, 2003). In order to provide the regulatory authorities with a well characterised quality control protocol and established analytical reference substances, characterisation not only of the mixture of compounds, but of pure ISM and isolated related substances is essential.

#### **5.1.1. Establishment of Quality Standards**

Since 1951 the World Health Organization (WHO) has been engaged in developing an International Pharmacopoeia (IP) for drugs and formulations used for the treatment of neglected diseases (WHO, 2003) which are not included in the existing Pharmacopoeias (British, European, U.S.A., etc.). These efforts have led to the recent publication of a 4<sup>th</sup> edition in 2006, that contains specifications for human-use trypanocides, which also had not been covered by any officially approved monograph previously (Karembé, 2008; WHO, 2008). If veterinary trypanocides were to be included in this collection of monographs, as well, this could largely improve the evaluation of their quality on the basis of efficacy and safety according to the EMLs (List of



Essential Medicines) and WHO treatment guidelines. There are eighteen steps to be followed in the development of a new monograph (WHO, 2009b), including the identification of pharmaceutical products for which quality control specifications need to be developed, development and validation of analysis methods, draft quality control specifications and the establishment of international chemical reference substances. Reference standards, not only of the active ingredient but also of known by-products, are required in order to provide a definition of the drug in question, its physicochemical properties, identification and quantification of the active principle as well as potential impurities (Karembe, 2008). The WHO's general guidelines for the establishment, maintenance, and distribution of chemical reference substances (WHO, 1997) advise that reference standards used in quantitative analysis preferably possess a purity of  $\geq 99.5\%$  and that the identity should be verified by several analytical techniques such as mass spectrometry, nuclear magnetic resonance spectroscopy, infrared and ultraviolet spectrophotometry. In order to establish ISM as an international chemical reference substance as required for a monograph in the IP, these data have to be obtained for each constituent of the ISM preparation, pure ISM and all the known by-products. Thus, instead of analysing the reference standard mixture, the individual compounds need to be isolated.

### **5.1.2. Preparative HPLC**

An efficient and versatile way to isolate, enrich and purify single components from a sample is the use of preparative liquid chromatography. Unlike an analytical separation, where the purpose is to obtain qualitative or quantitative information about a compound, preparative HPLC is carried out to recover a purified product from an impure sample preparation

(McDonald & Bidlingmeyer, 1987). While an analytical separation aims at a maximum peak capacity, high plate numbers (N) and good separation in the shortest possible time, the goal of a preparative separation is a maximum throughput, a substantial yield of sample purified in reasonable time. Columns used for such separations have an inner diameter of 1 - 3 cm, for so called semi-prep separations, and 3 - 10 cm or larger for a larger preparative scale. They are packed with particles of 5 - 7  $\mu\text{m}$  or  $> 7 \mu\text{m}$  diameter respectively. Flow rates of  $\geq 5 \text{ ml/min}$  are used and the detection conditions are set to a low sensitivity, as sample loads must be as large as possible to achieve a maximum yield of purified product (Bidlingmeyer, 1992; Snyder *et al.*, 1997c). However, preparative HPLC involves more than just scaling up column size and flow rate. As highly concentrated samples are required, sample solubility plays an important role in method development, as well as in the choice of mobile phase. As the compound collected from the detector outlet is dissolved in mobile phase, recovery of the isolated product should be feasible. Consequently the use of volatile mobile phases is preferred, without any addition of involatile additives, such as inorganic buffer salts or ion pairing reagents (Snyder *et al.*, 1997c). Contrary to an analytical separation which aims at baseline resolution of all compounds in a mixture, the separation in preparative LC is matched to its requirements for purity and recovery. Often moderate resolution of the major compound from present impurities is sufficient (Bidlingmeyer, 1992). Usually column-overload conditions are used in order to isolate milligram amounts of the compound of interest (Snyder *et al.*, 1997c). This means that the sample load is great enough to deform the solute band, resulting in a loss of resolution (figure 5.1). With sample concentrations in the  $\mu\text{g}$  region (analytical column) retention and bandwidth do not usually depend on sample size (figure 5.1 a).

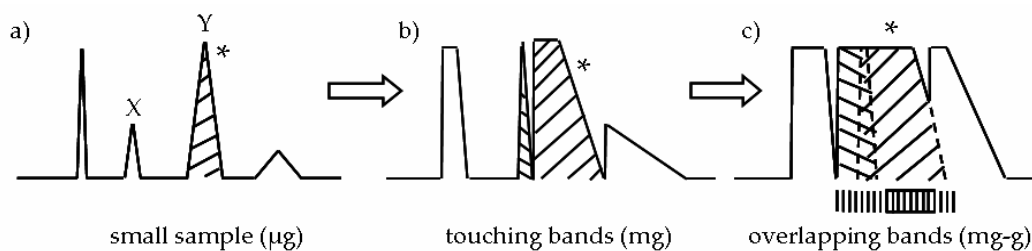


Figure 5.1: Theoretical separation as a function of sample weight, a) analytical conditions, b) lightly overloaded (touching band) separation, c) heavily overloaded (overlapping band) separation (Snyder *et al.*, 1997c)

With a greater sample load the compound band Y (\*) widens, resulting in a touching-band separation with the adjacent impurity X (figure 5.1 b).

Nevertheless, recovery and purity of up to 100 % can be achieved using this approach, while obtaining a much higher product yield than with use of smaller sample sizes (Snyder *et al.*, 1997c). Injections of still greater sample weights can result in a complete band overlap of product and impurities (figure 5.1 c). To obtain a pure sample using this method, small fractions across the product band can be collected, to obtain an enriched sample which needs further purification to recover a final product.

For the development of a preparative HPLC method for the isolation of a pure compound from an impure starting material it is useful if possible, to start with the HPLC conditions used to analyse the sample. Those conditions can be scaled up to a larger column, with a higher flow rate and larger sample sizes and optimized for a preparative LC separation (Snyder *et al.*, 1997c).

### 5.1.3. Synthesis of Isometamidium: Influence of Reaction Conditions on the Presence of Related Substances

As described in section 2.1.1 the synthesis of ISM results from an electrophilic substitution reaction (figure 2.2), where the diazonium salt, m-amidinobenzenediazonium chloride is coupled to the 8-amino group of

homidium (Wragg *et al.*, 1958). Reactivity of the weak electrophile is greatly enhanced by the presence of the electronegative amidino substituent leading to the production of, not only the principal isomer M&B4180A, which has the greatest trypanocidal activity (Berg, 1960), but also a positional isomer (M&B38897) and at least one doubly coupled product (M&B4596) (figure 5.2). The relatively high electron density of the carbon atoms in *ortho*- and *para*-positions of aromatic primary amines and the reactivity of the amidinobenzenediazonium ion can also result in formation of a purple aminoazo compound (M&B4250) (figure 5.2) by C-coupling at the 2- or 4- or 7- or 9-carbon atom of the homidium molecule (Berg, 1963). Rearrangement of the diazoamino-compounds at elevated temperature (60 – 100 °C), catalysed by addition of acid and the free amine could also lead to formation of the purple isomer.

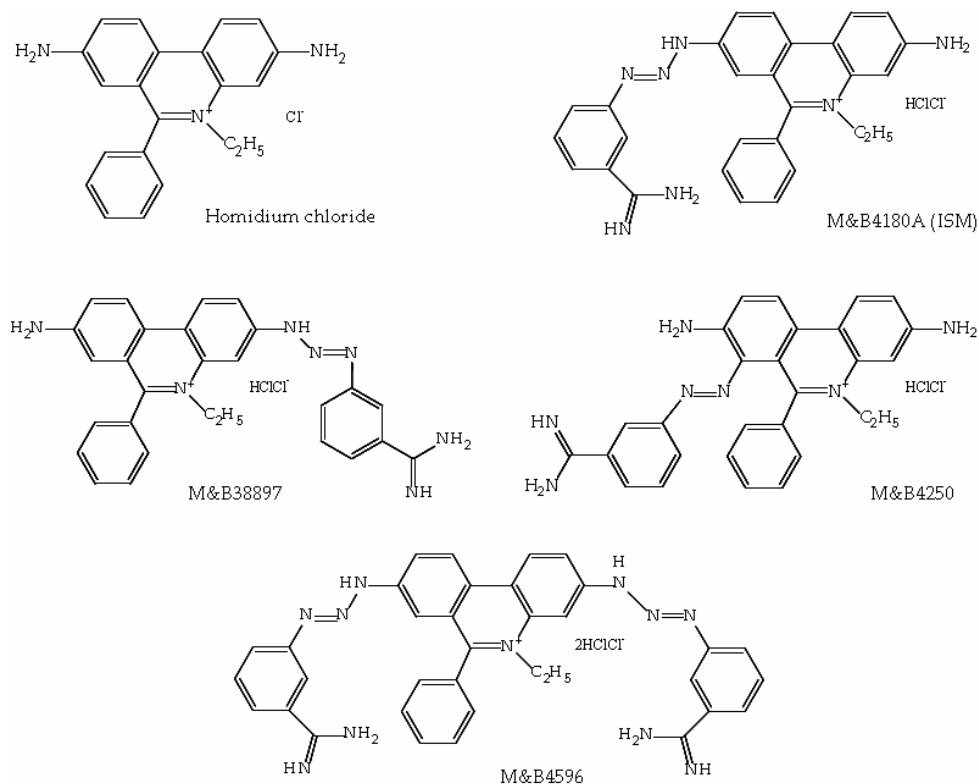


Figure 5.2: Proposed chemical structures of ISM and related substances (Tetty *et al.*, 1999)

In order to optimise the reaction in favour of the principal isomer M&B4180A, it should be carried out in strongly acidic media (pH 1 - 2), where *N*-coupling could occur on the weak base homidium, while the possibility of *C*-coupling is strongly reduced (Berg, 1963). It has been shown that diazotation of homidium results predominantly in the 8-diazonium analog rather than production of the 3-diazonium isomer (Firth *et al.*, 1983). The low reactivity of the 3-amino group is possibly due to the participation of its free electron pair in a resonance configuration with the quaternary nitrogen (figure 5.3), rendering it more stable and less available for attack by the diazonium ion (see section 2.1.1; figure 2.2) (Berg, 1963; Firth *et al.*, 1983).

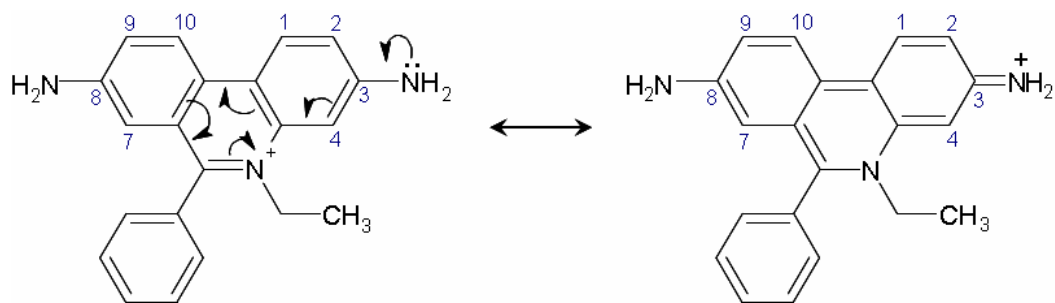


Figure 5.3: Participation of the 3-amino group in a resonance configuration with the quaternary nitrogen (Firth *et al.*, 1983)

The 8-amino group with its free electron pair is thus more reactive, as it does not participate in the resonance configuration. Similarly, if *C*-coupling does occur the 7- and 9-carbon are more likely to be attacked by the electrophilic reagent than the 1- or 2- carbon atoms, where the electron density of the ring system is reduced. Formation of the bis-substituted related compound M&B4596 (figure 5.2) is least favoured by the reaction conditions (Berg *et al.*, 1961; Berg *et al.*, 1963). Therefore it only occurs as a minor process-related impurity in ISM formulations (Samorin®). However, cleavage of the acid-labile triazene bond in ISM (Kinabo & Bogan, 1988d; Philips *et al.*, 1967) and

an incomplete reaction during synthesis can lead to substantial amounts of the starting material homidium in the final preparation. Even with an optimised and carefully controlled synthetic process the presence of all the known ISM related compounds (figure 5.2) is inevitable. Therefore, a preparative HPLC method for the preparation of pure ISM and related compounds needs to be able to sufficiently separate the principal isomer (M&B4180A) and all the process related by-products in a mixture, in order to isolate and characterise each single one of them.

#### 5.1.4. Structure Elucidation of ISM and Related Compounds

Wragg *et al.* (1958) introduced metamidium as a new trypanocidal drug, consisting of a mixture of two isomeric *p*-amidino-phenyldiazoamino-derivatives resulting from the coupling reaction of diazotised *p*-amino-benzamidine and homidium chloride in the presence of sodium acetate at a temperature of 0 to 5 °C. The resulting compounds could be separated due to their different solubilities. Precipitation from water with sodium chloride and subsequent fractional crystallization from water and methanol of the products resulted in isolation of a relatively water-insoluble purple (55 %) and a red isomer (45 %).

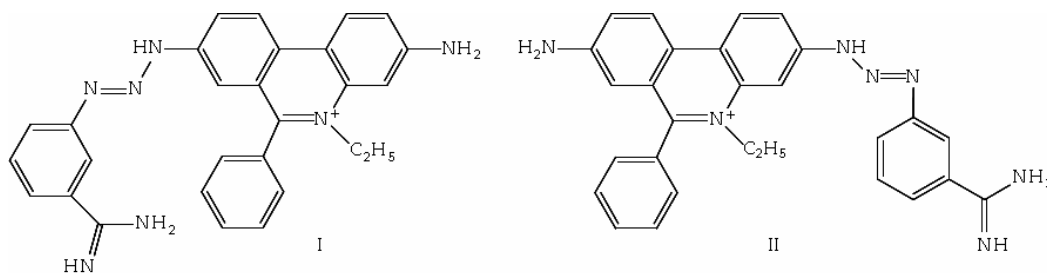


Figure 5.4: Provisionally assigned chemical structures by Wragg *et al.* (1958) for purple (I) and red (II) isomers contained in metamidium.

With paper electrophoresis and acetic acid as the electrolyte solution, the purple isomer was markedly more mobile than the red one. As the 8-amino group was known to be more prone to substitution and the purple isomer was the predominant product, structures I and II (figure 5.4) were provisionally assigned (Wragg *et al.*, 1958). Existence of stable tautomeric forms of the diazoamino group was ruled out based on distinct differences in their IR spectra (Berg, 1963). A diagnostic test for the presence of the diazoamino group in each isomer was carried out by measuring the volume of released nitrogen when boiled in dilute sulphuric acid (water : sulphuric acid; 5 : 1 v/v). Due to rapid evolution of nitrogen from both isomers, the presence of a diazoamino group in both structures was inferred, although the purple isomer yielded only about 65 % of the theoretical volume, while nearly 100 % evolved from the red isomer (Wragg *et al.*, 1958). Later these reaction conditions were found to be too drastic for this qualitative test. Boiling both compounds with milder conditions (cuprous chloride-3 M hydrochloric acid) revealed that the purple isomer did not contain a diazoamino group (Berg, 1960).

Structure I (figure 5.4) was consequently assigned to the red isomer, which was called isometamidium or M&B4180A by May and Baker, while the purple compound was suggested to be an aminoazo compound in which the amidinophenylazo-group is attached to one of the ring carbon atoms in *ortho*-position to the amino groups (figure 5.5) (Brown *et al.*, 1961).

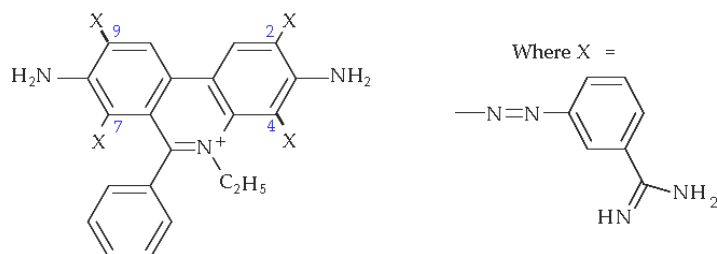


Figure 5.5: Proposed chemical structure of the purple isomer present in metamidium (Brown *et al.*, 1961)

However, C-coupling at position 2 and 4 is considered unlikely due to a resonance configuration involving the change in positive charge (section 5.1.3; figure 5.3) (Berg, 1963; Firth *et al.*, 1983). The only confirmation of the structure of the red isomer (ISM) was the deamination to the diazoamino compound, which could be synthesized selectively, for comparison. Unlike homidium, which has been extensively characterised (Firth *et al.*, 1983; Fraire *et al.*, 1981; Griggs *et al.*, 1980; Luedtke *et al.*, 2004), there are no unambiguous published reports on the structure elucidation of pure ISM or its isomers, by state of the art instrumentation like IR-, UV-, NMR- or high resolution mass spectrometry.

#### **5.1.5. Aims and Objectives**

Synthesis of the veterinary trypanocide ISM always results in production of a mixture of related compounds (Tetty *et al.*, 1998). So far there are no published reports on the isolation and characterisation of the single substances contained in the RSM and commercially available formulations. In order to establish official monographs and internationally agreed standards for the quality control of these formulations, pure and well characterised chemical reference standards of each of the constituents of ISM formulations need to be prepared. The aim of this part of the study is the computer assisted development of a preparative HPLC method for the isolation of ISM and process related by-products. Once isolated in pure form, they will be characterised using UV, mass and NMR spectroscopy.



## 5.2. Experimental

### 5.2.1. Materials

HPLC-grade acetonitrile and methanol were obtained from VWR International Ltd. (Poole, UK). Analytical reagent formic acid, anhydrous ammonia ( $\geq 99.99\%$ ), dimethyl sulfoxide-d<sub>6</sub> (99.96 atom %D) and 5 mm symmetrical Shigemi NMR microtube assemblies, matched with DMSO-d<sub>6</sub>, (bottom length 15 mm) were bought from Sigma-Aldrich (Dorset, UK). A secondary reference standard mixture (RSM) of isometamidium and related substances containing 8-(*m*-amidinophenyldiazoamino)-3-amino-5-ethyl-6-phenylphenanthridinium chloride [(58.6 %w/w), ISM, M&B4180A], 3-(*m*-amidinophenyldiazoamino)-8-amino-5-ethyl-6-phenylphenanthridinium chloride [(13.3 %w/w), M&B38897], 7-(*m*-amidinophenyldiazo)-3,8-diamino-5-ethyl-6-phenylphenanthridinium chloride [(13.7 %w/w), M&B4250] and 3,8-di(3-*m*-amidinophenyltriazeno)-5-ethyl-6-phenylphenanthridinium chloride [(8.1 %w/w), M&B4596] and pure homidium (3,8-diamino-5-ethyl-6-phenylphenanthridinium chloride) were generously donated by Merial Limited (Toulouse, France). An analytical (150 x 4.6 mm; 5  $\mu$ m) and a semi-preparative (250 x 10 mm; 5  $\mu$ m) ACE 5 C18 HPLC column from ACT were purchased from Hichrom Ltd.

*Mobile phase for semi-preparative separation: a mixture of 0.1 % ammonium formate solution (pH 6.0) and acetonitrile (77 : 23 v/v)*

Formic acid (1 ml) was accurately pipetted into 800 ml of distilled water using an Eppendorf pipette. The pH of the solution was adjusted to 6.0 using a dilute aqueous solution of ammonia, and made up to 1 L with distilled water. A volume of the ammonium formate solution (770 ml) was added to 230 ml of acetonitrile.

#### *Mixed standard solution (1 %w/v)*

A weight of the reference standard mixture (RSM) of ISM and related compounds (100 mg) was accurately weighed using a Mettler AT20 analytical balance (readability 0.01 mg) and transferred to a 10 ml volumetric flask. The flask was made up to the mark with water to produce a standard solution containing M&B4180A (5.86 mg/ml), M&B4596 (0.81 mg/ml), M&B38897 (1.32 mg/ml) and M&B4250 (1.37 mg/ml).

#### **5.2.2. HPLC - UV Analysis**

An Agilent HP1100 series quaternary pump with ChemStation® software version 10.02 for data acquisition equipped with a HP1100 series UV-Vis detector was used. M&B4180A and related substances were separated on analytical (150 × 4.6 mm; 5 µm) and semi-preparative (250 × 10 mm; 5 µm) ACE 5 C18 HPLC columns. The mobile phase was delivered at a flow rate of 1 ml/min for an analytical scale analysis and at 5 ml/min for the semi-preparative separations. Compounds were detected at a wavelength of 320 nm.

#### **5.2.3. HPLC - MS Analysis**

Stability of the isolated fractions was examined with an Agilent HP1100 series HPLC system equipped with a HP1100 series VWD detector. The system was also connected to a Finnigan LCQ Deca mass spectrometer (ThermoQuest Bremen, Germany) via an electrospray interface. High resolution MS analysis was performed using a Finnigan Surveyor HPLC system equipped with a Finnigan LTQ Orbitrap mass spectrometer (Thermo Electron Corporation). Data acquisition and evaluation was carried out with Xcalibur® software version 2.0.7. M&B4180A and related substances were

separated on an analytical (150 x 3.0 mm; 3  $\mu$ m) ACE 3 C18 HPLC column. The mobile phase was delivered at a flow rate of 0.4 ml/min. With the VWD detector, compounds were detected at a wavelength of 320 nm. For low resolution mass spectrometric analysis the following conditions were used: nebulising gas pressure, 10 psi; drying gas flow rate, 7 l/min; drying gas temperature, 300 °C; capillary voltage, 4000 V; positive ion mode; gain: 1; threshold: 150; step size: 0.10; peak width: 0.10 min; cycle time: 1.02 s/cycle. Data were acquired in full scan mode ( $m/z$  = 100–1000) at a fragmentor voltage of 70 V. For high resolution mass spectrometric analysis the conditions were: Source voltage: 4.50 kV; source current: 12.72  $\mu$ A, vaporizer temperature -63.88 °C; capillary voltage: 25.04 V; capillary temperature: 250.03 °C; tube lens voltage: 99.70.

#### 5.2.4. NMR Spectroscopy

Proton NMR spectra were recorded using a JEOL JNM-LA400 spectrometer operating at 400 MHz (Jeol Eching, Germany). Samples were dissolved in 200  $\mu$ L of deuteriated dimethyl-sulphoxide (DMSO- $d_6$ ) and referenced internally to the solvent (4.78 ppm at 25 °C). One- and two-dimensional techniques were used in assigning signals in homidium, M&B4180A (ISM) and M&B4250 spectra. Two-dimensional techniques used were COSY (Correlated SpectroscopY), TOCSY (Total Correlation SpectroscopY), ROESY (Rotating-frame Overhauser Effect SpectroscopY), HMBC (Heteronuclear Multiple Bond Connectivity) and HMQC (Heteronuclear Multiple Quantum Coherence). The data processing software in use was Delta<sup>®</sup> version 2.0.1 (Jeol) with data evaluation and formatting performed with MestreNova<sup>®</sup> NMR processing software (MacResearch).

### 5.2.5. DryLab® Input Data

Program: DryLab® 2000 plus version 3.6.1

Chromatographic input data: see section 4.3.2

– **Instrument Data**

- Dwell volume: 1.75 ml
- Extracolumn volume: 0.016 ml
- Time constant: 0.100 sec

– **Elution Data**

- Run Type: isocratic
- Temperature: 30 °C
- Isocratic data: 25, 30 and 35 %B
- Solvent A: A: 15 mM formate, pH 2.8 in water
- Solvent B: B: 15 mM formate, pH 2.8 in  
acetonitrile / water (80 : 20 v/v)

### 5.3. Results and Discussion

#### 5.3.1. Preparative HPLC

DryLab® computer modelling was used to obtain the optimum isocratic conditions for the separation of ISM and related compounds on a C18 semi-preparative column (250 x 10 mm, 5 µm). The 15 and 45 min gradients, run at 30 °C on an ACE 5 C18 column with a mobile phase containing ammonium formate and acetonitrile (see section 4.3.2) were used as DryLab® data input. The software was used to simulate isocratic separations with 25, 30 and 35 %B and the generated results were used as virtual input data set for an isocratic DryLab® model, providing an isocratic resolution map.

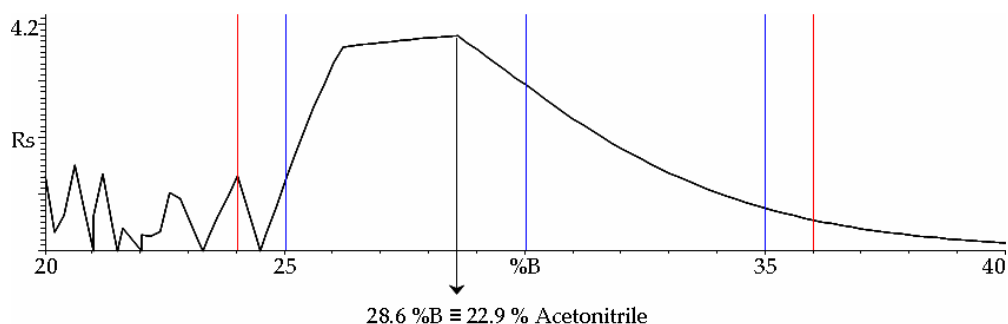


Figure 5.6: DryLab® generated resolution map, predicting isocratic conditions for optimum resolution of the compounds of interest on an ACE 5 C18, HPLC column with mobile phase consisting of ammonium formate in water and acetonitrile

The resolution map (figure 5.6) predicts an optimum isocratic separation with resolution for all compounds > 3.7 when using a mobile phase consisting of an ammonium formate solution and acetonitrile in a ratio of 77 : 23 (v/v). Unlike an analytical separation where high sensitivity and short analysis times are important parameters to consider, for the preparative HPLC method the main focus lies in good separation of the target compounds from any impurity, even under overload conditions (Snyder *et al.*, 1997c), in order to collect a concentrated sample as pure as possible.

With values for  $R_s > 3.7$  the compounds can be expected to elute far enough apart from each other to avoid the tailing of one solute band into the next eluting substance.

An analytical scale experiment was initially carried out to confirm the DryLab® predicted results (figure 5.7).

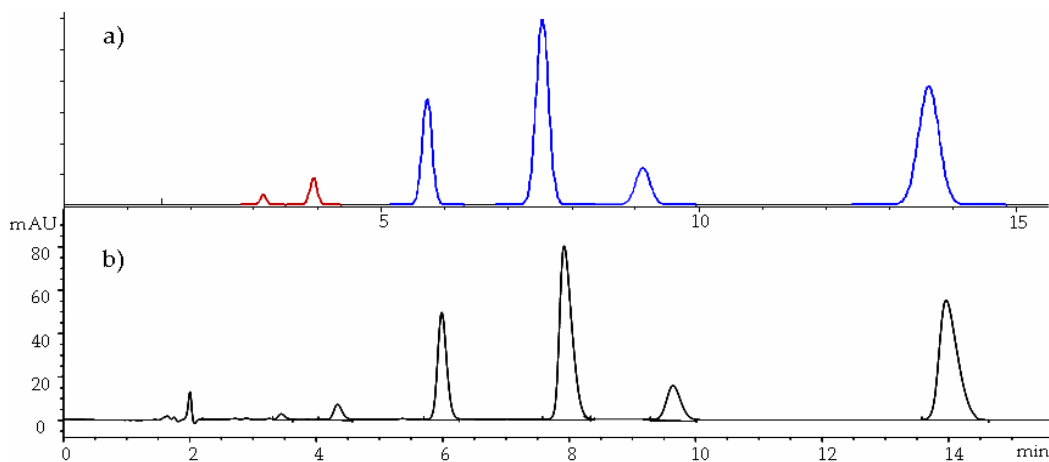


Figure 5.7: a) DryLab® prediction and b) experimental data of an isocratic separation of ISM and related compounds on an ACE 5 C18, HPLC column (150 x 4.6 mm) with mobile phase consisting of ammonium formate solution and acetonitrile at 28.6 %B (23 %v/v acetonitrile)

As can be seen, the experimental chromatogram was in good agreement with the one obtained from computer simulation (figure 5.7). The method was then transferred to a larger scale, so that the separation could be carried out with a semi-preparative column (ACE 5 C18, 250 x 10.0 mm). In order to keep the linear velocity constant and not change the selectivity of the separation when changing column dimensions, the flow rate had to be adjusted according to equation 14, where  $F_t$  is the target flow rate,  $F_a$  is the actual flow rate,  $d_t$  is the new inner diameter,  $d_a$  is the actual inner diameter and  $l_a$  and  $l_t$  are the actual and target column lengths, respectively.

Equation 14:

$$F_t = F_a \times \frac{d_t^2}{d_a^2} \times \frac{l_t}{l_a}$$

The new flow rate was calculated as 7.8 ml/min. However, an analytical HPLC system was used (section 5.2.2), with 5 ml/min as the highest possible flow rate. As a result using a lower linear velocity, the run time will increase as compared to the separation in analytical scale (figure 5.7).

To achieve the highest possible gain from every sample injection, the injection volume was set to a maximum value of 100  $\mu$ l and a concentrated sample containing 5.86 mg/ml ISM (1 %w/v RSM solution) was injected. The pH of the mobile phase was adjusted to 6.0 to avoid degradation of ISM to homidium (Kinabo & Bogan, 1988c). A typical chromatogram of the semi-preparative separation of ISM and related substances (figure 5.8 a) shows pronounced peak tailing, due to the high sample load.

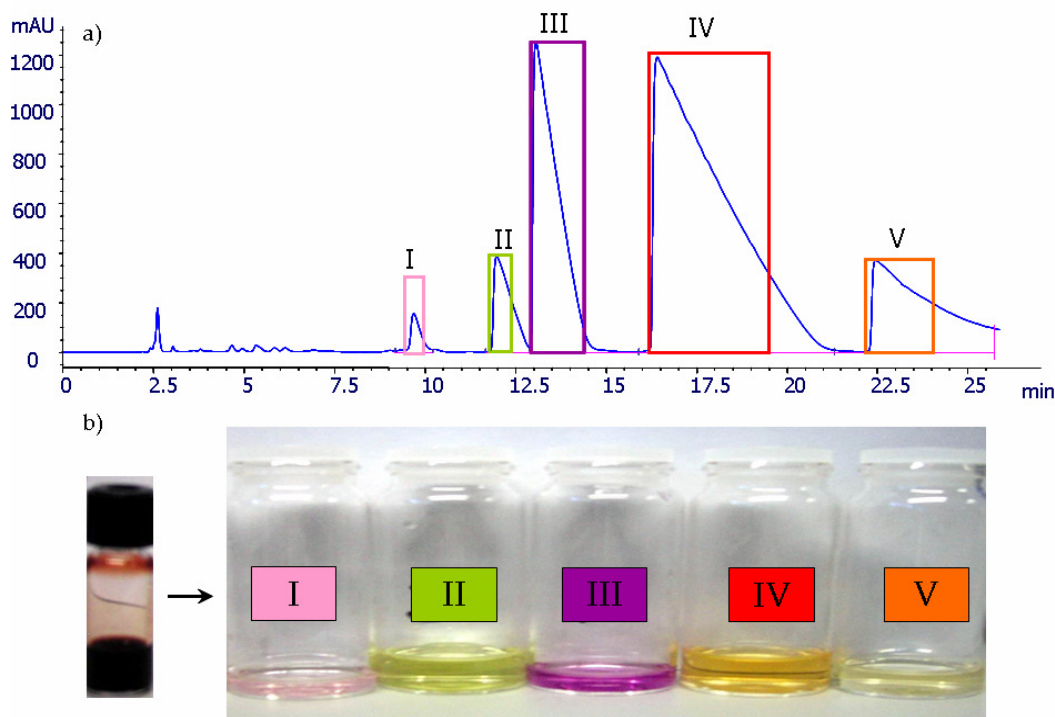


Figure 5.8: a) Representative chromatogram of the isocratic, semi-preparative separation of ISM and related compounds on an ACE 5 C18, HPLC column (250 x 10 mm) with mobile phase consisting of ammonium formate solution (pH 6.0) and acetonitrile (77 : 23 v/v)  
b) Fractions I - V obtained from a 1 %w/v RSM solution of ISM and related compounds

Each injection has a theoretical yield of ISM of 0.6 mg. The coloured boxes in the chromatogram (figure 5.8 a) indicate the time frame in which each fraction was collected to obtain a pure sample. The different colours of fractions II - V, yellow (M&B4596), purple (M&B4250), orange (M&B4180A) and orange (M&B38897) (figure 5.8 b) comply with those reported for the spots obtained in a TLC determination of ISM and related compounds (Tetty *et al.*, 1998) and indicate a successful separation of the analytes. To assess the stability of the samples and confirm their identity, the analyte fractions were subsequently analysed by LC-MS on the same day of collection. Analysis of each same sample was repeated after two, four and six hours (table 5.1).

Table 5.1: HPLC-MS data of stability testing of the fractions collected from semi-preparative separation of ISM and related compounds

Fraction I ( <i>unknown</i> )		Fraction II (M&B4596)		Fraction III (M&B4250)		Fraction IV (M&B4180A)		Fraction V (M&B38897)	
time o. i.	peak area	time o. i.	peak area	time o. i.	peak area	time o. i.	peak area	time o. i.	peak area
15:22	136.5	15:48	443.7	16:15	1683.3	16:42	1639.4	17:09	493.2
17:36	137.2	18:02	443.5	18:29	1685.0	18:56	1623.7	19:23	490.8
19:50	137.1	20:17	444.3	20:43	1691.7	21:10	1604.1	21:37	487.2
22:04	136.1	22:31	441.3	22:58	1696.9	23:24	1578.7	23:51	485.9
Mean	136.7		443.2		1689.2		1611.5		489.3
%RSD	0.38 %		0.30 %		0.37 %		1.63 %		0.68 %

Time o. i.: Time of injection

In addition to the little variation in peak areas with time (table 5.1) that indicated no degradation of the isolated compounds in the slightly acidic mobile phase (%RSD < 2 %), the MS data showed no sign of an ion due to the degradation product homidium ( $m/z = 314 M^+$ ) in fractions I - V, over six hours after collection (figure 5.9 b, d, f). The slightly increased values of %RSD for M&B4180A (ISM) could be due to the adsorption of the compound



to glassware. The results confirmed that the samples can be stored in the mobile phase for a short period of time before being frozen and freeze dried. MS data of fractions III - V showed the presence of ions at  $m/z = 230.5$  ( $M^{2+}$ ) as expected from ISM (M&B4180A) and its structural isomers M&B4250 and M&B38897 (see section 3.3.1.1). The mass chromatogram of fraction V (figure 5.9 e) shows the major signal for M&B38897 at 9.04 min, but also a minor one at 7.58 min, indicating that the separation of the critical pair M&B4180A (ISM) and M&B38897 was not complete and small amounts of M&B4180A are present in this sample. When 100 % purity is required, fraction V would need further purification by an additional separation.

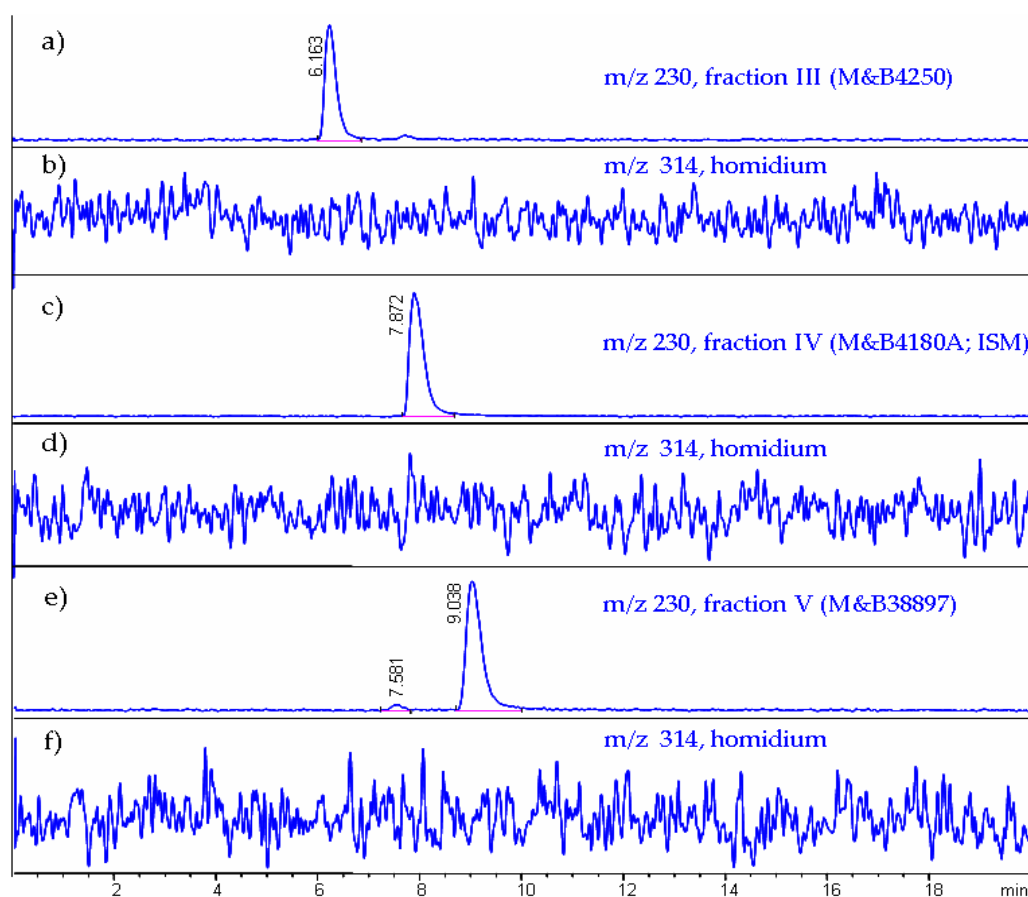


Figure 5.9: Representative HPLC-MS selected ion mass chromatograms of ions  $m/z = 230.5$  and  $m/z = 314$  obtained from fraction III (a + b), fraction IV (c + d) and fraction V (e + f) obtained from the semi-preparative separation of 1 %w/v ISM and related compounds RSM solution

MS data of fractions I and II had an ion at  $m/z = 606$  (figure 5.10), which is the singly charged molecular ion of the bis-substituted species.

The unknown compound (fraction I) is most probably also ISM related and a structural isomer of M&B4596 (fraction II).

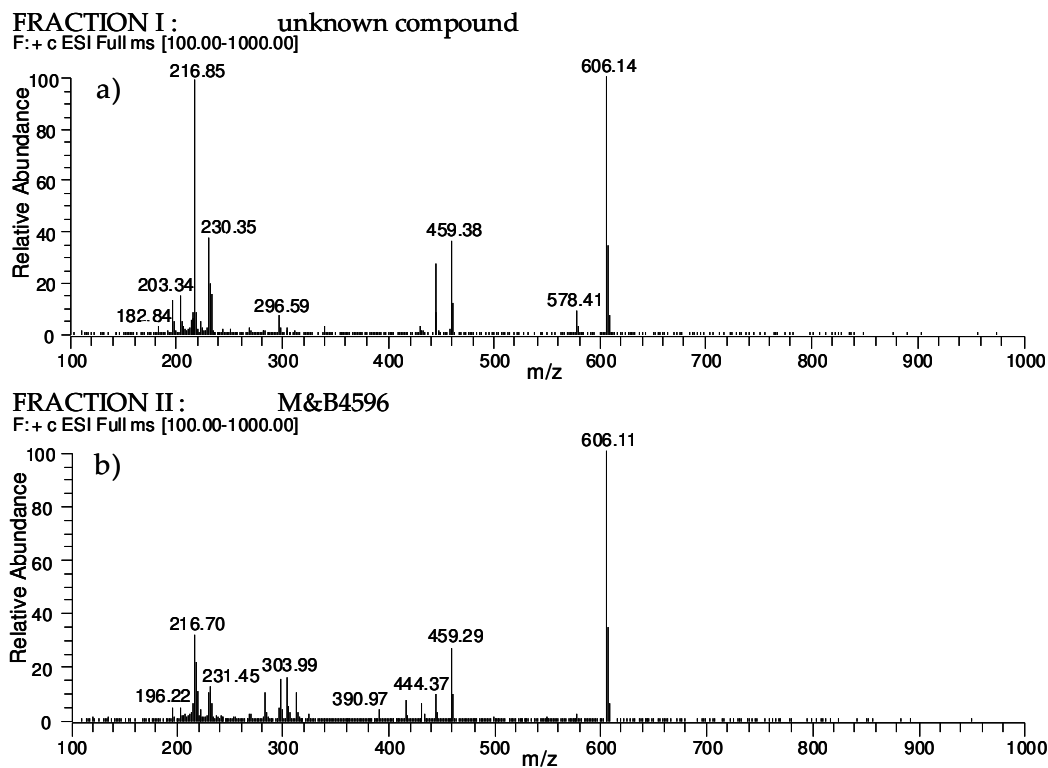


Figure 5.10: Mass spectra of a) fraction I and b) fraction II (M&B4596) obtained from semi-preparative separation of 1 %w/v ISM and related compounds RSM solution

In order to prepare the isolated compounds for NMR- and high resolution mass spectrometry, sample solutions were frozen, freeze dried and the residues reconstituted in DMSO- $d_6$  and a mixture of  $H_2O/MeCN$ , (75 : 25 v/v) respectively.

### 5.3.2. UV-Spectroscopy

UV spectra of each compound in the mobile phase were recorded with an Agilent 1100 series DAD-detector. A reference standard of the degradation product homidium, which is also the starting material in the synthesis of ISM exhibits a maximum absorption wavelength of 290 nm (figure 5.11). This value is in good agreement with a spectrum in aqueous acid reported by Clarke (1969).

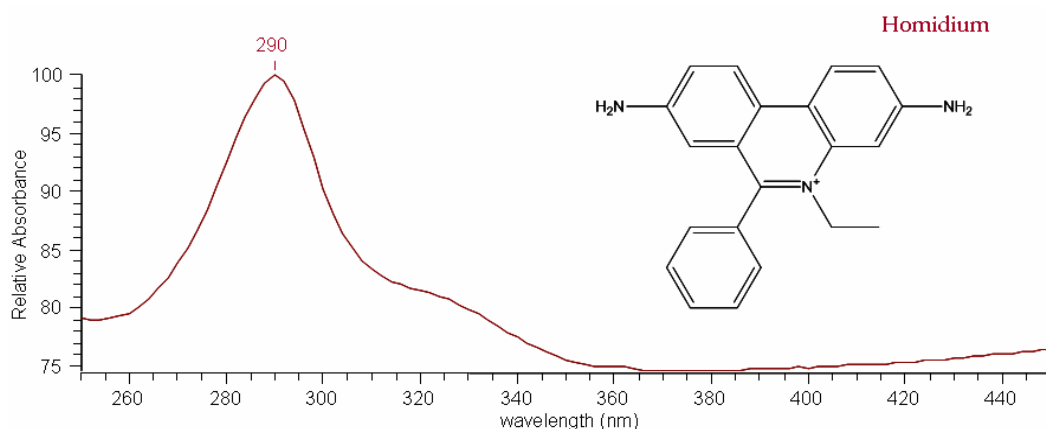


Figure 5.11: UV absorption spectrum of homidium in 15 mM ammonium formate solution (pH 2.8) : MeCN, 75 : 25 v/v

However, Clarke (1969) reported that the UV absorption spectrum for ISM has maxima at 284 nm and 317 nm, which do not agree with the values obtained in this study of 280 nm and 382 nm (figure 5.12 c). This difference is possibly due to the reported spectrum being one of the mixture of isomers and related compounds, while the spectrum in figure 5.12 c) is for a pure sample of ISM (M&B4180A).

The spectra of the three structural isomers M&B4250, M&B38897 and M&B4180A (ISM) (figure 5.12) show a shift of maxima to longer wavelengths when compared with homidium (figure 5.11). Substitution of the amidino moiety to the phenanthridine at the amine group at C-8 (figure 5.12 c) or C-3 (figure 5.12 b) positions causes bathochromic shifts to wavelengths of 386 nm

and 378 nm respectively. Substitution at C-7 demonstrates a UV transition at a distinctively lower wavelength of 312 nm (figure 5.12 a). This agrees with the theory, that the longer a conjugated system, the longer the wavelength of the absorption maximum (Williams & Fleming, 1995).

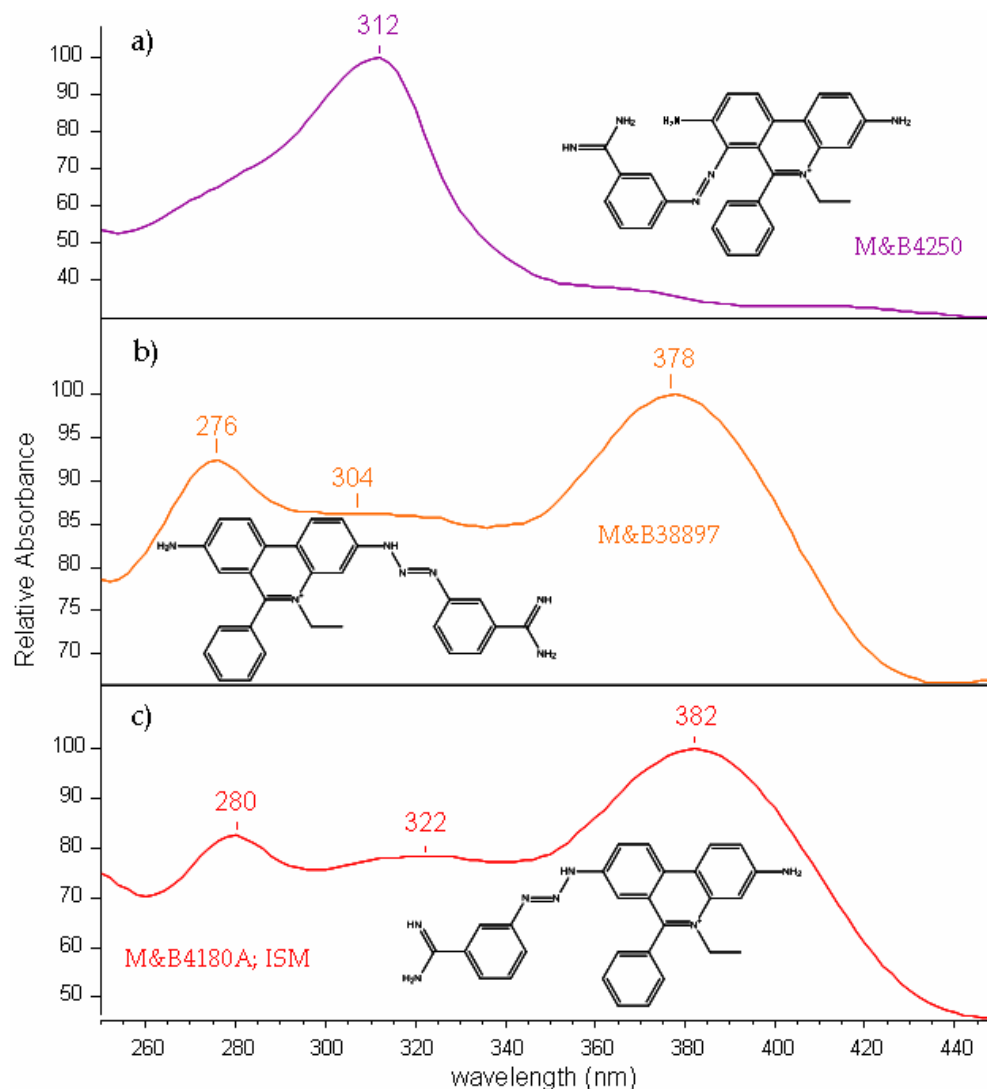


Figure 5.12: UV absorption spectra of isolated a) M&B4250 (fraction III), b) M&B38897 (fraction V) and c) M&B4180A (ISM; fraction IV) in 15 mM ammonium formate solution (pH 2.8) : MeCN, 75 : 25 v/v

M&B4180A and M&B38897 both contain a diazoamino-group whereas M&B4250 is an isomeric aminoazo compound, possessing less free electrons to participate in the conjugation.

Based on these observations and the distinct violet colour of fraction I, which M&B4250 also has (figure 5.8), it is proposed, that the uncharacterised compound is a structural isomer of the bis-substituted related compound M&B4596 containing one diazoamino and one aminoazogroup.

Compared with M&B4596 (figure 5.13 b), the UV maximum of fraction I (figure 5.13 a) shows a hypsochromic shift of the absorption maxima at 330 and 398 nm to 286 nm and 362 nm respectively.

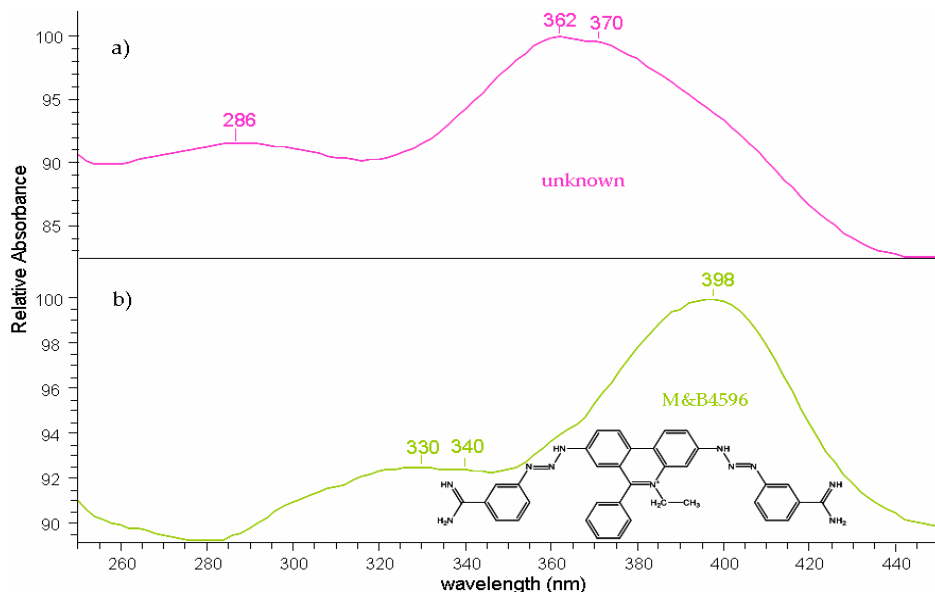


Figure 5.13: UV absorption spectra of pure samples of a) the isolated unknown compound (fraction I) and b) M&B4596 (fraction II) in 15 mM ammonium formate solution (pH 2.8) : MeCN, 75 : 25 v/v

### 5.3.3. NMR-Spectroscopy

Homidium, the starting material in the synthesis of ISM and its degradation product, has been well characterised by NMR spectroscopy (Firth *et al.*, 1983; Luedtke *et al.*, 2004).  $^1\text{H}$ -NMR,  $^{13}\text{C}$ -NMR and two dimensional NMR spectra of an authentic homidium standard in DMSO- $d_6$  were used to assign protons and carbon atoms to observed resonances, which complied well with previously reported data (Luedtke *et al.*, 2004). The coloured bonds in the

figure of the structure of homidium (figure 5.15) correspond to the  $^1\text{H}$ - $^1\text{H}$  correlations as evident in the total correlation spectrum (TOCSY) (figure 5.16).

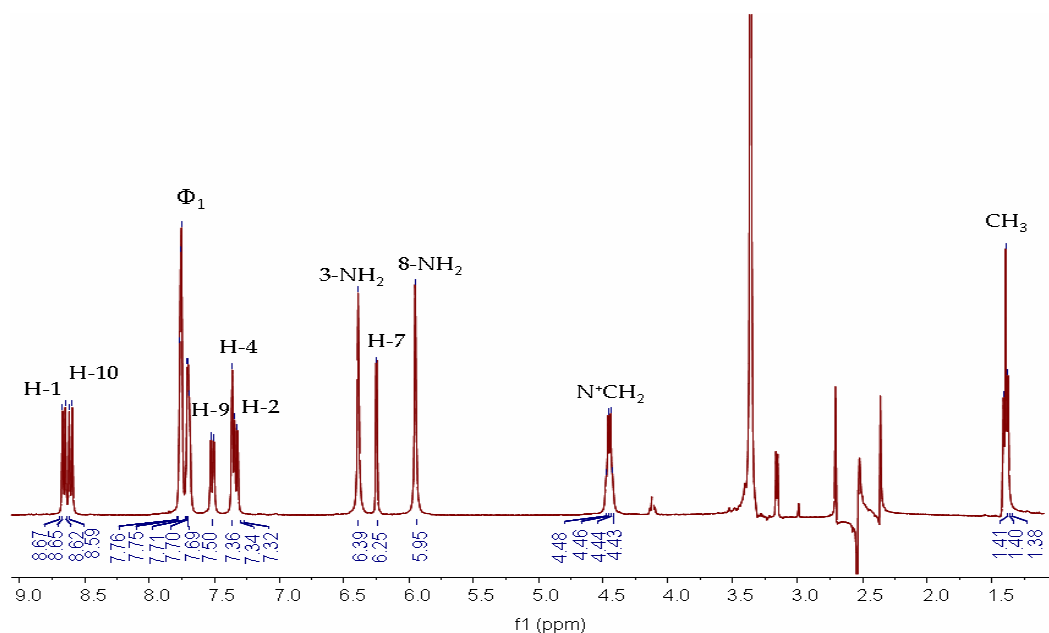


Figure 5.14: 400 MHz  $^1\text{H}$ -NMR spectrum of homidium in  $\text{DMSO-d}_6$

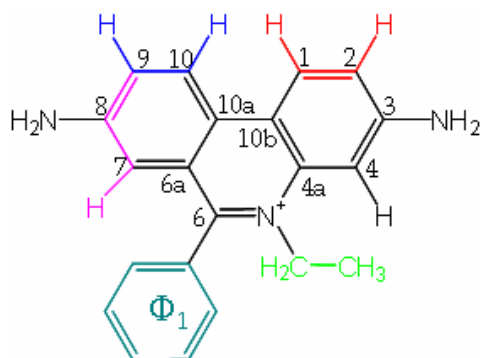


Figure 5.15: Chemical structure of homidium with coloured bonds correlating to  $^1\text{H}$ - $^1\text{H}$  TOCSY NMR correlations

The  $^1\text{H}$ -NMR chemical shifts for homidium (figure 5.14) were in perfect agreement with previously reported data (Firth *et al.*, 1983; Gaugain *et al.*, 1981; Luedtke *et al.*, 2004) and so was the assignment of the  $^{13}\text{C}$  spectrum (Luedtke *et al.*, 2004) (table 5.2). Heteronuclear multiple bond connectivity (HMBC) spectrum and  $^1\text{H}$ - $^{13}\text{C}$ -correlations are shown in figure 5.17.

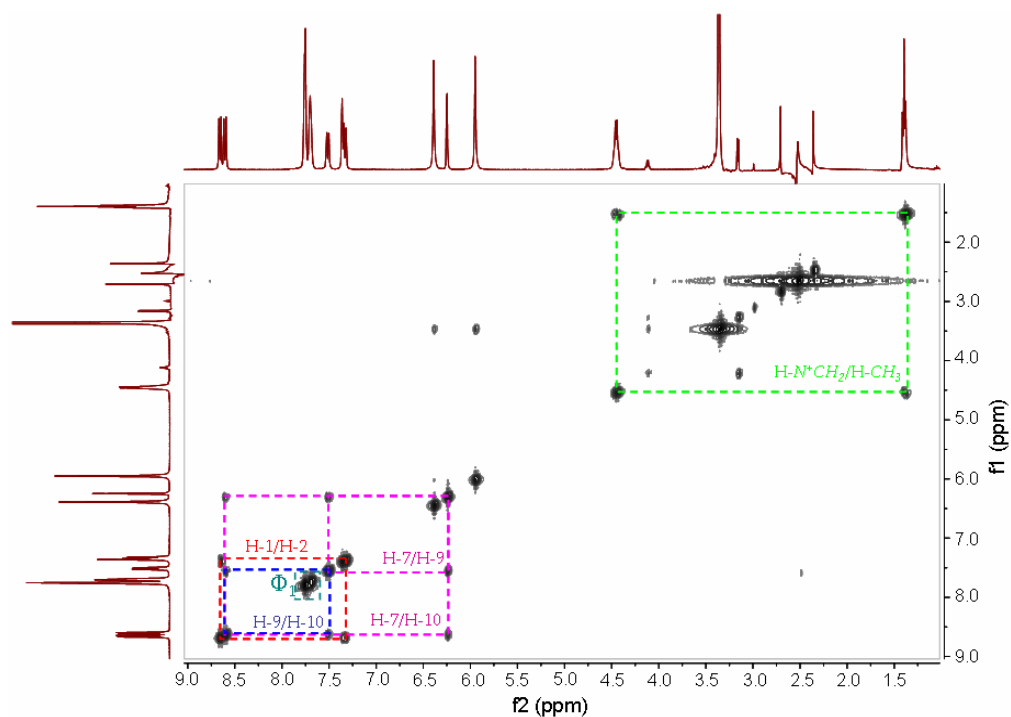


Figure 5.16: 400 MHz  $^1\text{H}$ - $^1\text{H}$  TOCSY spectrum of homidium in  $\text{DMSO-d}_6$  with coloured lines indicating  $^1\text{H}$ - $^1\text{H}$  correlations

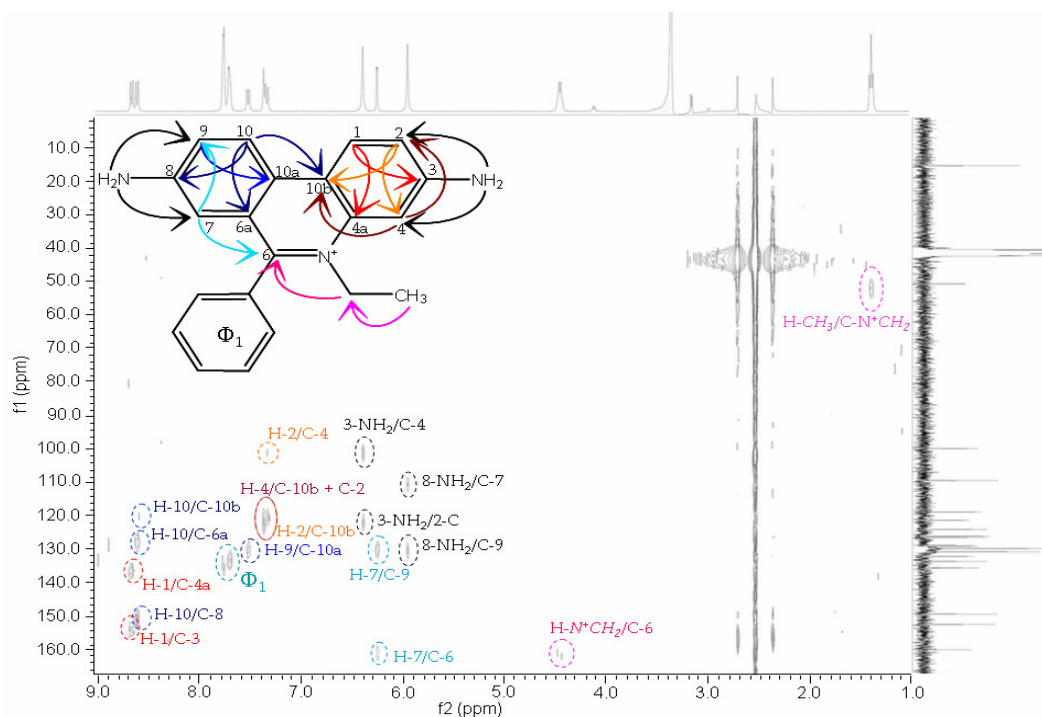


Figure 5.17: 400 MHz  $^1\text{H}$ - $^{13}\text{C}$  HMBC spectrum of homidium in  $\text{DMSO-d}_6$  with chemical structure of homidium; coloured arrows corresponding to  $^1\text{H}$ - $^{13}\text{C}$  HMBC correlations

$^1\text{H}$ - and  $^{13}\text{C}$ -NMR chemical shifts ( $\delta_{\text{H}}$ ,  $\delta_{\text{C}}$ ),  $^1\text{H}$ - $^1\text{H}$  coupling constants ( $J$ ) as well as TOCSY and HMBC correlations are summarised in table 5.2. Analysis of the HMQC spectrum (Appendix, figure A1) confirmed the assignments for all the carbons and protons in homidium.

Table 5.2:  $^1\text{H}$ -NMR and  $^{13}\text{C}$ -NMR data of homidium in DMSO- $d_6$  at 400 MHz

Position	$^1\text{H}$ -NMR		TOCSY	HMBC	$^{13}\text{C}$ -NMR
	$\delta_{\text{H}}$	$J$ (Hz)			
1	8.66 (d)	9.16	2	3, 4a	125.6
2	7.33 (bd)	9.16	1	4, 10b	120.4
3-NH <sub>2</sub>	6.39 (s)				151.6
4	7.36 (bs)			2, 10b	99.0
4a				1	134.7
6				7	159.2
6a				10	125.2
7	6.25 (d)	1.8	9, 10	6, 9, 10a	108.5
8-NH <sub>2</sub>	5.95 (s)			10	148.5
9	7.50 (dd)	8.8/1.8	7, 10	10a	127.9
10	8.60 (d)	8.8	7, 9	6a, 8, 10b	123.2
10a				7, 9	128.3
10b				2, 4, 10	118.0
N <sup>+</sup> CH <sub>2</sub>	4.46 (q)	7.0	CH <sub>3</sub>		49.9
CH <sub>3</sub>	1.40 (t)	7.0	N <sup>+</sup> CH <sub>2</sub>		14.3
Phenyl ( $\Phi_1$ )	7.71 (m)				128.9
	7.76 (m)				129.9
					131.3

The NMR spectra and assignments obtained for homidium were compared to NMR data of ISM and its isomers, in order to facilitate assignments of observed resonances to protons and carbons of the phenanthridinium ring. The amidino substituted isomers had very different spectra, with significant changes in chemical shifts, from those obtained for homidium, indicating major modifications in the electronic environment of its structure after introduction of the amidinobenzenediazonium moiety.

Neither  $^1\text{H}$ - nor  $^{13}\text{C}$ -NMR data of pure ISM and its isomers has been previously published. Hence,  $^1\text{H}$ - and  $^{13}\text{C}$ - assignments were confirmed



unambiguously using two dimensional  $^1\text{H}$ - $^1\text{H}$ - and  $^1\text{H}$ - $^{13}\text{C}$ -NMR data of the isolated fractions of ISM and M&B4250 in DMSO- $d_6$ . However, the sample yields obtained from preparative HPLC for fraction I, M&B4596 and M&B38897 were too small to produce useful NMR data.

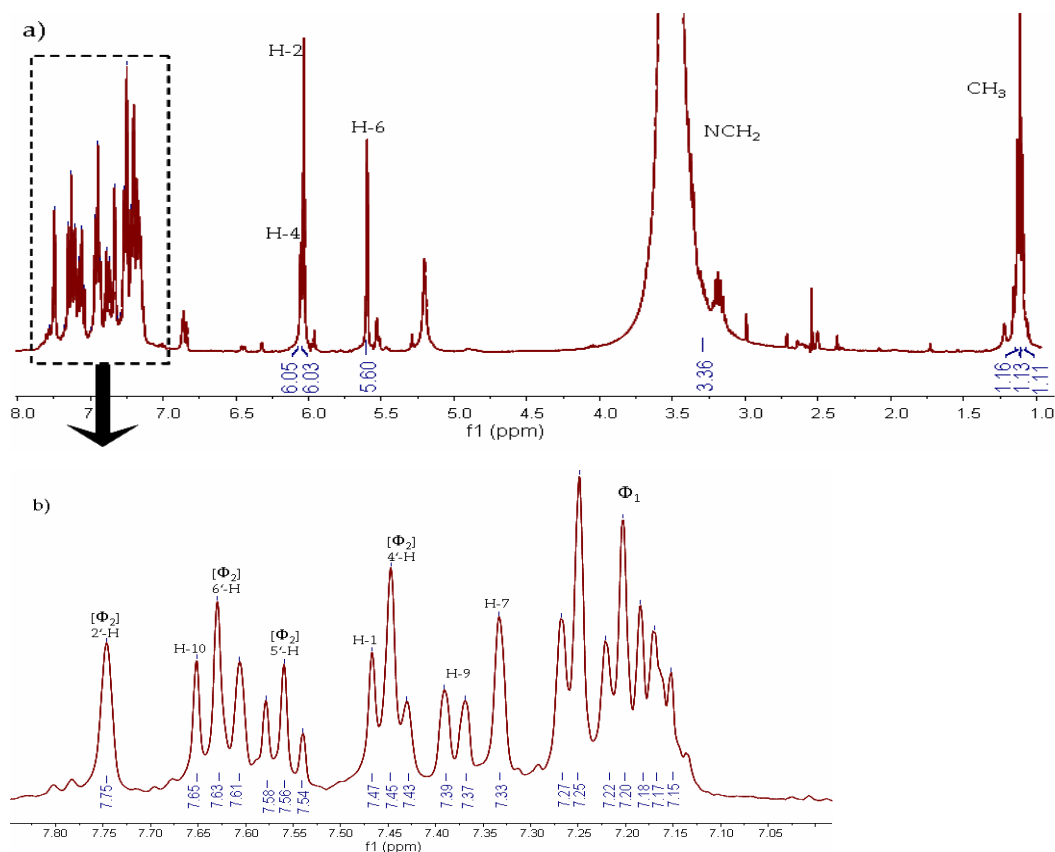


Figure 5.18: a) 400 MHz  $^1\text{H}$ -NMR spectrum of ISM in DMSO- $d_6$  and b) enhancement of the low field region from 7.0 - 8.0 ppm of the 400 MHz  $^1\text{H}$ -NMR spectra of ISM in DMSO- $d_6$

A very obvious difference is the upfield shift of the  $^1\text{H}$  resonances observed for ISM when compared with the  $^1\text{H}$ -NMR spectrum of homidium with a signal at 7.75 ppm instead of 8.67 ppm as previously found for the reference compound (figure 5.18). Other distinct features in the spectrum are the appearance of two quartet signals for the methylene protons of the NCH<sub>2</sub> group, vicinal to the methyl group (figure 5.20). These results indicate that the CH<sub>2</sub> protons, unlike in homidium, are no longer equivalent, but are in

different chemical and magnetic environments. These observations are further supported by the occurrence of an additional proton singlet at  $\delta_{\text{H}}$  5.60. This led to the assumption, that substitution on the homidium moiety resulted in cleavage of the double bond next to the quaternary nitrogen and introduction of an additional proton at the C-6 position (figure 5.19). The following loss of conjugation and planarity explains the upfield shift of the proton signals of the benzidine ring system, as well as the differences in the influence of the  $\Phi_1$  electron system on the  $\text{CH}_2$  protons.

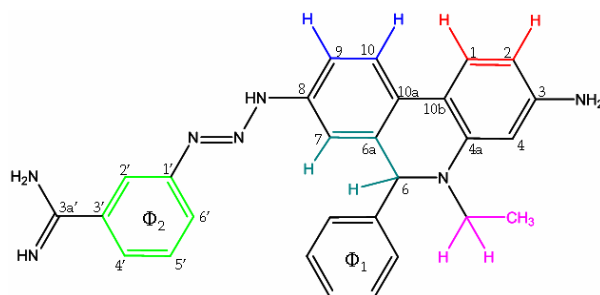


Figure 5.19: New proposed structure of ISM based on NMR data.  
Coloured bonds correspond to TOCSY correlations (figure 5.20)

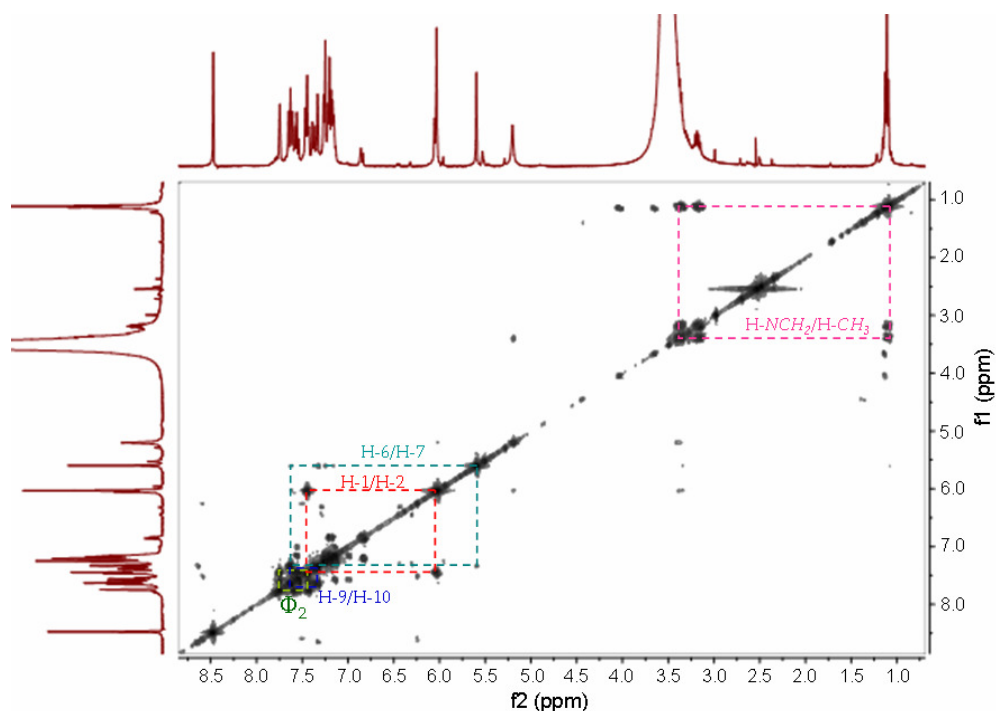


Figure 5.20: 400 MHz  $^1\text{H}$ - $^1\text{H}$  TOCSY spectrum of ISM in  $\text{DMSO-d}_6$  with coloured lines indicating  $^1\text{H}$ - $^1\text{H}$  correlations

TOCSY  $^1\text{H}$ - $^1\text{H}$  correlations (figure 5.20) confirm the assumption that the signal at 5.60 ppm is an additional proton which is absent in the homidium structure and that is found to connect to H-7 by  $\omega$ -coupling. In the HMBC spectrum (figure 5.22) of ISM (M&B4180A) this proton signal was found to correlate to C-4a, C-6a, C-7, C-10a, C-NCH<sub>2</sub> and the phenyl ring  $\Phi_1$  (figure 5.21).

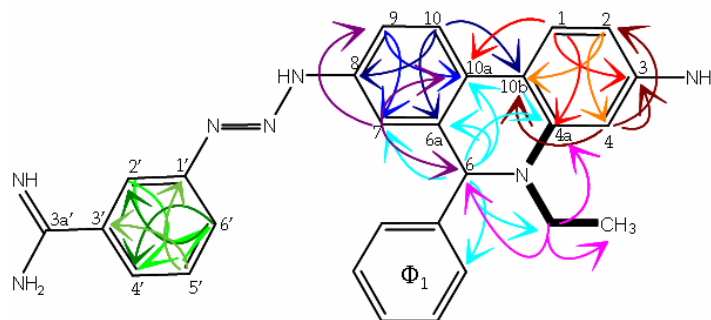
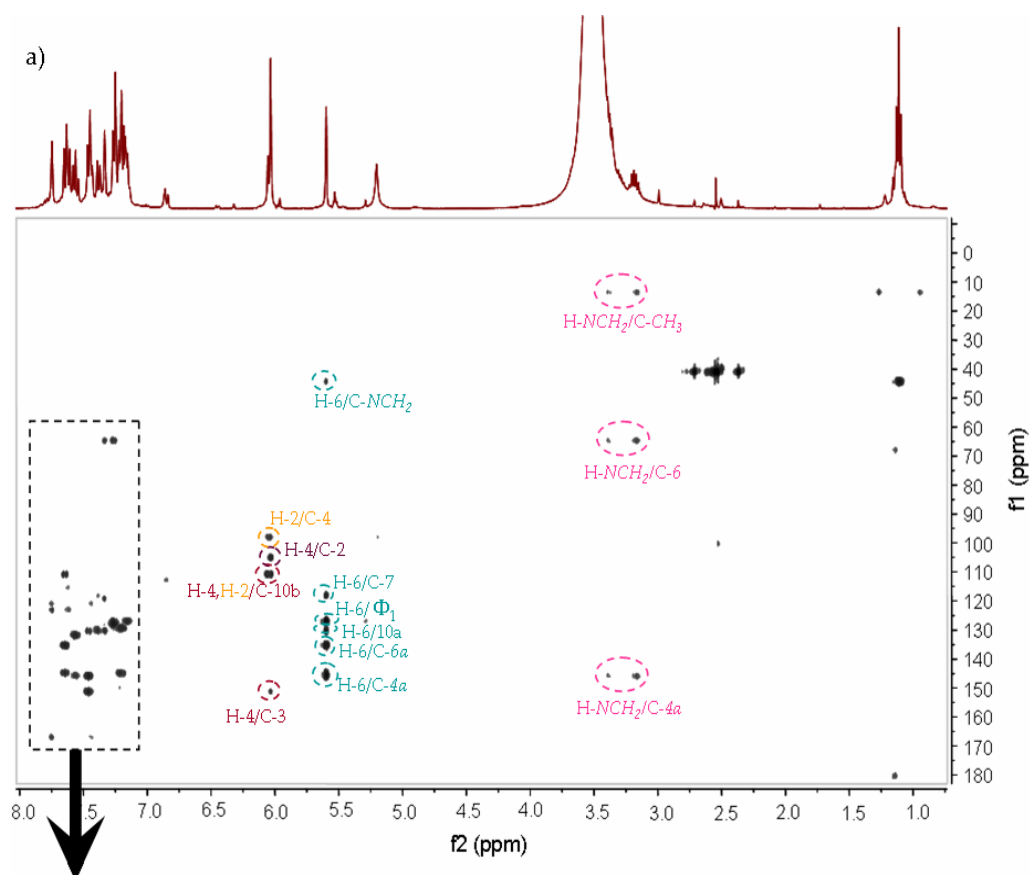


Figure 5.21: New proposed chemical structure of ISM with coloured arrows corresponding to  $^1\text{H}$ - $^{13}\text{C}$  correlations in figure 5.22



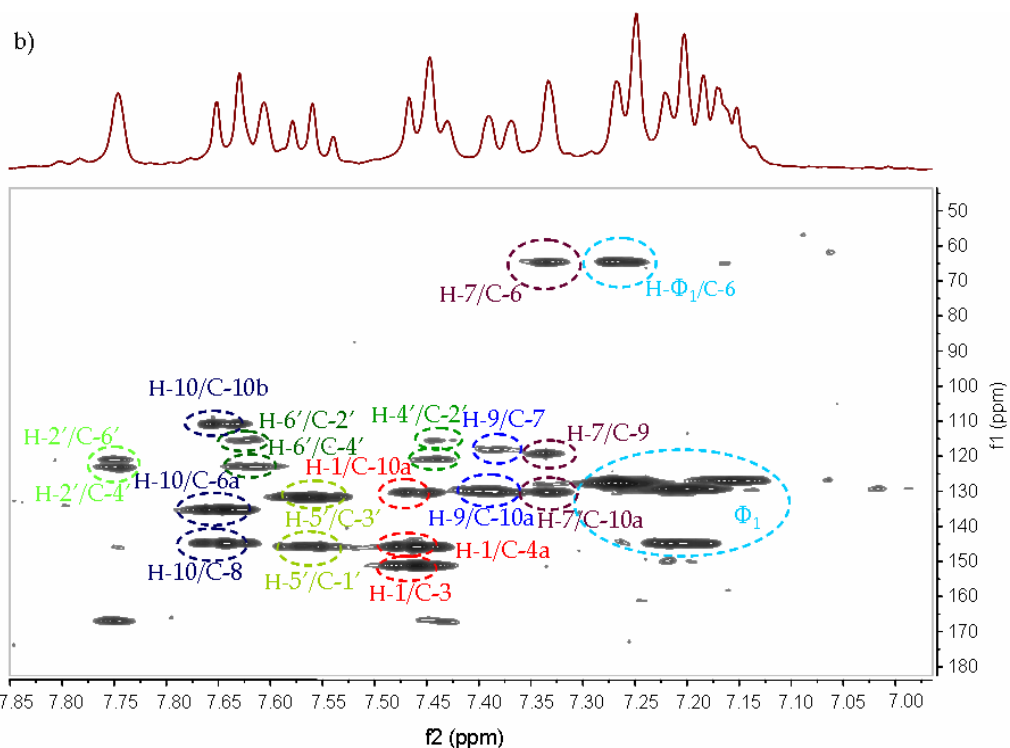
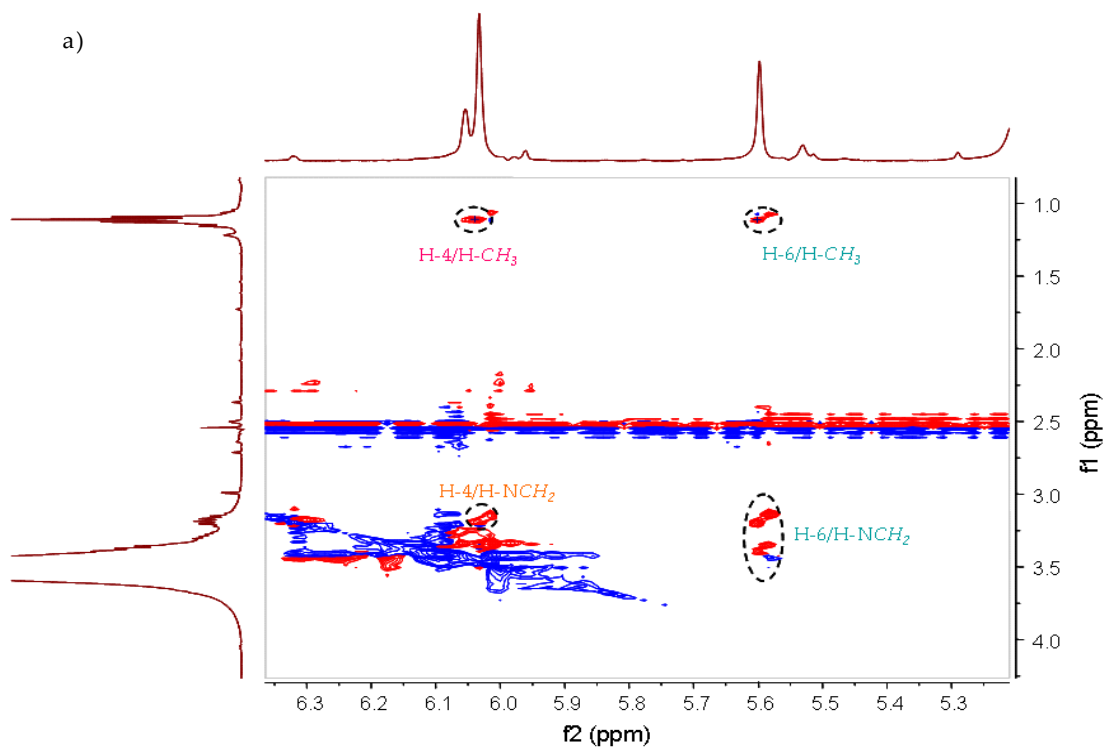


Figure 5.22: a) 400 MHz  $^1\text{H}$ - $^{13}\text{C}$  HMBC spectrum of ISM in  $\text{DMSO-d}_6$  and b) enhancement of the low field region from 7.0 - 8.0 ppm of the 400 MHz  $^1\text{H}$ - $^{13}\text{C}$  HMBC spectrum of ISM in  $\text{DMSO-d}_6$  with coloured numbering indicating  $^1\text{H}$ - $^{13}\text{C}$  correlations as shown in figure 5.21



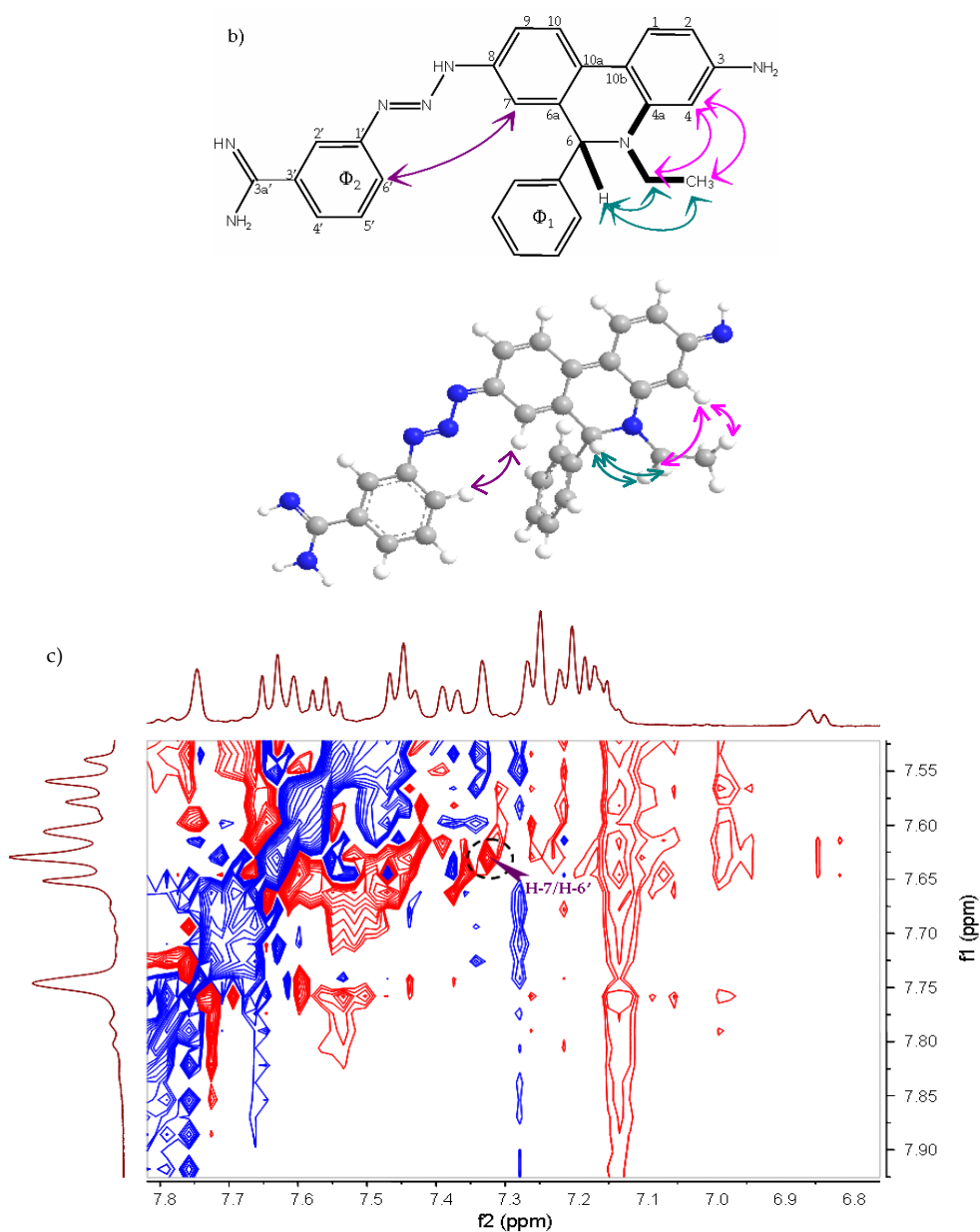


Figure 5.23: a) and c) 400 MHz  $^1\text{H}$ - $^1\text{H}$  ROESY spectra of ISM in  $\text{DMSO-d}_6$  with coloured numbering indicating  $^1\text{H}$ - $^1\text{H}$  correlations, b) new proposed chemical structure of ISM with coloured arrows corresponding to  $^1\text{H}$ - $^1\text{H}$  correlations in a) and c)

The ROESY spectra (figure 5.23) confirmed the substitution at 8- $\text{NH}_2$  and provides additional information on the steric configuration of the amidinobenzendiazonium ligand. A ROe correlation between H-7 and H-6' accounted for the deshielding effect on H-7.

HMQC data (Appendix, figure A2) confirmed the findings and facilitated complete assignment of the proton and carbon signal data by indicating one-bond correlations. It provided further evidence of an additional proton being introduced at C-6 with the loss of the double bond.  $^1\text{H}$ - and  $^{13}\text{C}$ -NMR chemical shifts ( $\delta_{\text{H}}$ ,  $\delta_{\text{C}}$ ),  $^1\text{H}$ - $^1\text{H}$  coupling constants ( $J$ ) as well as TOCSY and HMBC correlations are summarised in table 5.3.

Table 5.3:  $^1\text{H}$ -NMR and  $^{13}\text{C}$ -NMR data of ISM in DMSO- $d_6$  at 400 MHz

Position	$^1\text{H}$ -NMR		TOCSY	HMBC	$^{13}\text{C}$ -NMR
	$\delta_{\text{H}}$	$J$ (Hz)			
1	7.46 (d)	8.0	2	3, 4a	125.3
2	6.04 (d)	8.0	1	4, 10b	105.5
3					151.2
4	6.04 (s)			2, 10b	98.0
4a				1	135.3
6	5.60 (s)			7	64.6
6a				10	145.4
7	7.33 (s)		9	6, 9, 10a	118.0
8				10	142.4
9	7.37 (d)	8.0	7, 10	10a	119.1
10	7.66 (d)	8.0	9	6a, 8, 10b	122.3
10a				7, 9	127.0
10b				2, 4, 10	111.0
NHCH <sub>2</sub>	3.25 (q)	8.0			
	3.39*	*	CH <sub>3</sub>		44.3
CH <sub>3</sub>	1.15 (t)	8.0	NHCH <sub>2</sub>		13.2
					142.7
Phenyl ( $\Phi_1$ )					130.1
	7.71 (m)				129.2
	7.76 (m)				126.2
Phenyl ( $\Phi_2$ )					
1'					145.7
2'	7.75 (s)				116.4
3'					131.8
3a'					167.0
4'	7.44 (d)	8.0			123.1
5'	7.56 (dd)	8.0			130.9
6'	7.62 (d)	8.0			121.0

\*Resonances are underneath the water signal and were assigned accordingly through its COSY and HMQC correlations.

The experiments carried out for M&B4180A (ISM) were also undertaken for the structural isomer M&B4250, which gave comparable results. Cleavage of the double bond next to the quaternary nitrogen in the phenanthridine nucleus after introduction of the amidinobenzediazonium moiety was also evident. Chemical shifts of the ethyl group on the phenanthridine nitrogen are the same in the C-substituted isomer (M&B4250) as in the N-substituted ISM molecule ( $\delta_{\text{H}}[\text{CH}_3] = 1.13 \text{ ppm}$ ;  $\delta_{\text{H}}[\text{NCH}_2] = 3.36 \text{ ppm}$ ). However, there are some distinct differences in the downfield region of the spectra of the two isomeric compounds (figure 5.18; figure 5.24).

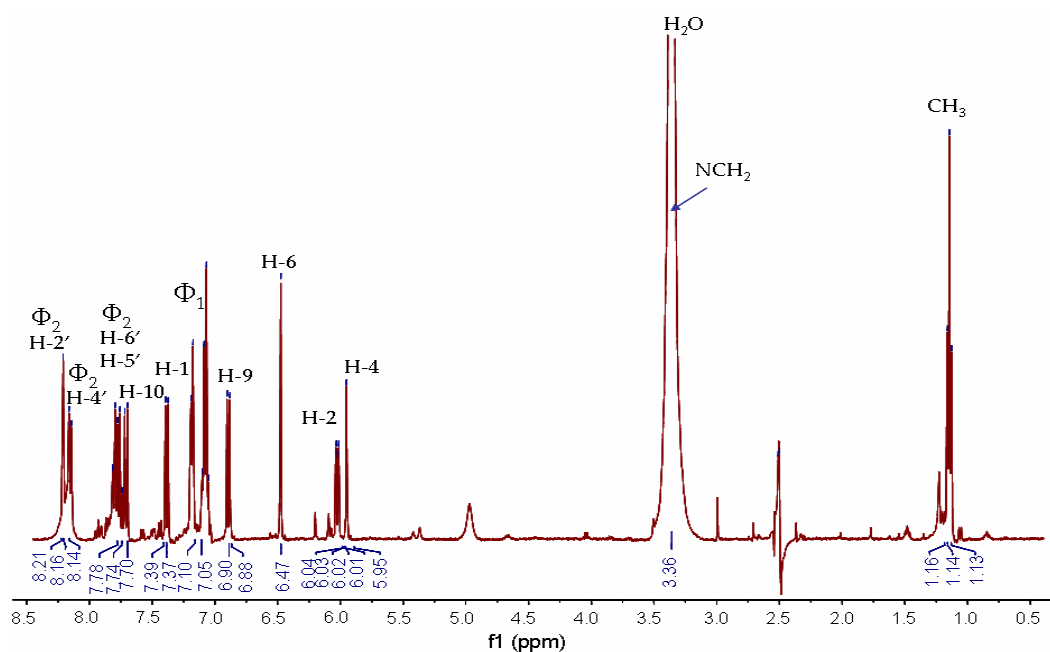


Figure 5.24: 400 MHz  $^1\text{H}$ -NMR spectrum of M&B4250 in  $\text{DMSO-d}_6$

Introduction of the azo group in the phenanthridine system has a pronounced deshielding effect on the H-6 proton, the signal of which shifts from 5.60 ppm in ISM to 6.47 ppm. The signal due to H-9 however is shifted upfield to 6.90 ppm, as there is no deshielding due to the phenyldiazo-substituent. Substitution on C-7 was also confirmed by loss of the H-7 proton in M&B4250 as seen in the TOCSY  $^1\text{H}$ - $^1\text{H}$  correlations (figure 5.26) where the H-6 proton does not show any evidence of through-bond correlations.

The spectrum shows three distinct signals due to  $\Phi_2$ -protons of the m-amidinobenzenediazonium ligand. The broad singlet at  $\delta_{\text{H}} = 8.20$  ppm is due to H-2' which couples to H-6' and H-4' at the meta-position (figure 5.25), but as the coupling constants in this case are only about  $J \sim 1.5$  Hz the peak splitting was not resolved. However, the H-4' signal exhibited a clear split into a doublet at 8.14 ppm, with a coupling constant  $> 8$  Hz (figure 5.24), which is also ortho coupled to H-5'.

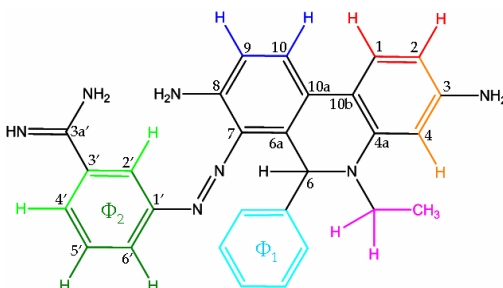


Figure 5.25: New proposed structure of M&B4250 based on obtained NMR data. Coloured bonds correspond to TOCSY correlations (figure 5.26)

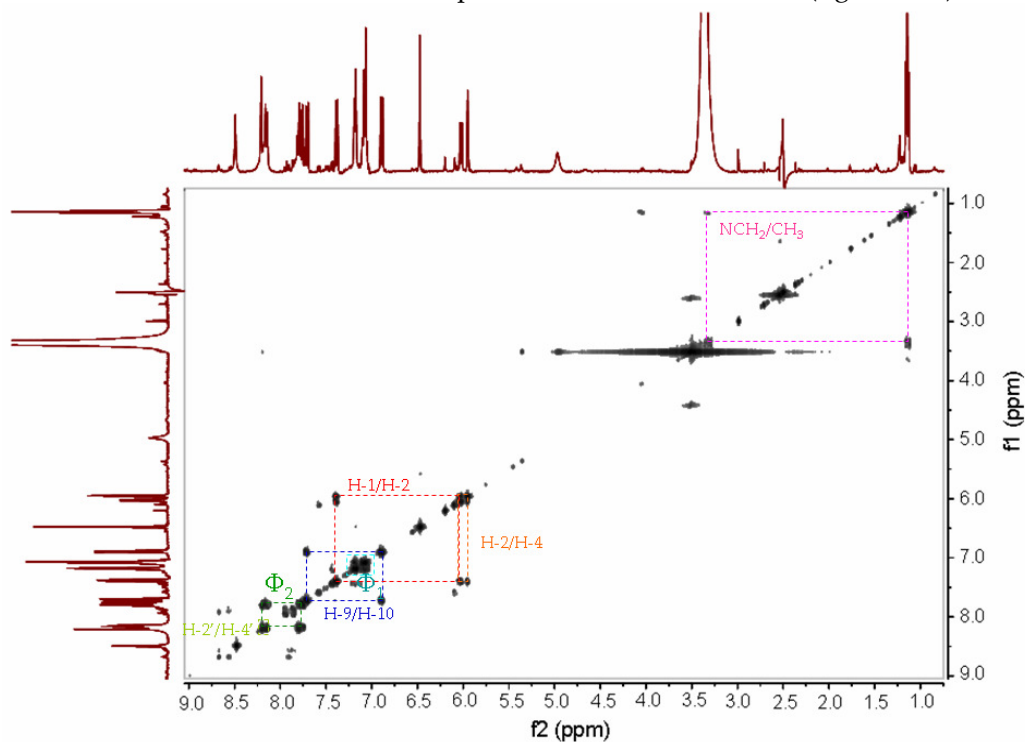


Figure 5.26: 400 MHz <sup>1</sup>H-<sup>1</sup>H TOCSY spectrum of M&B4250 in DMSO-d<sub>6</sub> with coloured lines indicating <sup>1</sup>H-<sup>1</sup>H correlations



H-5' and H-6' protons resonated as multiplet at 7.79 ppm where the doublet of doublets of H-5' overlapped with the doublet of H-6'. However, there was a clear separation of the  $^1\text{H}$  resonances in M&B4250 when compared to those of the  $\Phi_2$ -system obtained for ISM, which is another observed difference between the two compounds.

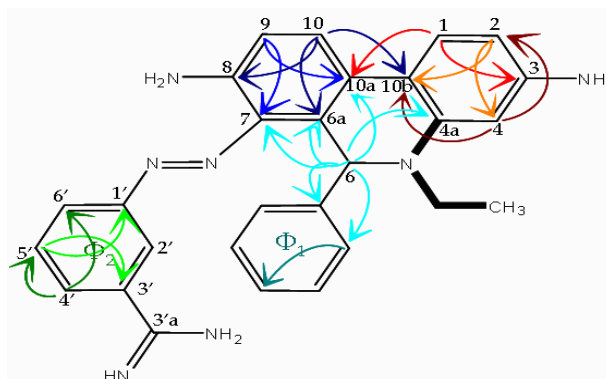


Figure 5.27: New proposed chemical structure of M&B4250 with coloured arrows corresponding to  $^1\text{H}$ - $^{13}\text{C}$  correlations in figure 5.28

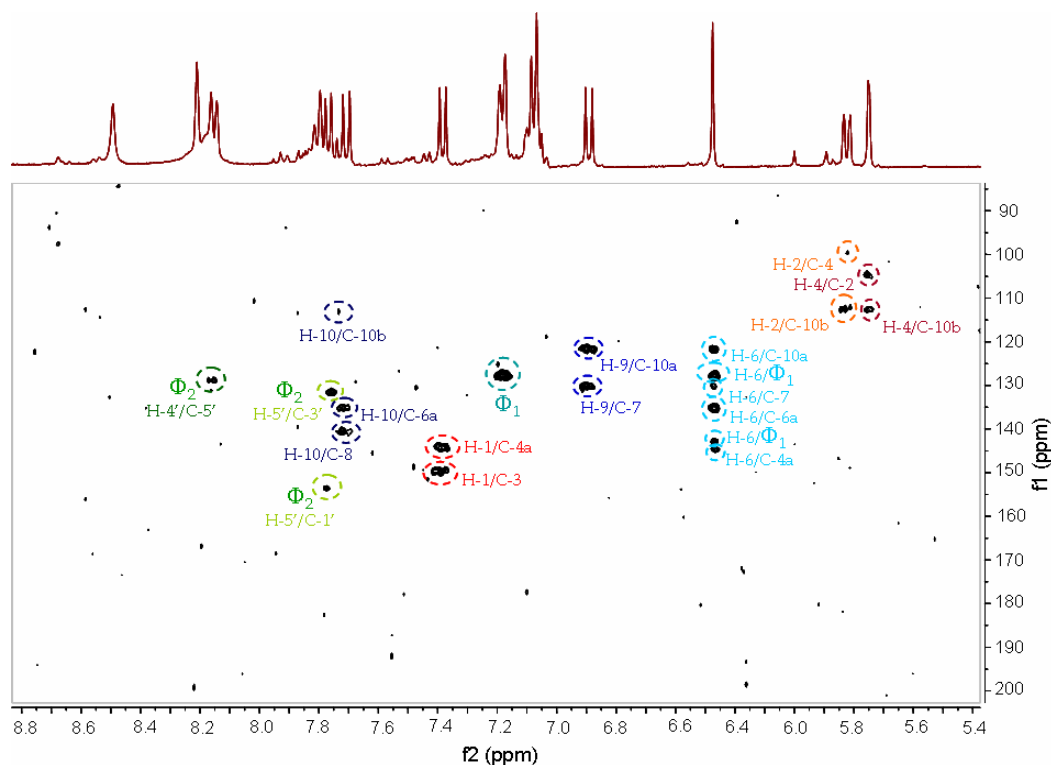
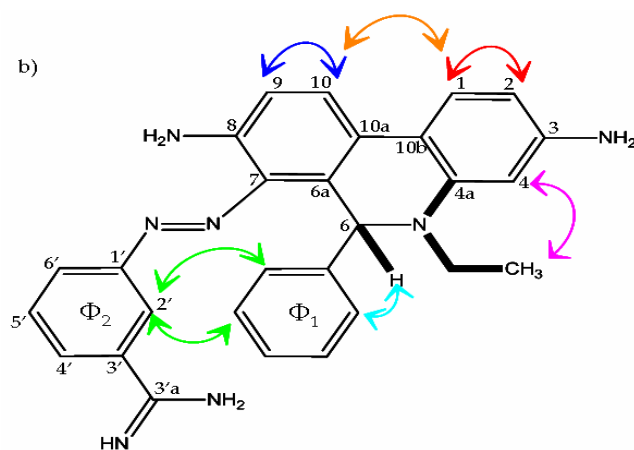
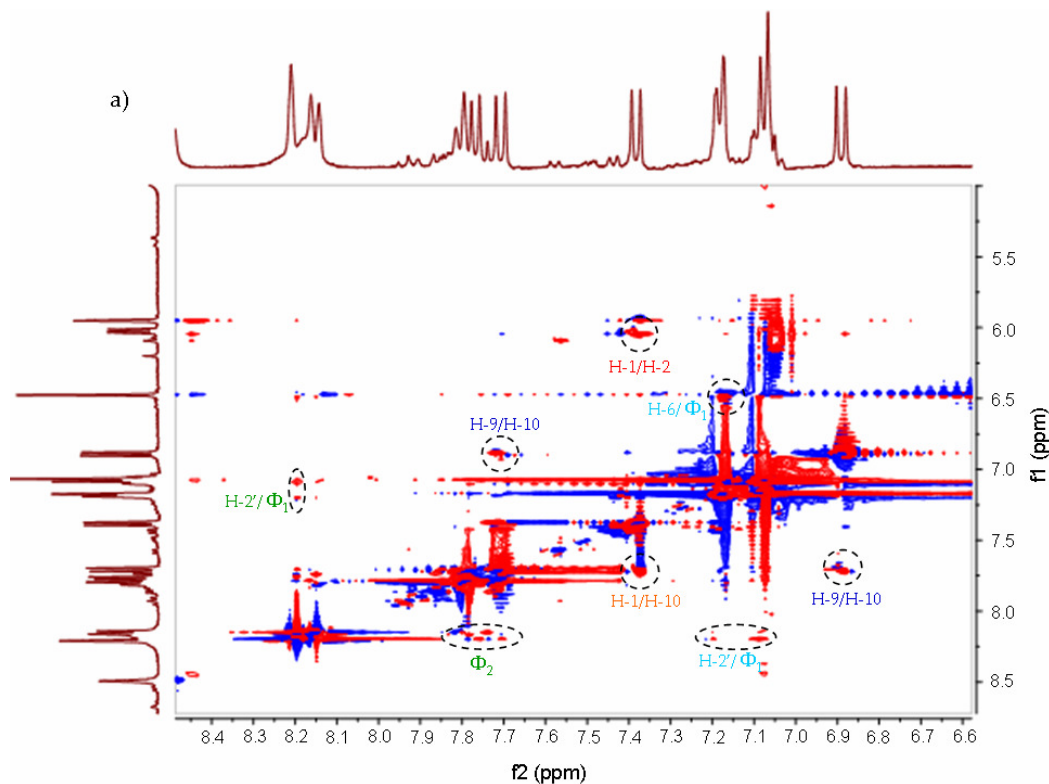


Figure 5.28: 400 MHz  $^1\text{H}$ - $^{13}\text{C}$  HMBC spectrum of M&B4250 in  $\text{DMSO-d}_6$  with coloured numbering indicating  $^1\text{H}$ - $^{13}\text{C}$  correlations as shown in figure 5.27

In the HMBC spectrum of M&B4250 (figure 5.28), the H-6 proton singlet was found to correlate to C-4a, C-6a, C-7, C-10a and the phenyl ring  $\Phi_1$  (figure 5.27), thus unambiguously confirming the new proposed chemical structure. Again a ROESY experiment (figure 5.29) provided an insight on the steric configuration of the amidinobenzenediazonium ligand. Through space correlations of H-2' with a  $\Phi_1$ -protons at  $\delta_H = 7.20$  and  $7.09$  ppm were detected (figure 5.29 a/b).



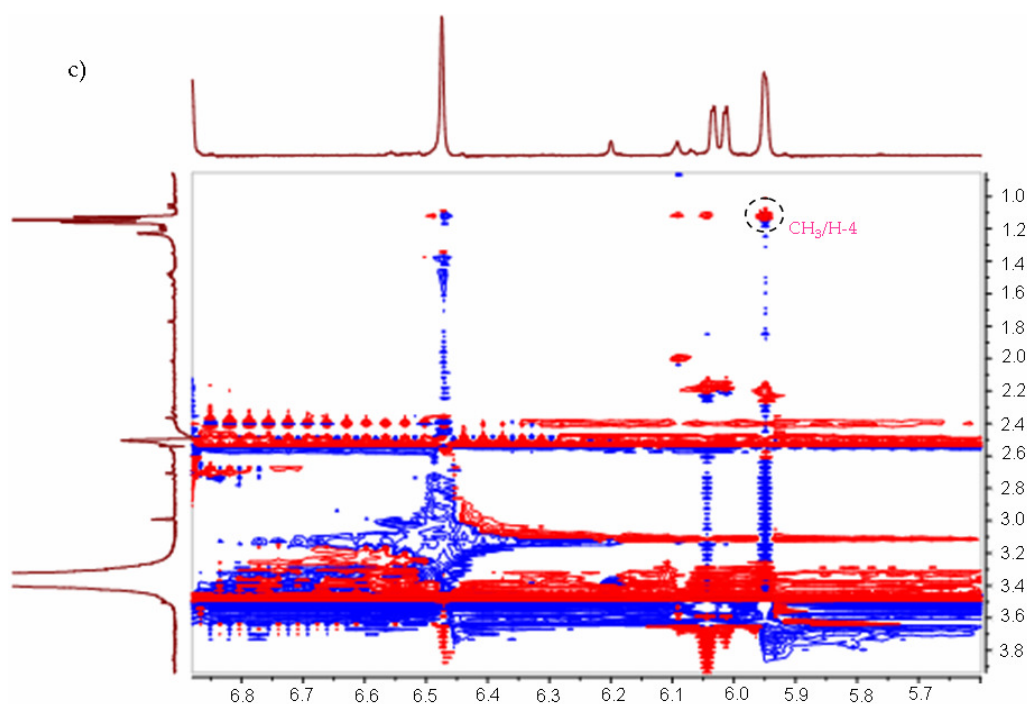


Figure 5.29: a) and c) 400 MHz  $^1\text{H}$ - $^1\text{H}$  ROESY spectra of M&B4250 in  $\text{DMSO-d}_6$  with coloured numbering indicating  $^1\text{H}$ - $^1\text{H}$  correlations, b) new proposed chemical structure of M&B4250 with coloured arrows corresponding to  $^1\text{H}$ - $^1\text{H}$  correlations in a) and c)

The HMQC spectrum (Appendix, figure A3) further confirmed the proposed new structure and allowed complete assignments of the proton and carbon shifts in M&B4250 by indicating correlations of  $^{13}\text{C}$  and the protons directly attached to it. Cleavage of the double bond between C-6 and the quaternary nitrogen in the phenanthridine moiety after introduction of the amidinobenzene substituent seems evident and the assumption is supported by all the NMR data obtained for both isomers.

$^1\text{H}$ - and  $^{13}\text{C}$ -NMR chemical shifts ( $\delta_{\text{H}}$ ,  $\delta_{\text{C}}$ ),  $^1\text{H}$ - $^1\text{H}$  coupling constants ( $J$ ) as well as TOCSY and HMBC correlations for M&B4250 are summarised in table 5.4. It was not possible to unambiguously interpret the NMR data obtained for the third isomer M&B38897, M&B4596 and the unknown related compound as there was insufficient material.

Table 5.4: <sup>1</sup>H-NMR and <sup>13</sup>C-NMR data of M&B4250 in DMSO-d<sub>6</sub> at 400 MHz

Position	<sup>1</sup> H-NMR		TOCSY	HMBC	<sup>13</sup> C-NMR
	δ <sub>H</sub>	J (Hz)			
1	7.40 (d)	8.0	2	3, 4a, 10a	123.8
2	6.03 (d)	8.0	1, 4	4, 10b	104.7
3					148.7
4	5.96 (s)		2	2, 10b	99.3
4a				1	144.5
6	6.46 (s)			Φ <sub>1</sub> , 4a, 6a, 7, 10a	60.7
6a				6, 10	135.2
7				6, 9	130.5
8				10	140.5
9	6.90 (d)	8.0	10	7, 10a	118.1
10	7.73 (d)	8.0	9	6a, 8, 10b	129.0
10a				1, 6, 9	121.8
10b				2, 4, 10	112.2
NHCH <sub>2</sub>	3.33*	*	CH <sub>3</sub>		44.3
CH <sub>3</sub>	1.14 (t)	8.0	NHCH <sub>2</sub>		13.7
Phenyl (Φ <sub>1</sub> )					142.9
	7.09 (m)		Φ <sub>1</sub>	Φ <sub>1</sub>	127.8
	7.20 (m)				127.7
Phenyl (Φ <sub>2</sub> )					
1'					153.6
2'	8.19 (s)		4'		122.6
3'				5'	131.6
3a'					167.0
4'	8.14 (d)	8.0	2', 5'	5', 6'	125.9
5'	7.79 (dd)	8.0	4', 6'	1', 3', 4'	129.0
6'	7.80 (d)	8.0	5'	4'	130.0

\*Resonances are underneath the water signal and were assigned accordingly through its COSY and HMQC correlations.

The new proposed structures of the isomer M&B4180A (ISM) and M&B4250, based on the NMR data would have molecular weights of 461.6 g/mol. However, these molecules bear no charge. Hence, a single charged protonated ion of ISM, as seen in the low resolution MS spectrum, should give a signal at  $m/z = 462.6$  instead of  $m/z = 460$  as detected. To determine whether the structure of the congeners only changed after or during the HPLC-MS experiments will require further studies.

### 5.3.4. High Resolution Mass Spectrometry

For the high resolution MS experiment the fractions had to be free of DMSO- $d_6$  in which they had been dissolved for the NMR studies. The DMSO solutions were frozen, freeze-dried, re-constituted in water and again frozen and freeze-dried twice in order to remove any residual solvent. For analysis by MS they were dissolved in a mixture of MeCN in water (25 : 75 v/v).

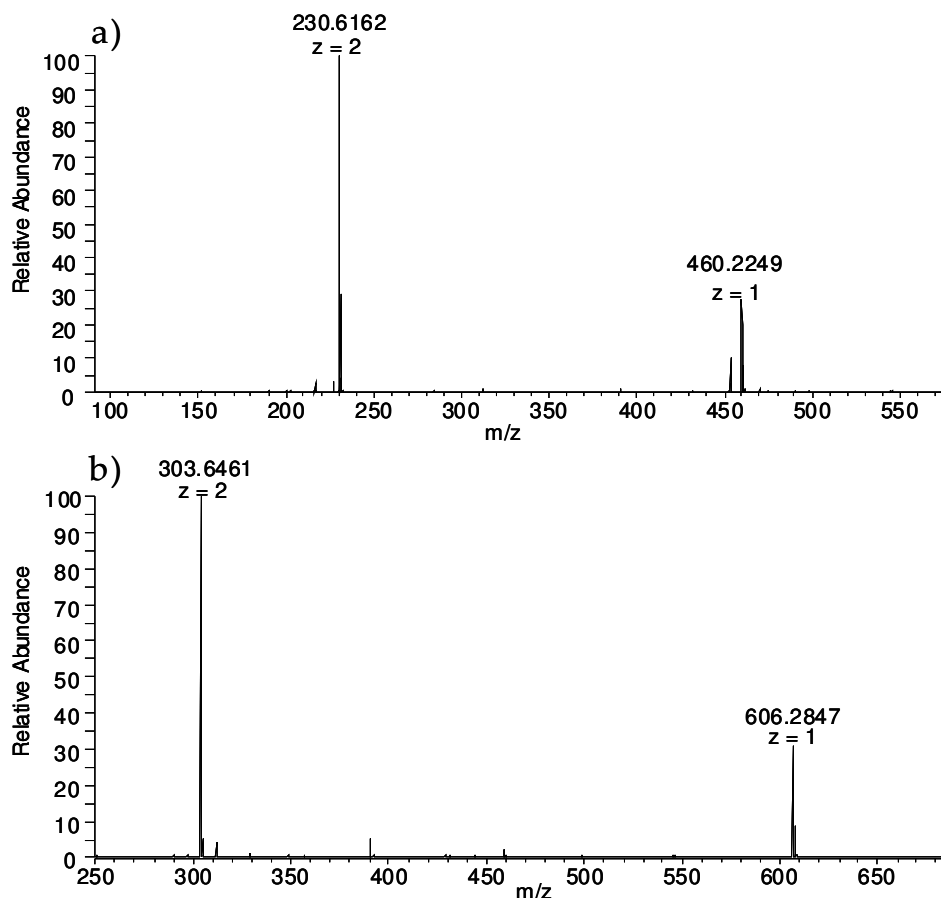


Figure 5.30: High resolution mass spectra of pure samples of a) ISM and b) M&B4596 obtained from semi-preparative separation of 1 %v/v ISM and related compounds RSM solution

The resulting data were very similar to those obtained in the low resolution experiments (section 5.3.1) with ions of  $m/z = 460.225$  and  $230.616$  for the three isomers M&B4180A (ISM) (figure 5.30 a), M&B4250 and M&B38897 and

$m/z = 606.285$  and  $303.646$  for M&B4596 (figure 5.30 b), suggesting a different molecular structure than proposed, based on an anticipated molecular weight of 461 amu as deduced from the NMR data. As the protonated ion possesses an exact mass of 460.225 g/mol, then the mass of the uncharged ISM molecule is expected to be 459.2 g/mol. However, the benzidine moiety seems to be affected by the pH and temperature conditions used during the MS experiments. The benzidine unit found within the structure of the phenanthridine ring system undergoes oxido-reduction to its diimine form during protonation (Yamazoe *et al.*, 1988). The stability and oxidation of the benzidine compounds at different pH values have been established using UV detection and emission spectrophotometry at longer wavelengths between 300 - 750 nm (Hmadeh *et al.*, 2008; Lakshmi *et al.*, 1994; Wise *et al.*, 1984; Yamazoe *et al.*, 1988). Due to the time constraints, this was beyond the scope of this study and further investigation on this would be interesting to pursue. Benzidinediimines has been shown by Yamazoe *et al.* (1988) to bind to guanine in DNA which plays a role in the activation of carcinogenicity in hepatic tissues. The proposed new structure, based on the NMR and high resolution MS experiments is shown in figure 5.31. This new structure is consistent with the theory of participation of the free electron pair of the 3-amino group in a resonance configuration with the quaternary nitrogen (figure 5.3) (Firth *et al.*, 1983), only after substitution of the benzenediazonium moiety there is no longer a quaternary nitrogen present in the molecule. After loss of a proton at the 3-amino position, these structures (figure 5.31 and 5.32) might be formed. With 34.27 kcal/mol, compared to 61.52 kcal/mol, it is energetically favourable over the previously reported configuration (approximate values calculated by ChemBioDraw Ultra version 12.0).

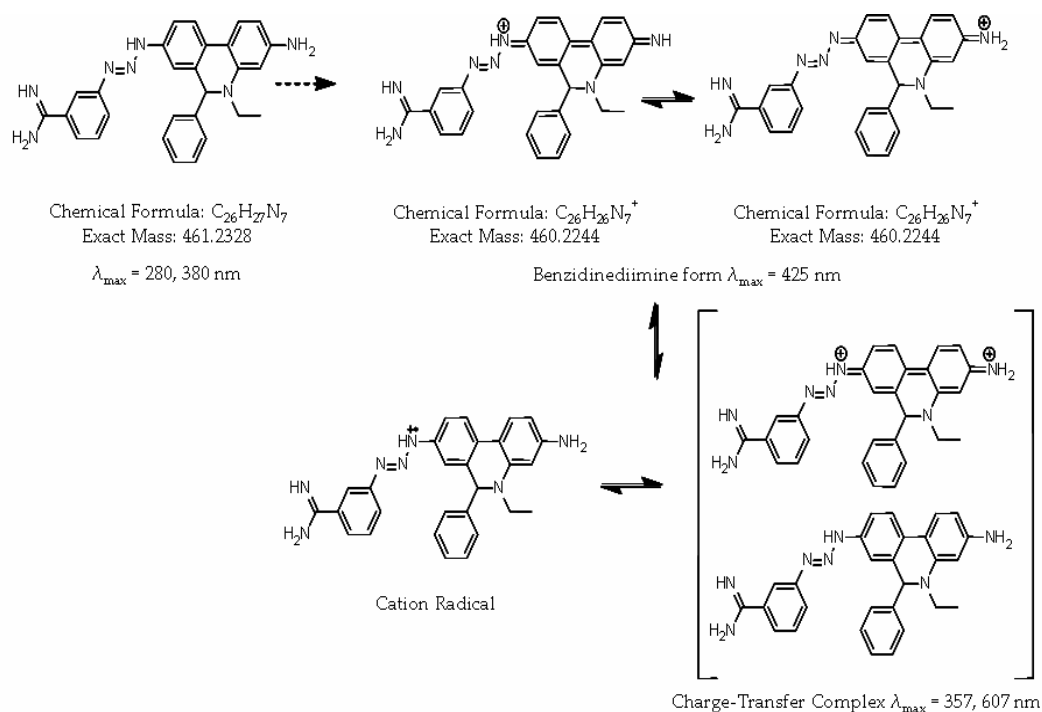


Figure 5.31: New proposed structure of ISM (M&B4180A) with an exact mass of 461.2328 g/mol and a protonated mass ion at  $m/z = 460.2244$  due to formation of the diimine reactive intermediate (Yamazoe *et al.*, 1988; Lakshmi *et al.* 1994)

Hence, new possible structures are proposed, also for the other two isomers M&B4250 and M&B38897, as well as the di-substituted related compound M&B4596 (figure 5.32) as supported by NMR and high resolution MS data.

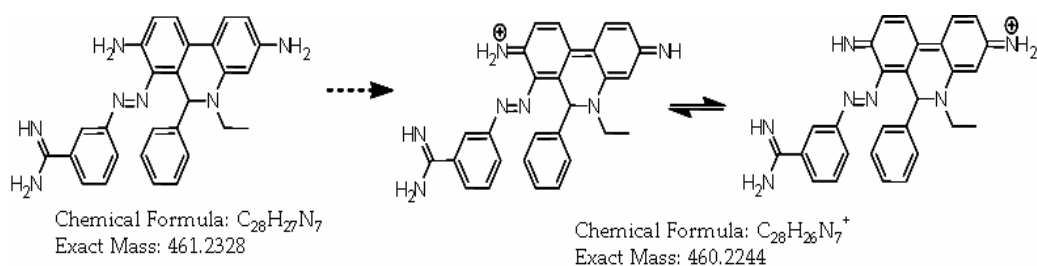


Figure 5.32: New proposed structure of M&B4250 as supported by NMR and high resolution MS data

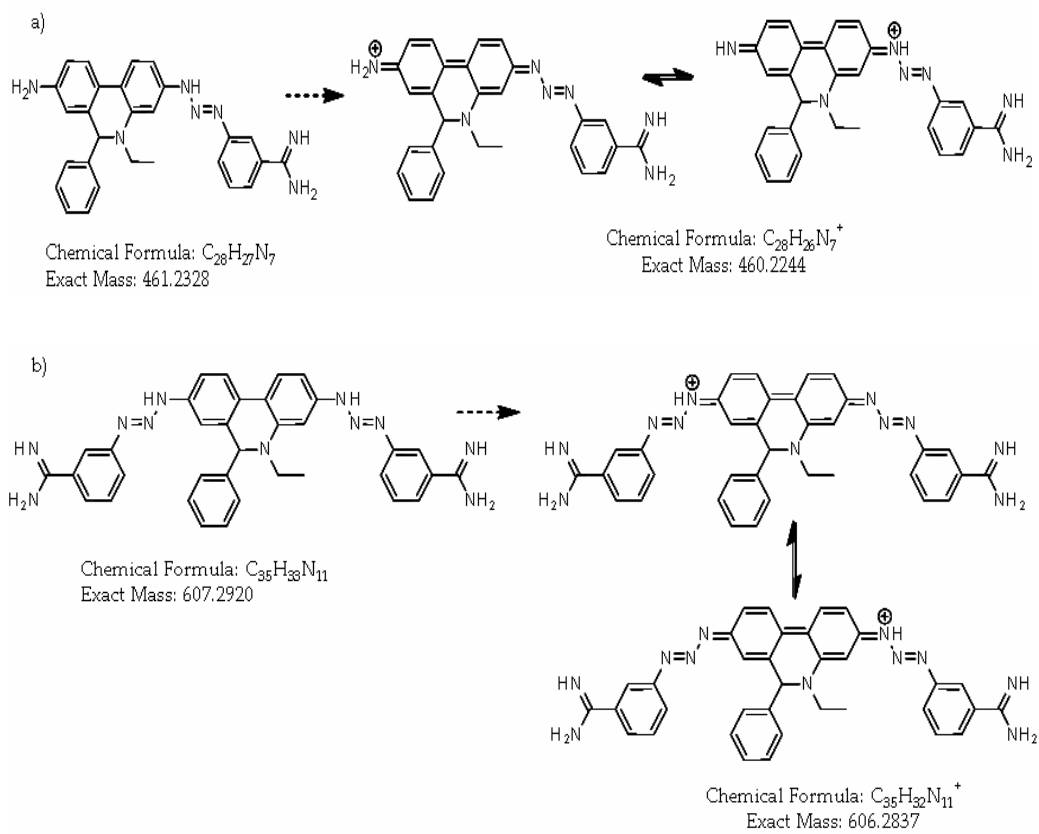


Figure 5.33: New proposed structure of a) M&B38897 and b) M&B4596 as supported by NMR and high resolution MS data



## 5.4. Conclusions

The existing isocratic, analytical assay of ISM and related compounds (chapter 2) was successfully scaled-up to provide a preparative HPLC separation of the compounds. Computer-assisted method development was used to develop a semi-preparative HPLC method for the specific isolation of single fractions of each of the components in a mixed reference standard material of ISM and related compounds. As ISM is susceptible to degradation under extreme acidic or basic pH conditions (Kinabo & Bogan, 1988c), the mobile phase was adjusted to pH 6.0. Once isolated the single compounds were analysed by LC-MS. They were shown to be reasonably pure and stable in the mobile phase. No major degradation to homidium was detected within 10 h after collection. A molecular weight of 460 g/mol for the three isomers M&B4180A, M&B4250 and M&B38897 was confirmed by low-resolution MS analysis, as well as a mass of 606 g/mol for the bis-substituted related compound, M&B4596. A second early eluting analyte was separated and collected during the semi-preparative assay, which also gave a MS signal at  $m/z = 606$ . Thus it could be assumed that there is a second bis-substituted related compound present in ISM formulations. Unambiguous differentiation between fractions I and II was given by their unequal colours. The solution of the unknown analyte shows a purple tone as opposed to the yellow colouring of M&B4596 (figure 5.8 b). Hence, it is unmistakably a matter of two different analytes. UV spectra of the five single compounds were obtained and they showed marked differences in their  $\lambda_{\max}$  values. Substitution of the amidino moiety to the phenanthridine nucleus at the amine group at C-8 (M&B4180A; ISM) or C-3 (M&B38897) positions resulted in bathochromic shifts of the absorption maxima of these compounds compared with homidium ( $\lambda_{\max} = 290$  nm) to wavelengths of 386 nm and

378 nm respectively. Substitution at C-7 (M&B4250) gave an UV transition at a distinctively lower wavelength of 312 nm, as with only one azo group instead of two the conjugated system in the C-substituted isomer is shorter. The unknown, possibly ISM-related compound with a mass of 606 g/mol has two absorption maxima at 286 nm and 360 nm. It exhibits a distinct hypsochromic shift as compared to the  $\lambda_{\max}$  of M&B4596 (330 and 398 nm). These UV transitions at lower wavelength, that give the violet colour very similar to that of M&B4250, lead to the conclusion that one of the two amidino-benzamidine rings in the unknown compound is C-coupled as in M&B4250.

Unambiguous structure elucidation for the major isomer M&B4180A and M&B4250 was achieved using NMR spectroscopy and high resolution mass spectrometry. The results provide evidence of a different structure than that formerly reported (figure 2.3) (Tetty *et al.*, 1998). The amidino phenanthridines no longer possess the quaternary nitrogen and seem to lose protons on residual amine groups in order to build a stable conjugated system with double bonded nitrogen atoms (figures 5.31 - 5.33). These findings are supported by several two-dimensional  $^1\text{H}$ - $^1\text{H}$  and  $^{13}\text{C}$ - $^1\text{H}$  NMR experiments with M&B4180A and M&B4250, which all confirmed the presence of an additional proton at the C-6 atom, and high resolution mass spectrometry analyses of all isolated fractions. An exact mass of 460.224 g/mol for the protonated ions of the three isomers M&B4180A (ISM), M&B4250 and M&B38897 was predicted and experimentally confirmed, as well as 606.285 g/mol for the bis-substituted compound M&B4596.

## 6. Conclusions and Future Work Suggestions

### 6.1. Conclusions

The veterinary trypanocide isometamidium (ISM) has been extensively studied in the work present in this thesis. The analytical investigation included the quality control of commercial formulations of ISM, bioanalysis and studies of its metabolism as well as the isolation and structure elucidation of the major isomer and all process-related by-products.

As the synthesis of ISM results in production of not only the principal trypanocidal component (ISM; M&B4180A), but also varying amounts of its isomers (M&B4250; M&B38896) and other structurally related impurities (M&B4596; homidium) (Tettey *et al.*, 1998), quality control of ISM formulations is required, which enables separation and quantification of each of these compounds.

The first part of this study (chapter 2) describes the development and validation of a simple isocratic HPLC-UV assay, which was successfully used for fast profiling of a range of ISM products. With the ammonium ion ( $\text{NH}_4^+$ ) in the mobile phase as a competing ion to the basic centres in ISM and related compounds and an acidic mobile phase pH value (pH 2.8) to suppress ionization of residual silanol groups, analyte-silanol interactions could be markedly reduced. Improved peak shape and good resolution of all analytes of interest were achieved. A full validation of the method showed it to be selective, precise and robust with respect to variations in pH, temperature and buffer strength (Kromidas, 1999). A linear relationship between detector response and concentration within a specified concentration range was shown, as well as good repeatability and reproducibility of the method.

The HPLC method which employs standard isocratic HPLC instrumentation with UV detection and widely available reagents and

chemicals was successfully employed for the quality evaluation of several generic ISM products obtained from the open market in Africa, amongst which several counterfeit products were identified (section 2.3.3).

The distribution of counterfeit or sub-standard drugs is a widespread problem that also contributes to the evolution of drug resistance. Since, at the moment, the possibility of the development of new veterinary trypanocides is small, the maintenance of the effectiveness of available drug substances is of vital importance. The reported assay provides a powerful tool for the control of ISM formulations and the identification of substandard and counterfeit products in international commerce. The relatively low cost and simple analytical method renders it suitable for transfer to laboratories in developing countries where improved quality control of veterinary trypanocides is an immediate need.

Furthermore with the elimination of mobile phase additives and use of volatile buffers the method is readily adapted for mass spectrometric detection. The determination of homidium ( $m/z = 314$ ), well separated from ISM ( $m/z = 460$ ; 230.5) and other related substances, shows selectivity of the method with respect to the main degradation product and its capability of indicating the stability of ISM.

Consequently, because of the increase in selectivity and sensitivity that LC-MS offers, it becomes possible to decrease the limit of detection and quantification markedly (40 fold), enabling the determination of very low concentrations (1 ng) of analytes as present in plasma and tissues from animals treated with ISM. Moreover, the development of a bioanalytical method (chapter 3) for the determination of residual ISM and related compounds in biological material would mean that the quality of ISM exposed meat products for human use could be monitored. The method

would also enable highly selective metabolic and bioavailability studies, leading to a better understanding of the mechanisms of action of the drug. A greater appreciation of the disposition and metabolism of ISM could limit the development of chemoresistance to existing trypanocides and help optimise the use of existing drugs in the field and the design of new compounds with trypanocidal activity.

ISM and related compounds were successfully extracted from spiked plasma samples by SPE using  $\text{NH}_4\text{Cl}$  saturated methanol as elution solvent. It was possible to minimize analyte adsorption to residual silanol groups in glass surfaces by using deactivated, silanized glassware and 1 %v/v iso-propanol in the reconstitution solvent. The problem of adverse matrix effects was overcome by preparing reference standards in blank plasma extracts.

Dimidium bromide was used as an internal standard, to compensate for any variations during sample preparation. Due to it lacking a highly basic amidino moiety it does not have the same physico-chemical properties as ISM. ISM and related compounds adsorb to glassware, while dimidium showed none of these losses during sample preparation. Hence, losses of ISM due to adsorption to glass surfaces during sample preparation are not accounted for when using dimidium as the internal standard (section 3.3.3). Dimidium bromide is more similar to homidium in its structure (figure 3.4). The two compounds differ in only one alkyl group and dimidium is an ideal internal standard for the determination of the degradation product. Results for accuracy and precision for homidium are far more satisfactory using this approach, than those for ISM and related substances (table 3.5). A related compound, possessing an amidino moiety in addition to the phenanthridine

group, which is not generally present in ISM formulations would be the better choice as an internal standard for this assay.

For the highly selective and sensitive determination of ISM, its isomers and related substances a MS detector was used in the selected ion mode (section 3.3.1.1). Limits of detection and quantification were considerably improved compared to previously reported HPLC-UV assays (Kinabo & Bogan, 1988c; Tettey *et al.*, 1998) with the further advantage of unambiguous specificity for all compounds present.

Although the linear relationship between peak area ratios of analyte and internal standard and sample concentration could be demonstrated, the method failed to provide good precision for all the analytes of interest. Repeatability and reproducibility of the determination of homidium was very good, but values of %RSD of up to 30.1 % in repeatability studies of the quantification and precision of M&B4180A and its structural isomers M&B4250 and M&B38897 were unsatisfactory. This problem could possibly be overcome by using a more suitable internal standard. However a compound with the desirable structure was not commercially available.

After development and optimisation of the sample preparation procedures of the bioanalytical method, focus centred on the optimisation of the HPLC-MS assay (chapter 4). Further enhancement of selectivity and sensitivity of the HPLC separation, would provide more precise data even at very low analyte concentrations.

A comparative study of the effect of stationary phase chemistry and mobile phase selectivity on the HPLC separation of ISM and related compounds was performed. As interactions of residual acidic silanol groups in the silica surface of the stationary phase with the highly basic amidino-phenanthridine compounds could produce pronounced peak tailing, new

generation, high purity silica phases were investigated. Also the use of various stationary phase chemistries with differing selectivity for the analytes was examined for possible improvements in the separation. Experiments with varying preliminary mobile phase compositions showed that the ammonium formate buffered mobile phase with an acidic pH of 2.8 suppresses silanol ionisation and provides optimum peak shapes for the charged basic analytes.

Changes of temperature between 30 and 50 °C did not seem to largely affect the separation. This allows the method to be used for field studies in laboratories situated in Africa without complications due to the hot climate.

Ten different stationary phases with varying surface chemistries were examined for their effect on the selectivity of the separation. It was found that the retention mechanism of the phenanthridine compounds is complex and affected by hydrophobic, aromatic and polar interactions of the analytes with the bonded organic layer or the silica support. Retention of ISM and related compounds on the reversed phase columns decreases with increasing surface coverage of the organic ligands, and increases with increasing polarity of the stationary phase, indicating that ionic interactions play an important part in the retention mechanism of these analytes (figure 4.10). Enhanced retention on columns with an aromatic functionality suggests that  $\pi$ - $\pi$  interactions of the stationary phase with the aromatic solutes also contribute to the retentive effect. A C8 HPLC column, rather than the previously reported C18 phase (section 4.3.2) was found to be the best choice for this separation.

Computer-assisted method development using the DryLab® simulation software was successfully employed to model optimum separation conditions for gradient and isocratic separations of ISM and

related substances. Gradient analysis was favoured for the trace analysis of ISM in plasma samples, as the constant increase of the content of organic solvent in the mobile phase lead to distinctively narrower, higher signals compared to an isocratic separation. With the increase in the response signal, the sensitivity of the method was markedly improved. Starting the gradient with a high % organic solvent content (30 %), lead to a reduction in gradient time from 21 min to 4 min and distinctively decreased column re-equilibration time and thus the overall analysis time. With the 4 min gradient on an ACE 5 C8 column, there was a dramatic improvement in peak shape and sensitivity due to improved column performance, yielding a better separation, compared to analysis using the original isocratic conditions on a Gemini 5u C18 column (figure 6.1).

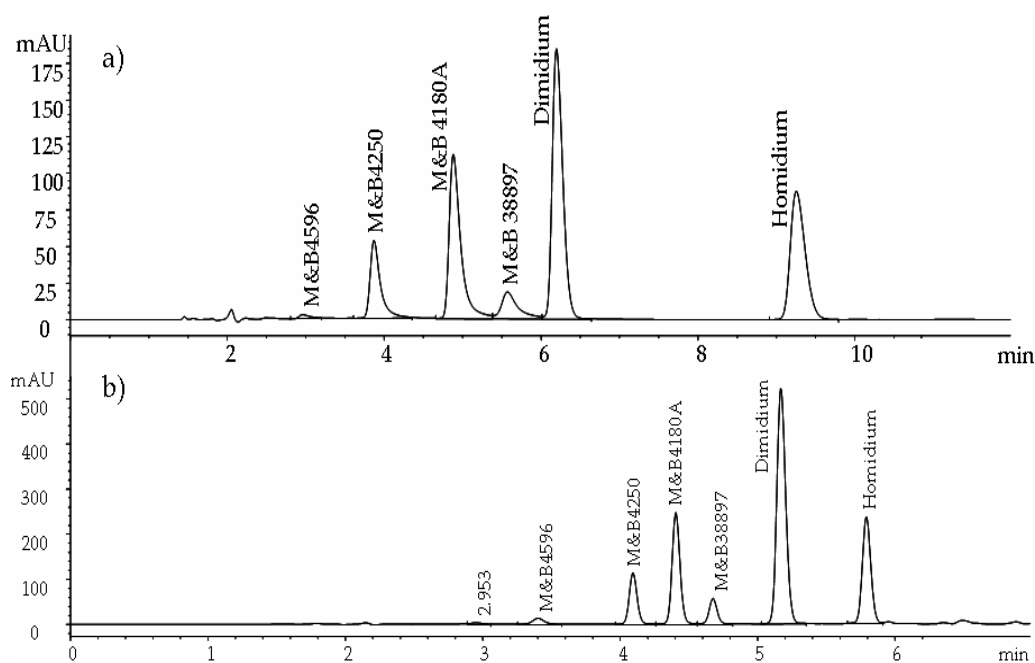


Figure 6.1: Chromatograms obtained with a) isocratic conditions (ammonium formate buffer, pH 2.8 / acetonitrile; 75 : 25 v/v) on Gemini 5u C18 and b) 4 min gradient on ACE 5 C8, 150 x 4.5 mm, 5  $\mu$ m HPLC columns, with mobile phase consisting of 15 mM ammonium formate and acetonitrile at 30  $^{\circ}$ C.



The last part of the study (chapter 5) involved the scaling up of the developed isocratic analytical assay (Chapter 2) to a preparative HPLC separation. Again, computer-assisted method development was successfully employed to develop a semi-preparative HPLC method for the specific isolation of pure ISM (M&B4180A) and related substances. As ISM readily degrades to homidium in an acidic environment, the mobile phase was adjusted to pH 6.0. Once isolated, the fractions containing the single compounds were analysed by LC-MS and shown to be reasonably pure and stable in the mobile phase for at least 10 hours after collection. No major degradation to homidium was detected. The molecular weight of 460 g/mol for the three isomers M&B4180A, M&B4250 and M&B38897 was confirmed, as well as a mass of 606 g/mol for the bis-substituted related compound M&B4596. A second early eluting peak was separated and collected during the semi-preparative assay, which also has a MS signal at  $m/z = 606$ . This led to the assumption, that there was a second bis-substituted related compound present in ISM formulations. This fraction had a violet colour as opposed to the yellow tone of the M&B4596 solution. Hence it was concluded, that the two components were different. UV spectra of the five isolated fractions had distinctive  $\lambda_{\max}$  values, indicating similarities and differences in absorption behaviour, and thus the structures of the related compounds. The two *N*-substituted isomers M&B4180A and M&B38897 exhibited very similar UV transitions with two absorption maxima around 280 and 380 nm. Substitution at C-7 as in M&B4250 produced a single absorption maximum at a much lower wavelength of 312 nm. The unknown, possibly ISM related compound with a mass of 606 g/mol and two  $\lambda_{\max}$  (286; 360 nm) gave a distinct hypsochromic shift when comparing the maximum absorption wavelengths of M&B4596 (330; 398 nm). This observation, as well as the

violet colour of fraction 1, suggests that one of the two amidino-benzamidine rings in the unknown compound is C-coupled as in M&B4250 (section 5.3.1 & 5.3.2).

Unambiguous structure elucidation of the major isomers M&B4180A and M&B4250 was achieved using two-dimensional  $^1\text{H}$ - $^1\text{H}$ - and  $^{13}\text{C}$ - $^1\text{H}$ -NMR spectroscopy, which suggested the presence of an additional proton at the C-6 atom (figure 6.2).

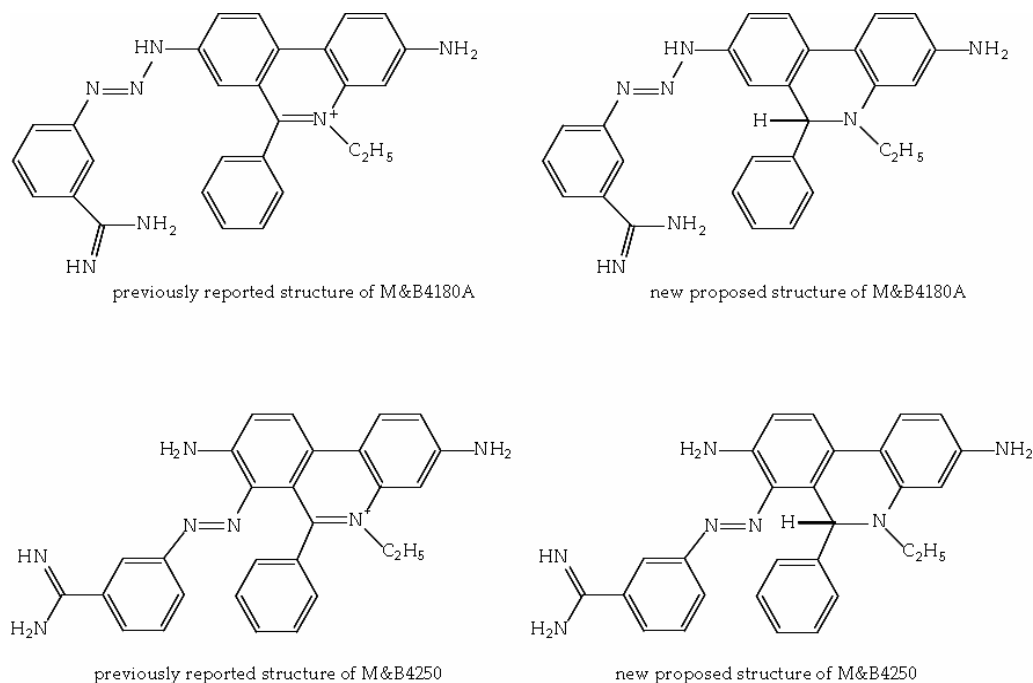


Figure 6.2: Previously reported and new proposed structures of M&B4180A (ISM) and M&B4250

High resolution mass spectrometry did not confirm the predicted mass of a protonated ion of 461 g/mol, but ions with exact masses of 460.224 g/mol for the protonated ions of the three isomers M&B4180A (ISM), M&B4250 and M&B38897 as well as 606.285 g/mol for the bis-substituted compound M&B4596 were found. These contradictory results are possibly due to formation of the diimine reactive intermediate during protonation (Yamazoe *et al.*, 1988) (figure 5.31) which has a predicted exact mass of 460.224 amu.

These data provide evidence that the structures of M&B4180A and M&B4250 are different from those previously reported (figure 6.2) in that the amidino phenanthridines no longer possess the quaternary nitrogen and seem to have lost protons on residual amine groups in the ionisation source of the MS detector, in order to build a stable conjugated system with double bonded nitrogen atoms (figure 5.31 - 5.33).

## **6.2. Suggestions for Future Work**

The 4 min gradient for the fast separation and selective quantification of ISM and related substances was only examined with UV detection. MS detection with an ESI interface requires the use of a lower flow rate, hence the method requires to be optimised with an equivalent column with narrower inner diameters containing smaller stationary phase micro-particles. If the method can be adapted to be compatible with conditions required for MS and validation of the modified method is successful it should provide a highly sensitive, while selective, alternative to ELISA analysis for the determination of residual trace amounts of ISM in the plasma of treated animals. During the course of this study it was not possible to obtain animal plasma samples from large animals treated in the field due to the strict regulations for shipping biological materials from outside the EU. Consequently all experiments were carried out using spiked bovine serum. This problem would be overcome by transferring the method to laboratories in Africa.

Further investigation of the '4 min gradient method' in terms of improving efficiency by using shorter columns, packed with smaller particles and a customised HPLC system with regard to dwell volume and detector response could lead to an even faster separation. Reduced analysis time and solvent consumption would lead to markedly decreased cost of analysis.

After validation, the assay could be used as an improved quality control method for quality assurance of commercial ISM formulations.

Larger amounts of pure samples of all the analytes should be obtained by scaling up the preparative method, so that further characterisation could be undertaken using UV-, IR-, NMR- and mass spectrometry. UV-titration could give further information on the pH dependency of the UV-spectra of the compounds. Solid state analysis could be used to give a better understanding of the preferred molecular orientations, residence of the positive charge, packing motifs and non-bonded interactions. Molecular modelling techniques could also be applied to investigate chemical effects and behaviour at the molecular level.

If the structure of each single compound is evaluated unambiguously, this would allow the investigation of structure-activity relationships, which might ultimately lead to the identification of new, therapeutically active compounds for the treatment of African trypanosomiasis.

Moreover, approved reference standards are needed in order to establish official protocols and monographs for the quality control and quality assurance of ISM based trypanocidal drugs.

## 7. References

- ACT (2007). ACE® HPLC Columns ACT - Advanced Chromatography Technologies.
- Ali, B. H. & Hassan, T. (1984). Preliminary pharmacokinetic study of isometamidium chloride in camels. *Research in Veterinary Science* 37, 376-377.
- Anene, B. M., Onah, D. N. & Nawa, Y. (2001). Drug resistance in pathogenic African trypanosomes: what hopes for the future? *Veterinary Parasitology* 96, 83-100.
- Bansal, S. & DeStefano, A. (2007). Key elements of bioanalytical method validation for small molecules. *The AAPS Journal* 9, E109-E114.
- Barrett, M. P., Burchmore, R. J., Stich, A., Lazzari, J. O., Frasc, A. C., Cazzulo, J. J. & Krishna, S. (2003). The trypanosomiasis. *The Lancet* 362, 1469-1480.
- Barry, J. D. (1997). Biology of Antigenic Variation in African Trypanosomes, Trypanosomiasis and Leishmaniasis, *Biology and Control*, edited by G. Hide, J. C. Mottram, G. H. Coombs, & P. H. Holmes, pp. 89-107.
- Berg, S. S. (1960). Structure of Isometamidium (M. and B. 4180A), 7-m-Amidinophenyldiazoamino-2-amino-10-ethyl-9-phenylphenanthridinium Chloride Hydrochloride, the Red Isomer present in Metamidium. *Nature* 188, 1106-1107.
- Berg, S. S. (1963). The search for new trypanocides. Part VIII. Coupling of *m*-amidinobenzenediazonium chloride with 3,8-diamino-5-ethyl-6-phenylphenanthridinium chloride. *Journal of the Chemical Society* 684, 3635-3640.
- Berg, S. S., Bretherick, K., Washbourn, K. & Wragg, W. R. (1963). The Search for New Trypanocides. Part IX. Amidinophenyldiazoamino- and Amidinophenylazo-phenanthridinium Salts. *Journal of the Chemical Society* 884, 4617-4622.

- Berg, S. S., Brown, K. N., Hill, J. & Wragg, W. R. (1961). A New Prophylactic Trypanocidal Drug, 2,7-di-(m-amidinophenyldiazoamino)-10-ethyl-9-phenyl-phenanthridinium Chloride Dihydrochloride (M&B 4596). *Nature* 192, 367-368.
- Bhalla, N. (2002). Pan African group takes lead against the tsetse fly. *The Lancet* 359, 686.
- Bidlingmeyer, B. A. (1992). *Practical HPLC methodology and applications*, 1<sup>st</sup> ed. New York: Wiley-Interscience.
- Boibessot, I., Tettey, J. N., Skellern, G. G., Watson, D. G. & Grant, M. H. (2006). Metabolism of isometamidium in hepatocytes isolated from control and inducer-treated rats. *Journal of Veterinary Pharmacology and Therapeutics* 29, 547-553.
- Boibessot, I., Turner, C. M., Watson, D. G., Goldie, E., Connel, G., McIntosh, A., Grant, M. H. & Skellern, G. G. (2002). Metabolism and distribution of phenanthridine trypanocides in *Trypanosoma brucei*. *Acta Tropica* 84, 219-228.
- Braide, V. B. & Eghianruwa, K. I. (1980). Isometamidium residues in goat tissues after parenteral administration. *Research in Veterinary Science* 29, 111-113.
- Brown, K. N., Hill, J. & Holland, A. E. (1961). Anti-trypanosomal activity of certain phenyldiazoamino- and phenylazoamino-phenanthridinium compounds. *British Journal of Pharmacology and Chemotherapy* 17, 396-405.
- Browning, C. H., Morgan G.T., Robb, J. V. M. & Walls, L. P. (1938). The trypanocidal action of certain phenanthridinium compounds. *The Journal of Pathology and Bacteriology* 46, 203-204.
- Budd, L. (1999). DFID-funded tsetse and trypanosome research and development since 1980. Vol. 2. Economic analysis. DFID Livestock Production, Animal Health and Natural Resources Systems Research Programmes.
- Bush, A. O., Fernández, J. C., Esch, G. W. & Seed, J.R (2001). The Protozoa, in: A. O. Bush, J. C. Fernández, G. W. Esch & J. R. Seed, *Parasitism: the diversity and ecology of animal parasites*, 1<sup>st</sup> ed. (pp. 42-95). Cambridge: Cambridge University Press.

Cech, N. B. & Enke, C. G. (2001). Practical implications of some recent studies in electrospray ionization fundamentals. *Mass Spectrometry Reviews* 20, 362-387.

Clair, M. (1988). The epidemiology of African animal trypanosomiasis, in: *FAO Corporate Document Repository: Proceedings of a meeting held 23-27 november. Nairobi, Kenya*  
[<http://www.fao.org/Wairdocs/ILRI/x5443E/x5443e0c.htm#9> the epidemiology of african animal trypanosomiasis]

Clarke, E. G. C. (1969). Isolation and identification of drugs in pharmaceuticals, body fluids, and post-mortem material, 1<sup>st</sup> ed. London: Pharmaceutical Press.

Coolbear, K. P. & Midgley, M. (1986). Characteristics of ethidium uptake by the trypanosomatid flagellates *Crithidia fasciculata* and *Leptomonas seymouri*. *Antimicrobial Agents and Chemotherapy* 29, 258-262.

Cox, F. E. G. (2004). History of sleeping sickness (African trypanosomiasis). *Infectious Disease Clinics of North America* 18, 231-245.

Croft, S. L., Barrett, M. P. & Urbina, J. A. (2005). Chemotherapy of trypanosomiasis and leishmaniasis. *Trends in Parasitology* 21, 508-512.

Cruz, E., Euerby, M. R., Johnson, C. M. & Hackett, C. A. (1997). Chromatographic Classification of Commercially Available Reverse-Phase HPLC Columns. *Chromatographia* 44, 151-161.

Dalan, T., McKeever, D., Teale, A. & Perry, B. (1989). Annual Report of the International Laboratory for Research on Animal Diseases.

de Raadt, P. (2005). The history of sleeping sickness  
[[http://www.who.int/trypanosomiasis\\_african/country/history/en/print.html](http://www.who.int/trypanosomiasis_african/country/history/en/print.html)]  
World Health Organisation.

Delespaux, V. & de Koning, H. P. (2007). Drugs and drug resistance in African trypanosomiasis. *Drug Resistance Updates* 10, 30-50.

Denise, H. & Barrett, M. P. (2001). Uptake and mode of action of drugs used against sleeping sickness. *Biochemical Pharmacology* 61, 1-5.

- Dolan, J. W., Lommen, D. C. & Snyder, L. R. (1989). Drylab® computer simulation for high-performance liquid chromatographic method development : II. Gradient Elution. *Journal of Chromatography A* 485, 91-112.
- Dolan, J. W., Snyder, L. R., Wolcott, R. G., Haber, P., Baczek, T., Kaliszan, R. & Sander, L. C. (1999). Reversed-phase liquid chromatographic separation of complex samples by optimizing temperature and gradient time: III. Improving the accuracy of computer simulation. *Journal of Chromatography A* 857, 41-68.
- Duong Thi, M. D., Grant, M. H., Mullen, A. B., Tettey, J. N. A., Mackay, S. P. & Clark, R. L. (2009). Metabolism of two new benzodiazepine-type anti-leishmanial agents in rat hepatocytes and hepatic microsomes and their interaction with glutathione in macrophages. *Journal of Pharmacy and Pharmacology* 61, 399-406.
- Eisler, M., Gault, E. A., Peregrine, A., Smith, H. V. & Holmes, P. (1993). Evaluation and improvement of an enzyme-linked immunosorbent assay for the detection of isometamidium in bovine serum. *Therapeutic Drug Monitoring* 15, 236-242.
- Eisler, M. C. (1996). Pharmacokinetics of the chemoprophylactic and chemotherapeutic trypanocidal drug isometamidium chloride (Samorin) in cattle. *Drug Metabolism and Disposition* 24, 1355-1361.
- Eisler, M. C., Elliott, C. T. & Holmes, P. H. (1996a). A simple competitive enzyme immunoassay for the detection of the trypanocidal drug isometamidium. *Therapeutic Drug Monitoring* 18, 73-79.
- Eisler, M. C., Maruta, J., Nqindi, J., Connor, R. J., Ushewokunze-Obatolu, U., Holmes, P. H. & Peregrine, A. S. (1996b). Isometamidium concentrations in the sera of cattle maintained under a chemoprophylactic regime in a tsetse-infested area of Zimbabwe. *Tropical Medicine and International Health* 1, 535-541.
- El-Sayed, N. M., Hegde, P., Quackenbush, J., Melville, S. E. & Donelson, J. E. (2000). The African trypanosome genome. *International Journal for Parasitology* 30, 329-345.
- Engelhardt, H., Löw, H. & Göttinger, W. (1991). Chromatographic characterization of silica-based reversed phases. *Journal of Chromatography A* 544, 371-379.



- Euerby, M. R. (2005). Personal Communication: Experimental design and optimisation
- Euerby, M. R. (2010). Personal Communication: Column equilibration between gradient runs
- Euerby, M. R. & Petersson, P. (2003). Chromatographic classification and comparison of commercially available reversed-phase liquid chromatographic columns using principal component analysis. *Journal of Chromatography A* 994, 13-36.
- Euerby, M. R., Petersson, P., Campbell, W. & Roe, W. (2007). Chromatographic classification and comparison of commercially available reversed-phase liquid chromatographic columns containing phenyl moieties using principal component analysis. *Journal of Chromatography A* 1154, 138-151.
- FAO (2006). Activities of the Food and Environmental Protection Section of the Joint FAO/IAEA Division of Nuclear Techniques in Food and Agriculture Related to the Work of the Codex Committee on Residues of Veterinary Drugs in Food [[http://www.fao.org/AG/AGAINFO/programmes/en/paat/documents/workshops/cancun\\_2006.pdf](http://www.fao.org/AG/AGAINFO/programmes/en/paat/documents/workshops/cancun_2006.pdf)]
- Firth, W. J., Watkins, C. L., Graves, D. E. & Yielding, L. W. (1983). Synthesis and Characterization of Ethidium Analogs: Emphasis on Amino and Azido Substituents. *Journal of Heterocyclic Chemistry* 20, 759-765.
- Folin, O. & Ciocalteu, V. (1927). On Tryrosine and Tryptophane Determinations in Proteins. *Journal of Biological Chemistry* 73, 627-650.
- Fraire, C., Lecoite, P. & Paoletti, C. (1981). Metabolism of ethidium bromide in rats. *Drug Metabolism and Disposition* 9, 156-160.
- Gambari, R. & Nastruzzi, C. (1994). DNA-binding activity and biological effects of aromatic polyamidines. *Biochemical Pharmacology* 47, 599-610.
- Gardiner, C. H., Fayer, R. & Dubey, J. P. (1988). *An Atlas of Protozoan Parasites in Animal Tissues*, Agriculture Handbook #651. Washington, DC: United States Department of Agriculture.
- Gaugain, B., Fraire, C., Lecoite, P., Paoletti, C. & Roques, B. P. (1981). Chemical structure of ethidium bromide metabolites extracted from rat bile. *FEBS Lett.* 129, 70-76.

Geerts, A. S. & Holmes, P. H. (1998). Drug management and parasite resistance in bovine trypanosomiasis in Africa, in: FAO Corporate Document Repository [<ftp://ftp.fao.org/docrep/fao/003/W9791E/W9791e01.pdf>]

Geerts, S., Holmes, P. H., Eisler, M. C. & Diall, O. (2001). African bovine trypanosomiasis: the problem of drug resistance. *Trends in Parasitology* 17, 25-28.

Gilbert, M., Jenner, C., Pender, J., Rogers, D., Slinghenbergh, J. & Wint, W. (2001). The Programme Against African Trypanosomiasis Information System (PAATIS)., *World class parasites: Vol.1 - the african trypanosomes*, edited by S. N. Black & J. R. Seed, pp. 11-24. Dordrecht, The Netherlands: Kluwer Academic Publishers.

Girgis-Takla, P. & James, D. M. (1974). In Vitro Uptake of Isometamidium and Diminazene by *Trypanosoma brucei*. *Antimicrobial Agents and Chemotherapie* 6, 372-374.

Greibrokk, T. & Andersen, T. (2003). High-temperature liquid chromatography. *Journal of Chromatography A* 1000, 743-755.

Griggs, B. G., Davidson, M. W., Wilson, W. D. & Withers Boykin, D. (1980). Assignment of the <sup>13</sup>C Chemical Shifts of Ethidium Bromide and Analogs in D<sub>2</sub>O Solution. *Organic Magnetic Resonance* 14, 371-373.

Haky, J. E. (2005). Resolution in HPLC: Selectivity, Efficiency and Capacity, in: J. Cazes (Ed.), *Encyclopedia of Chromatography*, Vol. 2, 2<sup>nd</sup> ed (pp. 1434-1436). New York: Taylor & Francis.

He, P. & Yang, Y. (2003). Studies on the long-term thermal stability of stationary phases in subcritical water chromatography. *Journal of Chromatography A* 989, 55-63.

Hide, G. (1999). History of Sleeping Sickness in East Africa. *Clin. Microbiol. Rev.* 12, 112-125.

Hill, J. & McFadzean, J. A. (1963). Studies on isometamidium : Depots of isometamidium in mice and rats and their importance for prophylaxis against *Trypanosoma congolense*. *Transactions of the Royal Society of Tropical Medicine and Hygiene* 57, 476-484.

Hmadeh, M., Traboulsi, H., Elhabiri, M., Braunstein, P., Albrecht-Gary, A. M. & Siri, O. (2008). Synthesis, characterization and photophysical properties of benzidine-based compounds. *Tetrahedron* 64, 6522-6529.

Jandera, P. (1998). Optimisation of gradient elution in normal-phase high-performance liquid chromatography. *Journal of Chromatography A* 797, 11-22.

Jandera, P. & Kucerov, M. (1997). Prediction of retention in gradient-elution normal-phase high-performance liquid chromatography with binary solvent gradients. *Journal of Chromatography A* 759, 13-25.

JECFA (2003). Isometamidium Chloride, in: JECFA directory of veterinary drug substances  
[[ftp://193.43.36.44/es/esn/jecfa/vetdrug/41-2-isometamidium\\_chloride.pdf](ftp://193.43.36.44/es/esn/jecfa/vetdrug/41-2-isometamidium_chloride.pdf)]

Kapp, C. (2002). Counterfeit drug problem "underestimated", says conference. *Lancet* 360, 1080.

Karembe, H. (2008). Improvement of control and harmonisation of international standards for quality of trypanocidal drugs, Proceedings of the OIE Conference on Veterinary Medicinal Products in Africa, Dakar, 25-27 March 2008

Kimata, K., Iwaguchi, K., Onishi, S., Jinno, K., Eksteen, R., Hosoya, K., Araki, M. & Tanaka, N. (1989). Chromatographic Characterization of Silica C<sub>18</sub> Packing Metrials. Correlation between a Preparation Method and Retention Behaviour of Stationary Phase. *Journal of Chromatographic Science* 27, 721-728.

Kinabo, L. D. (1993). Pharmacology of existing drugs for animal trypanosomiasis. *Acta Tropica* 54, 169-183.

Kinabo, L. D. & Bogan, J. A. (1988a). Development of a radioimmunoassay for isometamidium. *Veterinary Research Communications* 12, 375-382.

Kinabo, L. D. & Bogan, J. A. (1988b). Pharmacokinetic and histopathological investigations of isometamidium in cattle. *Research in Veterinary Science* 44, 267-269.

Kinabo, L. D. & Bogan, J. A. (1988c). Solid-phase extraction and ion-pair reversed-phase HPLC of isometamidium in bovine serum and tissues. *Acta Tropica* 45, 165-170.

Kinabo, L. D. & Bogan, J. A. (1988d). The pharmacology of isometamidium. *Journal of Veterinary Pharmacology and Therapeutics* 11, 233-245.

- Kinabo, L. D. & McKellar, Q. A. (1990). Isometamidium in goats: disposition kinetics, mammary excretion and tissue residues. *British Veterinary Journal* 146, 405-412.
- Kinabo, L. D., McKellar, Q. A. & Eckersall, P. D. (1991). Isometamidium in pigs: disposition kinetics, tissue residues and adverse reactions. *Research in Veterinary Science* 50, 6-13.
- Kratzer, R. D., Turkson, P. K., Karanja, W. M. & Ondiek, F. O. (1989) Studies in Cattle on the Pharmacokinetics, Residues and Bioavailability of the Anti-Trypanosomal Drug Isometamidium, in: *Proceedings of the 20<sup>th</sup> International Scientific Council for Trypanosomiasis Research and Control (ISCTRC) Meeting*
- Krisko, R. M., McLaughlin, K., Koenigbauer, M. J. & Lunte, C. E. (2006). Application of a column selection system and DryLab software for high-performance liquid chromatography method development. *Journal of Chromatography A* 1122, 186-193.
- Kromidas, S. (1999). *Validierung in der Analytik*, 1<sup>st</sup> ed. Weinheim: Wiley-VCH.
- Lakshmi, V. M., Zenser, T. V. & Davis, B. B. (1994). Mechanism of 3-(Glutathione-S-yl)-Benzidine Formation. *Toxicology and Applied Pharmacology* 125, 256-263.
- Lau, C. E., Falk, J. L., Dolan, S. & Tang, M. (1987). Simultaneous determination of flurazepam and five metabolites in serum by high-performance liquid chromatography and its application to pharmacokinetic studies in rats. *Journal of Chromatography* 423, 251-259.
- Lowe, D. (2009). The Great Acetonitrile Shortage. In the Pipeline, Corante Weblog Column [[http://pipeline.corante.com/archives/2009/01/22/the\\_great\\_acetonitrile\\_shortage.php](http://pipeline.corante.com/archives/2009/01/22/the_great_acetonitrile_shortage.php)]
- Lowry, O. H., Rosebrough, N. J., Farr, A. L. & Randall, R. J. (1951). Protein Measurement with the Folin Phenol Reagent. *J. Biol. Chem.* 193, 265-275.
- Luedtke, N. W., Liu, Q. & Tor, Y. (2004). On the Electronic Structure of Ethidium. *Chemistry - A European Journal* 11, 495-508.

- Maré, C. J. (1998). Foreign Animal Diseases, in: Committee on Foreign Animal Diseases of the United States Animal Health Association, The Gray Book, 6<sup>th</sup> ed (pp. 22-29). Richmond, Virginia: Pat Campbell & Associates and Carter Printing Company
- Marin, S. J., Jones, B. A., Dale, F. W. & Clark, J. (2004). Effect of high-temperature on high-performance liquid chromatography column stability and performance under temperature-programmed conditions. *Journal of Chromatography* 1030, 255-262.
- Mäser, P., Lüscher, A. & Kaminsky, R. (2003). Drug transport and drug resistance in African trypanosomes. *Drug Resistance Updates* 6, 281-290.
- Matovu, E., Seebeck, T., Enyaru, J. C. & Kaminsky, R. (2001). Drug resistance in *Trypanosoma brucei* spp., the causative agents of sleeping sickness in man and nagana in cattle. *Microbes and Infection* 3, 763-770.
- Matuszewski, B. K., Constanzer, M. L. & Chavez-Eng, C. M. (2003). Strategies for the Assessment of Matrix Effect in Quantitative Bioanalytical Methods Based on HPLC–MS/MS. *Analytical Chemistry* 75, 3019-3030.
- McDonald, P. D. & Bidlingmeyer, B. A. (1987). Strategies for successful preparative liquid chromatography, in: B. A. Bidlingmeyer (Ed.), *Preparative liquid chromatography*, 1<sup>st</sup> ed (pp. 1-95). Amsterdam: Elsevier
- Miller, C. & Fischer, S. (2000). Impact of Ion-Pair reagents on LC/MS Analysis. Agilent Technologies Application [<http://www.chem.agilent.com/Library/applications/5968-8659E.pdf>]
- Murilla, G. A., Mdachi, R. E. & Karanja, W. M. (1996). Pharmacokinetics, bioavailability and tissue residues of [<sup>14</sup>C]isometamidium in non-infected and *Trypanosoma congolense*-infected Boran cattle. *Acta Tropica* 61, 277-292.
- Neue, U. D. (2007). Stationary phase characterization and method development. *Journal of Separation Sciences* 30, 1611-1627.
- Neue, U. D., Alden, B. A. & Walter, T. H. (1999). Universal procedure for the assessment of the reproducibility and the classification of silica-based reversed-phase packings: II. Classification of reversed-phase packings. *Journal of Chromatography A* 849, 101-116.
- Neue, U. D., O'Gara, J. E. & Méndez, A. (2006). Selectivity in reversed-phase separations: Influence of the stationary phase. *Journal of Chromatography A* 1127, 161-174.

- Neugebauer, M. (2001). Hochleistungs-Flüssigchromatographie, Instrumentelle pharmazeutische Analytik, pp. 440-465. Wissenschaftliche Verlagsgesellschaft mbH Stuttgart.
- Newton, P. N., Green, M. D., Fernandez, F. M., Day, N. P. & White, N. J. (2006). Counterfeit anti-infective drugs. *Lancet Infectious Diseases* 6, 602-613.
- Olila, D., McDermott, J. J., Eisler, M. C., Mitema, E. S., Patzelt, R. J., Clausen, P.-H., Poetzsch, C. J., Zessin, K.-H., Mehlitz, D. & Peregrine, A. S. (2002). Drug sensitivity of trypanosome populations from cattle in a peri-urban dairy production system in Uganda. *Acta Tropica* 84, 19-30.
- PAAT/FAO (2008). Report of the 11th Meeting of the Programme Committee, Geneva, Switzerland, 24 - 25 April 2007 Food and Agriculture Organisation of the United Nations (FAO) [<http://www.fao.org/AG/AGAInfo/programmes/en/paat/documents/reports/Report-11th-PAAT-PC.pdf>].
- Perschke, H. & Vollner, L. (1985). Determination of the trypanocidal drugs homidium, isometamidium and quinapyramine in bovine serum or plasma using HPLC. *Acta Tropica* 42, 209-216.
- Petersson, P. & Euerby, M. R. (2005). An evaluation of the robustness of the Tanaka characterization protocol for reversed-phase liquid chromatography columns. *Journal of Separation Science* 28, 2120-2129.
- Philips, F. S., Sternberg, S. S., Cronin, A. P., Sodergren, J. E. & Vidal, P. M. (1967). Physiologic Disposition and Intracellular Localization of Isometamidium. *Cancer Res* 27, 333-349.
- Romanyshyn, L. A. & Tiller, P. R. (2001). Ultra-short columns and ballistic gradients: considerations for ultra-fast chromatographic liquid chromatographic-tandem mass spectrometric analysis. *Journal of Chromatography A* 928, 41-51.
- Russ-Kirschenbaum, R., Koziol, T. & Woolf, E. (1989). Solid Phase Extraction of Quaternary Ammonium Compounds on Diol Columns: Application to the HPLC determination of CK-1649 in Plasma. *Journal of Liquid Chromatography* 12, 3051-3059.
- Schwartz, M. A. & Postma E. (1970). Metabolism of flurazepam, a benzodiazepine, in man and dog. *Journal of Pharmaceutical Sciences* 59, 1800-1806.

- Seiter, A., Rago, L. & Jaehnke R. (2005). Pharmaceuticals: Quality Assurance in the Distribution Chain. HNP Brief #6  
[[http://siteresources.worldbank.org/HEALTHNUTRITIONANDPOPULATION/Resources/281627-1109774792596/HNPBrief\\_6.pdf](http://siteresources.worldbank.org/HEALTHNUTRITIONANDPOPULATION/Resources/281627-1109774792596/HNPBrief_6.pdf)]
- Shapiro, T. A. & Englund, P. T. (1990). Selective cleavage of kinetoplast DNA minicircles promoted by antitrypanosomal drugs. *Proceedings of the National Academy of Sciences* 87, 950-954.
- Sinyangwe, L., Delespaux, V., Brandt, J., Geerts, S., Mubanga, J., Machila, N., Holmes, P. H. & Eisler, M. C. (2004). Trypanocidal drug resistance in eastern province of Zambia. *Veterinary Parasitology* 119, 125-135.
- Snyder, L. R. & Dolan, J. W. (1996). Initial experiments in high-performance liquid chromatographic method development I. Use of a starting gradient run. *Journal of Chromatography A* 721, 3-14.
- Snyder, L. R., Dolan, J. W. & Carr, P. W. (2004). The hydrophobic-subtraction model of reversed-phase column selectivity. *Journal of Chromatography A* 1060, 77-116.
- Snyder, L. R., Dolan, J. W. & Lommen, D. C. (1989). Drylab® computer simulation for high-performance liquid chromatographic method development : I. Isocratic elution. *Journal of Chromatography A* 485, 65-89.
- Snyder, L. R., Kirkland, J. J. & Glajch, J. L. (1997a). Basics of Separation, Practical HPLC Method Development, pp. 21-58. John Wiley & Sons, Inc.
- Snyder, L. R., Kirkland, J. J. & Glajch, J. L. (1997b). Computer-Assisted Method Development, Practical HPLC Method Development, pp. 439-478. John Wiley & Sons, Inc.
- Snyder, L. R., Kirkland, J. J. & Glajch, J. L. (1997c). Preparative HPLC Separation, Practical HPLC Method Development, pp. 616-642. John Wiley & Sons, Inc.
- Sones, K. (2001). Pharmaceutical companies: partners or enemies? Newsletter on Integrated Control of Pathogenic Trypanosomes and their Vectors 3, 19-21.
- Song, D., Zhang, S. & Kohlhof, K. (1994). Gas chromatographic-mass spectrometric method for the determination of flurazepam and its major metabolites in mouse and rat plasma. *Journal of Chromatography B: Biomedical Sciences and Applications* 658, 142-148.

- Steiner, F., Teunissen, B., Morello, R., Maio, G. & Boos, K. S. A Miniaturized On-Line SPE-LC Solution for Direct Analysis of Drugs in Small-Volume Plasma Samples. Conference Proceedings Pittcon 2007
- Steverding, D. (2008). The history of African trypanosomiasis. *Parasites and Vectors* 1: 3.
- Supelco (1997). Guide to Derivatization Reagents for GC. Bulletin 909A. [[http://www.sigmaaldrich.com/etc/medialib/docs/Supelco/Application\\_Notes/4537.Par.0001.File.tmp/4537.pdf](http://www.sigmaaldrich.com/etc/medialib/docs/Supelco/Application_Notes/4537.Par.0001.File.tmp/4537.pdf)]
- Sutherland, I. A. & Holmes, P. H. (1993). Alterations in drug transport in resistant *Trypanosoma congolense*. *Acta Tropica* 54, 271-278.
- Swallow, B. M. (1999). Impacts of trypanosomiasis on African agriculture. PAAT technical and scientific series 2. Rome: FAO
- Tetty, J. N. (2006). Personal Communication: Pure standards of ISM and related compounds
- Tetty, J. N., Skellern, G. G., Grant, M. H. & Midgley, J. M. (1999). Investigation of the chemical equivalence of the trypanocidal products, Samorin and Veridium. *Journal of Pharmaceutical and Biomedical Analysis* 21, 1-7.
- Tetty, J. N., Skellern, G. G., Midgley, J. M. & Grant, M. H. (1998). HPTLC and HPLC determination of isometamidium in the presence of its manufacturing and degradation impurities. *Journal of Pharmaceutical and Biomedical Analysis* 17, 713-718.
- Trail, J. C. M., Wissocq, N., d'Ieteren, G. D. M., Kakiese, O. & Murray, M. (1994). Quantitative phenotyping of N'Dama cattle for aspects of trypanotolerance under field tsetse challenge. *Veterinary Parasitology* 55, 185-195.
- Tullo, A. (2008). A Solvent Dries Up. *Chemical & Engineering News* 86, 27-28.
- Vickerman, K. (1997). Landmarks in trypanosome research, in: G. Hide, J. C. Mottram, G. H. Coombs & P. H. Holmes (Eds.) *Trypanosomiasis and Leishmaniasis, Biology and Control* (pp. 1-37). Oxon: CAB International
- Walker, C. H., Hopkin, S. P., Sibly, R. M. & Peakall, D. B. (2006). *Principles of Ecotoxicology*, 3rd ed. London: Taylor & Francis Group.



- Watson, D. G. (1999). *Pharmaceutical Analysis*, 1<sup>st</sup> ed (pp. 195-205).  
Edinburgh: Elsevier
- Wesongah, J. O., Jones, T. W., Kibugu, J. K. & Murilla, G. A. (2004). A comparative study of the pharmacokinetics of isometamidium chloride in sheep and goats. *Small Ruminant Research* 53, 9-14.
- Whitelaw, D. D., Gault, E. A., Holmes, P. H., Sutherland, I. A., Rowell, F. J., Phillips, A. & Urquhart, G. M. (1991). Development of an enzyme-linked immunosorbent assay for the detection and measurement of the trypanocidal drug isometamidium chloride in cattle. *Research in Veterinary Science* 50, 185-189.
- WHO (1997). *Quality assurance of pharmaceuticals - A compendium of guidelines and related materials*.
- WHO (2003). *WHO Expert Committee on Specifications for Pharmaceutical Preparations*, Geneva: World Health Organization, 908.
- WHO (2006). *African trypanosomiasis (sleeping sickness)*  
[<http://www.who.int/mediacentre/factsheets/fs259/en/>]. World Health Organ Fact Sheet.
- WHO (2008). *The International Pharmacopoeia*, fourth edition (incl. First Supplement). [<http://apps.who.int/phint/en/p/about/>]
- WHO (2009a). *Joint FAO/WHO Food Standards Programme Codex Alimentarius Commission World Health Organization*, CAC/32 INF/6.  
[[ftp://ftp.fao.org/codex/CAC/CAC32/if32\\_06e.pdf](ftp://ftp.fao.org/codex/CAC/CAC32/if32_06e.pdf)]
- WHO (2009b). *Monograph Development for the International Pharmacopoeia*. [<http://www.who.int/medicines/publications/pharmacopoeia/mono-develop.pdf>]
- Williams, B., Dransfield, R., Brightwell, R. & Rogers, D. (1993). *Trypanosomiasis*. *Health Policy Plan.* 8, 85-93.
- Williams, D. H. & Fleming, I. (1995). *Ultraviolet and visible spectra*, in: *Spectroscopic Methods in Organic Chemistry*, 5<sup>th</sup> ed (pp. 1-27). Maidenhead: McGraw-Hill Publishing Company
- Wilson, N. S., Nelson, M. D., Dolan, J. W., Snyder, L. R. & Carr, P. W. (2002a). Column selectivity in reversed-phase liquid chromatography: II. Effect of a change in conditions. *Journal of Chromatography A* 961, 195-215.

- Wilson, N. S., Nelson, M. D., Dolan, J. W., Snyder, L. R., Wolcott, R. G. & Carr, P. W. (2002b). Column selectivity in reversed-phase liquid chromatography: I. A general quantitative relationship. *Journal of Chromatography A* 961, 171-193.
- Winkle, S. (2005). *Geißeln der Menschheit. Kulturgeschichte der Seuchen*. Düsseldorf: Artemis&Winkler.
- Wise, R. W., Zenser, T. V., & Davis, B. B. (1984). Characterization of benzidinediimine: a product of peroxidase metabolism of benzidine. *Carcinogenesis* 5, 1499-1503.
- Wolcott, R. G., Dolan, J. W., Snyder, L. R., Bakalyar, S. R., Arnold, M. A. & Nichols, J. A. (2000). Control of column temperature in reversed-phase liquid chromatography. *Journal of Chromatography A* 869, 211-230.
- Wragg, W. R., Washbourn, K., Brown, K. N. & Hill, J. (1958). Metamidium: a New Trypanocidal Drug. *Nature* 183, 1005-1006.
- Yamazoe, Y., Zenser, T. V., Miller, D. W., & Kadlubar, F. F. (1988). Mechanism of formation and structural characterisation of DNA adducts derived from peroxidative activation of benzidine *Carcinogenesis* pp. 1635-1641.
- Zilberstein, D., Wilkes, J., Hirumi, H., & Peregrine, A. S. (1993). Fluorescence analysis of the interaction of isometamidium with *Trypanosoma congolense*. *Biochemical Journal* 292, 31-35.

# APPENDIX

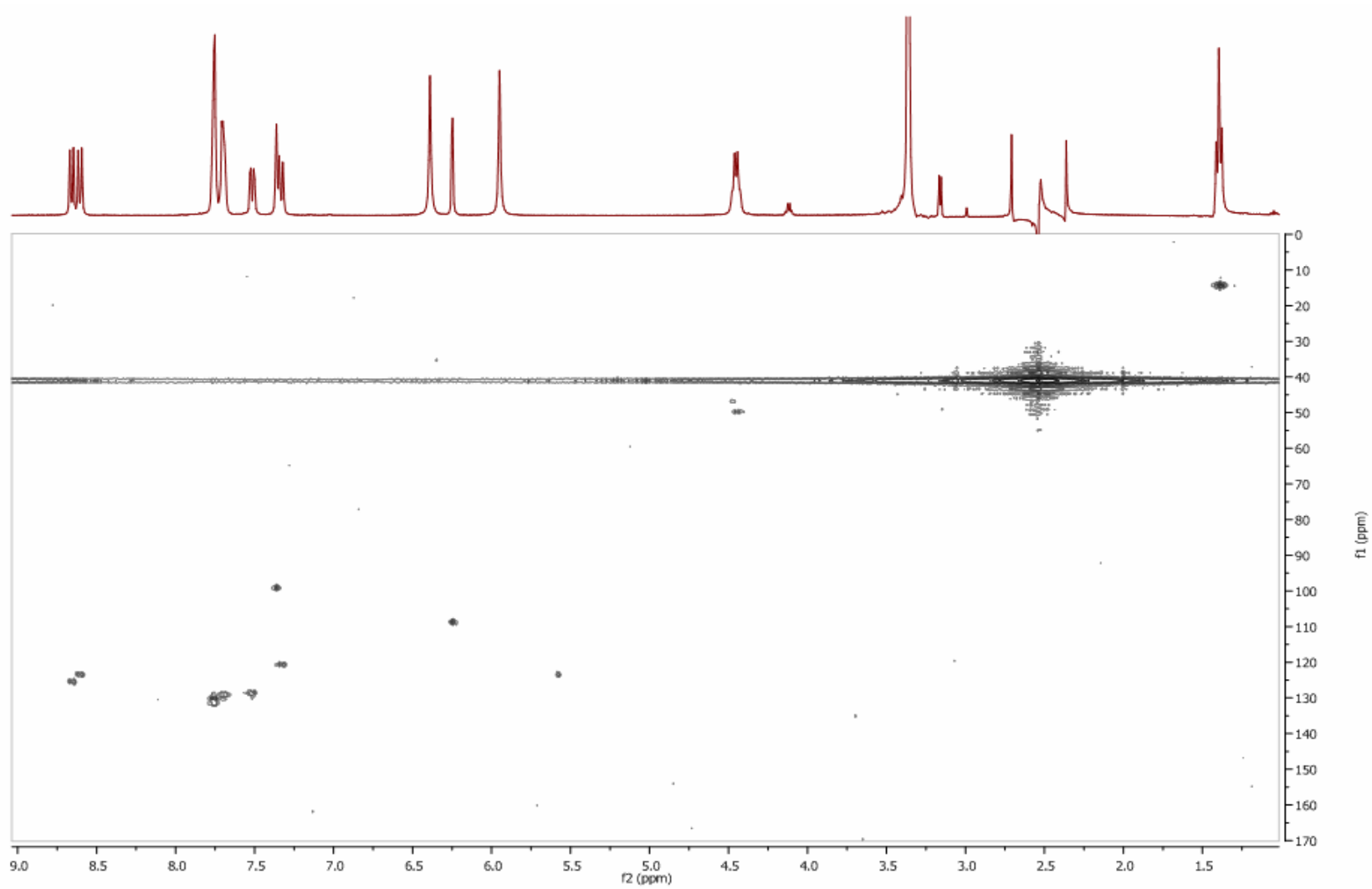


Figure A1: 400 MHz  $^1\text{H}$ - $^{13}\text{C}$  HMQC spectrum of homidium in  $\text{DMSO-d}_6$

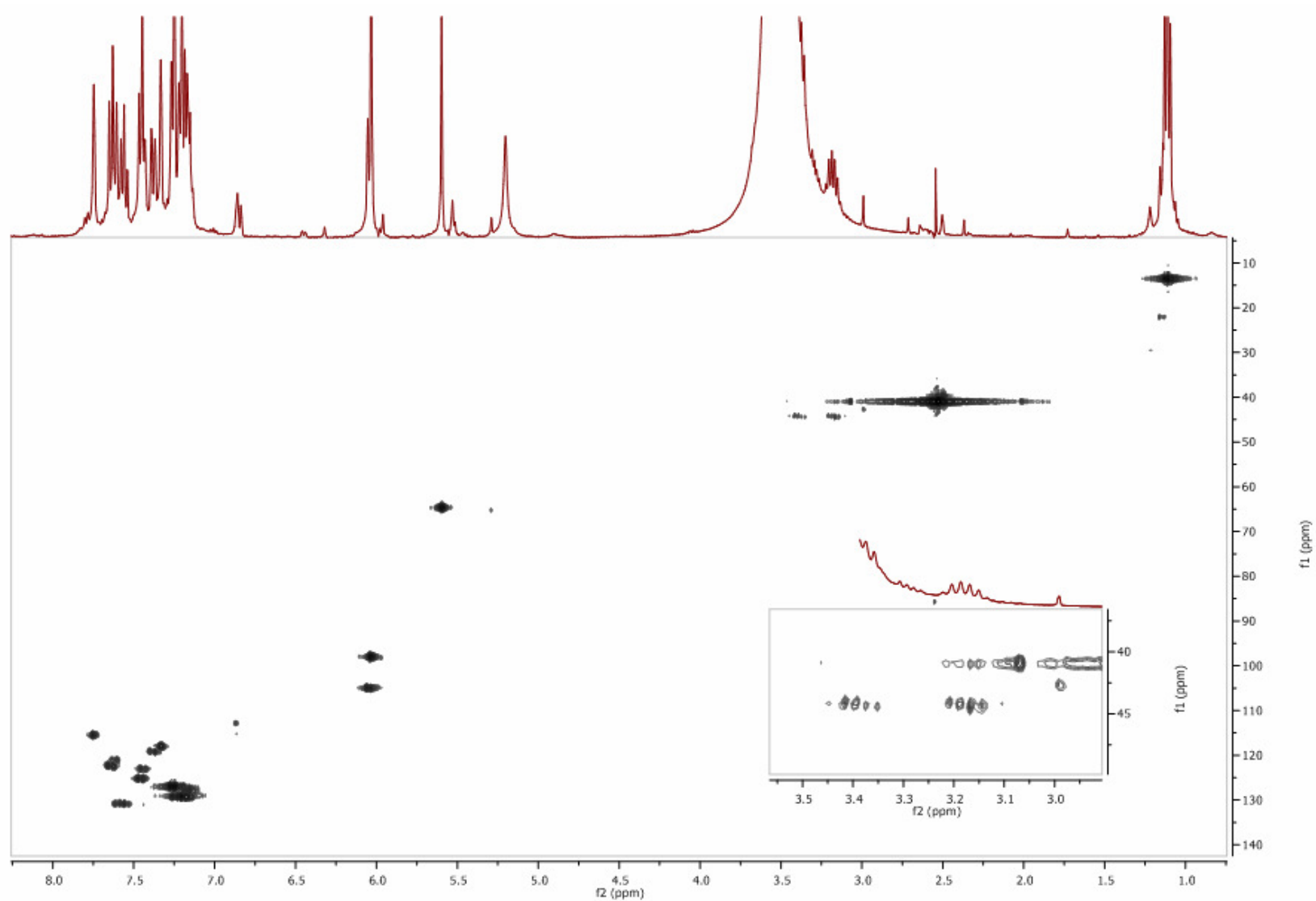


Figure A2: 400 MHz  $^1\text{H}$ - $^{13}\text{C}$  HMQC spectrum of ISM in  $\text{DMSO-d}_6$  with enhancement of the high field region from 3.0 – 3.5 ppm

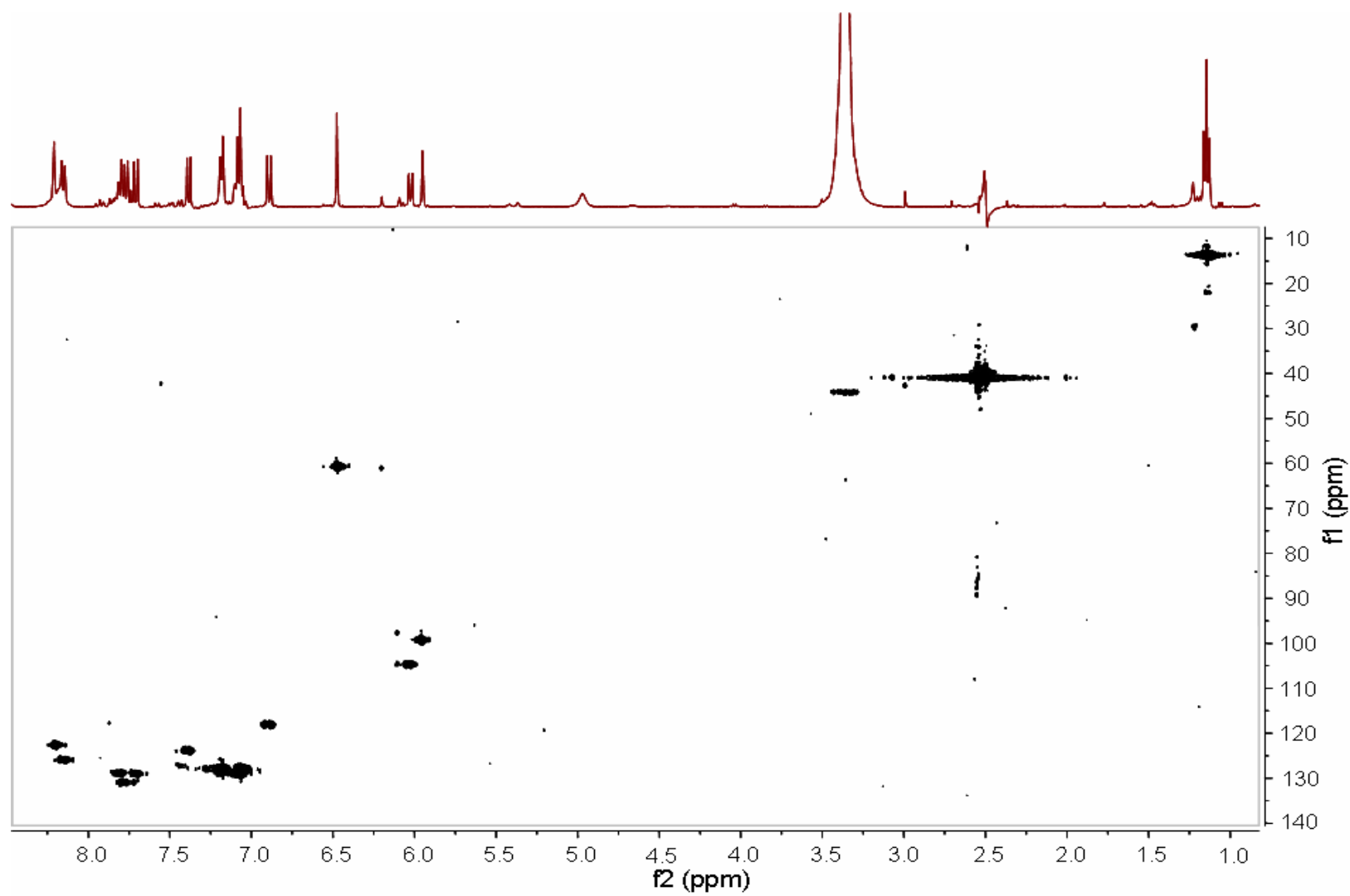


Figure A3: 400 MHz  $^1\text{H}$ - $^{13}\text{C}$  HMQC spectrum of M&B4250 in  $\text{DMSO-d}_6$

## Publication and Conference Proceedings

### Publication

Schad, G. J., Allanson, A., Mackay, S. P., Cannavan, A., Tettey, J. N. A. (2008). Development and validation of an improved HPLC method for the control of potentially counterfeit isometamidium products. *Journal of Pharmaceutical and Biomedical Analysis* 46, 45-51

### Conference Proceedings (Abstract)

Schad, G. J., Skellern, G. G., Euerby, M. R. (2008). Comparative study of the effect of stationary phase chemistry and mobile phase selectivity on the HPLC separation of isometamidium chloride hydrochloride and its structural isomers. Conference Proceedings of the 27<sup>th</sup> International Symposium on Chromatography (ISC2008) in Münster, Germany

Schad, G. J., Skellern, G. G., Euerby, M. R. (2008). Comparative study of the effect of stationary phase chemistry and mobile phase selectivity on the HPLC separation of isometamidium chloride hydrochloride and its structural isomers. Conference Proceedings of the 34<sup>th</sup> International Symposium on High-Performance Liquid Phase Separations and Related Techniques (HPLC2009) in Dresden, Germany